國立臺灣大學工學院材料科學與工程學研究所

博士論文

Graduate Institute of Material Sciences and Engineering
College of Engineering
National Taiwan University
Doctoral Dissertation

微流道中無電鍍問題之數學分析與數值分析

Mathematical and Numerical Analysis of Electroless Plating Problem in a Microchannel

吳柏毅

Po-Yi Wu

指導教授：高振宏 博士、Frédéric Hecht 博士

Advisor: Cheng-Hong Kao, Ph.D., Frédéric Hecht, Ph.D.

中華民國 111 年 03 月

March 2022

doi:10.6342/NTU202200609

Mathematical Modeling and Numerical Analysis of Electroless Plating Problem in a Microchannel

Po-Yi Wu
Advisor: Cheng-Hong Robert Kao, Tony Wen-Hann Sheu, Frédéric Hecht, Olivier Pironneau

Department of Materials Science and Engineering
National Taiwan University
Taipei, Taiwan

Laboratoire Jacques-Louis Lions
Sorbonne University
Paris, France

March 2022

doi:10.6342/NTU202200609

doi:10.6342/NTU202200609

致謝

首先我要感謝高振宏老師從我大二到現在給我非常多有趣的題目以及挑戰，讓我有機會能夠學習模擬相關的研究，也給我許多自由度讓我能做很多自己有興趣的題目。我也特別感謝許文翰老師對我的提拔以及教導，讓我對於數值分析領域有更深入的了解，也不吝於將我介紹到法國做研究，也因此能夠認識法國許多當代著名的計算領域大師。在法國期間，我特別感謝 Olivier Pironneau 對我非常有耐心的指導，剛到時我真的很多東西都不會，但 Olivier 總是願意從頭教我基本的觀念，因此短短的時間我學到很多看事情的角度，以及真正做研究的基本功，我也很感謝他花非常多時間在我身上並跟我討論問題。我也想感謝 Frédéric Hecht 在一些研究上還有很多行政的事情上幫我許多忙。對於能讓我畢業的關鍵文章，我想感謝 Vivette Girault 幫我們許多描述上的問題，她花很多時間幫助我們把許多數學的描述弄得更清楚，讓我原來糟糕的數學描述變得漂亮且清楚。除此之外我也想特別感謝那些曾參與過我博士生涯的老師：Maxim Solovchuk、Sidi Mahmoud Ould Kaber、Faker Ben Belgacem、Endre Süli、Zakaria Belhachmi、陳宜良老師、薛克民老師，以及周逸儒老師。

ACPL 是我從大學以來待最久的地方，這裡我們不知道打過多少種遊

doi:10.6342/NTU202200609

戲、喝醉嘔吐過幾次 (彥彬、朱子，特別標註)，糾團出遊也好幾次，302 辦公室真是個充滿回憶的地方。這段時間真的很感謝漢堂帶我種訓，喝咖啡，還有幫我很多事情一時說不完；瑞洋幫我買很多巧克力，對於做研究非常重要、Sean 是每次都留很晚的戰友，真的很少人這麼晚還在實驗室做事情、海洋教大家一口喝光啤酒的技巧、弘偉教大家如何把妹、氣質很會製造歡樂、立真示範如何兩年內做出很好的成果、億安示範如何逃脫 TSMC、穎暄幫我們拍了很多照片、柏融跟我排了好幾場吃雞，不過我們雙排好像還沒吃過? 感謝儀雯在實驗室期間幫我處理很多麻煩的行政事務；立宇是我大學以來的好同學，感謝你 4 等才單殺我，沒有 3 等就單殺；我也感謝清雲常常做甜點給我們吃，真的很厲害；柏紹幫助我研究實驗的部分，甚至最後要印論文的部分也幫我不少忙，真的很感謝；馬德也幫過我實驗的事情，還有子軒畢業時幫我們合照；家儀在謝師宴的時候幫忙喬很多事，也很會當獵人。有許多同學像是：珮慈、正豪、晉豪、Simon、至家、薇禎、復翎、詒嘉、晨婎、昱安，仁卡、靜涵、長弦、柏瑜，由於我很多時間在法國以及其他地方、跟你們較少接觸，祝福你們研究順利，畢業順利、未來也能找到好的工作。另外 Th in 並沒有被忘記，你被放在彭蒙惠那區。

我也要特別感謝彭蒙惠成員，這是我研究所期間的精神糧食，當年號稱材料系最大情報組織，感謝裡面的成員彥上、AJ、背骨仔、振寧、阿皮、Th in、胡老師、鵝魚、4 哲、高弟、米粒、宇凡、沈學長，很難找到比這更反社會的團體了。同樣的，整天改版標加上 Dcard rush 的聊天室也是一大精神支柱，感謝裡面的成員 (扣除與彭蒙惠重複的部分)：0J、大

doi:10.6342/NTU202200609

砲、中 X 胡、詠哥、Brian、尼克。這裡的垃圾話是讓人活下去的動力。這裡想特別提：Brian 在我出國前跟出國後先後送我好幾件衣服，都非常實用，真的非常感謝。也感謝振寧從日本寄了一封繞地球一圈的明信片到巴黎，上面都是亂七八糟的內容。還有彭蒙惠、B00 群組中陪我打 LOL、PUBG、AOE 等等的這些人，感謝這段時間的陪伴。

我感謝我爸媽、我的阿公阿嬤 (兩邊) 還有很多家人這段時間對我的支持。我要特別感謝子軒在這段期間一直鼓勵我也陪伴我度過很多艱難的時刻，沒有妳我真的會撐不住。我也感謝主送這麼多人來幫我，沒這些人 carry 我看是很難畢業。

Pour les personnes en France:

Tout d'abord, je tiens à remercier tous ceux que j'ai rencontrés au LJLL : Ludovic, qui m'a d'abord aidé à connaître l'environnement. On a joué à League of Legends ensemble assez souvent, même si d'habitude je le carried pour gagner. Olivier l'OG, qui m'a beaucoup aidé pendant la période où je suis en France. Merci pour vous très bon gourmet alsacien mais le munster peut être trop. Allen, qui est le mec clé de ma thèse. Il m'aide à gérer de nombreuses démarches administratives extrêmement pénibles. Je ne peux pas arriver à cette étape sans lui. Gontran, qui est très intéressant. Merci de m'avoir fourni de nombreuses informations sur les mangas français et de discuter avec moi assez souvent. Fatima, la grosse, merci pour toujours wesh à tout le monde. Mohammad, merci d'avoir envoyé une carte postale lorsque tu as été au Canada. On a partagé beaucoup d'idées à Paris. Anouk, qui

doi:10.6342/NTU202200609

aime toujours partager beaucoup de choses avec les autres. Tu es vraiment une bonne coéquipier pour attaquer les arènes. Je me suis excusé d'avoir été hors ligne pendant un certain temps. Valentin, merci de m'avoir invité à PontSakka. Tu es un très bon coéquipier. Lydie, je me souviens toujours d'une forme très incroyable de l'escape game. Merci beaucoup! Marc, qui est également membre d'attaquer les arènes. Merci pour l'appui-feu. Bien que tu nous aies trahi pour jouer à Sun & Moon. Ana, merci de m'avoir invité plusieurs fois à la fête chez vous. Alex, merci de m'avoir présenté l'ultimate, qui est vraiment cool et amusant. Elise, merci de tenir le thé du labo et de le garder en ligne pendant le covid. Ramon, merci d'avoir beaucoup discuté avec moi, même si tu es visiblement un gars calme. Federica, nous étions bons amis de l'alcool. je me souviendrai toujours de toi Shengquan, qui est un expert de Jay Chou. Merci de m'avoir beaucoup aidé à Paris. Mais je dois redire qu'un vélo est en effet un cheval de fer. Liudi, merci de m'avoir guidé de nombreux conseils sur l'administration de la soutenance de thèse. J'espère que nous pourrons jouer au mahjong quand je serai de retour à Paris. ShihJie, merci de m'avoir fait découvrir Bagneux pour jouer au foot. J'espère que tout va bien à Shanghai. Je tiens également à remercier Agua, Gabrielle, Amaury, Christophe, Gong, Yipeng, Li Rui, Katia, Haowan, Ivan, Eugenio, Greg, Ziad, Nicolas Clozeau, Nicolas Augier. Merci à tous d'avoir rejoint ma vie à Paris.

En outre, je tiens à remercier le club de go de Jussieu et l'équipe de

doi:10.6342/NTU202200609

football de Pontsakka de m'avoir fourni une vie riche en dehors de LJLL. Merci tout particulièrement Clément, Louise, Benjamin, Lucas, Nacho, et Juan.

doi:10.6342/NTU202200609

致謝

doi:10.6342/NTU202200609

摘要

微流道中的無電鍍製程是一項在工業中具有發展潛力的技術。從物理角度來看，這是一個多重物理耦合問題：需要考慮流體力學、質傳、化學反應、相變態等等，特別是在微小尺度下需要考慮更多細膩的物理行為。本論文主要從數學建模與數值分析的角度研究無電鍍問題，並將它們寫成三個章節：第一章將簡介無電鍍製程並回顧其相關文獻；第二章將討論無電鍍問題在單相流中的數學模型以及數值分析；第三章則是連無電鍍生成氣泡的狀況也一起討論，並探討如何模擬以及一些數值分析。

- 在第二章中，我們不考慮無電鍍反應中氣泡產生的效應，因此我們只考慮單相不可壓縮流與質傳的耦合問題，此外我們利用蒸發逼近的技巧來模擬物質上鍍造成的小幅度邊界移動。因此簡化的模型方程為 Navier-Stokes 方程以及擴散散對流方程的耦合並考慮非線性且非典型的邊界條件。我們將證明其中濃度方程解之存在性與唯一性並利用數值分析證明我們提出的數值方法與演算法之可行性。

- 氣體產生與氣相流體的移動問題在第三章中會被探討。由於氣泡會在整個物理空間中隨機地產生，因此我們採用平均形式的二相流方

doi:10.6342/NTU202200609

程以及擴散對流方程與通量邊界條件耦合作為模型方程，此外上鍍造成的邊界移動也有考慮。在數值方法方面，時間離散採用一階特徵線法；空間離散採用有限算法，且我們證明了數值方法的適定性。數值驗證方面我們將比較一、二維問題並與微流道實驗進行比較。

- 在附錄中，我們研究更加簡化的二相流模型。在這個模型中，我們忽略對流項的效應。我們考慮三條濃度方程：其中兩條代表參與無電鍍反應的化學物質傳輸以及一條代表溶解於水中的氣體傳輸，並與一條描述液體體積分率的常微分方程耦合。為了描述表面反應，我們考慮滿足電荷平衡的通量邊界條件。我們證明了此模型方程的解之存在性與唯一性，此證明將兩種化學物質推廣至 N 種化學物質也適用。

doi:10.6342/NTU202200609

Résumé

Le dépôt autocatalytique dans les microcanaux est une technologie en plein essor dans l'industrie. D'un point de vue physique, il s'agit d'un problème multiphysique incluant la dynamique des fluides, le transfert de masse, la réaction chimique, le changement de phase, etc. Surtout à l'échelle micrométrique, des phénomènes physiques plus subtils sont intéressants. Dans cette thèse, le problème du dépôt autocatalytique est principalement traité par la modélisation mathématique et l'analyse numérique. Il y a trois chapitres dans cette thèse: Un examen rapide et une introduction du dépôt autocatalytique sont donnés dans le chapitre 1. L'analyse d'un problème de dépôt autocatalytique dans un écoulement de liquide monophasique est présentée au chapitre 2. La simulation numérique du problème de dépôt électrolytique avec la production de gaz est abordée au chapitre 3.

- Dans le chapitre 2, la génération de gaz due au dépôt autocatalytique est négligée. Au lieu de cela, un écoulement incompressible monophasé couplé à un transfert de masse est considéré. Le petit mouvement de frontière dû aux espèces chimiques déposées est modélisé

doi:10.6342/NTU202200609

par une approximation de la transpiration. Avec cette simplification, le modèle mathématique se compose d'un écoulement Navier-Stokes et d'une équation pour la concentration du produit chimique de dépôt couplée par des conditions aux limites non standard et non linéaires. L'existence et l'unicité sont prouvées pour l'équation de concentration. Une analyse numérique est réalisée qui justifie les schémas numériques et l'algorithme non linéaire proposés.

- Dans le chapitre 3, la génération de gaz et le mouvement de la phase gazeuse sont pris en compte. Étant donné que les bulles sont générées de manière aléatoire et partout, un modèle d'écoulement à deux phases moyennées en volume est appliqué. Cette simplification est couplée à des équations de convection-diffusion soumises à des conditions aux limites de flux satisfaisant l'équilibre électronique. Une méthode conservatrice de volume de phase du premier ordre et une méthode d'éléments finis sont effectuées pour la simulation numérique et le bien-fondé du schéma numérique est prouvé. Des études numériques dans des cas uni et bidimensionnels avec comparaison à l'expérience sont réalisées pour justifier le modèle proposé.

- Dans l'annexe B, un autre modèle simplifié pour le transport d'espèces chimiques dans un écoulement à deux phases est considéré. Dans ce cas, les termes de convection sont négligés de sorte que la fraction volumique de phase liquide ne dépend que de la concentration en gaz de

doi:10.6342/NTU202200609

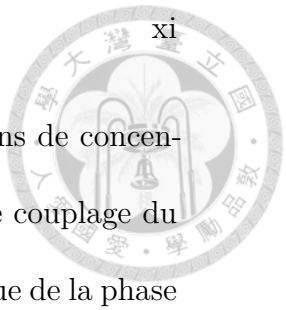

dissolution dans l'électrolyte. On considère trois équations de concentration pour le transport de deux espèces chimiques et le couplage du gaz de dissolution avec une ODE pour la fraction volumique de la phase liquide. La condition aux limites de flux sur la surface de réaction avec équilibre électronique est prise en compte. L'existence et l'unicité sont prouvées pour les équations de couplage. On montre que le cas des deux espèces peut être généralisé au cas des N-espèces.

doi:10.6342/NTU202200609

doi:10.6342/NTU202200609

Abstract

Electroless plating process in microchannel is a rising technology in industry. From a physical point of view, it is a multiphysics problem including fluid dynamics, mass transfer, chemical reaction, phase change, etc.. Especially in micrometer scale, more subtle physical phenomena are of interest. In this thesis, electroless plating problem is mostly taken care by mathematical modeling and numerical analysis. There are three chapters in this thesis: A quick review and introduction of electroless plating process are given in Chapter 1. Analysis of an electroless plating problem in a single phase liquid flow is presented Chapter 2. The numerical simulation on the electrolss plating plating problem with gas generation is discussed in Chapter 3.

- In Chapter 2, the gas generation due to the electroless plating is neglected. Instead, single phase incompressible flow coupled with mass transfer is considered. The small boundary motion owing to the deposited chemical species is modeled by a transpiration approximation. With this simplification, the mathematical model, consists of a Navier-Stokes flow and an equation for the concentration of the plating chem-

doi:10.6342/NTU202200609

ical coupled by non-standard and nonlinear boundary conditions. Existence and uniqueness are proven for the concentration equation. Numerical analysis is carried out and justifies the proposed numerical schemes and nonlinear algorithm.

- In Chapter 3, the gas generation and motion of gaseous phase are taken into account. Since the bubbles are generated randomly and everywhere, a volume averaged two phase flow model is applied. This simplification is coupled with convection-diffusion equations subject to flux boundary conditions satisfying electron balance. A first-order phase volume conservative method and finite element method are carried out for numerical simulation and the well-posedness of numerical scheme is proved. Numerical studies in one and two-dimensional cases with comparison to experiment are performed to justify the proposed model.

- In Appendix B, a further simplified model for chemical species transport in two phase flow is considered. In this case, the convection terms are neglected so that the volume fraction of liquid phase depends only on the concentration of dissolving gas in the electrolyte. Three concentration equations for two chemical species transport and dissolving gas coupling with an ODE for volume fraction of liquid phase are considered. The flux boundary condition on the reacting surface with electron balance is taken care. The existence and uniqueness are proven for the

doi:10.6342/NTU202200609

coupling equations. It is shown that the two species case can be generalized to N-species case.

doi:10.6342/NTU202200609

doi:10.6342/NTU202200609

Contents

doi:10.6342/NTU202200609

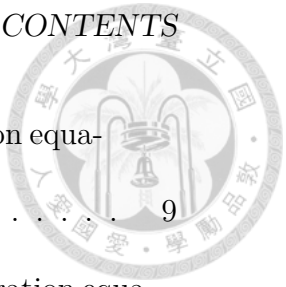

doi:10.6342/NTU202200609

doi:10.6342/NTU202200609

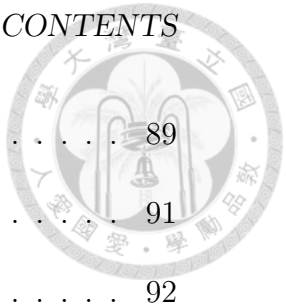

doi:10.6342/NTU202200609

doi:10.6342/NTU202200609

doi:10.6342/NTU202200609

List of Figures

doi:10.6342/NTU202200609

doi:10.6342/NTU202200609

doi:10.6342/NTU202200609

doi:10.6342/NTU202200609

doi:10.6342/NTU202200609

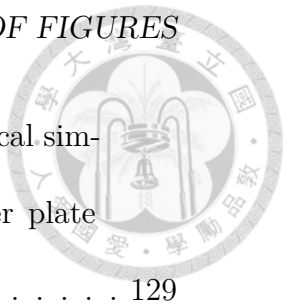

doi:10.6342/NTU202200609

List of Tables

doi:10.6342/NTU202200609

doi:10.6342/NTU202200609

Chapter 1

Introduction and state of the art

1.1 Electroless plating process

1.1.1 Overview

Electroless plating is a class of industrial chemical reaction process aimed at forming a film or layer on a base substrate by reducing complex metal cations in a liquid solution [2, 3, 4]. In contrast to electroplating processes, the reduction of matal cations can be achieved without the external current during electroless plating process. The metal coatings is created by autocatalytic chemical reduction of metal cations in a liquid bath. This technique has been widely applied in various industries. For instance, surface decoration, hard-wearing coating, manufacture of hard-disc drive, printed circuit

doi:10.6342/NTU202200609

boards, etc.[4, 5].

Recently, electroless process in microfluidic channels has been regarded as a promising micro or nano meter technology. Applications range from chemical etching process for electronic devices, to electrical packaging for food [6, 7]. Compared to the large-scale electroless process, the change of geometry to the micro- or nano-meter scale raises a critical issue for the deposition as the thickness becomes comparable to the dimension of flow channel. For instance, in the copper interconnecting process [8] by electroless plating, the thickness of the deposition layer of copper is large enough to risk a connection of the pillars.

1.1.2 Mechanism

In general, the chemical reaction of electroless plating can be expressed as

$$M^{z+}_{(aq)} + X^{z-}_{(aq)} \rightarrow M^{0}_{(s)} + Z,$$

where M is the metal, X^{z-} is the reducing agent, and Z is its oxidized by product.

In order to deposit the metal uniformly on a reaction surface, an initiator that is either an additional catalyst or the substrate itself shall be added in advance. Moreover, the reaction must be autocatylic so that it continues after the reaction surface has been covered by the metal. For the setting of the electroless plating process, see also Figure 1.1.

doi:10.6342/NTU202200609

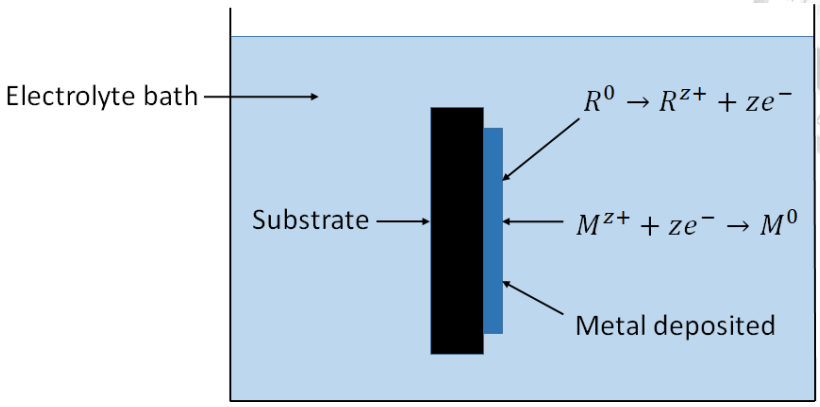

Figure 1.1: Schematic of electroless plating setup.

1.1.3 Mixed potential theory

Two assumption is made when the mixed potential theory is applied for the electroless plating process: (i) The overall chemical reaction can be divided into several partial reactions. Each partial reaction belongs to either anodic part or cathodic part. Here, the anodic reaction is the decomposition of the reducing agent

$$R^0 \rightarrow R^{z+} + ze^-, \tag{1.1}$$

and the cathodic reaction the reduction of the metal comples cations

$$M^{z+} + ze^- \rightarrow M^0. \tag{1.2}$$

(ii) The reaction must satisfy electron balance at all time. Therefore, the sum of the anodic current density and the cathodic current density is zero. That is,

$$\sum_{j \in \text{anodic}} I_j + \sum_{j \in \text{cathodic}} I_j = 0. \tag{1.3}$$

doi:10.6342/NTU202200609

We denote the equilirium potential for species j by E_j, the Butler-Volmer equation (see for example [9]) suggest that the current density I_j can be expressed as

$$I_j = i_j c_j^{\gamma_j} := A_j \Big[\exp\left(\frac{\alpha_j z_j F \xi_j}{R\theta}\right) - \exp\left(\frac{-\beta_j z_j F \xi_j}{R\theta}\right) \Big] c_j^{\gamma_j}, \tag{1.4}$$

where A_j is the ratio of the reference current density and the corresponding reference species concentration, α_j the anodic transfer coefficient, β_j the cathodic transfer coefficient, z_j the number of electrons, F the Faraday constant, R the gas constant, θ the temperature, c_j the species concentration, and γ_j the concentration dependency. In the above, ζ_j is the overpotential which can be expressed as

$$\zeta_j = E_{mix} - E_j, \tag{1.5}$$

where E_{mix} is the mixed potential (see also Figure 1.2).

1.1.4 Electroless plating in a microchannel

As the size of channel becomes smaller, more subtle issues influencing the deposition quality shall be taken into account. Those effects that do not play crucial roles in a large size problem become main characters in micro- or nano-scale. Some issues which are worthy of further consideration for electroless plating in a microchannel are listed below.

doi:10.6342/NTU202200609

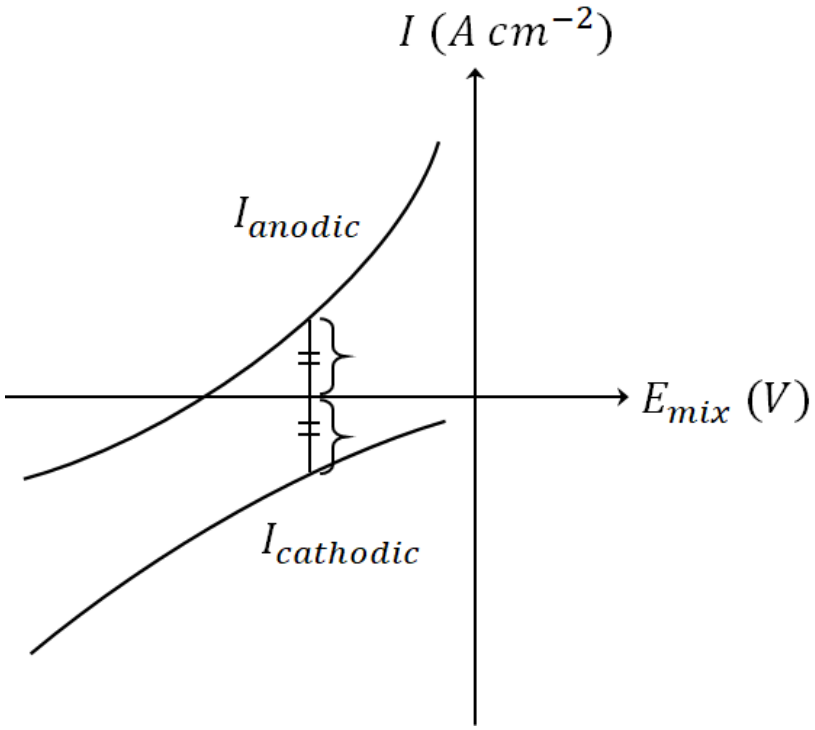

Figure 1.2: Current-potential curves for the system satisfying the hypotheses of the mixed potential theory.

doi:10.6342/NTU202200609

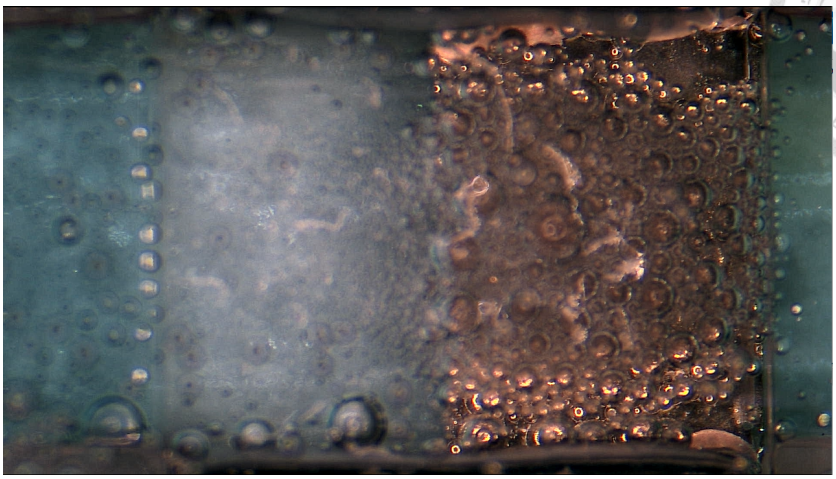

Figure 1.3: A microchannel of cross section 8 $mm \times 1$ mm with a copper plate where the electroless copper plating process occurs.

Gas generation

In a large scale problem, the gas generation in the electroless plating process is not important becuase it takes only slight space in comparison with the size of bath. In contrast, the effect that bubbles prevent the substrate from being plated is serious when the flow channel is of smaller size. Indeed, conducting a electroless copper plating in a microchannel with cross section of size 8 $mm \times 1$ mm for 2 minutes, the bubbles will have been taken over a large portion of the channel (see Figure 1.3).

Whether the gas generation occurs is determined by the electroless plating system being employed. Electroless nickel and copper plating systems generate hydrogen gas. On the other hand, electroless gold does not generate gas. Given this fact, both single phase and two-phase flow problems for the fluid motion in a electroless plating process play crucial roles.

doi:10.6342/NTU202200609

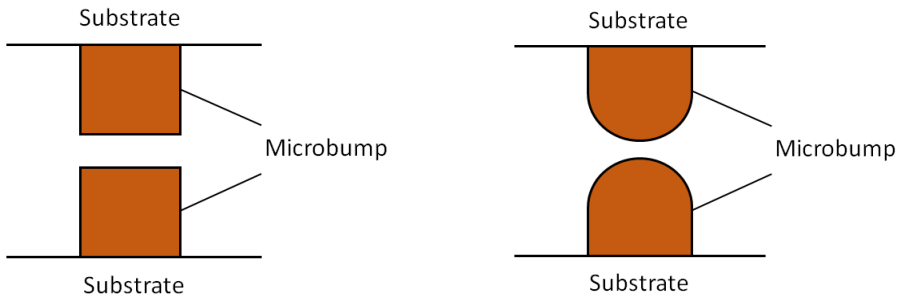

(a) Flap-topped microbumps. (b) Dome shape microbumps.

Figure 1.4: Comparison between flat-topped bump and dome shape microbumps.

Seams and voids between microbumbs

Microbump bonding is one of the important applications of electroless plating in microchannels. The geometry effect arising from the shape of microbumps is significant for the plating quality. For example, if two microbumps to be plated are flat-topped (see Figure 1.4a), then seams or voids may appear in the jointed bumps [8, 10]. This is owing to the fact that the region between two bumps is always of the lowest ionic concentration. The deposition rate of the outer region is always higher than the inner region between tp bumpes. Once the innter region is closed by the deposited metal of outer region, the seam or void remains due to the shortage of fresh electrolyte. On the other hand, if the dome-shaped microbumps (see Figure 1.4b) are adopted for electroless plating process, The bumbs can be jointed perfectly.

doi:10.6342/NTU202200609

Bridging

For a circuit pattern, It is essential to control precisely where to be plated and not to be plated. Let us take the bonding of face-to-face microbump array as an illustration. In most cases, the desired region to be plated is the gap between face-to-face bumps. Conversely, the plane within the bumbs installed on the same substrate are not desired to be deposited since the short circuit will be caused by the connection between to bumbs on the same plane. Such undesired phenomenon is called *bridging* [11, 12]. Bridging is due to the instability of the electrolyte which causes a homogeneous decomposition so that the metal particles accumulate everywhere. Indeed, this phenomenon is observed in the low flow velocity region where the ionic concentration is sufficient but the metal particles cannot be moved away.

Uniformity

For many circuit board, there always exists period structure so that the uniformity of plating quality is important. However, many physical conditions in such periodic space may not be uniform. For example, the bubble distribution is in general far from uniform even in a microchannel with simple geometry (see Figure. 1.3)

To see another uniformity issue, we take the bonding of face-to-face microbump arrays as an example again. Considering an face-to-face array of microbumps is placed in a microchannel, we observed that the plating condi-

doi:10.6342/NTU202200609

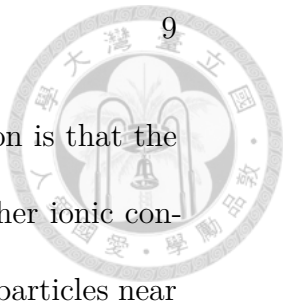

tion is highly nonuniform [12]. The most interesting observation is that the bumps near the flow entrance, which were in the region of higher ionic concentration, were not deposited. A hypothesis is that the metal particles near the entrance was washed away by the fluid flow but deposit behind. Indeed, when the entrance velocity is sufficiently high, None of the microbumps can be plated.

1.2 Mathematical model for electroless plating problem

Electroless plating problem can be regarded as a multiphysics problem which consists of surface reaction, fluid dynamics, heat transfer, chemical potential distribution, etc.. In a large scale deposition, simplified models would be adequate for describing the occuring physical phenomena, especially in a simple geometry case. In what follows, we review two kinds of one-dimensional models which well described the electroless plating process in the special cases.

1.2.1 One-dimensional steady state advection-diffusion equations

Kim and Sohn proposed a model describing the concentration profile of chemical species in the diffusion layer of a plated rotating disk with constant angular velocity [1]. In this situation, the fluid flow near the surface of rotating

doi:10.6342/NTU202200609

disk can be approximated by a uniformly disbributed flow directing to the surface. In addition, the thickness of diffusion layer is approximately uniform on the surface. Consequently, the physical domain for modeling can be reduced to be one-dimensional (see Chapter II, Section 11 in [13] for the derivation).

The modeling problem is given as follows: Let c_j be the concentration profile of the j-th species. The governing equations for steady state problem is

$$-D_j\frac{\partial^2 c_j}{\partial z^2}+v\frac{\partial c_j}{\partial z}=0, \tag{1.6}$$

where D_j is the diffusion coefficient, v the velocity field given by

$$v=-az^2\omega^{3/2}\nu^{-1/2}, \tag{1.7}$$

where $a=0.51023$, ω is the angular velocity of the rotating disk, and ν the kinematic viscosity of the electrolyte. The boundary conditions are given by

$$c_j=c_{b,j},\quad z^2+r^2\to\infty,\qquad -D_j\frac{\partial c_j}{\partial z}=\sum_{j\in R_j}\frac{|I_j|}{z_jF},\quad z=0, \tag{1.8}$$

where $c_{b,j}$ is the bulk concentration of species j, R_j the set collecting those species j participating in the reaction related to c_j, z_j the number of electrons, F the Faraday constant, and I_j the current density. We recall that I_j can be expressed by (1.4) with the overpotential (1.5).

For numerical simulation, the Dirichlet boundary condition $c_j=c_{b,j}$ shall be set at the diffusion layer-bulk interface. The diffusion layer thickness δ_j

doi:10.6342/NTU202200609

at steady state for a rotating disk can be expressed as

$$\delta_j = 1.61 D_j^{1/3} \omega^{-1/2} \nu^{1/6}. \tag{1.9}$$

Finally, the system of equations can be closed by the electron balance condition (1.3).

1.2.2 One-dimensional time-dependent diffusion-migration equations

To simulate electroless copper plating on a planar substrate, Ramasubramanian et. al. [14] applied a system of time-dependent diffusion-migration equations for solving the concentration profile of each species participating in the electroless process.

Let c_j, $j = 1, \dots N$ be the concentration profile of the j-th species. In the diffusion layer, the mass balance implies that

$$\frac{\partial c_j}{\partial t} = -\frac{\partial J_j}{\partial z} + Y_j, \tag{1.10}$$

where Y_j is the rate of homogeneous production or consumption of species j and the flux J_j is contributed by diffusion and migration:

$$J_j = -\frac{z_j D_j F c_j}{R\theta} \frac{\partial \Phi}{\partial z} - D_j \frac{\partial c_j}{\partial z}. \tag{1.11}$$

In the above Φ is the solution potential. In the electrolyte, water equilibrium holds at all times and therefore we have

$$\sum_j z_j c_j = 0, \tag{1.12}$$

doi:10.6342/NTU202200609

which closes the system with unknowns $(c_1, \ldots, c_N, \Phi)$.

The boundary conditions are similar to those proposed by Kim and Sohn [1]. At the diffusion layer-bulk interface, we let

$$c_j = c_{b,j}$$

At the electrode surface, the Neumann boundary conditions are given similarly the second equation of (1.8) but the current densities take the form

$$\begin{aligned} I_a &= A_a \left\{ \prod_{k \in R_a} c_k^{\gamma_k} \left(\exp\left(\frac{\alpha_a F}{R\theta} [V - \Phi - U_j^0 \right) - \exp\left(\frac{-\beta_a F}{R\theta} [V - \Phi - U_j^0] \right) \right) \right\}, \\ I_c &= A_c \left\{ \prod_{k \in R_c} c_k^{\gamma_k} \left(\exp\left(\frac{\alpha_c F}{R\theta} [V - \Phi - U_j^0] \right) - \exp\left(\frac{-\beta_c F}{R\theta} [V - \Phi - U_j^0] \right) \right) \right\}, \end{aligned} \tag{1.13}$$

where R_a and R_c are the set of species j involving in anodic reaction and cathodic reaction, respectively, V is the electrode potential, and U_j^0 is the open-circuit potential for the j-th species. Here, V plays a similar role as the mixed potential E_{mix} in (1.5). The full system can be closed by the electron balance on the reacting surface:

$$I_a + I_c = 0. \tag{1.14}$$

doi:10.6342/NTU202200609

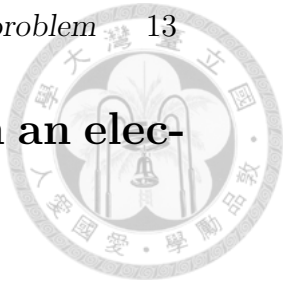

1.3 Governing equations of interest in an electroless plating problem

1.3.1 Navier-Stokes equations

To derive the Navier-Stokes equations, we assume that the fluid is a continuum and all the fields of interest, such as density, flow velocity, pressure, and temperature are differentiable.

Material derivative

Changes of a physical quantity can be measured in two different ways depending on where the observer is: One can measure a physical quantity either (i) on a fixed point (Eulerian), or (ii) by following a parcel of fluid along its streamine (Lagragian). The derivative of a physical quantity with respect to a fixed position in space is called a Eulerian derivatve, while the derivative following the flow velocity is called a Lagragian derivative. Based on the relation between Eulerian and Lagragian derivatve, we define the material derivative which connects these two concept:

$$\frac{D}{Dt} := \partial_t \mathbf{u} + \mathbf{u} \cdot \nabla, \tag{1.15}$$

where $\mathbf{u}$ is the flow velocity.

doi:10.6342/NTU202200609

Continuity equation

Let ϕ be any physical quantity defined over a control volume Ω, and Γ its boundary. The mass conservation can be expressed as

$$\frac{d}{dt}\int_\Omega \phi dx = \int_\Gamma \phi \mathbf{u}\cdot\mathbf{n}dS = \int_\Omega s dx, \tag{1.16}$$

where $\mathbf{u}$ is the flow velocity of teh field, $\mathbf{n}$ is the outward unit normal, and s is the sink or source in the flow. By the divergence theorem, we have

$$\frac{d}{dt}\int_\Omega \phi dx = -\int_\Omega \nabla\cdot(\phi\mathbf{u})dx - \int_\Omega s dx. \tag{1.17}$$

Applating the Reynolds transport theorem, we have

$$\int_\Omega \partial_t\phi dx = -\int_\Omega \nabla\cdot(\phi\mathbf{u})dx - \int_\Omega s dx. \tag{1.18}$$

The above equation must hold for any control volume. Therefore,

$$\partial_t\phi + \nabla\cdot(\phi\mathbf{u}) + s = 0 \tag{1.19}$$

Conservation of mass

Replacing ϕ by the density ρ in (1.19), and assuming that there is no source or sink of mass, we have

$$\partial_t\rho + \nabla\cdot(\rho\mathbf{u}) = 0. \tag{1.20}$$

Conservation of momentum

Let $\phi = \rho\mathbf{u}$ in (1.19), we have

$$\partial_t(\rho\mathbf{u}) + \nabla\cdot(\rho\mathbf{u}\otimes\mathbf{u}) = \mathbf{s}, \tag{1.21}$$

doi:10.6342/NTU202200609

where $\mathbf{s}$ is a vector function. The above equation can be split as

$$(\partial_t \rho)\mathbf{u} + \rho \partial_t \mathbf{u} + (\mathbf{u} \cdot \nabla \rho)\mathbf{u} + \rho(\mathbf{u} \cdot \nabla)\mathbf{u} + \rho(\nabla \cdot \mathbf{u})\mathbf{u} = \mathbf{s}. \tag{1.22}$$

The rearrangement gives

$$\begin{aligned} &(\partial_t \rho + \mathbf{u} \cdot \nabla \rho + \rho \nabla \cdot \mathbf{u})\mathbf{u} + \rho(\partial_t \mathbf{u} + (\mathbf{u} \cdot \nabla)\mathbf{u}) \\ &= (\partial_t \rho + \nabla \cdot (\rho \mathbf{u}))\mathbf{u} + \rho(\partial_t \mathbf{u} + (\mathbf{u} \cdot \nabla)\mathbf{u}) = \mathbf{s} \end{aligned} \tag{1.23}$$

By (1.15) and (1.20), we get

$$\rho \frac{D\mathbf{u}}{Dt} = \rho(\partial_t \mathbf{u} + (\mathbf{u} \cdot \nabla)\mathbf{u}) = \mathbf{s} \tag{1.24}$$

Cauchy momentum equation

The momentum source $\mathbf{s}$ can be split into two terms: one term for internal stresses and another for external forces. The momentum equation can be expressed as

$$\rho \frac{D\mathbf{u}}{Dt} = \nabla \cdot \boldsymbol{\sigma} + \mathbf{f}, \tag{1.25}$$

where $\boldsymbol{\sigma}$ is the Cauchy stress tensor and $\mathbf{f}$ is the body force.

In three dimensional space, $\boldsymbol{\sigma}$ is a rank two symmetric tensor which can be explicitly represented as a 3×3 matrix

$$\boldsymbol{\sigma} = \begin{pmatrix} \sigma_{xx} & \tau_{xy} & \tau_{xz} \\ \tau_{yx} & \sigma_{yy} & \tau_{yz} \\ \tau_{zx} & \tau_{zy} & \sigma_{zz} \end{pmatrix} \tag{1.26}$$

In the above, $\boldsymbol{\sigma}$ can be further split into isotropic part standing for the normal

doi:10.6342/NTU202200609

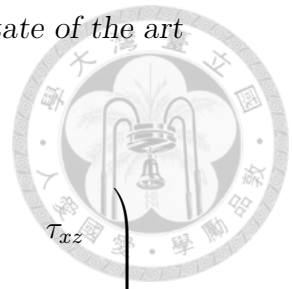

stresses and anisotropic part for shear stresses:

$$\boldsymbol{\sigma} = \begin{pmatrix} \sigma_{xx} & \tau_{xy} & \tau_{xz} \\ \tau_{yx} & \sigma_{yy} & \tau_{yz} \\ \tau_{zx} & \tau_{zy} & \sigma_{zz} \end{pmatrix} = - \begin{pmatrix} p & 0 & 0 \\ 0 & p & 0 \\ 0 & 0 & p \end{pmatrix} + \begin{pmatrix} \sigma_{xx}+p & \tau_{xy} & \tau_{xz} \\ \tau_{yx} & \sigma_{yy}+p & \tau_{yz} \\ \tau_{zx} & \tau_{zy} & \sigma_{zz}+p \end{pmatrix}$$

$$= -pI + \boldsymbol{\tau}, \tag{1.27}$$

where I is the identity matrix, and $\boldsymbol{\tau}$ is the deviatoric stress tenor. Since the tensor $\boldsymbol{\tau}$ should be zero when the fluid is motionless, we define the mechanical pressure p by

$$p = -\frac{1}{3}(\sigma_{xx} + \sigma_{yy} + \sigma_{zz}). \tag{1.28}$$

Finally, the Cauchy equation can be expressed as

$$\rho \frac{D\mathbf{u}}{Dt} = -\nabla p + \nabla \cdot \boldsymbol{\tau} + \mathbf{f}. \tag{1.29}$$

1.3.2 Compressible and incompressible flow

Compressible flow

We assume that the Cauchy stress tensor $\boldsymbol{\tau}$ in (1.29) satisfying the following assumptions

1. $\boldsymbol{\tau}$ is Galilean invariant: it depends only on the spatial derivatives of the flow velocity. That is, $\boldsymbol{\tau}$ is a function of $\nabla \mathbf{u}$.

2. The stress $\boldsymbol{\tau}$ is linear in the variable $\tau(\nabla \mathbf{u}) = C : \nabla \mathbf{u}$ for some fourth-order constant tensor.

doi:10.6342/NTU202200609

3. The fluid is isotropic. By Helmholtz decompositionm $\boldsymbol{\tau}$ can be expressed in terms of two scalar Lamé parameters: the bulk viscosity λ and the dynamic viscosity μ, i.e.

$$\boldsymbol{\tau} = \lambda(\nabla \cdot \mathbf{u})I + 2\mu\varepsilon, \tag{1.30}$$

where I is the identity tensor and $\varepsilon(\nabla\mathbf{u}) = \frac{1}{2}\nabla\mathbf{u} + \frac{1}{2}(\nabla\mathbf{u})^T$.

In three-dimension, given that $\mathrm{tr}(\varepsilon) = \nabla \cdot \mathbf{u}$ and $\mathrm{tr}(\boldsymbol{\tau}) = (3\lambda + 2\mu)\nabla\mathbf{u}$, $\boldsymbol{\tau}$ can be split into isotropic and deviatoric parts:

$$\boldsymbol{\tau} = (\lambda + \frac{2}{3}\mu)(\nabla \cdot \mathbf{u})I + \mu(\nabla\mathbf{u} + (\nabla\mathbf{u})^T - \frac{2}{3}(\nabla \cdot \mathbf{u})I). \tag{1.31}$$

Introducing the second viscosity $\zeta := \lambda + \frac{2}{3}\mu$, the linear stress constitutive equation can be expressed as

$$\boldsymbol{\tau} = \zeta(\nabla \cdot \mathbf{u})I + \mu(\nabla\mathbf{u} + (\nabla\mathbf{u})^T - \frac{2}{3}(\nabla \cdot \mathbf{u})I). \tag{1.32}$$

Let $\overline{p} := p - \zeta\nabla\mathbf{u}$, we obtain the Navier-Stokes momentum equation

$$\rho\left(\partial_t\mathbf{u} + (\mathbf{u} \cdot \nabla)\mathbf{u}\right) = -\nabla\overline{p} + \nabla \cdot \left(\mu(\nabla\mathbf{u} + (\nabla\mathbf{u})^T - \frac{2}{3}(\nabla \cdot \mathbf{u})I\right) + \mathbf{f}. \tag{1.33}$$

Applying the relation $\nabla \cdot (\nabla\mathbf{u})^T = \nabla(\nabla \cdot \mathbf{u})$, we finally get

$$\rho(\partial_t\mathbf{u} + (\mathbf{u} \cdot \nabla)\mathbf{u}) = -\nabla\overline{p} + \mu\Delta\mathbf{u} + \frac{1}{3}\mu\nabla(\nabla \cdot \mathbf{u}) + \mathbf{f}. \tag{1.34}$$

Remark 1.3.1 In two dimension, we have

$$\rho(\partial_t\mathbf{u} + (\mathbf{u} \cdot \nabla)\mathbf{u}) = -\nabla\overline{p} + \mu\Delta\mathbf{u} + \mathbf{f}. \tag{1.35}$$

doi:10.6342/NTU202200609

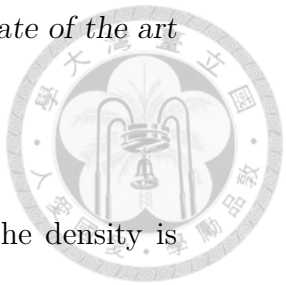

Incompressible flow

The incompressiblity implies that the mateiral derivative of the density is zero, i.e.,

$$\frac{D\rho}{Dt} = 0. \tag{1.36}$$

Combining the above equation with the continuity equation (1.20), we have

$$\nabla \cdot \mathbf{u} = 0. \tag{1.37}$$

Therefore, the linear stress constitutive equation for the incompressible flow can be written as

$$\tau = \mu(\nabla \mathbf{u} + (\nabla \mathbf{u})^T). \tag{1.38}$$

If μ is constant, divergence of the deviatoric stress is given by

$$\nabla \cdot \tau = \nabla \cdot (\nabla \mathbf{u} + (\nabla \mathbf{u})^T) = \mu \Delta \mathbf{u}. \tag{1.39}$$

Furthermore, if ρ is constant, the incompressible Navier-Stokes equation can be expressed as

$$\partial_t \mathbf{u} + (\mathbf{u} \cdot \nabla)\mathbf{u} - \nu \Delta \mathbf{u} = -\nabla \widetilde{p} + \widetilde{\mathbf{f}}, \tag{1.40}$$

where $\nu = \mu/\rho$, $\widetilde{p} = \overline{p}/\rho$, $\widetilde{\mathbf{f}} = \dfrac{1}{\rho}\mathbf{f}$.

1.3.3 Gas-liquid two phase flow

In electroless copper and nickel plating system, hydrogen gas generation is a crucial issue, especially in a microchannel, since the volume of gas is comparable to the size of the physical domain. Therefore, the governing equations for gas-liquid two phase flow should be considered.

doi:10.6342/NTU202200609

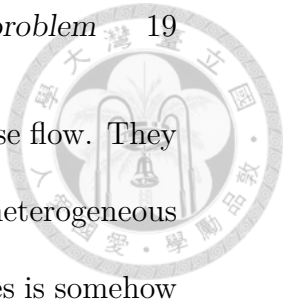

There are several versions of models describing the two phase flow. They can be roughly divided into two classes: (i) The interfaces of heterogeneous phases can be explicitly captured; (ii) The distribution of phases is somehow stochastic so that the problem can only be described in an average sense. For electroless plating process with gaseous phase generation, the problem at the beginning before a serious aggregation of bubbles is of class (ii). Once some large bubbles has accumulated in the microchannel, the problem becomes class (i) in a sense of approximation. Now we are in a position to introduce some governing equations in the aspect of these two classes.

Diffuse interface models

To formulate the thermodynamics and transport phenomena of multiphase systems, Reyleigh [15] and van der Waals [16] proposed a so-called diffuse interface model which assumes that the heterogeneous interfaces have a non-zero thickness. Based on this idea, several Navier-Stokes/Cahn-Hilliard system were proposed for modeling the multiphase flow [17, 18, 19]. For example, the *model H* for incompressible two phase flow proposed by Hohenberg

doi:10.6342/NTU202200609

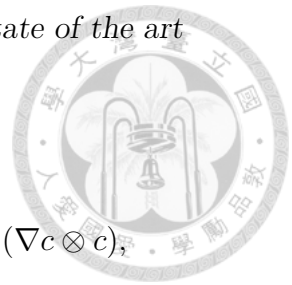

and Halperin [18] can be read as

$$\begin{aligned}
&\rho\partial_t\mathbf{u} + \rho(\mathbf{u}\cdot\nabla)\mathbf{u} - \nabla\cdot(\eta(c)(\nabla\mathbf{u} + (\nabla\mathbf{u})^T)) + \nabla p = \widehat{\sigma}\epsilon\nabla\cdot(\nabla c\otimes\nabla c),\\
&\nabla\cdot\mathbf{u} = 0,\\
&\partial_t c + \mathbf{u}\cdot\nabla c = \nabla\cdot(m\nabla\mu),\\
&\mu = \widehat{\sigma}\epsilon^{-1}\Psi'(c) - \widehat{\sigma}\epsilon\Delta c.
\end{aligned} \tag{1.41}$$

In the above, ρ is the density, $\mathbf{u}$ is the mean velocity of fluids, ρ is the pressure and c is an order parameter corresponding to the concnetration of the fluids (e.g. concentration of one component or concentration difference between two components), $\eta(c)$ is the viscosity of the mixture, $\widehat{\sigma}$ is the surface energy density ϵ is a parameter related to the thickness of the interface, Ψ is a homogeneous free energy density and μ is the chemical potential.

Another example proposed by Abels [17] is a thermodynaically consistent generalization of (1.41) to the case of non-matched densities based on a divergence-free velocity field $\mathbf{u}$. The governing equations can be expressed as

$$\begin{aligned}
&\partial_t(\rho\mathbf{u}) + \nabla\cdot(\rho\mathbf{u}\otimes\mathbf{u}) + \nabla\cdot(\mathbf{u}\otimes\frac{\widetilde{\rho}_1 - \widetilde{\rho}_2}{2}m(\varphi)\nabla\mu)\\
&- \nabla\cdot(\eta(\varphi)(\nabla\mathbf{u} + (\nabla\mathbf{u})^T) + \nabla p = -\widehat{\sigma}\epsilon\nabla\cdot(\nabla\varphi\otimes\nabla\varphi),\\
&\nabla\cdot\mathbf{u} = 0,\\
&\partial_t\varphi + \mathbf{u}\cdot\nabla\varphi = \nabla\cdot(m(\varphi)\nabla\mu)\\
&\mu = \widehat{\sigma}\epsilon^{-1}\Psi'(\varphi) - \widehat{\sigma}\epsilon\Delta\varphi,
\end{aligned} \tag{1.42}$$

where $\varphi = \varphi_2 - \varphi_1$ is the difference of the volume fracions and $\widetilde{\rho}_2 - \widetilde{\rho}_1$ is

doi:10.6342/NTU202200609

the difference of the densities. The above model has been widely used for numerical simulation (e.g. [20, 21, 22]).

Level set model

Unlike the diffuse interface model, the interface between two phases formulated by the level set model is sharp, i.e., the thickness of the interface between two phases is zero. In this case, the equation of motion for incompressible two phase flow is described by [23]

$$\begin{aligned} &\partial_t \mathbf{u} + (\mathbf{u}\cdot\nabla)\mathbf{u} = \frac{1}{\rho}\left(\nabla\cdot(\mu(\nabla\mathbf{u} + (\nabla\mathbf{u})^T)) - \nabla p + \sigma\kappa\delta(d)\mathbf{n}\right) + \widetilde{\mathbf{f}}, \\ &\nabla\cdot\mathbf{u} = 0, \end{aligned} \tag{1.43}$$

where $\mathbf{u} = \mathbf{u}(x,t)$ is the fluid velocity, $\rho = \rho(x,t)$ is the fluid density, $\mu = \mu(x,t)$ is the fluid viscosity, and $\widetilde{\mathbf{f}}$ is the body force. The surface tension is assumed to be a force exerting only on the interface. We denote by σ the surface tension, κ the curvature of the interface, d the normal distance to the interface, δ the Dirac delta function, and $\mathbf{n}$ the unit outward normal at the interface.

For immiscible fluids, the density and viscosity are constant along the path of velocity field. Therefore, we have

$$\begin{aligned} \partial_t\rho + (\mathbf{u}\cdot\nabla)\rho = 0 \\ \partial_t\mu + (\mathbf{u}\cdot\nabla)\mu = 0. \end{aligned} \tag{1.44}$$

Let ρ_1, μ_1 denote the density and viscosity of the gaseous phase fluid, respectively, and for liquid phase, ρ_2, μ_2. The level set ϕ is defined to discriminate

doi:10.6342/NTU202200609

the phases. For example, ϕ satisfies the following properties

$$\rho = \begin{cases} \rho_2, & \text{if } \phi > 0 \\ \rho_1, & \text{if } \phi < 0 \\ \dfrac{\rho_1 + \rho_2}{2}, & \text{if } \phi = 0 \end{cases} \tag{1.45}$$

and

$$\mu = \begin{cases} \mu_2, & \text{if } \phi > 0 \\ \mu_1, & \text{if } \phi < 0 \\ \dfrac{\mu_1 + \mu_2}{2}, & \text{if } \phi = 0. \end{cases} \tag{1.46}$$

Moreover, ϕ is carried by the velocity field

$$\partial_t \phi + (\mathbf{u} \cdot \nabla)\phi = 0. \tag{1.47}$$

If we initialize ϕ to be the signed distance function from the interface, ϕ is smooth, unlike ρ and μ. This shows the advantage to solve ϕ numerically.

To avoid the instability caused by the sharp changing of density and viscosity at the interface, a smoothing procedure on these two quantities is often applied to modify the governing equation, which leads to a similar idea as the diffuse interface model. Here is a common example of smoothing on the density: the density ρ can be smoothed by acting with a smoothed Heaviside function H_α defined by

$$H_\alpha(\phi) := \begin{cases} 1, & \text{if } \phi > \alpha, \\ 0, & \text{if } \phi < -\alpha, \\ \dfrac{1}{2}(1 + \dfrac{\phi}{\alpha} + \dfrac{1}{\pi}\sin(\dfrac{\pi\phi}{\alpha})), & \text{otherwise.} \end{cases} \tag{1.48}$$

doi:10.6342/NTU202200609

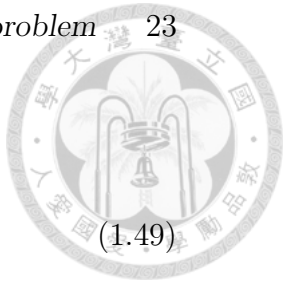

Now the smoothed density can be defined by

$$\rho(\phi) = \rho_2 H_\alpha(\phi) + \rho_1(1 - H_\alpha(\phi)). \tag{1.49}$$

It is worth noting that the smoothing in the diffuse interface model is by hypothesis but it is artificially made in the level set model.

Averaged two phase flow model

When the distribution of dispersive phases in a physical domain is stochastic, we may describe it in terms of the volume fraction of each phase at each point of the physical domain. The volume fraction of a phase can be regarded as the expectation that the phase occurs at a given point. This macroscopic aspect to the phase distribution is called volume averaging.

We review the derivation of volume averaging formulae introduced in [24, 25]. Let V_0 be an elementary volume to be observed in and V_k the volume in V_0 occupied by a single phase k and bounded by the interface A_k, which is assumed to be oriented. Let $\mathbf{n}_k$ be a outer normal to A_k and $\mathbf{w}_k$ the normal velocity of A_k.

The volume average of some quantity Ψ in phase k is

$$\langle \Psi \rangle_k = \frac{1}{V_0} \int_{V_0} \chi_k \Psi dx, \tag{1.50}$$

where χ_k is the indicator function that is 1 of V_k. The intrinsic volume average is defined by

$$\langle \Psi \rangle_k^{(k)} = \frac{1}{V_k} \langle \Psi \rangle_k \text{ where } V_k = \int_{V_0} \chi_k dx \tag{1.51}$$

doi:10.6342/NTU202200609

We define the volume fraction $r_k = \dfrac{V_k}{V_0}$ with the properties $\sum_k r_k = 1$ and

$$\langle \Psi \rangle_k = r_k \langle \Psi \rangle_k^{(k)}. \tag{1.52}$$

Some useful formulae in terms of the averaging are listed below[26, 27]:

$$\left\langle \frac{\partial \Psi}{\partial t} \right\rangle_k = \frac{\partial \langle \Psi \rangle_k}{\partial t} - \frac{1}{V_0} \int_{A_k} \Psi_k \mathbf{w}_k \cdot \mathbf{n}_k dA, \tag{1.53}$$

$$\langle \nabla \Psi \rangle_k = \nabla \langle \Psi \rangle_k + \frac{1}{V_0} \int_{A_k} \Psi_k \mathbf{n}_k dA. \tag{1.54}$$

If $\mathbf{\Psi}$ is a vector, we also have

$$\langle \nabla \cdot \mathbf{\Psi} \rangle_k = \nabla \cdot \langle \mathbf{\Psi} \rangle_k + \frac{1}{V_0} \int_{A_k} \mathbf{\Psi} \cdot \mathbf{n}_k dA. \tag{1.55}$$

Remark 1.3.2 If $\mathbf{\Psi} = 0$ outside V_k then we have

$$-\frac{1}{V_0} \int_{A_k} \mathbf{\Psi} \cdot \mathbf{n}_k dA = -\frac{1}{V_0} \int_{V_k} \nabla \cdot \mathbf{\Psi} dV = -\frac{1}{V_0} \int_{V_0} \chi_k \nabla \cdot \mathbf{\Psi} dV = -\langle \nabla \cdot \mathbf{\Psi} \rangle_k. \tag{1.56}$$

This implies that $\nabla \cdot \langle \mathbf{\Psi} \rangle_k = 0$.

By taking the volume averaging to (1.20), we have

$$\partial_t (r_k \rho_k) + \nabla \cdot (r_k \rho_k \langle \mathbf{u}_k \rangle_k^{(k)}) = \Gamma_k, \tag{1.57}$$

where

$$\Gamma_k = -\frac{1}{V_0} \int_{A_k} \rho_k (\mathbf{u}_k - \mathbf{w}_k) \cdot \mathbf{n}_k dA.$$

The interfacial terms Γ_k satisfy the conservation

$$\sum_k \Gamma_k = 0. \tag{1.58}$$

doi:10.6342/NTU202200609

For averaged equations of motion, we have

$$\partial_t(r_k\rho_k\langle\mathbf{u}_k\rangle_k^{(k)}) + \nabla\cdot(r_k\rho_k\langle\mathbf{u}_k\rangle_k^{(k)}\otimes\langle\mathbf{u}_k\rangle_k^{(k)}) = -\nabla(r_k\langle p_k\rangle_k^{(k)}) \\ + \nabla\cdot(\langle\boldsymbol{\tau}_k\rangle_k + \langle\boldsymbol{\tau}_k^T\rangle_k) + \mathbf{M}_k + r_k\langle\mathbf{f}_k\rangle_k^{(k)}, \tag{1.59}$$

where

$$\mathbf{M}_k = -\frac{1}{V_0}\int_{A_k}\rho_k\mathbf{u}_k(\mathbf{u}_k-\mathbf{w}_k)\cdot\mathbf{n}_k dA + \frac{1}{V_0}\int_{A_k}(\boldsymbol{\tau}_k - pI)\cdot\mathbf{n}_k dA$$

and

$$\langle\boldsymbol{\tau}_k^T\rangle = -\langle\rho_k\widehat{\mathbf{u}}_k\otimes\widehat{\mathbf{u}}_k\rangle, \quad \widehat{\mathbf{u}}_k = (\mathbf{u}_k - \langle\mathbf{u}_k\rangle_k^{(k)})\chi_k.$$

Since the sum of internal forces is zero, we have the interfacial balance condition

$$\sum_k \mathbf{M}_k + \mathbf{M}_i = 0. \tag{1.60}$$

In the above, $\mathbf{M}_i$ is the surfacial force such that

$$\mathbf{M}_i = \frac{1}{V_0}\int_{A_i}\sigma\kappa\mathbf{n}_i dA,$$

where A_i the collection of all the interfaces, σ the surface tension, κ the curvature, and $\mathbf{n}_i$ the outer normal on the interface.

Remark 1.3.3 If there are only two phases (say phase 1 and phase 2) in the physical domain of interest, then we have

$$\mathbf{M}_i = \frac{1}{V_0}\int_{A_i}\sigma\kappa n_1 dA = -\sigma\overline{\kappa}\nabla r_1, \tag{1.61}$$

where $\overline{\kappa}$ is the mean curvature. The above relation can be obtained by the constitutive relation

$$r_1 + r_2 = 1, \quad A_1 = A_2 = A_i \tag{1.62}$$

doi:10.6342/NTU202200609

1.3.4 Advection-diffusion in an electrolyte

The species transport is the core issue for studying the electroless plating process. We recall that for a concentration profile c_j of species j, the general mass conservation equation can be expressed as

$$\partial_t c_j + \nabla \cdot \mathbf{J}_j = R_j, \tag{1.63}$$

where $\mathbf{J}_j$ is the overall flux and R_j is the source or sink of c_j. If advection and diffusion are considered in the system, then there are two sources for J_j. First, the advective flux can be expressed as

$$\mathbf{J}_{j,adv} = \mathbf{u} c_j, \tag{1.64}$$

where $\mathbf{u}$ is the velocity field. Second, the diffusive flux can be approximated by the Fick's first law

$$\mathbf{J}_{j,diff} = -D_j \nabla c_j, \tag{1.65}$$

where D_j is the diffusion coefficient. Given that the total sum is the summation of these sources, we have

$$\mathbf{J}_j = \mathbf{J}_{j,adv} + \mathbf{J}_{j,diff} = \mathbf{u} c_j - D_j \nabla c_j. \tag{1.66}$$

Therefore, the advection-diffusion equation can be expressed as

$$\partial_t c_j + \nabla \cdot (\mathbf{u} c_j) - \nabla \cdot (D_j \nabla c_j) = R_j. \tag{1.67}$$

doi:10.6342/NTU202200609

Chapter 2

Single phase problem

2.1 Introduction

In this chapter, the mathematical analysis of the two or three-dimensional electroless plating problem neglecting the gas gneration is investigated. For numerical simulation, multi-dimensional electroless processes in geometrically varying micro- or nano-fluidic channels remain computationally expensive so we have investigated on bidimensional cases.

We consider a single chemical species in the electrolyte. The flux of the chemical species on the reacting surface is described in terms of the exchange current. In our case, the exchange current I_0 is given by the Butler-Volmer equation (see for example [13, 28]); it is a linear function of the electrolyte concentration c

$$I_0 = i_0 c := A\Big[\exp\left(\frac{\alpha_0 z F\xi}{R\theta}\right) - \exp\left(\frac{-\beta_0 z F\xi}{R\theta}\right)\Big]c, \tag{2.1}$$

doi:10.6342/NTU202200609

where A, α_0, β_0 are physical constants, R is the perfect gas constant, F the Faraday constant and z the atomic number of the electrolyte; θ is the temperature, and ξ is the excess potential related to the interaction with other chemical species which, for our purpose is constant [1, 14]. The temperature is also assumed uniform and constant.

The plating occurs on a boundary $S(t)$ of the electrolyte, causing this interface to move inward the fluid domain but this motion is small because it is only due to plating. The plating being proportional to the concentration c, the velocity of $S(t)$ is normal to itself and given by a linear law

$$\mathbf{u} = -\alpha i_0 c \mathbf{n}$$

and α is small. On the other hand the flux of metal ion through $S(t)$ is proportional to c

$$D\frac{\partial c}{\partial \mathbf{n}} = -i_0 c$$

where D is a diffusion constant.

The concentration of the chemical species c satisfies a convection diffusion equation while the electrolyte flow is modelled by the Navier-Stokes equations.

In order to analyse this coupled problem, we approximate the small displacement of the reaction surface $S(t)$ by a transpiration approximation [29, 30] on a fixed mean surface S. It leads to an integro-differential con-

doi:10.6342/NTU202200609

dition on S:

$$-D\frac{\partial c}{\partial n} + i_0 c\left(1 + \frac{\alpha i_0^2}{D}\int_0^t c(s)ds\right) = 0. \tag{2.2}$$

The mathematical analysis of the Navier-Stokes equations coupled with a convection-diffusion equation for c is somewhat problematic because of the non-homogenous condition on S for the velocity. So we restrict the study to the existence of the weak solution to the convection-diffusion equation with a given fluid velocity $\boldsymbol{u}$ and even this study is not straightforward. First a time-discretized approximation is shown to have a unique solution using a version of Minty-Browder's theorem and the maximum principle to prove that $0 \leq c \leq 1$. The solution of the time continuous problem is obtained as the weak limit of the of the solution of the time-discretized solutions. Some numerical tests are given to justify the transpiration approximation and the convergence of the backward Euler nonlinear scheme.

2.2 Modeling of the Physical System

The plating chemicals flow in a thin channel between a top and a bottom plate. Due to an electro-potential applied between the two plates the chemicals will deposit on the top plate. Hence the depth of the channel varies with time. A vertical cross section of the 3D system is depicted in Figure 2.1.

doi:10.6342/NTU202200609

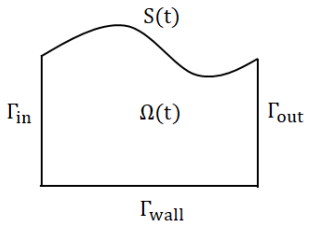

Figure 2.1: The physical domain is the domain occupied by the flow $\Omega(t)$; the chemical deposit is above the free boundary $S(t)$. The chemicals flow from the left boundary, Γ_{in}, to the right Γ_{out}. The bottom Γ_{wall} is a solid wall.

2.2.1 The Fluid Flow

The geometry of the fluid part is a two or three-dimensional domain $\Omega(t)$ bounded on the left by an inflow boundary Γ_{in}, on the right by an outflow boundary Γ_{out}, on the bottom by a flat wall Γ_{wall} and on the top by a time dependent boundary $S(t)$. In the three-dimensional case, the remaining boundaries are assumed to be walls. The fluid is viscous, Newtonian and incompressible, so the flow is governed by the Navier-Stokes equations for the velocity $\boldsymbol{u}(\mathbf{x}, t)$ and pressure $p(\mathbf{x}, t)$:

$$\partial_t \boldsymbol{u} + \boldsymbol{u} \cdot \nabla \boldsymbol{u} - \nu \Delta \boldsymbol{u} + \nabla p = 0, \qquad \nabla \cdot \boldsymbol{u} = 0, \ \forall \mathbf{x} \in \Omega(t), \ \forall t \in [0, T], \quad (2.3)$$

where ν is the (constant) kinematic viscosity of the fluid. The initial velocity is given and denoted by $\boldsymbol{u}_0$; the inflow velocity $\boldsymbol{u}_{in}$ is also given on Γ_{in}; a no slip condition holds on $\Gamma_{wall} \cup S(t)$, and we impose a traction-free outflow

doi:10.6342/NTU202200609

condition at Γ_{out}. So at all $t \in [0, T]$ we have:

$$\boldsymbol{u} = \boldsymbol{u}_{in} \text{ on } \Gamma_{in}, \quad \boldsymbol{u} = 0 \text{ on } \Gamma_{wall}, \quad -\nu \frac{\partial \boldsymbol{u}}{\partial n} + p\boldsymbol{n} = 0 \text{ on } \Gamma_{out}. \tag{2.4}$$

We assume that there is no back-flow on Γ_{out}: $\boldsymbol{u} \cdot \boldsymbol{n} \geq 0$.

Remark 2.2.1 In general, the traction-free boundary condition on Γ_{out}, $-\nu \frac{\partial \boldsymbol{u}}{\partial n} + p\boldsymbol{n} = 0$ does not imply $\boldsymbol{u} \cdot \boldsymbol{n} \geq 0$. However, for electroless plating process, the fluid velocity field near the outlet is near to a Poiseuille flow. We note that the Poiseuille flow in a fixed cross section domain satisfies $\boldsymbol{u} \cdot \boldsymbol{n} \geq 0$ on Γ_{out} and the traction-free condition. For mathematical convenience, the assumption: $\boldsymbol{u} \cdot \boldsymbol{n} \geq 0$ on Γ_{out} is made.

2.2.2 The Metal Ion Concentration

The metal ion concentration $c(\mathbf{x}, t)$ solves a convection-diffusion equation

$$\partial_t c + \boldsymbol{u} \cdot \nabla c - D\Delta c = 0, \quad \forall \mathbf{x} \in \Omega(t), \quad \forall t \in [0, T] \tag{2.5}$$

with given initial concentration c_0; D is the diffusion constant. The concentration is given on Γ_{in} and a no-flux condition holds on Γ_{wall} and Γ_{out} :

$$c = c_{in} \text{ on } \Gamma_{in}, \quad \frac{\partial c}{\partial n} = 0 \quad \text{on } \Gamma_{wall} \cup \Gamma_{out}. \tag{2.6}$$

On $S(t)$ a reaction condition is written as suggested in [1, 14],

$$-D\frac{\partial c}{\partial n} = i_0 c, \quad \boldsymbol{u} = -\alpha i_0 c \boldsymbol{n}, \quad \forall x \in S(t), \tag{2.7}$$

where i_0 and α are constants. Most important for our study: α is small.

doi:10.6342/NTU202200609

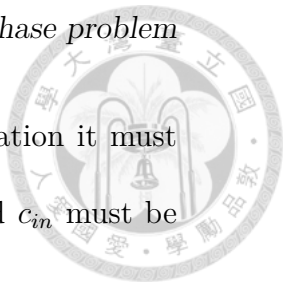

It is also important to remember that c, being a concentration it must be non-negative and less or equal to one. In particular c_0 and c_{in} must be chosen in $[0, 1]$.

2.2.3 The case $\alpha = 0$

When $\alpha = 0$, there is no free boundary; consider the case $\Omega = (0, L) \times (0, 1)$. With appropriate initial and inflow conditions, the fluid velocity is

$$\boldsymbol{u} = (u_1, u_2)^T, \quad u_1 = y(1-y), \quad u_2 = 0$$

Similarly, with appropriate initial and inflow conditions, the concentration depends only on time t and $y := x_2$ and solves

$$\partial_t c - D\partial_{yy} c = 0, \quad -D\partial_y c = i_0 c \text{ at } y = 1, \quad \partial_y c = 0 \text{ at } y = 0.$$

It has a closed solution $c = e^{-D\lambda^2 t}\cos(\lambda y)$ provided λ satisfies: $\lambda \tan \lambda = \frac{i_0}{D}$.

When $0 < \alpha << 1$,$\boldsymbol{u}_{in} = (y(1-y), 0)^T$, $c_{in} = e^{-D\lambda^2 t}\cos(\lambda y)$, $\boldsymbol{u}_0 = \boldsymbol{u}_{in}$, $c_0 = c_{in}|_{t=0}$, the solution will be a linear perturbation of the above.

2.2.4 Transpiration Approximation

Experimental observation show that the evolution of $S(t)$ is small. Following [29, 30], we approximate (2.7) with a transpiration approximation as follows.

Let S be the initial position of $S(t)$ and let η be the distance between $S(t)$ and S normally to S, i.e.

$$S(t) = \{\mathbf{x} + \eta(\mathbf{x}, t)\boldsymbol{n}(\mathbf{x}) \ : \ \mathbf{x} \in S\}, \qquad \eta(0) = 0$$

doi:10.6342/NTU202200609

where $\eta(0) = 0$ is short for $\eta(\mathbf{x}, 0) = 0$ for all $\mathbf{x} \in S$. If the radius of curvature of $S(t)$ and the derivative of η along S are not large it can be shown that the difference between the normals of S and $S(t)$ is second order in η (see [29]). By definition of $\boldsymbol{u}$ and by the second equation in (2.7),

$$\frac{d\eta}{dt} = \boldsymbol{u} \cdot \boldsymbol{n} = -\alpha i_0 c, \quad \eta(0) = 0, \quad \Rightarrow \quad \eta(t) = -\alpha i_0 \int_0^t c(s)ds. \tag{2.8}$$

By a Taylor expansion, the first equation in (2.7) can be written on S rather than $S(t)$:

$$\begin{aligned} &-D\frac{\partial c}{\partial n}(\mathbf{x} + \eta(\mathbf{x}, t)\boldsymbol{n}(\mathbf{x}), t) = -D\left(\frac{\partial c}{\partial n}(\mathbf{x}, t) + \eta(\mathbf{x}, t)\frac{\partial^2 c}{\partial n^2}(\mathbf{x}, t)\right) + o(\eta) \\ &= i_0 c(\mathbf{x} + \eta(\mathbf{x}, t)\boldsymbol{n}(\mathbf{x}), t) = i_0\left(c(\mathbf{x}, t) + \eta(\mathbf{x}, t)\frac{\partial c}{\partial n}(\mathbf{x}, t)\right) + o(\eta). \end{aligned} \tag{2.9}$$

By (2.8), it is rewritten as

$$-D\left(1 - \alpha\frac{i_0^2}{D}\int_0^t c(s)ds\right)\frac{\partial c}{\partial n}(\mathbf{x}, t) - i_0 c(\mathbf{x}, t) = \eta(\mathbf{x}, t)D\frac{\partial^2 c}{\partial n^2}(\mathbf{x}, t) + o(\eta) = O(\eta). \tag{2.10}$$

A first order in α approximation of this condition is

$$-D\frac{\partial c}{\partial n}(\mathbf{x}, t) - i_0 c(\mathbf{x}, t) = 0 \tag{2.11}$$

Neglecting $o(\eta)$ and using $\dfrac{1}{1-y} \approx 1 + y$ and neglecting $D\dfrac{\partial^2 c}{\partial n^2}$ leads to

$$D\frac{\partial c}{\partial n} + i_0 c\left(1 + \frac{\alpha i_0^2}{D}\int_0^t c(s)ds\right) = 0 \quad \text{on } S. \tag{2.12}$$

In the discussion below we argue in favor of this approximation where $\eta D\dfrac{\partial^2 c}{\partial n^2}$ is neglected.

doi:10.6342/NTU202200609

The second equation of (2.7) is simply written on S instead of $S(t)$. Indeed a similar Taylor expansion shows that

$$\boldsymbol{u} + \eta \frac{\partial \mathbf{u}}{\partial n} = -\alpha i_0 \left(c + \eta \frac{\partial c}{\partial n} \right) \mathbf{n} + o(\eta\alpha), \tag{2.13}$$

The second equation in (2.7) implies that $\mathbf{u}$ is $O(\alpha)$; so when all normal derivatives are bounded

$$\boldsymbol{u} = -\alpha i_0 c \mathbf{n} + O(\eta\alpha), \quad \text{on } S \tag{2.14}$$

2.2.5 The Final Problem (P)

The domain and the top boundary are now fixed and denoted by Ω and S; the boundary of Ω is

$$\Gamma := \partial\Omega = \Gamma_{in} \cup \Gamma_{wall} \cup \Gamma_{out} \cup S.$$

We propose to solve (2.3) and (2.5) in $\Omega \times (0, T)$ subject to initial conditions and boundary conditions (2.4) and (2.6) and

$$D \frac{\partial c}{\partial n} + \left(1 + \frac{\alpha i_0^2}{D} \int_0^t c(s) ds \right) i_0 c = 0 \quad \text{on } S, \tag{2.15}$$

$$\boldsymbol{u} = -\alpha i_0 c \boldsymbol{n} \quad \text{on } S. \tag{2.16}$$

2.2.6 Discussion:

If we had kept the term $\eta(\mathbf{x}, t) D \frac{\partial^2 c}{\partial n^2}(\mathbf{x}, t)$ in (2.12), this condition would have been second order. But even without it we expect it to be near second

doi:10.6342/NTU202200609

order when c varies slowly and Ω is elongated, because (2.5) will not be far from $-D\frac{\partial^2 c}{\partial \mathbf{n}^2} \approx 0$.

One of the purpose of this article is to analyse the additional nonlinear term in (2.15). In the numerical section , it will be compared to the first order condition obtained by setting $\alpha = 0$ in (2.15).

A third condition can be obtained as follows. If s denotes arc length on S, the PDE which governs c tells us that near S

$$\partial_t c + \boldsymbol{u} \cdot \boldsymbol{n} \frac{\partial c}{\partial n} = D\frac{\partial^2 c}{\partial n^2} + D\frac{\partial^2 c}{\partial s^2}$$

Assuming that the variations in s are much smaller than those in n, we obtain

$$D\frac{\partial^2 c}{\partial n^2} = \partial_t c - \alpha i_0 c \frac{\partial c}{\partial n} = \partial_t c + O(\alpha). \tag{2.17}$$

Inserting the above equation into (2.10), we get

$$-D\left(1 - \alpha\frac{i_0^2}{D}\int_0^t c(s)ds\right)\frac{\partial c}{\partial n}(\mathbf{x},t) - i_0 c(\mathbf{x},t) = -\left(\alpha i_0 \int_0^t c(s)ds\right)(\partial_t c + O(\alpha)). \tag{2.18}$$

As for getting (2.12), by a first order approximation ($\frac{1}{1-y} \approx 1 + y$) and a discard of the term of order $O(\alpha^2)$, leads to

$$D\frac{\partial c}{\partial n} + i_0 c + \alpha i_0 \left(\frac{i_0^2}{D}c - \partial_t c\right)\int_0^t c(s)ds = 0 \quad \text{on } S. \tag{2.19}$$

2.2.7 Plan

If it wasn't for the boundary conditions, the mathematical analysis of (2.3), (2.5,and (2.11),(2.16) is somewhat classical, so we shall focus on the problem

doi:10.6342/NTU202200609

raised by the nonlinear boundary conditions (2.3),(2.5,(2.15),(2.16). Then, at the end we shall argue that there is no essential new difficulty if the term $\partial_t c$ is added, namely problem (2.3),(2.5,(2.19),(2.16).

Once more, existence of c will be shown for a given flow $\boldsymbol{u}, p$. The coupled problem is analysed only in the numerical section.

2.3 Variational formulation

2.3.1 Notations

For convenience, C, $C^{'}$ and C_i, $i = 1, 2, 3, \ldots$, denote generic constants independent of $\boldsymbol{u}$ and $\boldsymbol{c}$. We denote $d = 2, 3$ the dimension.

We use the standard notations: $f^+ = \max\{f, 0\}$ and $f^- = -\min\{f, 0\}$.

We denote by $\|\cdot\|_s$ the norm of $H^s(\Omega)$ and by $\|\cdot\|_{s,\Gamma}$ the norm of $H^s(\Gamma)$ for $\Gamma \subset \partial\Omega$.

If B is a Banach space, $B^{'}$ denotes its dual space. The $L^2(\Omega)$ inner product is $(\cdot,\cdot)$ and the duality product between B and $B^{'}$ is $\langle\cdot,\cdot\rangle_{B,B'}$.

We define

$$W = \Big\{ w \in H^1(\Omega) : \quad w|_{\Gamma_{in}} = 0 \Big\};$$

since W is closed in $H^1(\Omega)$ and $H^1(\Omega)$ is a Hilbert space, then so is W.

We assume that $\boldsymbol{u} \in L^2(0, T; \boldsymbol{V}_{div}) \cap L^\infty(0, T; L^2(\Omega)^d)$ is given, where

$$\boldsymbol{V}_{div} := \{ \boldsymbol{v} \in H^1(\Omega)^d : \quad \nabla \cdot \boldsymbol{v} = 0 \}.$$

doi:10.6342/NTU202200609

In view of (2.16) with nonnegative concentration c and assuming that there is no back-flow on Γ_{out}, we make the following assumptions for $\boldsymbol{u}$:

$$\begin{aligned} &\text{(U1)} \qquad \boldsymbol{u}\cdot\boldsymbol{n} \le 0 \ \text{ on } S, \\ &\text{(U2)} \qquad \boldsymbol{u}\cdot\boldsymbol{n} \ge 0 \ \text{ on } \Gamma_{out}. \end{aligned} \tag{2.20}$$

In variational form (2.5), (2.6), (2.15) is: Let $w(x,t)$ be a sufficiently smooth function defined in $\Omega\times[0,T]$ and vanishing on Γ_{in}. Multiplying $w(x,t)$ with (2.5), integrating over Ω, and using (2.6), (2.15), (2.16), we have

$$\begin{aligned} &\int_\Omega(\partial_t c+\boldsymbol{u}\cdot\nabla c-D\Delta c)w dx \\ &=\int_\Omega(\partial_t c)w dx+\frac{1}{2}\int_\Omega(\boldsymbol{u}\cdot\nabla c)w dx-\frac{1}{2}\int_\Omega(\boldsymbol{u}\cdot\nabla w)c dx+\frac{1}{2}\int_{\partial\Omega}(\boldsymbol{u}\cdot\boldsymbol{n})cw \\ &+\int_\Omega D\nabla c\cdot\nabla w dx-\int_{\partial\Omega}D\frac{\partial c}{\partial n}w \\ &=\int_\Omega(\partial_t c)w dx+\frac{1}{2}\int_\Omega[(\boldsymbol{u}\cdot\nabla c)w-(\boldsymbol{u}\cdot\nabla w)c]dx+\int_\Omega D\nabla c\cdot\nabla w dx \\ &+\frac{1}{2}\int_{\Gamma_{out}}(\boldsymbol{u}\cdot\boldsymbol{n})cw+\int_S\left(1-\frac{\alpha c}{2}+\frac{\alpha i_0^2}{D}\int_0^t c(s)ds\right)i_0 cw. \end{aligned} \tag{2.21}$$

The resulting variational formulation reads:

Problem (P)

Given $c_0\in H^1(\Omega)$, $c_0(x)\in[0,1]$, $c_{in}\in H^{1/2}(\Gamma_{in})$, $c_{in}(x)\in[0,1]$, and $\boldsymbol{u}\in L^2(0,T;\boldsymbol{V}_{div})$ satisfying (U1), (U2), find $c\in L^2(0,T;H^1(\Omega))$ $\partial_t c\in L^2(0,T;W')$, such that, $c(0)=c_0$, $c|_{\Gamma_{in}}=c_{in}$ and, for all $w\in W$,

$$\begin{aligned} &\langle\partial_t c,w\rangle_{W',W}+\int_\Omega D\nabla c\cdot\nabla w dx+\frac{1}{2}\int_\Omega[(\boldsymbol{u}\cdot\nabla c)w-(\boldsymbol{u}\cdot\nabla w)c]dx \\ &\quad+\frac{1}{2}\int_{\Gamma_{out}}(\boldsymbol{u}\cdot\boldsymbol{n})cw+\int_S\left(1-\frac{\alpha c}{2}+\frac{\alpha i_0^2}{D}\int_0^t c(s)ds\right)i_0 cw=0. \end{aligned} \tag{2.22}$$

The following result, central to this chapter, shows existence of the concentration profile c when the velocity field $\boldsymbol{u}$, is known:

doi:10.6342/NTU202200609

Theorem 2.3.1 Given $c_0 \in H^1(\Omega)$, $c_0(x) \in [0,1]$, $c_{in} \in H^{1/2}(\Gamma_{in})$, $c_{in}(x) \in [0,1]$, and $\boldsymbol{u} \in L^2(0,T;\boldsymbol{V}_{div})$ satisfying (U1) and (U2), there exists a unique $c \in L^2(0,T;H^1(\Omega))$ with $\partial_t c \in L^2(0,T;W')$ such that

$$\begin{aligned}
&\int_0^T \langle \partial_t c, w\rangle_{W',W} dt + \frac{1}{2}\left(\int_0^T \int_\Omega [(\boldsymbol{u}\cdot\nabla c)w - (\boldsymbol{u}\cdot\nabla w)c] dx dt\right) \\
&+ D\int_0^T \int_\Omega \nabla c\cdot\nabla w dx dt + \int_0^T \int_S \left(1 - \frac{\alpha c}{2} + \frac{\alpha i_0^2}{D}\int_0^t c(s)ds\right) i_0 c w dt \\
&+ \int_0^T \int_S \frac{\alpha i_0^3}{D} c\left(\int_0^t c(s)ds\right) w dt + \frac{1}{2}\int_0^T \int_{\Gamma_{out}} (\boldsymbol{u}\cdot\boldsymbol{n}) c w dt \\
&= 0.
\end{aligned} \tag{2.23}$$

for all $w \in L^2(0,T;W)$, and $c(0) = c_0 \in H^1(\Omega)$, and $c|_{\Gamma_{in}} = c_{in} \in H^{1/2}(\Gamma_{in})$.

Remark 2.3.1 The existence and regularity of the coupled problem $\{\boldsymbol{u}, c\}$ will not be studied. Mostly because it would require minute and perhaps hard to obtain estimates due to the corners in the domain as in [31, 32, 33], the traction-free boundary condition, etc, but also because, $\boldsymbol{u}$ is merely weakly coupled with c only through the boundary condition on S. Furthermore, due to the numerical values of the physical constants, $\boldsymbol{u}$ is small on Γ_{in}. Therefore, we focus on the solution to the convection-diffusion equation (2.22), for which, as we shall see, the functional setting is not so simple.

2.3.2 Convexification

The term $c - \dfrac{\alpha c^2}{2}$ in the integral on S is problematic because it is not monotone so it makes the problem non-coercive. Indeed its primitive $\psi(c) := \dfrac{c^2}{2} - \dfrac{\alpha c^3}{6}$ is nonconvex beyond $c > \dfrac{1}{\alpha}$. But the physics require that $c \in [0,1]$

doi:10.6342/NTU202200609

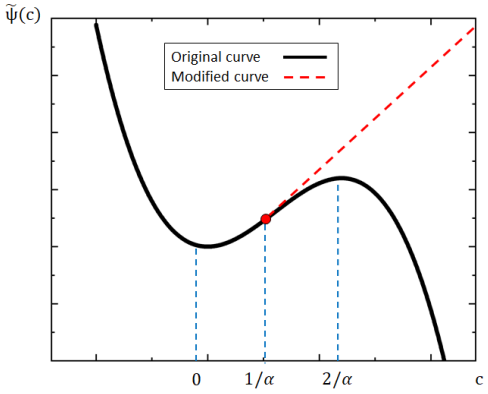

Figure 2.2: Graphic showing the modification of the nonconvex function $c \mapsto \frac{c^2}{2} - \frac{\alpha c^3}{6}$ into a convex one.

and the maximum principle will insure it. So any modification of ψ outside $(0,1)$ will not affect the solution; hence to work with a convex potential let us replace ψ by (see Figure 2.2).

$$\Psi(c) = \begin{cases} \frac{c^2}{2} - \frac{\alpha c^3}{6} & \text{if } \ c < \frac{1}{\alpha}, \\ \frac{c}{2\alpha} - \frac{1}{6\alpha^2} & \text{otherwise.} \end{cases} \tag{2.24}$$

Let ρ be any time dependent function defined on $[0,T]$. We define

$$(\phi(\rho))(t) = i_0 \dot{\Psi}(\rho(t)) + \frac{\alpha i_0^3}{D} \rho(t) \int_0^t |\rho(s)| ds, \quad t \in [0,T], \tag{2.25}$$

where $\dot{\Psi}(c)$ is the derivative of Ψ with respect to c:

$$\dot{\Psi}(c) = \begin{cases} c - \frac{\alpha c^2}{2} & \text{if } c < \frac{1}{\alpha}, \\ \frac{1}{2\alpha} & \text{otherwise.} \end{cases} \tag{2.26}$$

Naturally $\dot{\Psi}$ is monotone increasing. Note that Ψ is strictly convex and $\dot{\Psi}$ is strictly increasing in $[0, \frac{1}{\alpha}]$.

doi:10.6342/NTU202200609

The convexified variational formulation replacing (2.22) is

Problem (P_c)

Given $c_0 \in H^1(\Omega)$, $c_0(x) \in [0,1]$, $c_{in} \in H^{1/2}(\Gamma_{in})$, $c_{in}(x) \in [0,1]$, and $\boldsymbol{u} \in L^2(0,T;\boldsymbol{V}_{div})$ satisfying (U1), (U2), find $c \in L^2(0,T;H^1(\Omega))$ satisfying $c|_{\Gamma_{in}} = c_{in} \in H^{1/2}(\Gamma_{in})$, $\partial_t c \in L^2(0,T;W')$, $\phi(c) \in L^2(0,T;L^2(S))$, and

$$\begin{aligned}\langle \partial_t c, w\rangle_{W',W} + \int_\Omega D\nabla c\cdot\nabla w dx + \frac{1}{2}\int_\Omega [(\boldsymbol{u}\cdot\nabla c)w - (\boldsymbol{u}\cdot\nabla w)c]dx \\ + \frac{1}{2}\int_{\Gamma_{out}} (\boldsymbol{u}\cdot\boldsymbol{n})cw + \int_S \phi(c)w = 0, \quad \forall w \in W.\end{aligned} \tag{2.27}$$

Note that when $0 \le c \le 1$, then both c and $\phi(c) \in L^\infty(\Omega\times(0,T))$.

The proof of existence goes by steps. We assume that $\boldsymbol{u} \in L^2(0,T;\boldsymbol{V}_{div}) \cap L^\infty(0,T;L^2(\Omega)^d)$, so as to focus on the equation for c with $\boldsymbol{u}$ given. We will first discretize in time, show existence for the time discretized problem and then let the time step tend to zero.

2.4 Existence for the Time-discretized Problem

Let $N \in \mathbb{N}^+$ and let $\delta t = \dfrac{T}{N}$ be the time step.

Discrete velocity field $\boldsymbol{u}$

Since functions in a Bochner space $L^p(0,T;X)$ for all Banach space $(X, \|\cdot\|)$ can be approximated by step functions on a uniform discretization of $(0,T)$ (see for instance [34, 35]), we define $\boldsymbol{u}_\delta : (0,T] \to \boldsymbol{V}_{div}$ by

$$\boldsymbol{u}_\delta(t) = \sum_{m=0}^{N-1} \boldsymbol{u}^{m+1}\chi_{(m\delta t,(m+1)\delta t]}(t), \tag{2.28}$$

doi:10.6342/NTU202200609

where $\boldsymbol{u}^j = \frac{1}{\delta t}\int_{j\delta t}^{(j+1)\delta t} \boldsymbol{u}(s)ds$ for $j = 0, \dots N-1$. For convenience, we further define $\boldsymbol{u}^0 = \boldsymbol{u}(0) \in \boldsymbol{V}_{div}$. Obviously, $\boldsymbol{u}^j \in \boldsymbol{V}_{div}$ for all $0 \le j \le N$. To show that $\boldsymbol{u}_\delta$ converges to $\boldsymbol{u}$ strongly in $L^2(0,T;H^1(\Omega)^d)$, we need a lemma:

Lemma 2.4.1 Let $f \in L^2([a,b])$ for $a, b \in \mathbb{R}$, $a < b$, and $N > 0$ be an integer. Defining $\delta t = \frac{b-a}{N}$, we have

$$\delta t \sum_{j=0}^{N-1} \int_{a+j\delta t}^{a+(j+1)\delta t} \int_{a+j\delta t}^{a+(j+1)\delta t} \frac{|f(s)-f(t)|^2}{\delta t^2} dsdt \to 0, \quad \text{as } \delta t \to 0 \tag{2.29}$$

Proof. Given $\epsilon_1 > 0$, there exists $g \in C([a,b])$ such that

$$\int_a^b |f-g|^2 dt < \epsilon_1$$

We note that choice of g is independent to δt. With given g in hand, for every $\epsilon_2 > 0$, there exists $\delta > 0$ such that for every $s, t \in [a,b]$, we have

$$|g(s)-g(t)| < \epsilon_2, \quad \text{whenever } |s-t| < \delta.$$

Choosing $\delta t < \delta$, we have the estimate:

$$\begin{aligned}
&\sum_{j=0}^{N-1} \int_{a+j\delta t}^{a+(j+1)\delta t} \int_{a+j\delta t}^{a+(j+1)\delta t} |f(s)-f(t)|^2 dsdt \\
&\le 3\sum_{j=0}^{N-1} \int_{a+j\delta t}^{a+(j+1)\delta t} \int_{a+j\delta t}^{a+(j+1)\delta t} (|f(s)-g(s)|^2 + |g(s)-g(t)|^2 + |f(t)-g(t)|^2) dsdt \\
&\le 6\sum_{j=0}^{N} \delta t \left(\int_{a+j\delta t}^{a+(j+1)\delta t} \int_{a+j\delta t}^{a+(j+1)\delta t} |f(s)-g(s)|^2 ds \right) + 3\sum_{j=0}^{N-1} \int_{a+j\delta t}^{a+(j+1)\delta t} \int_{a+j\delta t}^{a+(j+1)\delta t} |g(s)-g(t)|^2 dsdt \\
&\le 6\delta t\epsilon_1 + 3(b-a)\delta t\epsilon_2
\end{aligned} \tag{2.30}$$

Therefore,

$$\delta t \sum_{j=0}^{N-1} \int_{a+j\delta t}^{a+(j+1)\delta t} \int_{a+j\delta t}^{a+(j+1)\delta t} \frac{|f(s)-f(t)|^2}{\delta t^2} dsdt \le 6\epsilon_1 + 3(b-a)\epsilon_2. \tag{2.31}$$

doi:10.6342/NTU202200609

By the arbitrariness of ϵ_1 and ϵ_2, the proof is completed. Q.E.D.

Proposition 2.4.1 Let $\boldsymbol{u}_\delta$ be defined by (2.28), we have the following:

$$\|\boldsymbol{u} - \boldsymbol{u}_\delta\|_{L^2(0,T;H^1(\Omega))} \to 0 \quad \text{as } \delta t \to 0. \tag{2.32}$$

Proof.

$$\begin{aligned}
&\int_0^T \|\boldsymbol{u}_\delta(t) - \boldsymbol{u}(t)\|_1^2 dt \\
&= \sum_{j=0}^{N-1} \int_{j\delta t}^{(j+1)\delta t} \|\boldsymbol{u}^{j+1} - \boldsymbol{u}(t)\|_1^2 dt \\
&= \sum_{j=0}^{N-1} \int_{j\delta t}^{(j+1)\delta t} \left\| \frac{1}{\delta t} \int_{j\delta t}^{(j+1)\delta t} (\boldsymbol{u}(s) - \boldsymbol{u}(t)) ds \right\|_1^2 dt \\
&\leq \sum_{j=0}^{N-1} \int_{j\delta t}^{(j+1)\delta t} \left(\frac{1}{\delta t} \int_{j\delta t}^{(j+1)\delta t} \|\boldsymbol{u}(s) - \boldsymbol{u}(t)\|_1^2 ds \right) dt \\
&= \delta t \sum_{j=0}^{N-1} \int_{j\delta t}^{(j+1)\delta t} \int_{j\delta t}^{(j+1)\delta t} \frac{\|\boldsymbol{u}(s) - \boldsymbol{u}(t)\|_1^2}{\delta t^2} ds dt
\end{aligned} \tag{2.33}$$

Defining the function $f : [0, T] \to \mathbb{R}$ by $s \mapsto \|\boldsymbol{u}(s)\|_1^2$ and applying Lemma 2.4.1, the proof is completed. Q.E.D.

We observe that $\boldsymbol{u}_\delta$ is strongly convergent to $\boldsymbol{u}$ in $L^2(0, T; H^1(\Omega)^d)$. Thus,

Corollary 2.4.1 There exists a constant C depending only on $\Omega, T, \boldsymbol{u}$ so that

$$\|\boldsymbol{u}_\delta\|_{L^2(0,T;H^1(\Omega)^d)} \leq C \quad \forall \delta t \geq 0. \tag{2.34}$$

Problem (P_c^m)

For each integer $m \in (0, N-1)$, given $c^m \in H^1(\Omega)$, and $\boldsymbol{u}^{m+1} = \boldsymbol{u}_\delta((m+$

doi:10.6342/NTU202200609

1)δt) satisfying (U1), (U2), find $c^{m+1} \in H^1(\Omega)$ such that for all $w \in W$,

$$\begin{aligned} &\int_\Omega \frac{c^{m+1}-c^m}{\delta t} w dx + D\int_\Omega \nabla c^{m+1}\cdot\nabla w dx \\ &+ \frac{1}{2}\int_\Omega [(\boldsymbol{u}^{m+1}\cdot\nabla c^{m+1})w - (\boldsymbol{u}^{m+1}\cdot\nabla w)c^{m+1}]dx \\ &+ \int_S \phi_m(c^{m+1})w + \frac{1}{2}\int_{\Gamma_{out}} (\boldsymbol{u}^{m+1}\cdot\boldsymbol{n})c^{m+1}w = 0 \end{aligned} \tag{2.35}$$

with $c^{m+1}|_{\Gamma_{in}} = c_{in} \in H^{1/2}(\Gamma_{out})$, where $\phi_m(c^{m+1})$ is the following time approximation of $\phi(c)$,

$$\phi_m(c^{m+1}) = i_0\dot{\Psi}(c^{m+1}) + \frac{\alpha i_0^3}{D}\left(\sum_{j=0}^{m} c^j \delta t\right) c^{m+1}.$$

The boundary condition is given by $c|_{\Gamma_{in}} = c_{in} \in H^{1/2}(\Gamma_{in})$, $0 \le c_{in} \le 1$. The initial value is $c^0 = c_0$ with $c_0 \in H^1(\Omega)$, $c_0|_{\Gamma_{in}} = c_{in} \in H^{1/2}(\Gamma_{in})$, $0 \le c_0 \le 1$.

2.4.1 Existence of the Solution to the Time-discretized Problem (P_c^m)

To prove the existence, the Minty-Browder Theorem (see Theorem 9.14.1 in [36] and a series of works by Minty and Browder[37, 38, 39]) will be used.

Theorem 2.4.1 (Minty-Browder) Let B be a reflexive Banach space and $\|\cdot\|$ its norm. Let $A : B \to B'$ a continuous mapping such that

(i) $\langle Au - Av, u - v\rangle > 0 \ \ \forall u, v \in B, \ \ u \neq v$

(ii) $\lim_{\|u\|\to\infty} \|u\|^{-1}\langle Au, u\rangle = +\infty.$

Then, for any $b \in B'$, there is a unique u such that $Au = b$.

doi:10.6342/NTU202200609

Remark 2.4.1 The continuity of A in Theorem 2.4.1 can be generalized to hemicontinuity, or demicontinuity.

The theorem will be applied to $c^m - \widetilde{c}_{in}$ where $\widetilde{c}_{in} \in H^1(\Omega)$ is a lift of the boundary conditions defined as the unique solution of

$$\int_\Omega D\nabla\widetilde{c}_{in} \cdot \nabla w dx = 0, \quad \forall w \in W \tag{2.36}$$

such that $\widetilde{c}_{in} = c_{in}$ on Γ_{in}. With $c_{in} \in H^{1/2}(\Gamma_{in})$, the existence and uniqueness of $\widetilde{c}_{in}$ can be guaranteed (see Section 7 in [40]).

Lemma 2.4.2 If $0 \le c_{in} \le 1$, then $\widetilde{c}_{in}$ satisfies $0 \le \widetilde{c}_{in} \le 1$ a.e.

Proof. The argument is classical; let us recall it for the reader's convenience. Note that $(\widetilde{c}_{in} - 1)^+$ and $(\widetilde{c}_{in})^-$ belong to W. Choosing $w = (\widetilde{c}_{in})^-$ in (2.36), gives $\|\nabla(\widetilde{c}_{in})^-\|_0^2 = 0$. Hence $(\widetilde{c}_{in})^- = 0$ i.e. $\widetilde{c}_{in} \ge 0$.

Now choosing $w = (\widetilde{c}_{in} - 1)^+$ in (2.36) implies $\|\nabla(\widetilde{c}_{in} - 1)^+\|_0^2 = 0$. Hence $(\widetilde{c}_{in} - 1)^+ = 0$, i.e. $\widetilde{c}_{in} \le 1$ a.e. in Ω. Q.E.D.

Proposition 2.4.2 Let $m \ge 0$. If $0 \le c^j \le 1$ a.e. in Ω, $c^j \in H^1(\Omega)$ for all $j \le m$, then $c^{m+1} \in H^1(\Omega)$ and $0 \le c^{m+1} \le 1$ a.e. in Ω.

Proof. Letting $w = (c^{m+1})^-$ in (2.35), gives

$$\begin{aligned} &-\frac{1}{\delta t}\|(c^{m+1})^-\|_0^2 - D\|\nabla(c^{m+1})^-\|_0^2 - \frac{1}{2}\int_{\Gamma_{out}} (\boldsymbol{u}^{m+1} \cdot \boldsymbol{n})(c^{m+1})^{-2} \\ &+ \int_S i_0 \dot{\Psi}(c^{m+1})(c^{m+1})^- - \frac{\alpha i_0^3}{D}\sum_{j=0}^{m} c^j \delta t (c^{m+1})^{-2} = \frac{1}{\delta t}\int_\Omega c^m (c^{m+1})^- \ge 0 \end{aligned} \tag{2.37}$$

All terms on the left are obviously negative except $\dot{\Psi}(c^{m+1})(c^{m+1})^-$. Two cases: if $c \ge \frac{1}{\alpha}$ then $c^- = 0$ and $\dot{\Psi}(c)c^- = 0$; if $c < \frac{1}{\alpha}$ then $\dot{\Psi}(c)c^- =$

doi:10.6342/NTU202200609

$(c-\frac{\alpha}{2}c^2)c^- = -(c^-)^2 - \frac{\alpha}{2}c^2c^- \le 0$. Hence $\dot{\Psi}(c^{m+1})(c^{m+1})^- \le 0$ always; thus (2.37) leads to $\|(c^{m+1})^-\|_0^2 = 0$.

Define $\overline{c}^{m+1} = c^{m+1} - 1$. It satisfies

$$\begin{aligned}
&\int_\Omega \frac{\overline{c}^{m+1}-\overline{c}^m}{\delta t}w + \int_\Omega D\nabla\overline{c}^{m+1}\cdot\nabla w dx \\
&+ \frac{1}{2}\int_\Omega [(\boldsymbol{u}^{m+1}\cdot\nabla\overline{c}^{m+1})w - (\boldsymbol{u}^{m+1}\cdot\nabla w)\overline{c}^{m+1}]dx \\
&- \frac{1}{2}\int_{S\cup\Gamma_{out}}(\boldsymbol{u}^{m+1}\cdot\boldsymbol{n})w + \int_S i_0\dot{\Psi}(c^{m+1})w + \int_S \frac{\alpha i_0^3}{D}\sum_{j=0}^m c^j\delta t c^{m+1}w \\
&+ \frac{1}{2}\int_{\Gamma_{out}}(\boldsymbol{u}^{m+1}\cdot\boldsymbol{n})(\overline{c}^{m+1}+1)w = 0
\end{aligned} \tag{2.38}$$

Testing with $w = (\overline{c}^{m+1})^+$, gives

$$\begin{aligned}
&\frac{1}{\delta t}\|(\overline{c}^{m+1})^+\|_0^2 - \frac{1}{\delta t}\int_\Omega \overline{c}^m(\overline{c}^{m+1})^+ + D\|\nabla(\overline{c}^{m+1})^+\|_0^2 - \frac{1}{2}\int_S(\boldsymbol{u}^{m+1}\cdot\boldsymbol{n})(\overline{c}^{m+1})^+ \\
&\int_S i_0\dot{\Psi}(c^{m+1})(\overline{c}^{m+1})^+ + \frac{\alpha i_0^3}{D}\int_S\sum_{j=0}^m c^j\delta t c^{m+1}(\overline{c}^{m+1})^+ \\
&+ \frac{1}{2}\int_{\Gamma_{out}}(\boldsymbol{u}^{m+1}\cdot\boldsymbol{n})((\overline{c}^{m+1})^+ + 1)(\overline{c}^{m+1})^+ = 0.
\end{aligned} \tag{2.39}$$

By the induction hypothesis, $\overline{c}^m$ is negative; observe that $\boldsymbol{u}^{m+1}\cdot\boldsymbol{n} \le 0$ on S by (U1), $\boldsymbol{u}^{m+1}\cdot\boldsymbol{n} \ge 0$ on Γ_{out} by (U2) and $\dot{\Psi}(c^{m+1}) \ge 0$ because $c^{m+1} \ge 0$. So we have that $\|(\overline{c}^{m+1})^+\|_0^2 = 0$. Q.E.D.

Let us define.

$$\widetilde{c}^m := c^m - \widetilde{c}_{in} \in W, \quad m = 0, 1, \ldots, N.$$

Remark 2.4.2 As $\widetilde{c}^m \in [-1, 1]$ and $\dot{\Psi}(c^m) \in [0, 1]$, therefore $|\dot{\Psi}(c^m)\widetilde{c}^m| \le 1$.

doi:10.6342/NTU202200609

By construction, (2.35), which defines Problem P_c^m, can be rewritten as

Problem ($\widetilde{P}_c^m$)

For each integer $m \in (0, N-1)$, given $\widetilde{c}^m \in H^1(\Omega)$, $\widetilde{c}_{in} \in H^1(\Omega)$, $\widetilde{c}_{in}(x) \in [0,1]$, and $\boldsymbol{u}^{m+1} = \boldsymbol{u}_\delta((m+1)\delta t)$ satisfying (U1), (U2), find $\widetilde{c}^{m+1} \in W$ such that for all $w \in W$,

$$\begin{aligned}
&\frac{1}{\delta t}\int_\Omega \widetilde{c}^{m+1} w dx + \frac{1}{2}\int_\Omega [(\boldsymbol{u}^{m+1}\cdot\nabla\widetilde{c}^{m+1})w - (\boldsymbol{u}^{m+1}\cdot\nabla w)\widetilde{c}^{m+1}]dx \\
&+ D\int_\Omega \nabla\widetilde{c}^{m+1}\cdot\nabla w dx + \int_S \phi_m(c^{m+1})w + \frac{1}{2}\int_{\Gamma_{out}}(\boldsymbol{u}^{m+1}\cdot\boldsymbol{n})\widetilde{c}^{m+1}w \\
&= -\frac{1}{2}\int_\Omega [(\boldsymbol{u}^{m+1}\cdot\nabla\widetilde{c}_{in})w - (\boldsymbol{u}^{m+1}\cdot\nabla w)\widetilde{c}_{in}]dx + \frac{1}{\delta t}\int_\Omega \widetilde{c}^m w dx - \frac{1}{2}\int_{\Gamma_{out}}(\boldsymbol{u}^{m+1}\cdot\mathbf{n})\widetilde{c}_{in}w
\end{aligned} \tag{2.40}$$

Now define the mapping $A : W \to W'$ by

$$\begin{aligned}
\langle A\rho, w\rangle &= \frac{1}{\delta t}\int_\Omega \rho w dx + \frac{1}{2}\int_\Omega [(\boldsymbol{u}^{m+1}\cdot\nabla\rho)w - (\boldsymbol{u}^{m+1}\cdot\nabla w)\rho]dx \\
&+D\int_\Omega \nabla\rho\cdot\nabla w dx + \int_S \phi_m(\rho+\widetilde{c}_{in})w + \frac{1}{2}\int_{\Gamma_{out}}(\boldsymbol{u}^{m+1}\cdot\boldsymbol{n})\rho w
\end{aligned} \tag{2.41}$$

Since W is closed in $H^1(\Omega)$ and $H^1(\Omega)$ is a Hilbert space, then so is W.

Lemma 2.4.3 Let $m \geq 0$. We suppose that $c_j \in H^1(\Omega)$ for all $j \leq m$, then $A : W \to W'$ defined by (2.41) is locally Lipschitz continuous.

The proof is fairly straightforward but long, so it is postponed to Appendix A so as not to break the thread of the proof of existence of ($\widetilde{P}_c^m$). From the definition of A by (2.41), there is no essential difficulty to arrive, via a sequence of inequalities, at

$$\begin{aligned}
&|\langle A\rho_1 - A\rho_2, w\rangle| \\
&\leq \left(C_1 + C_2\|\boldsymbol{u}^{m+1}\|_1 + C_3(\|\rho_1\|_1 + \|\rho_2\|_1) + C_4\delta t\sum_{j=0}^m \|c^j\|_1\right)\|\rho_1-\rho_2\|_1\|w\|_1,
\end{aligned} \tag{2.42}$$

doi:10.6342/NTU202200609

Lemma 2.4.4 Let $\rho_1, \rho_2, \rho \in W$ and $m \geq 0$. We suppose that $0 \leq c^j \leq 1$ a.e. in Ω for all $j \leq m$. $A : W \to W'$ defined by (2.41) satisfies

(i) $\langle A\rho_1 - A\rho_2, \rho_1 - \rho_2 \rangle > 0$ if $\rho_1 \neq \rho_2$

(ii) $\lim_{\|\rho\|_1 \to +\infty} \|\rho\|_1^{-1} \langle A\rho, \rho \rangle = +\infty$.

Proof. To show (i), we use (2.41) with $\rho_1, \rho_2 \in W$,

$$\begin{aligned}
&\langle A\rho_1 - A\rho_2, w \rangle = \frac{1}{\delta t} \int_\Omega (\rho_1 - \rho_2) w dx \\
&+ \frac{1}{2} \int_\Omega [(\boldsymbol{u}^{m+1} \cdot \nabla(\rho_1 - \rho_2))w - (\boldsymbol{u}^{m+1} \cdot \nabla w)(\rho_1 - \rho_2)] dx + D \int_\Omega \nabla(\rho_1 - \rho_2) \cdot \nabla w dx \\
&+ \int_S (\phi_m(\rho_1 + \widetilde{c}_{in}) - \phi_m(\rho_2 + \widetilde{c}_{in}))w + \frac{1}{2} \int_{\Gamma_{out}} (\boldsymbol{u}^{m+1} \cdot \boldsymbol{n})(\rho_1 - \rho_2) w.
\end{aligned} \tag{2.43}$$

By the definition of ϕ_m, c^j are given for $j \leq m$ irrespectively of ρ. Let $w = \rho_1 - \rho_2$ in the above equation, one obtain

$$\begin{aligned}
&\langle A\rho_1 - A\rho_2, \rho_1 - \rho_2 \rangle = \\
&\int_\Omega \frac{1}{\delta t} (\rho_1 - \rho_2)^2 dx + D \int_\Omega |\nabla(\rho_1 - \rho_2)|^2 dx + \frac{1}{2} \int_{\Gamma_{out}} (\boldsymbol{u}^{m+1} \cdot \boldsymbol{n})(\rho_1 - \rho_2)^2 \\
&\int_S \frac{\alpha i_0^3}{D} \sum_{j=0}^{m} c^j \delta t (\rho_1 - \rho_2)^2 + \int_S (\dot{\Psi}(\rho_1 + \widetilde{c}_{in}) - \dot{\Psi}(\rho_2 + \widetilde{c}_{in}))(\rho_1 - \rho_2).
\end{aligned} \tag{2.44}$$

Recall that $\boldsymbol{u}^{m+1} \cdot \boldsymbol{n} \geq 0$ on Γ_{out}. All the terms on the right are obviously positive, except the last one. Without loss of generality, we assume that $\rho_2 > \rho_1$; we know that $\dot{\Psi}$ is strictly increasing. That is, $\dot{\Psi}(\rho_2 + \widetilde{c}_{in}) > \dot{\Psi}(\rho_1 + \widetilde{c}_{in})$. Hence $(\dot{\Psi}(\rho_2 + \widetilde{c}_{in}) - \dot{\Psi}(\rho_1 + \widetilde{c}_{in}))(\rho_2 - \rho_1) > 0$. Hence

$$\langle A\rho_1 - A\rho_2, \rho_1 - \rho_2 \rangle > \frac{1}{\delta t} \|\rho_1 - \rho_2\|_0^2 + D \|\nabla(\rho_1 - \rho_2)\|_0^2.$$

Finally (ii) can be proved by taking $\rho_1 = 0$ in (i). Q.E.D.

doi:10.6342/NTU202200609

By Theorem 2.4.1 and Lemmas 2.4.3, 2.4.4, we have

Corollary 2.4.2 There exists a unique solution to Problem $(\widetilde{P}_c^m)$ and hence also to (P_c^m) defined by (2.35).

2.5 Stability of the Time-discretized Problem

$$P_c^m$$

Proposition 2.5.1 Let $\widetilde{c}^{m+1}$ be the solution of (2.40) for each integer $m \in (0, N-1)$ with given $\widetilde{c}^j \in H^1(\Omega)$, $\widetilde{c}^j(x) \in [-1,1]$ for $j = 0, \ldots, m$, $\widetilde{c}_{in} \in H^1(\Omega)$, $\widetilde{c}_{in}(x) \in [0,1]$, and $\boldsymbol{u}^{m+1} \in H^1(\Omega)^d$ satisfying (U1), (U2). We have

$$\begin{aligned} \|\widetilde{c}^{m+1}\|_0^2 + \quad & \|\widetilde{c}^{m+1} - \widetilde{c}^m\|_0^2 + D\delta t \|\nabla \widetilde{c}^{m+1}\|_0^2 + \delta t \int_{\Gamma_{out}} (\boldsymbol{u}^{m+1} \cdot \boldsymbol{n})(\widetilde{c}^{m+1})^2 \\ & \le \|\widetilde{c}^m\|_0^2 + C_1 \delta t + C_2 \delta t \|\boldsymbol{u}^{m+1}\|_1^2 + C_3 \delta t \|\nabla \widetilde{c}_{in}\|_0^2 \end{aligned} \tag{2.45}$$

Proof. By (2.40) with $w = \widetilde{c}^{m+1}$ we have

$$\begin{aligned} & \frac{1}{2\delta t}\|\widetilde{c}^{m+1}\|_0^2 + \frac{1}{2\delta t}\|\widetilde{c}^{m+1} - \widetilde{c}^m\|_0^2 + D\|\nabla \widetilde{c}^{m+1}\|_0^2 + \frac{1}{2}\int_{\Gamma_{out}} (\boldsymbol{u}^{m+1} \cdot \boldsymbol{n})(\widetilde{c}^{m+1})^2 \\ & = -\int_S i_0 \dot{\Psi}(c^{m+1})\widetilde{c}^{m+1} - \int_S \frac{\alpha i_0^3}{D} \sum_{j=0}^{m} c^j \delta t c^{m+1} \widetilde{c}^{m+1} - \frac{1}{2}\int_{\Gamma_{out}} (\boldsymbol{u}^{m+1} \cdot \boldsymbol{n}) \widetilde{c}_{in} \widetilde{c}^{m+1} \\ & - \frac{1}{2}\int_\Omega (\boldsymbol{u}^{m+1} \cdot \nabla \widetilde{c}^{m+1}) \widetilde{c}_{in} dx + \frac{1}{2}\int_\Omega (\boldsymbol{u}^{m+1} \cdot \nabla \widetilde{c}_{in}) \widetilde{c}^{m+1} dx + \frac{1}{2\delta t}\|\widetilde{c}^m\|_0^2 \end{aligned} \tag{2.46}$$

doi:10.6342/NTU202200609

We estimate each term of the right hand side

$$
\begin{aligned}
&-\int_S i_0\dot{\Psi}(c^{m+1})\widetilde{c}^{m+1} \le i_0\int_S|\dot{\Psi}(c^{m+1})\widetilde{c}^{m+1}| \le i_0|S|.\\
&-\int_S \frac{\alpha i_0^3}{D}\left(\sum_{j=0}^m c^j\delta t\right)c^{m+1}\widetilde{c}^{m+1} \le \frac{\alpha i_0^3}{D}\int_S\left(\sum_{j=0}^m c^j\delta t\right)c^{m+1}|\widetilde{c}^{m+1}| \le \frac{\alpha i_0^3}{D}\int_S m\delta t \le \frac{\alpha i_0^3 T}{D}|S|.\\
&-\int_{\Gamma_{out}}(\boldsymbol{u}^{m+1}\cdot\boldsymbol{n})\widetilde{c}_{in}\widetilde{c}^{m+1} \le |\Gamma_{out}|^{\frac{1}{2}}\left(\int_{\Gamma_{out}}|\boldsymbol{u}^{m+1}|^2\right)^{\frac{1}{2}} \le C\|\boldsymbol{u}^{m+1}\|_1^2.\\
&-\int_\Omega(\boldsymbol{u}^{m+1}\cdot\nabla\widetilde{c}^{m+1})\widetilde{c}_{in}dx \le \int_\Omega|\boldsymbol{u}^{m+1}\cdot\nabla\widetilde{c}^{m+1}|dx \le \frac{1}{2D}\|\boldsymbol{u}^{m+1}\|_0^2+\frac{D}{2}\|\nabla\widetilde{c}^{m+1}\|_0^2.\\
&\int_\Omega(\boldsymbol{u}^{m+1}\cdot\nabla\widetilde{c}_{in})\widetilde{c}^{m+1}dx \le \int_\Omega|\boldsymbol{u}^{m+1}\cdot\nabla\widetilde{c}_{in}|dx \le \frac{1}{2D}\|\boldsymbol{u}^{m+1}\|_0^2+\frac{D}{2}\|\nabla\widetilde{c}_{in}\|_0^2.
\end{aligned}
$$

Collecting all terms leads to

$$
\begin{aligned}
&\frac{1}{2\delta t}\|\widetilde{c}^{m+1}\|_0^2+\frac{1}{2\delta t}\|\widetilde{c}^{m+1}-\widetilde{c}^m\|_0^2+\frac{D}{2}\|\nabla\widetilde{c}^{m+1}\|_0^2+\frac{1}{2}\int_{\Gamma_{out}}(\boldsymbol{u}^{m+1}\cdot\boldsymbol{n})(\widetilde{c}^{m+1})^2\\
&\qquad\le \frac{1}{2\delta t}\|\widetilde{c}^m\|^2+C_1+C_2\|\boldsymbol{u}^{m+1}\|_1^2+C_3\|\nabla\widetilde{c}_{in}\|_0^2
\end{aligned}
\tag{2.47}
$$

Multiplying both sides by $2\delta t$ completes the proof. Q.E.D.

Summing (2.45) from 0 to m, leasds to the following:

Corollary 2.5.1 Let $\boldsymbol{u}^{j+1}\in H^1(\Omega)^d$ be given satisfying (U1), (U2) for all $j=0,\dots,N-1$. If $\widetilde{c}^0\in H^1(\Omega)$, $\widetilde{c}^0(x)\in[-1,1]$, $\widetilde{c}_{in}\in H^1(\Omega)$, $\widetilde{c}_{in}(x)\in[0,1]$, then (2.40) implies that

$$
\begin{aligned}
&\|\widetilde{c}^{m+1}\|_0^2+\sum_{j=0}^m\|\widetilde{c}^{j+1}-\widetilde{c}^j\|_0^2+D\delta t\sum_{j=0}^m\|\nabla\widetilde{c}^{j+1}\|_0^2+\sum_{j=0}^m\delta t\int_{\Gamma_{out}}(\boldsymbol{u}^{j+1}\cdot\boldsymbol{n})(\widetilde{c}^{j+1})^2\\
&\qquad\le \|\widetilde{c}^0\|_0^2+C_1T+C_2\delta t\sum_{j=0}^m\|\boldsymbol{u}^{j+1}\|_1^2+C_3T\|\nabla\widetilde{c}_{in}\|_0^2.
\end{aligned}
\tag{2.48}
$$

Proposition 2.5.2 Let $\boldsymbol{u}^{j+1}\in H^1(\Omega)^d$ be given satisfying (U1), (U2) for all $j=0,\dots,N-1$. If $\widetilde{c}^0\in H^1(\Omega)$, $\widetilde{c}^0(x)\in[-1,1]$, $\widetilde{c}_{in}\in H^1(\Omega)$, $\widetilde{c}_{in}(x)\in[0,1]$,

doi:10.6342/NTU202200609

then (2.40) implies that

$$\delta t \sum_{j=1}^{m} \left\| \frac{\widetilde{c}^{j+1} - \widetilde{c}^{j}}{\delta t} \right\|_{W'}^{2} \quad \text{is uniformly bounded.} \tag{2.49}$$

Proof. By definition

$$\left\| \frac{\widetilde{c}^{m+1} - \widetilde{c}^{m}}{\delta t} \right\|_{W'} = \sup_{w_0 \in W} \frac{1}{\|w_0\|_1} \left\langle \frac{\widetilde{c}^{m+1} - \widetilde{c}^{m}}{\delta t}, w_0 \right\rangle. \tag{2.50}$$

By (2.40), with $w = \dfrac{w_0}{\|w_0\|_1} \in W$,

$$\begin{aligned} \left\| \frac{\widetilde{c}^{m+1} - \widetilde{c}^{m}}{\delta t} \right\|_{W'} = \sup_{w \in W, \|w\|=1} \Big\{ & - \int_{\Omega} D \nabla \widetilde{c}^{m+1} \cdot \nabla w dx \\ & - \frac{1}{2} \int_{\Omega} [(\boldsymbol{u}^{m+1} \cdot \nabla \widetilde{c}^{m+1}) w - (\boldsymbol{u}^{m+1} \cdot \nabla w) \widetilde{c}^{m+1}] dx - i_0 \int_{S} \dot{\Psi}(c^{m+1}) w \\ & - \int_{S} \frac{\alpha i_0^3}{D} \left(\sum_{j=0}^{m} c^j \delta t \right) c^{m+1} w - \frac{1}{2} \int_{\Gamma_{out}} (\boldsymbol{u}^{m+1} \cdot \boldsymbol{n}) c^{m+1} w \\ & - \frac{1}{2} \int_{\Omega} [(\boldsymbol{u}^{m+1} \cdot \nabla \widetilde{c}_{in}) w - (\boldsymbol{u}^{m+1} \cdot \nabla w) \widetilde{c}_{in}] dx \Big\}. \end{aligned} \tag{2.51}$$

We estimate all terms on the right hand side of (2.51)

$$- D \int_{\Omega} \nabla \widetilde{c}^{m+1} \cdot \nabla w dx \le D \|\nabla \widetilde{c}^{m+1}\|_0 \|\nabla w\|_0 \le D \|\widetilde{c}^{m+1}\|_1 \|w\|_1 = D \|\widetilde{c}^{m+1}\|_1, \tag{2.52}$$

$$\int_{\Omega} (\boldsymbol{u}^{m+1} \cdot \nabla w) \widetilde{c}^{m+1} dx \le \int_{\Omega} |\boldsymbol{u}^{m+1} \cdot \nabla w| \le \|\boldsymbol{u}^{m+1}\|_0, \tag{2.53}$$

$$\begin{aligned} & - \int_{\Omega} (\boldsymbol{u}^{m+1} \cdot \nabla \widetilde{c}^{m+1}) w dx = \int_{\Omega} (\boldsymbol{u}^{m+1} \cdot \nabla w) \widetilde{c}^{m+1} dx - \int_{\partial \Omega} (\boldsymbol{u}^{m+1} \cdot \boldsymbol{n}) \widetilde{c}^{m+1} w \\ & \le \|\boldsymbol{u}^{m+1}\|_0 + \|\boldsymbol{u}^{m+1}\|_{\partial \Omega} \|w\|_{\partial \Omega} \le C \|\boldsymbol{u}^{m+1}\|_1, \end{aligned} \tag{2.54}$$

$$- \int_{S} \dot{\Psi}(c^{m+1}) w \le C |S|^{\frac{1}{2}} \|w\|_1 = C |S|^{\frac{1}{2}}, \tag{2.55}$$

$$- \int_{S} \left(\sum_{j=0}^{m} c^j \delta t \right) c^{m+1} w \le \int_{S} T |w| \le C T |S|^{\frac{1}{2}} \|w\|_1 = C T |S|^{\frac{1}{2}}, \tag{2.56}$$

doi:10.6342/NTU202200609

$$-\int_{\Gamma_{out}} (\boldsymbol{u}^{m+1}\cdot\boldsymbol{n})c^{m+1}w \le \|\boldsymbol{u}^{m+1}\|_{\Gamma_{out}}\|w\|_{\Gamma_{out}} \le C\|\boldsymbol{u}^{m+1}\|_1\|w\|_1 = C\|\boldsymbol{u}^{m+1}\|_1, \tag{2.57}$$

$$\int_\Omega (\boldsymbol{u}^{m+1}\cdot\nabla w)\widetilde{c}_{in}dx \le \int_\Omega |\boldsymbol{u}^{m+1}\cdot\nabla w| \le \|\boldsymbol{u}^{m+1}\|_0\|w\|_1 = \|\boldsymbol{u}^{m+1}\|_0, \tag{2.58}$$

$$-\int_\Omega (\boldsymbol{u}^{m+1}\cdot\nabla\widetilde{c}_{in})w dx \le C\|\boldsymbol{u}^{m+1}\|_1 \ \text{ (see (2.54))}. \tag{2.59}$$

Collecting (2.52)-(2.59) with (2.51), all multiplied by δt, gives

$$\delta t\left\|\frac{\widetilde{c}^{m+1}-\widetilde{c}^m}{\delta t}\right\|^2_{W'} \le C\delta t(1+\|\widetilde{c}^{m+1}\|_1^2+\|\boldsymbol{u}^{m+1}\|_1^2). \tag{2.60}$$

By summing (2.60) from 0 to $N-1$ and the boundedness given by Corollary 2.4.1 and Corollary 2.5.1, the proof is completed. Q.E.D.

2.6 Passage to the Limit $\delta t \to 0$

Let us define

$$c_\delta : [0,T] \to H^1(\Omega), \quad c_\delta(t) = c^j \quad \text{if } t \in ((j-1)\delta t, j\delta t], \tag{2.61}$$

$$c_h : [0,T] \to H^1(\Omega), \ c_h(t) = \frac{t-(j-1)\delta t}{\delta t}c^j + \frac{j\delta t - t}{\delta t}c^{j-1} \quad \text{if } t \in ((j-1)\delta t, j\delta t], \tag{2.62}$$

$$c_{\delta-} : [0,T] \to H^1(\Omega), \quad c_{\delta-}(t) = c^{j-1} \quad \text{if } t \in [(j-1)\delta t, j\delta t), \tag{2.63}$$

$$C_{\delta-} : [0,T] \to H^1(\Omega), \quad C_{\delta-}(t) = \sum_{k=1}^{j} c^{k-1}\delta t \quad \text{if } t \in [(j-1)\delta t, j\delta t), \tag{2.64}$$

for $j = 1,\dots,N$. Note that c_δ, c_h, and $c_{\delta-}$ are in $L^2(0,T;H^1(\Omega))$ and $L^\infty(\Omega\times(0,T))$. With these notations, problem (P_c^m) reads

$$(\partial_t c_h, w) + \frac{1}{2}[(\boldsymbol{u}_\delta\cdot\nabla c_\delta, w) - (\boldsymbol{u}_\delta\cdot\nabla w, c_\delta)]$$
$$+D(\nabla c_\delta, \nabla w) + \int_S i_0\dot{\Psi}(c_\delta)w + \int_S \frac{\alpha i_0^3}{D}c_\delta C_{\delta-}w + \frac{1}{2}\int_{\Gamma_{out}}(\boldsymbol{u}_\delta\cdot\boldsymbol{n})c_\delta w = 0. \tag{2.65}$$

doi:10.6342/NTU202200609

Lemma 2.6.1 $C_{\delta-}$ is in $L^2(0,T;H^1(\Omega))$.

Proof.

$$\int_T \int_\Omega |\partial_{x_i} C_{\delta-}(t)|^2 dxdt \le \int_0^T \int_\Omega \left(\delta t \sum_{k=1}^N |\partial_{x_i} c^{k-1}|\right)^2 dxdt$$
$$= \int_0^T \int_\Omega \delta t^2 \left(\sum_{k=1}^N |\partial x_i c^{k-1}|\right)^2 dxdt \le \int_0^T \delta t^2 \cdot \frac{T}{\delta t} \sum_{k=1}^N |\partial_{x_i} c^{k-1}|^2 dx$$
$$= T^2 \delta t \sum_{k=1}^N \int_\Omega |\partial_{x_i} c^{k-1}|^2 dx \le C$$

The last inequality is due to Corollary 2.5.1.

Lemma 2.6.2

$$\|c_\delta - c_h\|_{L^2((0,T)\times\Omega)} \le \sqrt{\frac{\delta t}{3}} \left(\sum_{j=1}^N \|c^{j+1} - c^j\|_0^2\right)^{\frac{1}{2}} \tag{2.66}$$

Proof.

$$c_\delta(t) - c_h(t) = \frac{t - j\delta t}{\delta t}(c^j - c^{j-1}) \quad \text{for } (j-1)\delta t < t \le j\delta t,$$
$$\int_{(j-1)\delta t}^{j\delta t} \|c_\delta(t) - c_h(t)\|_0^2 dt = \frac{\delta t}{3} \|c^j - c^{j-1}\|_0^2.$$

The proof can be completed by taking summation from $j = 1$ to N.

Corollary 2.6.1

$$c_\delta - c_h \to 0 \quad \text{in } L^2((0,T)\times\Omega) \text{ as } \delta t \to 0. \tag{2.67}$$

By the boundedness given by Proposition 2.4.2, 2.5.2, and Corollary 2.5.1, there are subsequences of c_δ and c_h (still denoted by c_δ and c_h), respectively

doi:10.6342/NTU202200609

such that

$$c_\delta \to c \qquad \text{in } L^2(0,T;H^1(\Omega)) \text{ weakly}, \tag{2.68}$$

$$c_h \to c_* \qquad \text{in } L^2(0,T;H^1(\Omega)) \text{ weakly}, \tag{2.69}$$

$$c_h \to c_* \qquad \text{in } L^\infty(\Omega\times(0,T)) \text{ weak star}, \tag{2.70}$$

$$\partial_t c_h \to g \qquad \text{in } L^2(0,T;W^{'}) \text{ weakly}. \tag{2.71}$$

By Corollary 2.6.1, we have $c = c_*$.

By a classical argument, see for instance [41], we have

$$g = \partial_t c. \tag{2.72}$$

Let

$$Y = \left\{ w \in L^2(0,T;H^1(\Omega)),\ \partial_t w \in L^2(0,T;W^{'}) \right\}.$$

By the Aubin-Lions Lemma, Y is compactly embedded in $L^2(0,T;L^q(\Omega))$ with $q < 6$ when $d = 3$ and $q < \infty$ when $d = 2$. Therefore, we have in particular

$$c_h \to c \quad \text{in } L^2((0,T)\times\Omega) \text{ strongly}. \tag{2.73}$$

Using Corollary 2.6.1 again, we get

$$c_\delta \to c \quad \text{in } L^2((0,T)\times\Omega) \text{ strongly}. \tag{2.74}$$

To see the convergence of the boundary term, we need the following lemma:

Lemma 2.6.3 Let X be a normed linear space, D a dense subset of $X^{'}$, x_n, $n = 1, 2, \ldots$ a uniform bounded sequence in X. If $g(x_n) \to g(x)$ for all

doi:10.6342/NTU202200609

$g \in D$, then $x_n \to x$ weakly in X.

The above Lemma can be found in Theorem 10.1 of [42].

Lemma 2.6.4 Given c_δ defined by (2.61), there exists a subsequence (still denoted by c_δ) satisfying (2.68) and the followings:

$$\dot{\Psi}(c_\delta) \to \dot{\Psi}(c) \quad \text{in } L^2(0,T;H^{\frac{1}{2}}(S)) \text{ weakly}, \tag{2.75}$$

$$c_\delta \int_0^t c_\delta(s)ds \to c\int_0^t c(s)ds \quad \text{in } L^2(0,T;H^{\frac{1}{2}}(S)) \text{ weakly}. \tag{2.76}$$

Proof. Let us prove that $\dot{\Psi}(c_\delta)$ tends to $\dot{\Psi}(c)$ weakly in $L^2(0,T;H^1(\Omega))$. First, we know that $\dot{\Psi}(c_\delta)$ is bounded in $\Omega \times [0,T]$ and we have $\dot{\Psi}(c_\delta) = c_\delta - \dfrac{\alpha c_\delta^2}{2}$ a.e. since $c_\delta \le 1$ a.e.. Moreover, since $\alpha < 1$, we have

$$\begin{aligned}
&\int_0^T \int_\Omega |\partial_{x_i}\dot{\Psi}(c_\delta)|^2 dxdt = \int_0^T |\partial_{x_i}c_\delta - \alpha c_\delta \partial_{x_i}c_\delta|^2 dxdt \\
&= \int_0^T \int_\Omega |(1-\alpha c_\delta)\partial_{x_i}c_\delta|^2 dxdt = \int_0^T \int_\Omega |1-\alpha c_\delta|^2 |\partial_{x_i}c_\delta|^2 dxdt \\
&\le \int_0^T \int_\Omega |\partial_{x_i}c_\delta|^2 dxdt < \infty.
\end{aligned}$$

Therefore, $\dot{\Psi}$ converges weakly in $L^2(0,T;H^1(\Omega))$. To identify its limit, let $w \in C([0,T]\times\overline{\Omega})$. Then (2.74) implies that

$$\int_0^T \int_\Omega \dot{\Psi}(c_\delta) w dxdt \to \int_0^T \int_\Omega \dot{\Psi}(c) w dxdt$$

and (2.74) and (2.68) imply that

$$\int_0^T \int_\Omega \partial_{x_i}\dot{\Psi}(c_\delta) w dxdt \to \int_0^T \int_\Omega \partial_{x_i}\dot{\Psi}(c) w dxdt.$$

This gives the desired convergence. By the continuity of the trace mapping

$$\phi \mapsto \phi|_{\partial\Omega}$$

doi:10.6342/NTU202200609

for the weak topology, we deduce that

$$\dot{\Psi}(c_\delta) \to \dot{\Psi}(c) \ \text{ weakly in } L^2(0,T;H^{\frac{1}{2}}(S)). \tag{2.77}$$

For (2.76), we define $r(t,c_\delta) := c_\delta \int_0^t c_\delta(s)ds$ in $(0,T)\times\Omega$. To begin with, we observe that $\int_0^t c_\delta(s)ds \to \int_0^t c(s)ds$ strongly in $L^2((0,T)\times\Omega)$. This can be checked by the estimate:

$$\begin{aligned}\int_0^T\int_\Omega \left|\int_0^t (c_\delta(s)-c(s))ds\right|^2 dxdt &\le \int_0^T\int_\Omega t\int_0^t |c_\delta(s)-c(s)|^2 dsdxdt\\ \le \int_0^T t\int_0^T\int_\Omega |c_\delta(s)-c(s)|^2 dxdsdt &= \frac{1}{2}T^2\int_0^T\int_\Omega |c_\delta(s)-c(s)|^2 dxds\\ &\to 0 \ \text{ as } \delta t\to 0.\end{aligned}$$

Let $w \in C([0,T]\times\overline{\Omega})$. Since c_δ strongly converges to c in $L^2((0,T)\times\Omega)$, we have

$$\int_0^T\int_\Omega r(t,c_\delta)w dxdt \to \int_0^T\int_\Omega r(t,c)w dxdt. \tag{2.78}$$

We differentiate $r(t,c_\delta)$:

$$\partial_{x_i} r(t,c_\delta) = \partial_{x_i}c_\delta \int_0^t c_\delta(s)ds + c_\delta\int_0^t \partial_{x_i}c_\delta(s)ds. \tag{2.79}$$

We have the boundedness for the first term on the right hand side:

$$\begin{aligned}\int_0^T\int_\Omega |\partial_{x_i}c_\delta|^2\left|\int_0^t c_\delta(s)ds\right|^2 dxdt &\le \int_0^T\int_\Omega t|\partial_{x_i}c_\delta|^2 dxdt\\ &\le T\int_0^T\int_\Omega |\partial_{x_i}c_\delta|^2 dxdt < \infty\end{aligned} \tag{2.80}$$

Using the fact that both $\partial_{x_i}c_\delta \to \partial_{x_i}c$ weakly in $L^2((0,T)\times\Omega)$ and $\int_0^t c_\delta(s)ds \to \int_0^t c(s)ds$ strongly in $L^2((0,T)\times\Omega)$, we have

$$\int_0^T\int_\Omega \partial_{x_i}c_\delta\left(\int_0^t c_\delta(s)ds\right)w dxdt \to \int_0^T\int_\Omega \partial_{x_i}c\left(\int_0^t c(s)ds\right)w dxdt. \tag{2.81}$$

doi:10.6342/NTU202200609

The second term is bounded as well:

$$\int_0^T \int_\Omega \left| \int_0^t \partial_{x_i} c_\delta(s) ds \right|^2 dxdt \le \int_0^T \int_\Omega t \int_0^t |\partial_{x_i} c_\delta(s)|^2 ds dx dt$$
$$= \int_0^T t \int_0^t \int_\Omega |\partial_{x_i} c_\delta(s)|^2 dx ds dt \le \int_0^T t \int_0^T \int_\Omega |\partial_{x_i} c_\delta(s)|^2 dx ds dt \qquad (2.82)$$
$$= \frac{1}{2} T^2 \int_0^T \int_\Omega |\partial_{x_i} c_\delta(s)|^2 dx dt < \infty$$

And we observe that

$$\int_0^T \int_\Omega \left(\int_0^t \partial_{x_i} c_\delta(s) ds \right) w dx dt$$
$$= \int_0^T \int_0^t \left(\int_\Omega \partial_{x_i} c_\delta(s) w dx \right) ds dt \to \int_0^T \left(\int_0^t \int_\Omega \partial_{x_i} c(s) w dx ds \right) dt$$

because $w(t)$ for fixed t is continuous in Ω. Now, we have $c_\delta \to c$ in $L^2((0,T) \times \Omega)$ strongly and $\int_0^t \partial_{x_i} c_\delta(s) ds \to \int_0^t \partial_{x_i} c(s) ds$ weakly in $L^2((0,T) \times \Omega)$. This implies that

$$\int_0^T \int_\Omega c_\delta \left(\int_0^t \partial_{x_i} c_\delta(s) ds \right) w(t) dx dt \to \int_0^T \int_\Omega c \left(\int_0^t \partial_{x_i} c(s) ds \right) w dx dt$$

By (2.82) and Lemma A.3.3 below, we have $c_\delta \int_0^t \partial_{x_i} c_\delta(s) ds \to c \int_0^t \partial_{x_i} c(s) ds$ weakly in $L^2((0,T) \times \Omega)$.

Collecting all the weak convergence results above, we conclude that $r(t, c_\delta) \to r(t, c)$ in $L^2(0,T; H^1(\Omega))$ weakly. By the continuity of the trace for the weak topology, we have $r(t, c_\delta) \to r(t, c)$ in $L^2(0,T; H^{\frac{1}{2}}(S))$ weakly. Q.E.D.

Lemma 2.6.5 $C_{\delta-}$ defined in (2.64) satisfies

$$\left\| C_{\delta-} - \int_0^t c_\delta(s) ds \right\|_{L^2(0,T;H^1(\Omega))} \le C\delta t \qquad (2.83)$$

Proof. For all $t \in [(j-1)\delta t, j\delta t)$,

$$C_{\delta-}(t) - \int_0^t c_\delta(s) ds = \sum_{k=1}^{j} c^{k-1} \delta t - \sum_{k=1}^{j-1} c^k \delta t - c^j (t - (j-1)\delta t)$$
$$= c^0 \delta t - c^j (t - (j-1)\delta t).$$

doi:10.6342/NTU202200609

But for $t \in [(j-1)\delta t, j\delta t)$, we have $0 \le t-(j-1)\delta t \le \delta t$. Therefore

$$\left| C_{\delta -}(t) - \int_0^t c_\delta(s)ds \right| \le \delta t |c^0 + c^j|.$$

On the other hand,

$$\begin{aligned}\partial_{x_i} C_{\delta -}(t) - \partial_{x_i} \int_0^t c_\delta(s)ds &= \partial_{x_i} C_{\delta -}(t) - \int_0^t \partial_{x_i} c_\delta(s)ds \\ &= \partial_{x_i} c^0 \delta t - \partial_{x_i} c^j (t-(j-1)\delta t).\end{aligned}$$

Hence, we have

$$\left| \partial_{x_i} \left(C_{\delta -}(t) - \int_0^t c_\delta(s)ds \right) \right| \le \delta t |\partial_{x_i}(c^0 + c^j)|.$$

Therefore,

$$\begin{aligned}&\left\| C_{\delta -} - \int_0^t c_\delta(s)ds \right\|^2_{L^2(0,T;H^1(\Omega))} = \int_0^T \left\| C_{\delta t -}(t) - \int_0^t c_\delta(s)ds \right\|_1^2 \\ &\le \sum_{j=1}^N \int_{(j-1)\delta t}^{j\delta t} (\delta t)^2 \|c^0 + c^j\|_1^2 \\ &\le 2\sum_{j=1}^N \int_{(j-1)\delta t}^{j\delta t} (\delta t)^2 \left(\|c^0\|_1^2 + \|c^j\|_1^2 \right) \\ &\le 2\|c^0\|_1^2 (\delta t)^2 + 2(\delta t)^2 \sum_{j=1}^N \delta t \|c^j\|_1^2 \\ &\le C(\delta t)^2\end{aligned}$$

Q.E.D.

Proof of Theorem 2.3.1.

Now, we are in a position to pass to the limit in (2.65). Take any $w = v(x)\lambda(t)$, where $v \in W \cap W^{1,\infty}(\Omega)$ and $\lambda \in W_0^{1,\infty}(0,T)$. Then

$$\begin{aligned}&-\int_0^T (c_h, v)\lambda'(t)dt + \frac{1}{2}\int_0^T [(\boldsymbol{u}_\delta \cdot \nabla c_\delta, v) - (\boldsymbol{u}_\delta \cdot \nabla v, c_\delta)]\lambda dt \\ &+ \int_0^T D(\nabla c_\delta, \nabla v)\lambda dt + \int_0^T \int_S i_0 \dot{\Psi}(c_\delta) v \lambda(t) dt + \int_0^T \int_S \frac{\alpha i_0^3}{D} c_\delta C_{\delta -} v \lambda(t) dt \\ &+ \frac{1}{2}\int_0^T \int_{\Gamma_{out}} (\boldsymbol{u}_\delta \cdot \boldsymbol{n}) c_\delta v \lambda(t) dt = 0.\end{aligned}$$

doi:10.6342/NTU202200609

Since $\boldsymbol{u}_\delta \to \boldsymbol{u}$ strongly in $L^2(\Omega \times (0,T))$ and $\nabla c_\delta \to \nabla c$ weakly in $L^2(\Omega \times (0,T))$, the regularity of v and λ implies that

$$-\int_0^T (c_h, v)\lambda'(t)dt \to -\int_0^T (c, v)\lambda'(t)dt = \int_0^T \langle \partial_t c, v\rangle_{W',W}\lambda dt, \tag{2.84}$$

$$\frac{1}{2}\int_0^T [(\boldsymbol{u}_\delta \cdot \nabla c_\delta, v) - (\boldsymbol{u}_\delta \cdot \nabla v, c_\delta)]\lambda dt \to \frac{1}{2}\int_0^T [(\boldsymbol{u} \cdot \nabla c, v) - (\boldsymbol{u} \cdot \nabla v, c)]\lambda dt, \tag{2.85}$$

$$\int_0^T D(\nabla c_\delta, \nabla c)\lambda dt \to \int_0^T D(\nabla c, \nabla v)\lambda dt. \tag{2.86}$$

Similarly, the weak convergence of $\dot{\Psi}(c_\delta)$ to $\dot{\Psi}(c)$ in $L^2(0,T; H^{\frac{1}{2}}(S))$ implies that

$$\int_0^T \int_S i_0 \dot{\Psi}(c_\delta) v\lambda(t)dt \to \int_0^T \int_S \dot{\Psi}(c) v\lambda(t)dt, \tag{2.87}$$

and the weak convergence of $c_\delta C_{\delta -}$ to $c\int_0^t c$ in $L^2(0,T; H^{\frac{1}{2}}(S))$ implies that

$$\int_0^T \int_S c_\delta C_{\delta -} v\lambda(t)dt \to \int_0^T \int_S c\left(\int_0^t c(s)ds\right) v\lambda(t)dt. \tag{2.88}$$

Finally, we consider the last term $\frac{1}{2}\int_0^T \int_{\Gamma_{out}} (\boldsymbol{u}_\delta \cdot \boldsymbol{n}) c_\delta v\lambda(t)$. Given the construction of $\boldsymbol{u}_\delta$ in Section 2.4, we have: $\boldsymbol{u}_\delta \to \boldsymbol{u}$ weakly in $L^2(0,T; H^1(\Omega)^d)$ and $\boldsymbol{u}_\delta \to \boldsymbol{u}$ strongly in $L^2(0,T; L^4(\Omega)^d)$ (thanks to the strong convergence of $\boldsymbol{u}_\delta$ by (2.32), $H^1(\Omega)^d$ can be replaced by any space X so that $H^1(\Omega) \subset\subset X$. Here we take $X = L^4(\Omega)^d$, which is compatible with $d = 3$; the exponent has to be less than 6). We use Green's formula:

$$\int_0^T \int_{\Gamma_{out}} (\boldsymbol{u}_\delta \cdot \boldsymbol{n}) c_\delta v\lambda = \int_0^T \int_\Omega \nabla \cdot (\boldsymbol{u}_\delta c_\delta) v\lambda + \int_0^T \int_\Omega (c_\delta \boldsymbol{u}_\delta \cdot \nabla v)\lambda \tag{2.89}$$

for all $\lambda \in L^\infty(0,T)$ and for all smooth v that vanish on $\partial\Omega \setminus \Gamma_{out}$. It is suffices to prove the convergence of each term to the desired limit.

doi:10.6342/NTU202200609

1) For all $v \in L^4(\Omega)$ and for all $\lambda \in L^\infty(0,T)$:

$$\int_0^T \int_\Omega \nabla \cdot (\boldsymbol{u}_\delta c_\delta) v\lambda = \int_0^T \int_\Omega \boldsymbol{u}_\delta \cdot \nabla c_\delta v\lambda$$
$$= \int_0^T \int_\Omega (\boldsymbol{u}_\delta - \boldsymbol{u}) \cdot \nabla c_\delta v\lambda + \int_0^T \int_\Omega \boldsymbol{u} \cdot \nabla c_\delta v\lambda$$
$$\leq \|\boldsymbol{u}_\delta - \boldsymbol{u}\|_{L^2(0,T;L^4(\Omega))} \|\nabla c_\delta\|_{L^2(\Omega\times(0,T))} \|\lambda\|_{L^\infty(0,T)} \|v\|_{L^4(\Omega)} + \int_0^T \int_\Omega \boldsymbol{u} \cdot \nabla c_\delta v\lambda.$$

It is noted that $\boldsymbol{u}v\lambda \in L^2(0,T;L^2(\Omega)^d)$ and $\nabla c_\delta \to \nabla c$ weakly in $L^2(0,T;L^2(\Omega)^d)$, we have

$$\int_0^T \int_\Omega \nabla \cdot (\boldsymbol{u}_\delta c_\delta) v\lambda \to \int_0^T \int_\Omega (\boldsymbol{u} \cdot \nabla c) v\lambda = \int_0^T \int_\Omega \nabla \cdot (\boldsymbol{u}c) v\lambda. \tag{2.90}$$

2) For all $v \in H^1(\Omega)$, $\lambda \in L^\infty(\Omega)$

$$\int_0^T \int_\Omega (c_\delta \boldsymbol{u}_\delta \cdot \nabla v)\lambda = \int_0^T \int_\Omega c_\delta (\boldsymbol{u}_\delta - \boldsymbol{u}) \cdot \nabla v\lambda + \int_0^T \int_\Omega \boldsymbol{u}(c_\delta - c) \cdot \nabla c\lambda + \int_0^T \int_\Omega c(\boldsymbol{u} \cdot \nabla v)\lambda$$
$$\leq \|\boldsymbol{u}_\delta - \boldsymbol{u}\|_{L^2(0,T;L^2(\Omega)^d)} \|c_\delta\|_{L^\infty(\Omega\times(0,T))} \|\nabla v\|_0 \|\lambda\|_{L^\infty(\Omega)}$$
$$+ \|\boldsymbol{u}\|_{L^2(0,T;L^4(\Omega)^d)} \|c_\delta - c\|_{L^2(0,T;L^4(\Omega)^d)} \|\nabla v\|_0 \|\lambda\|_{L^\infty(\Omega)} + \int_0^T \int_\Omega c(\boldsymbol{u} \cdot \nabla v)\lambda.$$

Therefore

$$\begin{aligned} &\int_0^T \langle \partial_t c, v\rangle_{W',W} \lambda dt + \frac{1}{2} \int_0^T ((\boldsymbol{u} \cdot \nabla c, v) - (\boldsymbol{u} \cdot \nabla v, c))\lambda dt \\ &+ \int_0^T D(\nabla c, \nabla v)\lambda dt + \int_0^T \int_S i_0 \dot{\Psi}(c) v\lambda dt + \int_0^T \int_S \frac{\alpha i_0^3}{D} c \left(\int_0^t c(s) ds \right) v\lambda dt \\ &+ \frac{1}{2} \int_0^T \int_{\Gamma_{out}} (\boldsymbol{u} \cdot \boldsymbol{n}) cv\lambda dt = 0 \end{aligned} \tag{2.91}$$

for all $\lambda \in W_0^{1,\infty}(0,T)$ and for all $v \in W^{1,\infty}(\Omega)$. This gives the equations a.e. in $(0,T)$.

To recover the initial condition, we take $\lambda \in W^{1,\infty}(0,T)$, $\lambda(T) = 0$, $\lambda(0) \neq 0$, and $v \in W^{1,\infty}(\Omega)$. We consider (2.65) such that all terms are identical except the first:

$$\int_0^T (\partial_t c_h, v)\lambda dt = \int_0^T \partial_t (c_h, v)\lambda dt = -\int_0^T (c_h, v)\lambda'(t) - (c^0, v)\lambda(0). \tag{2.92}$$

doi:10.6342/NTU202200609

When passing to the limit, we obtain

$$\begin{aligned}\int_0^T \langle \partial_t c, v\rangle_{W',W}\lambda dt &= -\int_0^T (c,v)\lambda'(t) - (c^0,v)\lambda(0)\\ &= \int_0^T \frac{d}{dt}(c,v)\lambda + (c(0),v)\lambda(0) - (c^0.v)\lambda(0)\\ &= \int_0^T \langle \partial_t c, v\rangle_{W',W}\lambda dt + (c(0),v)\lambda(0) - (c^0,v)\lambda(0).\end{aligned} \tag{2.93}$$

Therefore

$$(c(0),v) = (c^0,v), \qquad \forall v \in W \cap W^{1,\infty}(\Omega).$$

This implies that $c(0) = c^0$.

The above shows that Problem (P_c) has a unique solution, which satisfies $0 \le c \le 1$; it is also the solution of (P). Q.E.D.

2.6.1 On the boundary condition (2.19) which contains $\partial_t c$

To prove existence a similar strategy is taken: $\partial_t c$ is replaced by $(c^{m+1} - c^m)/\delta t$, existence is shown and then convergence when $\delta t \to 0$.

The proof of existence of the time-discretized problem is exactly the same but with ϕ redefined as

$$\phi_m(c^{m+1}) = i_0\dot{\Psi}(c^{m+1}) + \alpha i_0\left(\frac{i_0^2}{D} - \frac{1}{\delta t}\right)\left(\sum_{j=0}^{m} c^j \delta t\right) c^{m+1}.$$

Convergence with $\delta t \to 0$ requires more regularity, which can be obtained from the PDE differentiated in time.

doi:10.6342/NTU202200609

2.7 Numerical Simulations

The rectangular domain of size $0.025\ mm \times 0.005\ mm$ is the initial physical domain. The electroprocess is simulated up to time $T = 5000$.

2.7.1 Scalings

The simulation will be done with dimensionless variables. Let L, C and U be representative length, concentration and velocity of the physical system. Then it is easy to see that the dimensionless equation for c is the same as the original equation but with $\widetilde{D}/(LU)$ instead of D, where $\widetilde{D}$ is the physical molecular diffusion. Similarly because (2.7) becomes

$$-D\frac{\partial c}{\partial n} = \frac{i_0}{U}c, \quad \mathbf{u} = -\alpha\, C\frac{i_0}{U}c\mathbf{n},$$

the original form holds but with i_0/U redefined as i_0 and $\alpha\, C$ redefined as α.

It is well known that the dimensionalized Navier-Stokes equation has the inverse Reynolds number $\widetilde{\nu}/(UL)$ redefined as ν, where $\widetilde{\nu}$ being the kinematic viscosity.

The parameters of nickel ion given in [1] are $i_0 = \widetilde{i_0}/(zF)$ with $\widetilde{i_0} = 0.001\ A \cdot mm^{-2}$, the number of electrons involves in the reaction $z = 2$ and the Faraday constant $F = 96487\ s \cdot A \cdot mol^{-1}$, $C = 3 \times 10^{-7}\ mol \cdot mm^{-3}$.

For electrodeless plating we may take $U = 1\ mm \cdot s^{-1}$, $L = 0.005\ mm$, $\widetilde{D} = 1 \times 10^{-4}\ mm^2 \cdot s^{-1}$, $\alpha = 6590\ mm^3 \cdot mol^{-1}$, and $\widetilde{\nu} = 1.2\ mm^2 \cdot s^{-1}$.

So in the end the numerical tests are done on a rescaled domain $\Omega =$

doi:10.6342/NTU202200609

$(0,5)\times(0,1)$ with

$$\alpha = 0.002085, \quad i_0 = 0.017273, \quad D = 0.02, \quad \nu = 240,$$

2.7.2 Numerical algorithm

The finite element method is used for spacial discretization. Let $\mathcal{T}_h$ be a triangulation consisting of K traingles $\{T_k\}_{k=1}^K$ with the standard conformity hypothesis. We define the finite element space which will be used in this section:

$$\begin{aligned}
W_h &:= \{w \in C^0(\overline{\Omega}) :\ w|_{T_k} \in P^1\ \forall T_k \in \mathcal{T}_h,\ w|_{\Gamma_{in}} = 0\},\\
C_h &:= \{w \in C^0(\overline{\Omega}) :\ w|_{T_k} \in P^1,\ \forall T_k \in \mathcal{T}_h\},\\
\boldsymbol{V}_h &:= \{\boldsymbol{v} \in C^0(\overline{\Omega})^2 :\ \boldsymbol{v}|_{T_k} \in (P^2)^2,\ \forall T_k \in \mathcal{T}_h\},\\
\boldsymbol{J}_h &:= \{\boldsymbol{v} \in C^0(\overline{\Omega})^2 :\ \boldsymbol{v}|_{T_k} \in (P^2)^2\ \forall T_k \in \mathcal{T}_h,\ \boldsymbol{v}|_{\partial\Omega\setminus\Gamma_{out}} = 0\},\\
Q_h &:= C_h.
\end{aligned} \tag{2.94}$$

Solving concentration profile c_h^{m+1} with known velocity field $\boldsymbol{u}_h^{m+1}$

We use the P^1 finite element method for Problem (P_c^m) to define $\{c_h^m\}_{m>0}$. Given $\boldsymbol{u}_h^{m+1} \in \boldsymbol{V}_h$, one must solve the finite dimensional problem (P_h^m) defined to be (P_c^m) with W_h instead of W in (2.35): find $c_h^{m+1} \in C_h$ satisfying,

doi:10.6342/NTU202200609

for all $w_h \in W_h$,

$$\int_\Omega \frac{c_h^{m+1}-c_h^m}{\delta t} w_h dx + \int_\Omega [(\boldsymbol{u}_h^{m+1}\cdot\nabla c_h^{m+1}) w_h + D\int_\Omega \nabla c_h^{m+1}\cdot\nabla w_h dx + \int_S \left(1+\frac{\alpha i_0^2}{D}\left(\sum_{j=1}^m c_h^j \delta t\right)\right) i_0 c_h^{m+1} w_h = 0, \quad (2.95)$$

$$c_h^{m+1}|_{\Gamma_{in}} = c_{inh}$$

In the above, c_{inh} is the piecewise linear interpolate of c_{in}.

Since $\boldsymbol{u}_h^{m+1}$ and $\{c_h^j\}_{j\le m}$ are given, (2.95) leads to a linear system by assigning w_h to be the P1 hat functions in a standard way. We apply UMFPACK[43] for solving the linear system at each time step.

Solving velocity field $\boldsymbol{u}_h^{m+1}$ with known concentration profile c_h^{m+1}

For the Navier-Stokes equation we use the P^2/P^1 triangular Taylor-Hood element [44] and we denote by $\boldsymbol{u}_h^m$, p_h^m the finite element solution and by $\boldsymbol{V}_h$, Q_h the corresponding finite element space. The variational formulation is: Find $\boldsymbol{u}_h^{m+1} \in V_h$ and $p_h^{m+1} \in Q_h$ satisfying

$$\int_\Omega \frac{\boldsymbol{u}_h^{m+1}-\boldsymbol{u}_h^m}{\delta t}\cdot\boldsymbol{v}_h dx + \int_\Omega [(\boldsymbol{u}_h^m\cdot\nabla)\boldsymbol{u}_h^{m+1}]\cdot\boldsymbol{v}_h dx + \nu\int_\Omega \nabla\boldsymbol{u}_h^{m+1}:\nabla\boldsymbol{v}_h dx - \int_\Omega (p_h^{m+1}\nabla\cdot\boldsymbol{v}_h + q_h\nabla\cdot\boldsymbol{u}_h^{m+1} + \epsilon p_h q_h)dx = 0,$$

$$\boldsymbol{u}_h^{m+1} = \boldsymbol{u}_{inh} \text{ on } \Gamma_{in}, \quad \boldsymbol{u}_h^{m+1} = 0 \text{ on } \Gamma_{wall}, \quad \boldsymbol{u}_h^{m+1} = -\alpha i_0 c_h^{m+1}\boldsymbol{n} \text{ on } S \quad (2.96)$$

for all $\boldsymbol{v}_h \in \boldsymbol{J}_h$ and $q_h \in Q_h$; ϵ is a small regularization parameter which is taken to be 10^{-12} in our computer implementation. In the above, $\boldsymbol{u}_{inh}$ is the P^2 interpolation of $\boldsymbol{u}_{in}$.

With known $\boldsymbol{u}_h^m$ and c_h^{m+1}, (2.96) leads to a linear system for the degrees

doi:10.6342/NTU202200609

of freedom of $\boldsymbol{u}_h^{m+1}$ and p_h^{m+1} which is solved with the numerical library UMFPACK[43], at each m.

Remark 2.7.1 If mass-lumping is used and the triangulation has no obtuse angle, the positivity of (2.95) can be guaranteed by the same argument in the proof of Proposition 2.4.2. Therefore, the assumption (U1) holds for $\boldsymbol{u}_h^{m+1}$. Again, (U2) does not hold for the system (2.96) in general. In practical numerical implementation, the natural outflow boundary condition

$$-\nu \frac{\partial \boldsymbol{u}_h^{m+1}}{\partial n} + p_h^{m+1}\boldsymbol{n} = 0$$

does no harm to (U2) when the velocity field is closed to a Poiseuille flow (for instance, the numerical tests conducted in Sections 7.3 and 7.4).

Iteration algorithm

The coupled system (2.95)-(2.96) is solved iteratively. We replace c_h^{m+1} by c^* in (2.95) and solve (2.96). We denote the solution by $\boldsymbol{u}^*$. Then we replace $\boldsymbol{u}_h^{m+1}$ by $\boldsymbol{u}^*$ in order to get the new c^*, until $\|\boldsymbol{u}_{new}^* - \boldsymbol{u}_{old}^*\|_0 + \|c_{new}^* - c_{old}^*\|_0$ is sufficiently small.

To validate the method we need to compare with the original free boundary problem. It is solved with a similar iterative fixed point like process but the mesh needs to be rebuilt when the free boundary is updated. It is done by a scaling on y-coordinate at each time step t^j: $y \mapsto (1 - \alpha i_0 c_h^j \delta t)y$.

doi:10.6342/NTU202200609

Data: $\boldsymbol{u}_h^m$, p_h^m, c_h^m, and y

Set initial data $\boldsymbol{u}_0$, c_0;

for m **do**

  $c^* = c_h^m$;

  while $\|\boldsymbol{u}_{new}^* - \boldsymbol{u}_{old}^*\|_0 + \|c_{new}^* - c_{old}^*\|_0 \geq tolerance$ **do**

    Solve (2.95) to get c_{new}^*;

    Solve (2.96) to get $\boldsymbol{u}_{new}^*$ and p_{new}^*;

  end

  $c_h^{m+1} = c_{new}^*$;

  $\boldsymbol{u}_h^{m+1} = \boldsymbol{u}_{new}^*$;

  For the free boundary case change the mesh by

  $y \leftarrow (1 - \alpha i_0 c_h^{m+1} \delta t) y$;

end

2.7.3 Numerical results at low Reynolds number

The initial and inflow values are

$$c_0 = \cos(\lambda y), \quad \boldsymbol{u}_0 = y(1-y); \qquad c_{in} = c_0|_{\Gamma_{in}} \exp(-D\lambda^2 t), \quad \boldsymbol{u}_{in} = \boldsymbol{u}_0|_{\Gamma_{in}}.$$

A uniform triangular mesh 150×30 for the initial domain for each test so that the time-discrete error can be emphasized.

We compare the results obtained using a time dependent domain (Figure 2.3a) with the results using a fixed domain and the linear condition (2.7) (see Figure 2.3b) and finally with the nonlinear condition (2.12) (see Figure

doi:10.6342/NTU202200609

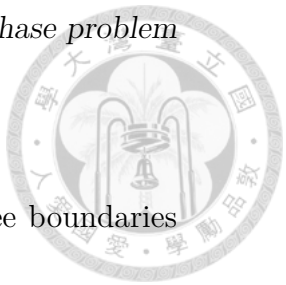

2.3c).

On Figure 2.4 the free boundary and the reconstructed free boundaries are displayed using η given by (2.8).

The convergence with respect to time step size is shown on Table 2.1, computed at an intermediate time $T = 100$. Since no exact solution is available, the numerical solution with time step $\delta t = 0.01$ is taken as the reference solution. The numerical results in Table 2.1 show a first order convergence in L^2 error conformed with the estimates given in Appendix B (see Figure 2.5).The weak first order convergence of H^1 error is also proved in Appendix B. However the numerical results show strong first order H^1 convergence for this test problem (see Figure 2.6).

2.7.4 Numerical results at larger Reynolds number

In the previous example, where the values of the parameters correspond to the physical design of [45], we could have neglected the inertial terms and work with the Stokes approximation. In order to validate the algorithm at higher Reynolds number, which may be the case for other plating problems, we keep all parameters given in the end of Section 7.1 but change the Reynolds number to the inverse of $\nu = 0.01$. The same experiments are conducted as in Section 7.3. The numerical results obtained for the low Reynolds number and the larger Reynolds number are very similar; no visible changes can be seen (see the right side of Figure 2.4) so we do not display the plots of Figure

doi:10.6342/NTU202200609

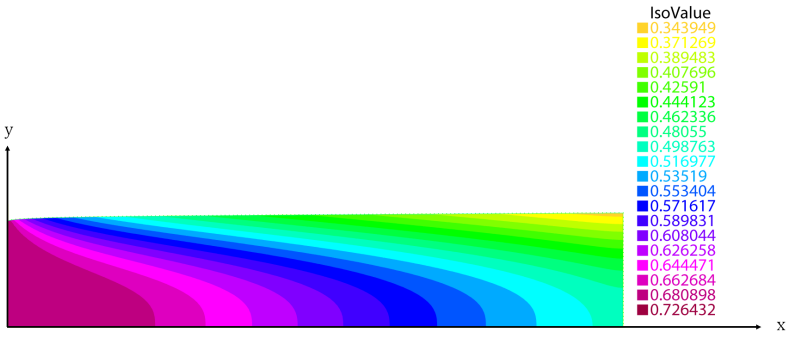

(a) Intensity map of c computed with a free boundary on a moving mesh.

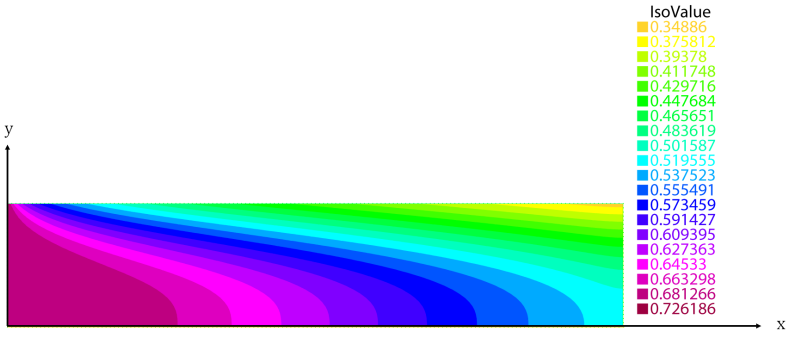

(b) Intensity map of c computed by the linear transpiration approximation.

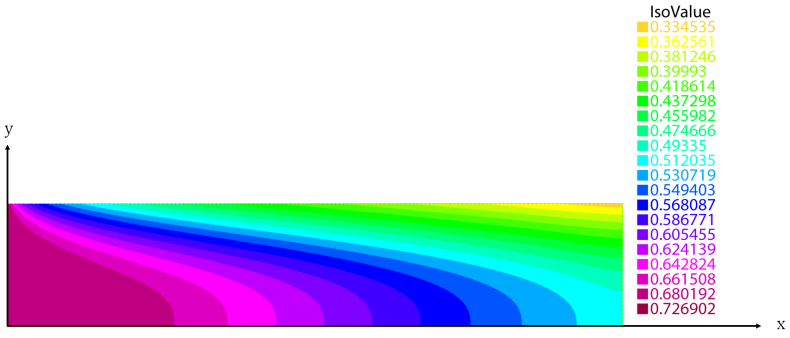

(c) Intensity map of c computed by nonlinear transpiration approximation.

Figure 2.3: The solution profiles of numerical experiments with $\nu = 240$.

doi:10.6342/NTU202200609

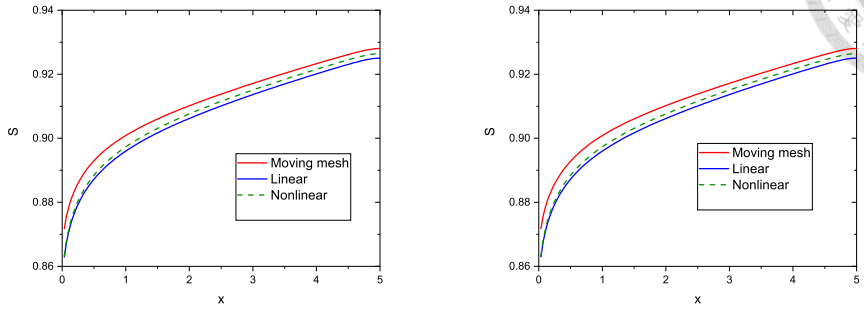

Figure 2.4: $S(T)$ calculated by 3 experiments at $T = 5000$. The red curve is the height of $S(T)$ computed by moving mesh. The blue curve is computed by the displacement $\eta(T)$ with linear condition. The green dash curve is computed by the displacement $\eta(T)$ with nonlinear condition. If the curve of moving mesh is regarded as the reference solution, it is easy to see that the nonlinear approximation does better than the linear approximation. Left figure corresponds to with $\nu = 240$ and Right figure to $\nu = 0.01$.

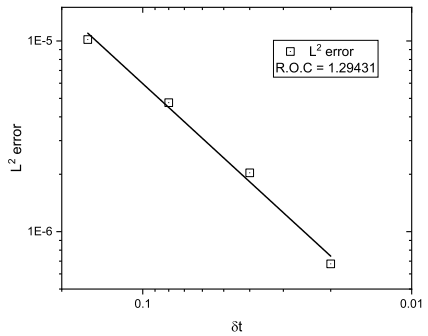

Figure 2.5: L^2 relative error versus δt at $T = 100$

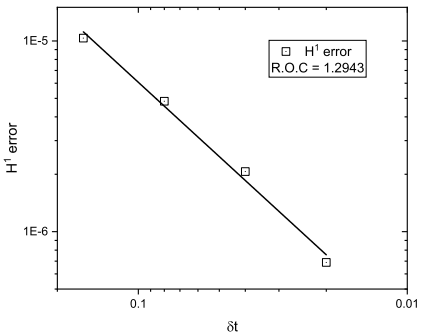

Figure 2.6: H^1 relative error versus δt at $T = 100$.

doi:10.6342/NTU202200609

δt	L^2 error
0.16	1.01723×10^{-5}
0.08	4.74704×10^{-6}
0.04	2.03444×10^{-6}
0.02	6.78147×10^{-7}

δt	H^1 error
0.16	1.03365×10^{-5}
0.08	4.82368×10^{-6}
0.04	2.06729×10^{-6}
0.02	6.89107×10^{-7}

δt	L^2 error
0.16	1.01722×10^{-5}
0.08	4.74701×10^{-6}
0.04	2.03443×10^{-6}
0.02	6.78142×10^{-7}

δt	H^1 error
0.16	1.03365×10^{-5}
0.08	4.82367×10^{-6}
0.04	2.06729×10^{-6}
0.02	6.89103×10^{-7}

Table 2.1: Convergence when $\delta t \to 0$: L^2 and H^1 relative error at $T = 100$ for the scheme with the nonlinear transpiration approximation and $\nu = 240$ (left columns) and $\nu = 0.01$ (right columns). A uniform triangular mesh 150×30 is used.; $c_{\delta t=0.01}$ is used as reference solution.

doi:10.6342/NTU202200609

2.3 for the high Reynolds number case.

Furthermore, several numerical experiments show no visible change by choosing the Reynolds number between the inverse of 240 and the inverse of 0.01.

2.7.5 Influence of the term $\partial_t c$ in (2.19)

For the geometry considered in these numerical test no visible difference could be observed between (2.12) and (2.19) .

2.8 Conclusion

We have proposed a simplified model which approximates the Electroless process of [45] by replacing the time dependent domain occupied by the reacting chemical by a fixed domain using a transpiration approximation. We have validated the approximation numerically with a finite element method in space and a fully implicit in time approximation. We have constructed an existence proof by using variational convex analysis or fixed point arguments. The proof is technical and long because the nonlinearity is on the boundary condition and because it required a convexification of the energy potential and the maximum principle. However it was worth the effort because it gives a stable ground for the numerical studies and it may be useful for other similar problems. We plan to extend this study to two phase flows to take

doi:10.6342/NTU202200609

into account the formation of bubbles.

2.A Proof of Lemma 2.4.3.

Let $\rho_1, \rho_2 \in W$. Formula (2.41) gives

$$\begin{aligned}\langle A\rho_1 - A\rho_2, w\rangle &= \frac{1}{\delta t}\int_\Omega (\rho_1-\rho_2)w dx \\ &+ \frac{1}{2}\int_\Omega [(\boldsymbol{u}^{m+1}\cdot\nabla(\rho_1-\rho_2))w - (\boldsymbol{u}^{m+1}\cdot\nabla w)(\rho_1-\rho_2)]dx + D\int_\Omega \nabla(\rho_1-\rho_2)\cdot\nabla w dx \\ &+ \int_S (\phi_m(\rho_1+\widetilde{c}_{in}) - \phi_m(\rho_2+\widetilde{c}_{in}))w + \frac{1}{2}\int_{\Gamma_{out}} (\boldsymbol{u}^{m+1}\cdot\boldsymbol{n})(\rho_1-\rho_2)w\end{aligned} \tag{2.97}$$

We estimate each term on the right hand side of (2.97):

$$\frac{1}{\delta t}\int_\Omega (\rho_1-\rho_2)w dx \le \frac{1}{\delta t}\|\rho_1-\rho_2\|_0\|w\|_0 \le \frac{1}{\delta t}\|\rho_1-\rho_2\|_1\|w\|_1 \tag{2.98}$$

$$\begin{aligned}&\int_\Omega (\boldsymbol{u}^{m+1}\cdot\nabla(\rho_1-\rho_2))w dx \le \|\boldsymbol{u}^{m+1}\|_{L^4(\Omega)}\|\nabla(\rho_1-\rho_2)\|_0\|w\|_{L^4(\Omega)} \\ &\le C\|\boldsymbol{u}^{m+1}\|_1\|\rho_1-\rho_2\|_1\|w\|_1\end{aligned} \tag{2.99}$$

$$\begin{aligned}&\int_\Omega (\boldsymbol{u}^{m+1}\cdot\nabla w)(\rho_1-\rho_2) dx \le \|\boldsymbol{u}^{m+1}\|_{L^4(\Omega)}\|\nabla w\|_0\|\rho_1-\rho_2\|_{L^4(\Omega)} \\ &\le C\|\boldsymbol{u}^{m+1}\|_1\|\rho_1-\rho_2\|_1\|w\|_1\end{aligned} \tag{2.100}$$

$$\int_\Omega \nabla(\rho_1-\rho_2)\cdot\nabla w dx \le \|\nabla(\rho_1-\rho_2)\|_0\|\nabla w\|_0 \le \|\rho_1-\rho_2\|_1\|w\|_1 \tag{2.101}$$

Let $x_1, x_2 \in \mathbb{R}$. If $x_1+\widetilde{c}_{in}$, and $x_2+\widetilde{c}_{in} > \frac{1}{2\alpha}$, then $|\overline{\psi}_{,c}(x_1+\widetilde{c}_{in}) - \overline{\psi}_{,c}(x_2+\widetilde{c}_{in})| = 0$. If $x_1+\widetilde{c}_{in} \le \dfrac{1}{2\alpha}$ and $x_2+\widetilde{c}_{in} > \dfrac{1}{2\alpha}$, then

$$\begin{aligned}&|\overline{\psi}_{,c}(x_1+\widetilde{c}_{in}) - \overline{\psi}_{,c}(x_2+\widetilde{c}_{in})| \le |\overline{\psi}_{,cc}(x_1+\widetilde{c}_{in})||x_1-x_2| \\ &\le |1-\alpha(x_1+\widetilde{c}_{in})||x_1-x_2| \le (1+\alpha+\alpha|x_1|)|x_1-x_2|.\end{aligned}$$

doi:10.6342/NTU202200609

If $x_1 + \widetilde{c}_{in}$, and $x_2 + \widetilde{c}_{in} \leq \frac{1}{2\alpha}$, then

$$\begin{aligned}|\overline{\psi}_{,c}(x_1 + \widetilde{c}_{in}) - \overline{\psi}_{,c}(x_2 + \widetilde{c}_{in})| &= |x_1 + \widetilde{c}_{in} - \frac{\alpha}{2}(x_1 + \widetilde{c}_{in})^2 - (x_2 + \widetilde{c}_{in}) + \frac{\alpha}{2}(x_2 + \widetilde{c}_{in})^2| \\ &= |x_1 - x_2 - \frac{\alpha}{2}(x_1 + \widetilde{c}_{in})^2 + \frac{\alpha}{2}(x_2 + \widetilde{c}_{in})^2| \\ &= |x_1 - x_2 - \frac{\alpha}{2}(x_1 + x_2)(x_1 - x_2) - \alpha\widetilde{c}_{in}(x_1 - x_2)| \\ &\leq (1 + \alpha + \frac{\alpha}{2}|x_1| + \frac{\alpha}{2}|x_2|)|x_1 - x_2|.\end{aligned}$$

Now we can conclude that

$$\begin{aligned}&\int_S (\overline{\psi}_{,c}(\rho_1 + \widetilde{c}_{in}) - \overline{\psi}_{,c}(\rho_2 + \widetilde{c}_{in}))w \leq \int_S (1 + \alpha + \frac{\alpha}{2}|\rho_1| + \frac{\alpha}{2}|\rho_2|)|\rho_1 - \rho_2||w| \\ &\leq (1 + \alpha)\|\rho_1 - \rho_2\|_S\|w\|_S + \frac{\alpha}{2}(\|\rho_1\|_{L^3(S)} + \|\rho_2\|_{L^3(S)})\|\rho_1 - \rho_2\|_{L^3(S)}\|w\|_{L^3(S)} \\ &\leq C_1\|\rho_1 - \rho_2\|_1\|w\|_1 + C_2(\|\rho_1\|_1 + \|\rho_2\|_1)\|\rho_1 - \rho_2\|_1\|w\|_1.\end{aligned} \tag{2.102}$$

Now,

$$\begin{aligned}&\int_S \sum_{j=0}^{m} c^j \delta t((\rho_1 + \widetilde{c}_{in}) - (\rho_2 + \widetilde{c}_{in}))w \\ &= \int_S \sum_{j=0}^{m} c^j \delta t(\rho_1 - \rho_2)w \leq \delta t \int_S \sum_{j=0}^{m} |c^j||\rho_1 - \rho_2||w| \\ &\leq \delta t \sum_{j=0}^{m} \|c^j\|_{L^3(S)}\|\rho_1 - \rho_2\|_{L^3(S)}\|w\|_{L^3(S)} \leq C\delta t \sum_{j=0}^{m} \|c^j\|_1\|\rho_1 - \rho_2\|_1\|w\|_1\end{aligned} \tag{2.103}$$

And finally,

$$\begin{aligned}&\int_{\Gamma_{out}} (\boldsymbol{u}^{m+1} \cdot \boldsymbol{n})(\rho_1 - \rho_2)w \leq \int_{\Gamma_{out}} |\boldsymbol{u}^{m+1} \cdot \boldsymbol{n}||\rho_1 - \rho_2||w| \\ &\leq \|\boldsymbol{u}^{m+1}\|_{L^3(\Gamma_{out})}\|\rho_1 - \rho_2\|_{L^3(\Gamma_{out})}\|w\|_{L^3(\Gamma_{out})} \leq C\|\boldsymbol{u}^{m+1}\|_1\|\rho_1 - \rho_2\|_1\|w\|_1\end{aligned} \tag{2.104}$$

doi:10.6342/NTU202200609

Combining (2.98)-(2.104), we have

$$
\begin{aligned}
&|\langle A\rho_1 - A\rho_2, w\rangle| \\
&\leq \left(C_1 + C_2\|\boldsymbol{u}^{m+1}\|_1 + C_3(\|\rho_1\|_1 + \|\rho_2\|_1) + C_4\delta t \sum_{j=0}^{m} \|c^j\|_1 \right) \|\rho_1 - \rho_2\|_1 \|w\|_1
\end{aligned} \tag{2.105}
$$

This completes the proof. Q.E.D.

2.B Error estimates

In this section, we further assume that

$$
\begin{aligned}
&\text{(A1)} \quad \int_0^T \|\partial_{tt} c\|_{-1}^2 dt \leq M_1 \ \text{ for some constant } M_1 \text{ and} \\
&\text{(A2)} \quad \sup_{t\in[0,T]} \|\partial_t c\|_{H^1(\Omega)'} < M_2 \ \text{ for some constant } M_2.
\end{aligned} \tag{2.106}
$$

For convenience, we define

$$
\begin{aligned}
B(u,v) &:= \left(1 + \frac{\alpha i_0^2}{D} u\right) i_0 v, \\
b(u,v,w) &:= \int_S \left(1 + \frac{\alpha i_0^2}{D} u\right) i_0 v w, \\
G(u,v,w) &:= \int_S \frac{\alpha i_0^3}{D} u v w.
\end{aligned} \tag{2.107}
$$

The difference equation for the exact solution of c defined by (2.5) can be expressed as:

$$
\frac{c(t^{m+1}) - c(t^m)}{\delta t} + \boldsymbol{u}^{m+1} \cdot \nabla c(t^{m+1}) - D\Delta c(t^{m+1}) = R^m, \tag{2.108}
$$

where

$$
R^m = \frac{1}{\delta t} \int_{t^m}^{t^{m+1}} (t - t^m) \partial_{tt} c(t) dt \tag{2.109}
$$

doi:10.6342/NTU202200609

Defining $\epsilon^j = c(t^j) - c^j$, the error equation can be expressed by

$$\frac{\epsilon^{m+1} - \epsilon^m}{\delta t} + \boldsymbol{u}^{m+1} \cdot \nabla \epsilon^{m+1} - D\Delta \epsilon^{m+1} = R^m \tag{2.110}$$

subject to the boundary condition

$$\begin{aligned} \epsilon^{m+1} = 0 \ \text{ on } \Gamma_{in}, \qquad \frac{\partial \epsilon^{m+1}}{\partial n} = 0 \ \text{ on } \Gamma_{wall} \cup \Gamma_{out} \\ D\frac{\partial \epsilon^{m+1}}{\partial n} + B(\int_0^{t^{m+1}} c(s)ds, c(t^{m+1})) - B(\sum_{j=0}^{m} c_j \delta t, c^{m+1}) = 0 \ \text{ on } S. \end{aligned} \tag{2.111}$$

The symmetrized weak formulation to (2.108) is

$$\begin{aligned} &\int_\Omega \frac{c(t^{m+1}) - c(t^m)}{\delta t} w + D\int_\Omega \nabla c(t^{m+1}) \cdot \nabla w \\ &+ \frac{1}{2}\int_\Omega [(\boldsymbol{u}^{m+1} \cdot \nabla c(t^{m+1}))w - (\boldsymbol{u}^{m+1} \cdot \nabla w)c(t^{m+1})]dx + \int_{\Gamma_{out}} (\boldsymbol{u}^{m+1} \cdot \boldsymbol{n})c^{m+1} w \\ &+ \int_S \left(1 - \frac{\alpha c^{m+1}}{2} + \frac{\alpha i_0^2}{D}\sum_{j=0}^{m} c^j\right) i_0 c^{m+1} w = \int_\Omega R^m w dx \end{aligned} \tag{2.112}$$

Subtracting (2.112) by (2.35), we have

$$\begin{aligned} &\int_\Omega \frac{\epsilon^{m+1} - \epsilon^m}{\delta t} w dx + D\int_\Omega \nabla \epsilon^{m+1} \cdot \nabla w dx \\ &+ \frac{1}{2}\int_\Omega [(\boldsymbol{u}^{m+1} \cdot \nabla \epsilon^{m+1})w - (\boldsymbol{u}^{m+1} \cdot \nabla w)\epsilon^{m+1}]dx + \int_{\Gamma_{out}} (\boldsymbol{u}^{m+1} \cdot \boldsymbol{n})\epsilon^{m+1} w \\ &- \int_S \frac{\alpha i_0}{2}(c(t^{m+1}) + c^{m+1})\epsilon^{m+1} w + b(\int_0^{t^{m+1}} c(s)ds, c(t^{m+1}), w) \\ &- b(\sum_{j=0}^{m} c^j \delta t, c^{m+1}, w) = \int_\Omega R^m w dx \end{aligned} \tag{2.113}$$

Before investigating the error estimate, some auxiliary results are needed. We collect them in the Remark below:

doi:10.6342/NTU202200609

Remark 2.B.1 We have

$$\begin{aligned} & B(\int_0^{t^{m+1}} c(s)ds, c(t^{m+1})) - B(\sum_{j=0}^{m} c^j \delta t, c^{m+1}) \\ &= \left(1 + \frac{\alpha i_0^2}{D} \sum_{j=0}^{m} c^j \delta t\right) i_0 \epsilon^{m+1} + \frac{\alpha i_0^3}{D} \left[\int_0^{t^{m+1}} c(s)ds - \sum_{j=0}^{m} c^j \delta t\right] c(t^{m+1}) \end{aligned} \tag{2.114}$$

Defining

$$\xi^m = \int_0^{t^{m+1}} c(s)ds - \sum_{j=0}^{m} c^j \delta t \tag{2.115}$$

we have

$$\xi^m = \sum_{j=0}^{m} \epsilon^j \delta t + \phi^m, \tag{2.116}$$

where $\phi^m = \sum_{j=0}^{m} \partial_t c(\theta^j)\delta t^2$ for some $\theta^j \in (t^j, t^{j+1})$. By (2.114), (2.115), (2.116) and letting $w = \epsilon^{m+1}$ in (2.113), we have

$$\begin{aligned} & \frac{1}{\delta t}\|\epsilon^{m+1}\|^2 - \frac{1}{\delta t}\int_\Omega \epsilon^{m+1}\epsilon^m dx + D\|\nabla \epsilon^{m+1}\|^2 + b(\sum_{j=0}^{m} c^j \delta t, \epsilon^{m+1}, \epsilon^{m+1}) \\ & + G(c(t^{m+1}), \sum_{j=0}^{m} \epsilon^j \delta t, \epsilon^{m+1}) + G(c(t^{m+1}), \phi^m, \epsilon^{m+1}) + \int_{\Gamma_{out}} (\boldsymbol{u}^{m+1} \cdot \boldsymbol{n})(\epsilon^{m+1})^2 \\ & - \int_S \frac{\alpha i_0}{2}(c(t^{m+1}) + c^{m+1})(\epsilon^{m+1})^2 = \int_\Omega R^m w dx \end{aligned} \tag{2.117}$$

Multiplying the both sides by δt, we get

$$\begin{aligned} & \|\epsilon^{m+1}\|^2 + D\delta t\|\nabla \epsilon^{m+1}\|^2 + \delta t b(\sum_{j=0}^{m} c^j \delta t, \epsilon^{m+1}, \epsilon^{m+1}) \\ & + \delta t G(c(t^{m+1}), \sum_{j=0}^{m} \epsilon^j \delta t, \epsilon^{m+1}) + \delta t G(c(t^{m+1}), \phi^m, \epsilon^{m+1}) + \delta t \int_{\Gamma_{out}} (\boldsymbol{u}^{m+1} \cdot \boldsymbol{n})(\epsilon^{m+1})^2 \\ & - \delta t \int_S \frac{\alpha i_0}{2}(c(t^{m+1}) + c^{m+1})(\epsilon^{m+1})^2 = \delta t \int_\Omega R^m w dx + \int_\Omega \epsilon^{m+1}\epsilon^m dx \end{aligned} \tag{2.118}$$

Q.E.D.

doi:10.6342/NTU202200609

Theorem 2.B.1 There is a generic constant C such that

$$\|\epsilon^{m+1}\| \leq C\delta t \quad \forall\ 0 \leq m \leq \frac{T}{\delta t} - 1 \tag{2.119}$$

and

$$\|\epsilon^{m+1}\|_1 \leq C\delta t^{\frac{1}{2}} \quad \forall\ 0 \leq m \leq \frac{T}{\delta t} - 1. \tag{2.120}$$

Proof. By a recurrence argument, we are going to show that if the statements (2.119) and (2.120) hold simultaneously for all ϵ^j and for all $j \leq m$, then they hold as well for ϵ^{m+1}. Notice that it is true when $m = 0$.

Defining $G_1 = |G(c(t^{m+1}), \sum_{j=0}^{m} \epsilon^j \delta t, \epsilon^{m+1})|$ and $G_2 = |G(c(t^{m+1}), \phi^m, \epsilon^{m+1})|$, we have the estimates:

$$\begin{aligned} G_1 &\leq \frac{\alpha i_0^3}{D} \sum_{j=0}^{m} \int_S |c(t^{m+1})\epsilon^j \epsilon^{m+1} \delta t| \\ &\leq \frac{\alpha i_0^3}{D} \sum_{j=0}^{m} \int_S |\delta t \epsilon^j \epsilon^{m+1}| \leq \frac{\alpha i_0^3}{D} \left(\sum_{j=0}^{m} \|\epsilon^j\|_S \delta t \right) \|\epsilon^{m+1}\|_S \\ &\leq C \left(\sum_{j=0}^{m} \|\epsilon^j\|_1 \delta t \right) \|\epsilon^{m+1}\|_1 \leq C(m+1)\delta t^{\frac{3}{2}} \|\epsilon^{m+1}\|_1 \leq C\|\epsilon^{m+1}\|\delta t^{\frac{1}{2}}. \end{aligned} \tag{2.121}$$

Using (A2), we have

$$\begin{aligned} G_2 &\leq \frac{\alpha i_0^3}{D} \int_S |c(t^{m+1})\phi^m \epsilon^{m+1}| \leq \frac{\alpha i_0^3}{D} \int_S |\phi^m \epsilon^{m+1}| \\ &\leq \frac{\alpha i_0^3}{D} \|\phi^m\|_S \|\epsilon^{m+1}\|_S \leq C\|\phi^m\|_1 \|\epsilon^{m+1}\|_1 \leq C\delta t^2 \|\epsilon^{m+1}\|_1. \end{aligned} \tag{2.122}$$

doi:10.6342/NTU202200609

By (A1), we have

$$\begin{aligned}
&\delta t\left|\int_\Omega R^m\epsilon^{m+1}dx\right| \\
&\le \frac{D}{4}\delta t\|\epsilon^{m+1}\|_1^2 + C\delta t^{-1}\|R^m\|^2_{H^1(\Omega)'} \\
&= \frac{D}{4}\|\epsilon^{m+1}\|_1^2 + C\delta t^{-1}\left\|\int_{t^m}^{t^{m+1}}(t-t^m)\partial_{tt}c dt\right\|^2_{H^1(\Omega)'} \\
&\le \frac{D}{4}\|\epsilon^{m+1}\|_1^2 + C\delta t^{-1}\int_{t^m}^{t^{m+1}}\|\partial_{tt}c\|^2_{H^1(\Omega)'}dt\int_{t^m}^{t^{m+1}}(t-t^m)^2dt \\
&\le \frac{D}{4}\|\epsilon^{m+1}\|_1^2 + C\delta t^{2}\int_{t^m}^{t^{m+1}}\|\partial_{tt}c\|^2_{H^1(\Omega)'}dt \\
&\le \frac{D}{4}\|\epsilon^{m+1}\|_1^2 + C\delta t^2
\end{aligned} \tag{2.123}$$

$$\begin{aligned}
&b(\sum_{j=0}^m c^j\delta t,\epsilon^{m+1},\epsilon^{m+1}) - \int_S\frac{\alpha i_0}{2}(c(t^{m+1})+c^{m+1})(\epsilon^{m+1})^2 \\
&\ge \int_S\left(1+\frac{\alpha i_0^2}{D}\sum_{j=0}^m c^j\delta t\right)i_0(\epsilon^{m+1})^2 - \int_S\alpha i_0(\epsilon^{m+1})^2 \\
&\ge \int_S\left((1-\alpha)+\frac{\alpha i_0^2}{D}\sum_{j=0}^m c^j\delta t\right)i_0(\epsilon^{m+1})^2 \ge 0.
\end{aligned} \tag{2.124}$$

$$\int_\Omega\epsilon^{m+1}\epsilon^m dx \le \frac{1}{2}\|\epsilon^m\|^2 + \frac{1}{2}\|\epsilon^{m+1}\|^2. \tag{2.125}$$

Combining (2.118), (2.121)-(2.125), and since the boundary term of Γ_{out} in (2.118) is nonnegative, we have

$$(\frac{1}{2}-\frac{1}{4}D\delta t)\|\epsilon^{m+1}\|^2 + \frac{3}{4}D\delta t\|\epsilon^{m+1}\|_1^2 \le C\|\epsilon^{m+1}\|_1\delta t^{\frac{3}{2}} + C\delta t^2. \tag{2.126}$$

This implies (2.120). Now using (2.126) and (2.120), we get (2.119). Q.E.D.

Theorem 2.B.2 (Improved estimate) For $0 \le m \le \dfrac{T}{\delta t} - 1$, we have

$$\delta t\sum_{j=0}^m\|\epsilon^{j+1}\|_1^2 \le C\delta t^2 \tag{2.127}$$

doi:10.6342/NTU202200609

Proof. Putting $w = 2\epsilon^{m+1}$ in (2.118) and using the estimates in Theorem 2.B.1, we have

$$\|\epsilon^{m+1}\|^2 + 2D\delta t\|\nabla\epsilon^{m+1}\|^2 \le 2\delta tC_1\|\epsilon^{m+1}\|_1\left(\sum_{j=0}^{m}\|\epsilon^j\|_1\delta t\right)$$
$$+2C_2\delta t^3\|\epsilon^{m+1}\|_1 + \frac{D}{4}\delta t\|\epsilon^{m+1}\|_1^2 + C_3\delta t^2\int_{t^m}^{t^{m+1}}\|\partial_{tt}c\|^2_{H^1(\Omega)'}dt + \|\epsilon^m\|^2 \tag{2.128}$$

Note that

$$\|\epsilon^{m+1}\|^2 + 2D\delta t\|\epsilon^{m+1}\|_1^2 = (1-2D\delta t)\|\epsilon^{m+1}\|^2 + 2D\delta t\|\epsilon^{m+1}\|_1^2.$$

Taking the sum of (2.128) from 0 to m and using (A1), we have

$$(1-\frac{9}{4}D\delta t)\|\epsilon^{m+1}\|^2 + \frac{7}{4}\sum_{j=0}^{m}D\delta t\|\epsilon^{j+1}\|_1^2 \le \sum_{j=0}^{m}2\delta tC_1\|\epsilon^{j+1}\|_1\left(\sum_{k=0}^{j}\|\epsilon^k\|_1\delta t\right)$$
$$+\sum_{j=0}^{m}2C_2\delta t^3\|\epsilon^{j+1}\|_1 + C_3\delta t^2. \tag{2.129}$$

The first term on the right hand side of (2.129) can be estimated by

$$\sum_{j=0}^{m}2\delta tC\|\epsilon^{m+1}\|_1\left(\sum_{k=0}^{k}\|\epsilon^k\|_1\delta t\right)$$
$$\le \sum_{j=0}^{m}\frac{D}{4}\delta t\|\epsilon^{j+1}\|_1^2 + C\delta t^2\sum_{j=0}^{m}\sum_{k=0}^{j}\|\epsilon^k\|_1^2 \tag{2.130}$$
$$\le \frac{D}{4}\delta t\|\epsilon^{m+1}\|_1^2 + C\delta t\sum_{j=0}^{m}\|\epsilon^j\|_1^2.$$

Similarly, the second term can be estimated by

$$\sum_{j=0}^{m}2C_2\delta t^3\|\epsilon^{m+1}\|_1 \le \sum_{j=0}^{m}2C\delta t^3\left(\frac{1}{2\nu}\|\epsilon^{m+1}\|_1^2 + \frac{\nu}{2}|\Omega|\right)$$
$$\le \nu CT|\Omega|\delta t^2 + \frac{C}{\nu}\delta t^2\sum_{j=0}^{m}\|\epsilon^{m+1}\|_1^2 \tag{2.131}$$
$$\le C\delta t^2 + \frac{D}{4}\delta t\sum_{j=0}^{m}\|\epsilon^j\|_1^2 + \frac{D}{4}\delta t\|\epsilon^{m+1}\|_1^2$$

doi:10.6342/NTU202200609

for every $\nu > 0$.

Finally, employing (2.129)-(2.131), we have

$$\left(1 - \frac{11}{4} D\delta t\right) \|\epsilon^{m+1}\|^2 + \frac{5}{4} D\delta t \sum_{j=0}^{m} \|\epsilon^{j+1}\|_1^2 \leq C_1 \delta t^2 + C_2 \delta t \sum_{j=0}^{m} \|\epsilon^j\|_1^2. \quad (2.132)$$

By induction on m, we can easily show that

$$\frac{5}{4} D\delta t \sum_{j=0}^{m} \|\epsilon^{j+1}\|_1^2 \leq C\delta t^2. \quad (2.133)$$

Q.E.D.

doi:10.6342/NTU202200609

doi:10.6342/NTU202200609

Chapter 3

Simulation on electroless plating problem with gas generation

3.1 Introduction

When emphasizing on micro-scale electroless plating problem, gas generation will be a serious issue. The existence of relatively large bubbles in a microchannel has been an important issue in the study of microfluid[46, 47, 48]. In electroless plating process, the bubbles may prevent electrolyte from going into the region needed to be plated. In view of the trouble caused by bubble generation, we are motivated to understand the mechanism of bubble motion and bubble generation in electroless process. From a theoretical point

doi:10.6342/NTU202200609

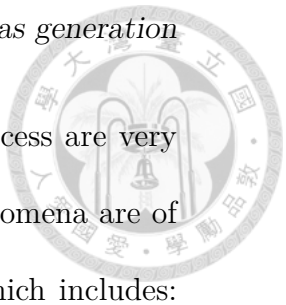

of view, the physical phenomena for describing electroless process are very complicated. In practical simulation, not all the physical phenomena are of interest. Therefore, for the simulation, we chose a system which includes: gas-liquid two phase flow, chemical species transport, surface reaction, and moving boundary caused by deposition.

Numerous papers about modeling and simulation of gas-liquid two phase flow have been published [49, 50, 51, 52, 53]. In terms of how we resolve the motion of the gaseous phase flows, the working models in most of these papers can be sorted into two classes: (i) phase field or level set models where the gas-liquid interface is tracted[17, 20, 23, 54]; (ii) averaged models [55, 56, 25]. Several reasons support our choice for an averaged model: (i) The bubble generation is random, we only know that there is a higher chance of gas generation occurring in regions of higher concentration of dissolving gas; (ii) Even if the bubble generation can be well predicted, vast amounts of bubbles are generated in a short moment for electroless process; furthermore, the computational cost for capturing each bubble is prohibitive; (iii) Interfacial terms (e.g. terms caused by phase change) can be easily estimated if the averaged model is applied (see Appendix A); (iv) it simplifies substantially the modeling.

Experimentally, the bubbles are seen to get stuck somewhere in the microchannel. This indicates that the velocities of two phases are quite different. To allow a disparity of motion between the liquid phase and gaseous

doi:10.6342/NTU202200609

phase, a two velocities model will be used. To our knowledge, such approach is new for incompressible two phase flows in thin microchannels.

A system of linear convection-diffusion equations with additional phase change terms is applied for depicting the concentration profiles of chemical species. We use the mixed potential theory (see for instance [13]) to model the reaction boundary condition describing the electroless process, which is a Robin boundary condition subject to electron balance constraints. We further consider the boundary motion induced by the chemical species deposition on reaction surface. Combining all with the average model for gas-liquid two phase flow, we propose a set of coupled equations for a system which includes gas-liquid fluid motion, chemical species transport and moving boundary to simulate an electroless plating process. Note that, in absence of bubbles, the proposed model reduces to the usual single phase model (i.e. neglecting the existence of gas) which is compatible with previous studies on electroless process such as [57].

For numerical simulations, the Galerkin characteristic method[58] is applied for time discretization. The Finite element method of degree one is used for space discretization. The well-posedness of the numerical scheme for the coupling system is proved. We reproduce a one-dimensional numerical simulation on electroless nickel plating problem to compare with [1]. The numerical code for the full system is implemented as well and we compare the numerical results with a real-world experiment done by one of the authors

doi:10.6342/NTU202200609

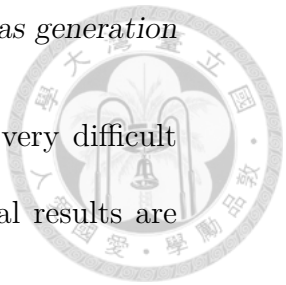

for this purpose. Unfortunately the numerical experiment is very difficult to make and it gave only qualitative results. So the numerical results are compared qualitatively only with the experiment.

So the numerical simulations seems more reliable than experiment and they give detail information on the free boundary and on the speeds and concentrations of the chemical, highly important for the design of commercial systems.

3.2 Modeling equations for liquid-gas flow

Let $\Omega(t)$ be the time-dependent physical domain which is a thin channel between a top and a bottom plate. The boundary of Ω consists of the inlet Γ_{in}, the outlet Γ_{out}, the solid wall Γ_{wall} and the reacting surface $S(t)$ (see Figure 3.1).

3.2.1 Volume averaging

We review the derivation proposed by Ni and Beckermann [24].

Let $\Omega_0(x,t)$ be an small open set to be observed in $\Omega(t)$ and $\Omega_k \subset \Omega_0$ the set occupied by phase k and bounded by the interface $\partial\Omega_k$, which is assumed to be oriented. Assume that $\cup_k \Omega_k = \Omega_0$ and $\Omega_k \cap \Omega_j = 0,\ k \neq j$. Let $\boldsymbol{n}_k$ be a outer normal to $\partial\Omega_k$ and $\boldsymbol{w}_k$ the normal velocity of $\partial\Omega_k$.

Let Ψ be a function of a slow variable x and a fast variable y due to

doi:10.6342/NTU202200609

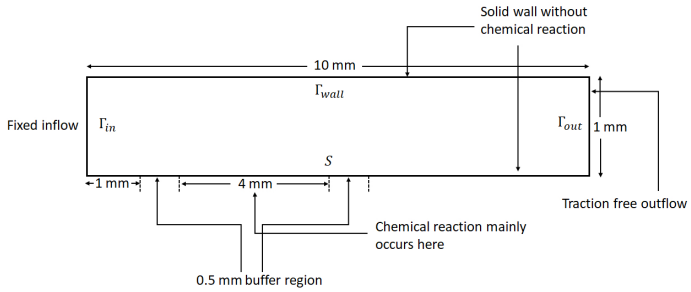

Figure 3.1: The computational domain $\Omega(t)$ for the test problem in Section 3.5.2 is initially a rectangle of size $10mm \times 1mm$. We assume a fixed inflow velocity and given chemical concentrations from the left on Γ_{in}, a solid wall on the top side with a no-slip condition for the velocity, and a traction-free outflow on Γ_{out}. On the bottom side, $S(t)$ is a free boundary and its motion is given by (3.23). However as the reaction site is active mostly for $x \in (1.5mm, 5.5mm)$, we may block the chemical reactions for $x < 1mm$ to avoid a corner singularity at the entrance and also for $x > 6mm$ because experiments show that almost no plating occurs there. In the regions $x \in (1.0mm, 1.5mm) \cup (5.5mm, 6.0mm)$ the numerical simulations may not be accurate due to the singularity caused by the discontinuity in the boundary conditions (see figure 3.17 for details).

doi:10.6342/NTU202200609

the phase change. The volume average of Ψ in phase k is $\langle\Psi\rangle_k(x,t) = \frac{1}{V_0}\int_{\Omega_0(x,t)}\chi_k(y)\Psi(x,y)dy$, where χ_k is the indicator function of the domain of phase k and $V_0 = \int_{\Omega_0} dx$, assumed constant. The intrinsic volume average is defined as

$$\langle\Psi\rangle_k^{(k)} = \frac{V_0}{V_k}\langle\Psi\rangle_k \text{ where } V_k = \int_{\Omega_0}\chi_k dy \tag{3.1}$$

The volume fraction $r_k = \dfrac{V_k}{V_0}$ has the properties $\sum_k r_k = 1$ and $\langle\Psi\rangle_k = r_k\langle\Psi\rangle_k^{(k)}$. Some useful formulas in terms of the averaging are listed below[26, 27]:

$$\left\langle\frac{\partial\Psi}{\partial t}\right\rangle_k = \frac{\partial\langle\Psi\rangle_k}{\partial t} - \frac{1}{V_0}\int_{\partial\Omega_k}\Psi_k\boldsymbol{w}_k\cdot\boldsymbol{n}_k dA, \qquad \langle\nabla\Psi\rangle_k = \nabla\langle\Psi\rangle_k + \frac{1}{V_0}\int_{\partial\Omega_k}\Psi_k\boldsymbol{n}_k dA. \tag{3.2}$$

In principle one should introduce also fast and slow time variables but it is assumed that spatially averaged functions are no longer varying fast in time.

3.2.2 Mass conservation

We consider a gas and a liquid phase. Let ρ_g be the density of gas, ρ_l the density of liquid. We have the mass conservation for both phases (l for liquid and g for gas):

$$\partial_t(r_j\rho_j) + \nabla\cdot(r_j\rho_j\boldsymbol{u}_j) = \dot{S}_j, \quad l = l, g \tag{3.3}$$

where $\dot{S}_g$ is the mass gained owing to the precipitation of dissolved gas, $\dot{S}_l$ is the mass loss when liquid is replaced by the gas, and $\boldsymbol{u}_g(x,t)$, $\boldsymbol{u}_l(x,t)$ are the volume averaged fluid flow of gas and liquid, respectively. Since the mass

doi:10.6342/NTU202200609

gained in gas balances the mass loss in liquid, we have

$$\dot{S}_g = -\dot{S}_l. \tag{3.4}$$

For chemical species, we assume that the ions are transported only by the liquid electrolyte. Let c_s be the volume averaged concentration of metallic ions destined to be deposited on the reacting surface, c_g the volume averaged concentration of dissolved gas and c_k, $k = k_1, \ldots, k_M$ the volume averaged concentration of other chemical species participating to the chemical reaction. The equations for the concentrations are

$$\partial_t(r_l\rho_l c_j) + \nabla\cdot(r_l\rho_l c_j \boldsymbol{u}_l) - \nabla\cdot(r_l\rho_l D_j \nabla c_j) - G_j = 0, \quad j = s, g, k. \tag{3.5}$$

where G_j, $j = s, k$ are interfacial terms due to the phase change. By (3.3) , we can rewrite the above equation by

$$r_l\rho_l(\partial_t c_j + \boldsymbol{u}_l\cdot\nabla c_j) - \nabla\cdot(r_l\rho_l D_j\nabla c_j) - G_j + \dot{S}_l c_j = 0, \quad j = s, g, k. \tag{3.6}$$

where D_j are the diffusion coefficients. In particular, since the gas is consumed by the phase change, we have

$$G_g = -\frac{1}{V_0}\int_{\partial\Omega_l} \rho_l c_g(\boldsymbol{u}_l - \boldsymbol{w}_l)\cdot\boldsymbol{n}_l dA - \rho_l M_g K r_l (c_g - c_{sat})^+ \tag{3.7}$$

by assuming the gas precipitation is linearly dependent on the dissolving gas concentration[59, 60].

doi:10.6342/NTU202200609

In the above, $\boldsymbol{w}_l$ is the interface velocity of $\partial\Omega_l$ and where K is a constant independent of r_g, r_l and c_{sat} is the saturated concentration of the gas, M_g is the reciprocal of the molar mass of the gas,

$$\dot{S}_g = Kr_l(c_g - c_{sat})^+. \tag{3.8}$$

Moreover, G_j, $j = s, k, g$ can be estimated by (see Appendix A)

$$G_j \approx \dot{S}_l c_j, \quad j = s, k, \quad G_g \approx \dot{S}_l c_g - \rho_l M_g K r_l (c_g - c_{sat})^+. \tag{3.9}$$

For incompressible fluids, a volume conservation is derived from (3.3):

$$\sum_{\alpha=g,l} \frac{1}{\rho_\alpha} \left[\partial_t(r_\alpha \rho_\alpha) + \nabla \cdot (r_\alpha \rho_\alpha \boldsymbol{u}_\alpha) - \dot{S}_\alpha\right] = 0. \tag{3.10}$$

By (3.4), the above reduces to

$$\nabla \cdot (r_g \boldsymbol{u}_g + r_l \boldsymbol{u}_l) = \dot{S}_g \left(\frac{1}{\rho_g} - \frac{1}{\rho_l}\right). \tag{3.11}$$

Recall that the physical domain is occupied either by gas or liquid, therefore $r_g(t) + r_l(t) = 1$ at all times.

3.2.3 Equations of motion

Let μ_g, μ_l be the viscosity of the gas and the liquid, respectively. The volume averaged Navier-Stokes equations are used for momentum balance (see [24]):

$$\partial_t(r_j \rho_j \boldsymbol{u}_j) + \nabla \cdot (r_j \rho_j \boldsymbol{u}_j \otimes \boldsymbol{u}_j) + r_j \nabla p_j - \mu_j \nabla \cdot (r_j D(\boldsymbol{u}_j)) + M_{D,j} = \boldsymbol{F}_j, \quad j = g, l \tag{3.12}$$

doi:10.6342/NTU202200609

where $p_j,\ M_{D,j},\ \boldsymbol{F}_j,\ j = l, g$ are pressure, drag force terms[25, 24]

$$\begin{aligned} M_{D,g} &= C_D r_g |\boldsymbol{u}_g - \boldsymbol{u}_l|(\boldsymbol{u}_g - \boldsymbol{u}_l) \\ M_{D,l} &= C_D r_g |\boldsymbol{u}_g - \boldsymbol{u}_l|(\boldsymbol{u}_l - \boldsymbol{u}_g), \end{aligned} \tag{3.13}$$

where C_D is drag coefficient, and interfacial terms $\boldsymbol{F}_j = -\frac{1}{V_0}\int_{\partial\Omega_j} \rho_j \boldsymbol{u}_j(\boldsymbol{u}_j - \boldsymbol{w}_j)\cdot \boldsymbol{n}_j dA,\ j = l, g$, $D(\boldsymbol{v}) = \nabla \boldsymbol{v} + (\nabla \boldsymbol{v})^T$ is the viscous stress tensor for any vector-valued function $\boldsymbol{v}$; $\boldsymbol{F}_j$, $j = l, g$ can be estimated by (see Appendix A)

$$\boldsymbol{F}_g \approx \dot{S}_g \boldsymbol{u}_g, \quad \boldsymbol{F}_l \approx \dot{S}_l \boldsymbol{u}_l, \tag{3.14}$$

In view of (3.11), following [61, 62], we assume a constitutive relation $p = p_l = p_g$ in order to close the system of equations. The velocity fields of both phases are assumed to be 0 outside their own single phase region, respectively. Consequently, and by (3.3), (3.12), the momentum equations simplify to

$$\begin{aligned} r_j \rho_j(\partial_t \boldsymbol{u}_j + (\boldsymbol{u}_j \cdot \nabla)\boldsymbol{u}_j) + r_j \nabla p - \mu_j \nabla \cdot (r_j D(\boldsymbol{u}_j)) + \gamma_j C_D r_g |\boldsymbol{u}_g - \boldsymbol{u}_l|(\boldsymbol{u}_g - \boldsymbol{u}_l) = 0, \\ j = g, l, \quad \text{with } \gamma_g = 1 \text{ and } \gamma_l = -1 \end{aligned} \tag{3.15}$$

3.2.4 Boundary conditions

We consider a fluid flow from an input boundary Γ_{in} to an output boundary Γ_{out} with a solid wall at the bottom, Γ_{wall}:

$$\begin{aligned} &\boldsymbol{u}_j = \boldsymbol{u}_{in} \quad \text{on } \Gamma_{in}, \qquad \boldsymbol{u}_j = 0 \quad \text{on } \Gamma_{wall}, \\ &-\mu_j D(\boldsymbol{u}_j)\cdot \boldsymbol{n} + p\boldsymbol{n} = 0 \quad \text{on } \Gamma_{out}, \quad j = l, g. \end{aligned} \tag{3.16}$$

doi:10.6342/NTU202200609

The boundary conditions for r_j, $j = g, l$ are

$$\begin{aligned} r_g = \epsilon, \quad r_l = 1 - \epsilon \ \text{ on } \Gamma_{in}, \\ \frac{\partial r_g}{\partial n} = \frac{\partial r_l}{\partial n} = 0 \ \text{ on } \partial\Omega \setminus \Gamma_{in}, \end{aligned} \tag{3.17}$$

where ϵ is a fixed positive small constant.

The boundary conditions for the concentrations of chemical species are, with $c_{j,in}$ given:

$$c_j = c_{j,in} \quad \text{on } \Gamma_{in}, \qquad \frac{\partial c_j}{\partial n} = 0 \quad \text{on } \Gamma_{wall} \cup \Gamma_{out}, \quad j = s, g, k \tag{3.18}$$

With F the Faraday constant, and z the atomic number of the material.

Referring to Figure 3.2, if $S(t)$ is the reaction surface , we denote $S_l(t) \subset S(t)$ the region occupied by the liquid and $S_g(t) := S(t) \setminus S_l(t)$ the region occupied by gas. Choosing an arbitrary subset $W \subset S(t)$, the surface reaction takes place only on $W \cap S_l(t)$. Assuming that the concentration profile is uniform near the small region W, we have: $-\int_W \rho_l D_j \frac{\partial c_j}{\partial n} dA = \int_{W \cap S_l(t)} \rho_l \frac{|I_j|}{z_j F} dA$. Therefore by dividing both sides by $\int_W 1 dA$:

$$-D_j \frac{\partial c_j}{\partial n} = \frac{|I_j|}{z_j F}, \quad j = s, k, \qquad -D_g \frac{\partial c_g}{\partial n} = -\frac{\beta |I_s|}{z_s F} \tag{3.19}$$

for a positive number β indicating the chemical equivalence for gaseous molecular generation.

In the above, I_j is the current density satisfying the Butler-Volmer equation

$$I_j = i_j(E_{mix}) c_j^{\kappa_j} := L_j \Big[\exp\left(\frac{\alpha_j z_j F (E_{mix} - E_j)}{R\theta} \right) - \exp\left(\frac{-\beta_j z_j F (E_{mix} - E_j)}{R\theta} \right) \Big] c_j^{\kappa_j}, \quad j = s, k, \tag{3.20}$$

doi:10.6342/NTU202200609

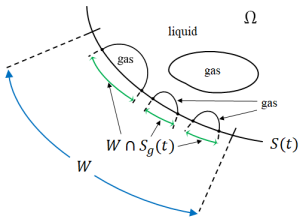

Figure 3.2: The reaction surface.

where R is the gas constant, E_j are the chemical potentials of species j, θ is the temperature, α_j, β_j, L_j, κ_j are constants, E_{mix} is given by writing electrical neutrality :

$$I_s + \sum_k I_k = 0. \tag{3.21}$$

On $S(t)$, the fluid velocity induced by the deposition is

$$\boldsymbol{u}_g = \boldsymbol{u}_l = \frac{r_l V_s |I_s|}{z_s F} \boldsymbol{n}. \tag{3.22}$$

where V_s is a constant. Hence $S(t)$ moves according to

$$\dot{x}(t) = (\boldsymbol{u}_g \cdot \mathbf{n})\mathbf{n}|_{x(t)}, \quad x(t) \in S(t) \tag{3.23}$$

3.2.5 Single phase flow

If there is no gaseous phase in the system and no dissolved gas in liquid, i.e. $r_g = c_g = 0$, then $\boldsymbol{u} = \boldsymbol{u}_l$ and $\dot{S}_g = 0$ and mass conservation reduces to $\nabla \cdot \boldsymbol{u} = 0$. The convection-diffusion of chemicals become,

$$\partial_t c_j + \boldsymbol{u} \cdot \nabla c_j - D_j \Delta c_j = 0, \quad j = s, k, \tag{3.24}$$

and the fluid system reduce to the Navier-Stokes equations:

$$\rho_l(\partial_t \boldsymbol{u} + (\boldsymbol{u} \cdot \nabla)\boldsymbol{u}) - \mu_l \Delta \boldsymbol{u} + \nabla p = 0, \qquad \nabla \cdot \boldsymbol{u} = 0. \tag{3.25}$$

doi:10.6342/NTU202200609

The above system of equations exactly describes the chemical species transported by the fluid flow satisfying the incompressible Navier-Stokes equation.

3.3 Numerical method

3.3.1 Notations

If $f \in \mathbb{R}$, we denote by $f^+ := \max(f, 0)$ and by $f^- := -\min(f, 0)$. We denote by $\|\cdot\|_{L^p} := \|\cdot\|_{L^p(\Omega(t))}$ the L^p norm on $\Omega(t)$, $\|\cdot\|_{W^{k,p}} := \|\cdot\|_{W^{k,p}(\Omega(t))}$ the $W^{k,p}$ norm on $\Omega(t)$, and $\|\cdot\|_{H^k} = \|\cdot\|_{W^{k,2}}$, $0 \le k \le +\infty$, $1 \le p \le +\infty$. Remembering that $c_k(x,t)$ is a vector, let us denote $C = (c_s, c_k^T, c_g)^T$.

We assume the densities ρ_j constant and denote $\alpha_j = r_j \rho_j$ and the kinematic viscosities $\nu_j = \mu_j/\rho_j$. The system is

$$\partial_t \alpha_j + \boldsymbol{u}_j \cdot \nabla \alpha_j + \alpha_j \nabla \cdot \boldsymbol{u}_j - \alpha_l \frac{\gamma_j K}{\rho_l}(c_g - c_{sat})^+ = 0, \quad j = l, g \tag{3.26}$$

$$\alpha_j \left(\partial_t \boldsymbol{u}_j + \boldsymbol{u}_j \cdot \nabla \boldsymbol{u}_j + \rho_j^{-1} \nabla p\right) - \nu_j \nabla \cdot (\alpha_j D(\boldsymbol{u}_j)) + \gamma_j C_D r_g |\boldsymbol{u}_g - \boldsymbol{u}_l|(\boldsymbol{u}_g - \boldsymbol{u}_l) = 0, \quad j = g, l \tag{3.27}$$

$$\alpha_l(\partial_t C + \boldsymbol{u}_l \cdot \nabla C) - \nabla \cdot (\alpha_l \boldsymbol{D} \cdot \nabla C) + (0, 0, M_g K \alpha_l (c_g - c_{sat})^+)^T = 0, \tag{3.28}$$

where $\boldsymbol{D}$ is the appropriate diffusion matrix compatible with (3.15). In addition as $\dot{S}_g = -\dot{S}_l = K\alpha_l(c_g - c_{sat})^+/\rho_l$, we may use the redundant equation (3.11):

$$\nabla \cdot \left(\frac{\alpha_g}{\rho_g}\boldsymbol{u}_g + \frac{\alpha_l}{\rho_l}\boldsymbol{u}_l\right) = \dot{S}_g \left(\frac{1}{\rho_g} - \frac{1}{\rho_l}\right). \tag{3.29}$$

doi:10.6342/NTU202200609

3.3.2 Semi-discrete schemes

Let T be the final time and δt a time step. We denote by ϕ^m, $m = 0, 1, \ldots, N := T/\delta t$ the numerical solution of any physical quantity ϕ at time $m\delta t$. Convection terms are approximated in time by the method of characteristics. Let $X_j^m(x) \approx x - \boldsymbol{u}_j^m(x)\delta t$. Then

$$(\partial_t \alpha_j + \boldsymbol{u}_j \cdot \nabla \alpha_j)|_{x,t=t^{m+1}} \approx \frac{1}{\delta t}\left(\alpha_j^{m+1}(x) - \alpha^m(X_j^m(x))\right).$$

Consider the following scheme

$$\frac{1}{\delta t}(\alpha_l^{m+1} - \alpha_l^m \circ X_l^m) + \alpha_l^{m+1}\left(\nabla \cdot \boldsymbol{u}_l^m + \frac{1}{\rho_l}K(c_g^m - c_{sat})^+\right) = 0, \tag{3.30}$$

$$r_l^{m+1} = \alpha_l^{m+1}/\rho_l, \quad r_g^{m+1} = 1 - r_l^{m+1}, \quad \alpha_g^{m+1} = \rho_g r_g^{m+1} \tag{3.31}$$

$$\frac{1}{\delta t}\alpha_j^{m+1}(\boldsymbol{u}_j^{m+1} - \boldsymbol{u}_j^m \circ X_j^m) + \rho_j^{-1}\alpha_j^{m+1}\nabla p^{m+1} - \nu_j \nabla \cdot (\alpha_j^{m+1} D(\boldsymbol{u}_j^{m+1}))$$
$$+\gamma_j \rho_g^{-1} C_D \alpha_g^{m+1} |\boldsymbol{u}_g^{m+1} - \boldsymbol{u}_l^{m+1}|(\boldsymbol{u}_g^{m+1} - \boldsymbol{u}_l^{m+1}) = 0, \quad j = g, l, \tag{3.32}$$

$$\nabla \cdot (\rho_g^{-1}\alpha_g^{m+1}\boldsymbol{u}_g^{m+1} + \rho_l^{-1}\alpha_l^{m+1}\boldsymbol{u}_l^{m+1}) = {\rho_l}^{-1} K \alpha_l^{m+1}(c_g^{m+1} - c_{sat})^+ \left(\rho_g^{-1} - \rho_l^{-1}\right), \tag{3.33}$$

$$\frac{1}{\delta t}\alpha_l^{m+1}(C^{m+1} - C^m \circ X_j^m) - \nabla \cdot (\alpha_l^{m+1}\boldsymbol{D} \cdot \nabla C^{m+1}) + (0, 0, M_g K \alpha_l^m (c_g^m - c_{sat})^+)^T = 0, \tag{3.34}$$

For electroless plating the domain is $\Omega^m = \{(x, y) \ : \ 0 < y < y^m(x), \ x \in (0, L)\}$, so it is updated by

$$y^{m+1}(x) = y^m(x) + \delta t {u_g}_2^{m+1}(x), \quad x \in (0, L)$$

doi:10.6342/NTU202200609

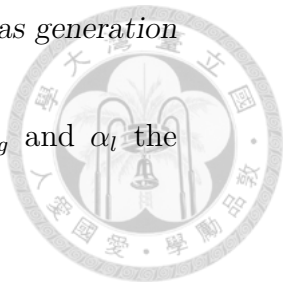

Remark 3.3.1 Because of the asymmetrical treatment of α_g and α_l the scheme (3.30) does *not* imply that

$$\frac{1}{\delta t}(\alpha_g^{m+1} - \alpha^m \circ X_g^m) + \alpha_g^{m+1}\nabla \cdot \boldsymbol{u}_g^m = \rho_l^{-1}\alpha_l^{m+1}K(c_g^m - c_{sat})^+. \tag{3.35}$$

However, by (3.30),(3.31), (3.33), we have

$$\begin{aligned}
&\frac{1}{\delta t}(\alpha_g^{m+1} - \alpha_g^m \circ X_g^m) + \alpha_g^{m+1}\nabla \cdot \boldsymbol{u}_g^m + \frac{\rho_g}{\rho_l}(\alpha_l^{m+1} - \alpha_l^m)\nabla \cdot (\boldsymbol{u}_l^m - \boldsymbol{u}_g^m) \\
&+ \frac{1}{\delta t}(\alpha_g^m \circ X_g^m - \alpha_g^m \circ X_l^m) + (\boldsymbol{u}_g^m - \boldsymbol{u}_l^m) \cdot \nabla \alpha_g^m \\
&= \rho_l^{-1}\alpha_l^{m+1}K(c_g^m - c_{sat})^+ + \rho_l^{-1}(\frac{\rho_g}{\rho_l} - 1)(\alpha_l^{m+1} - \alpha_l^m)K(c_g^m - c_{sat})^+.
\end{aligned} \tag{3.36}$$

By a Taylor expansion at x, we obtain

$$\alpha_g^m(X_l^m(x)) - \alpha_g^m(X_g^m(x)) = \delta t(\boldsymbol{u}_g^m - \boldsymbol{u}_l^m) \cdot \nabla \alpha_g^m(x) + O(\delta t^2), \tag{3.37}$$

and

$$\alpha_l^{m+1} - \alpha_l^m = -\delta t(\boldsymbol{u}_l \cdot \nabla \alpha_l^m + \alpha_l^{m+1}\nabla \cdot \boldsymbol{u}_l^m) - \delta t K \alpha_l^{m+1}(c_g^m - c_{sat})^+ + O(\delta t^2). \tag{3.38}$$

Plugging (3.37) and (3.38) into (3.36), we have

$$\frac{1}{\delta t}(\alpha_g^{m+1} - \alpha_g^m \circ X_g^m) + \alpha_g^{m+1}\nabla \cdot \boldsymbol{u}_g^m = \rho_l^{-1}\alpha_l^{m+1}K(c_g^m - c_{sat})^+ + O(\delta t). \tag{3.39}$$

So the scheme is consistent with the equation for α_g.

3.3.3 Positivity

Positivity of α_l^{m+1} holds only if δt is small enough. When positivity is required absolutely, an $O(\delta t)$ modification of (3.30) forces the positivity of

doi:10.6342/NTU202200609

α_l:

$$\frac{1}{\delta t}\left(\alpha_l^{m+1}(x)-\alpha_l^m(X_l^m(x))\right)+\alpha_l^{m+1}\left(\nabla\cdot\boldsymbol{u}_l^m+\frac{1}{\rho_l}K(c_g^m-c_{sat})^+\right)^+ = \alpha_l^m\left(\nabla\cdot\boldsymbol{u}_l^m+\frac{1}{\rho_l}K(c_g^m-c_{sat})^+\right)^- . \tag{3.40}$$

Indeed assume that α_l^m is strictly positive, or more precisely that $\alpha_l^m \geq \epsilon > 0$ for all x; then we have

$$\alpha_l^{m+1}\left[1+\delta t(\nabla\cdot\boldsymbol{u}_l^m+\frac{1}{\rho_l}K(c_g^m-c_{sat})^+)^+\right] = \alpha_l^m(X_l^m)+\delta t\alpha_l^m\left[\nabla\cdot\boldsymbol{u}_l^m+\frac{1}{\rho_l}K(c_g^m-c_{sat})^+\right]^- \geq \epsilon(1+\delta t(\nabla\cdot\boldsymbol{u}_l^m+\frac{1}{\rho_l}K(c_g^m-c_{sat})^+)^-). \tag{3.41}$$

1. Let us show first that (3.30) generates a bounded sequence $\{\alpha_l^m\}_{m=1..N}$.

   For clarity we assume homogeneous data at the boundaries. With simplified notations

   $$\frac{1}{\delta t}(\alpha^{m+1}-\alpha^m\circ X^m)+\alpha^{m+1}\left(\nabla\cdot\boldsymbol{u}^m+\phi^m\right)=0$$

   A multiplication by α^{m+1} and an integration on Ω^{m+1} leads to

   $$\|\alpha^{m+1}\|_{L^2}^2=\int_{\Omega^{m+1}}\left[\alpha^{m+1}\left(\alpha^m\circ X^m-\delta t\left(\alpha^{m+1}\nabla\cdot\boldsymbol{u}^m+\phi^m\right)\right)\right]dx$$

   By the Cauchy Schwarz inequality and the positivity of ϕ^m,

   $$\|\alpha^{m+1}\|_{L^2}^2\leq\|\alpha^{m+1}\|_{L^2}\left(\int_{\Omega^{m+1}}\left[\alpha^m\circ X^m-\delta t\alpha^{m+1}\nabla\cdot\boldsymbol{u}^m\right]^2dx\right)^{\frac{1}{2}}.$$

   The inverse of the determinant of the Jacobian of the transformation $x\mapsto X^m(x)$ is $1+\delta t\nabla\cdot u+O(\delta t^2)$; therefore, for any smooth function f, in particular with $f=\alpha^m\circ X^m-\delta t\alpha^{m+1}\nabla\cdot\boldsymbol{u}^m=\alpha^m\circ X^m(1-$

doi:10.6342/NTU202200609

$\delta t \nabla \cdot \boldsymbol{u}^m \circ X^m + O(\delta t^2))$,

$$\int_{\Omega^{m+1}} f^m \circ X^m = \int_{\Omega^m} f^m (1 + \delta t \nabla \cdot \boldsymbol{u}^m + O(\delta t^2)) dx$$

$$\Rightarrow \qquad \|\alpha^{m+1}\|_{L^2} \leq \|\alpha^m\|_{L^2} (1 + C(\|\nabla^2 \boldsymbol{u}^m\|_{L^\infty}) \delta t^2).$$

where $C()$ is a generic constant bounded by the Hessian of $\boldsymbol{u}^m$. Thus $\{\alpha_l^m\}_{m=1..N}$ is bounded.

2. Stability of the scheme for C is shown by the same argument.

3. Stability of the scheme for $\boldsymbol{u}_g$ and $\boldsymbol{u}_l$ is a consequence of a similar argument combined with the Ladhyzenskaya-Babuska-Brezzi saddle point theory (LBB) [63].

We denote by $(\cdot, \cdot)$ the L^2 inner product. For tensor-valued functions such that $\boldsymbol{f}, \boldsymbol{g} \in L^2(\Omega(t))^{mn}$, $m, n \in \mathbb{N}^+$, $(\boldsymbol{f}, \boldsymbol{g}) = \sum_{i=1}^m \sum_{j=1}^n (f_{ij}, g_{ij})$. With self explanatory notations, the equations for the velocities (3.32),(3.33) are written in variational form as:

Find $\boldsymbol{u}_g, \boldsymbol{u}_l$ and p satisfying the Dirichlet conditions and such that, $\forall \widehat{\boldsymbol{v}}_g, \widehat{\boldsymbol{v}}_l \in \boldsymbol{V}_0^{m+1} := \left(H_0^1(\Omega^{m+1})\right)^2$ and $\forall \widehat{q} \in P^{m+1} := L^2(\Omega^{m+1})/\mathbb{R}$,

$$(\beta_g \boldsymbol{u}_g, \widehat{\boldsymbol{v}}_g) + (\beta_l \boldsymbol{u}_l, \widehat{\boldsymbol{v}}_l) + \frac{1}{2}(\alpha_g D(\boldsymbol{u}_g), D(\widehat{\boldsymbol{v}}_g)) + \frac{1}{2}(\alpha_l D(\boldsymbol{u}_l), D(\widehat{\boldsymbol{v}}_l))$$
$$- \left(p, \nabla \cdot (\frac{\alpha_g}{\rho_g} \widehat{\boldsymbol{v}}_g + \frac{\alpha_l}{\rho_l} \widehat{\boldsymbol{v}}_l)\right) + \left(\widehat{q}, \nabla \cdot (\frac{\alpha_g}{\rho_g} \boldsymbol{u}_g + \frac{\alpha_l}{\rho_l} \boldsymbol{u}_l)\right) = (\boldsymbol{L}_g, \widehat{\boldsymbol{v}}_g) + (\boldsymbol{L}_l, \widehat{\boldsymbol{v}}_l) + (\widehat{q}, f)\,. \tag{3.42}$$

where, for $j = g, l$, $\alpha_j := \alpha_j^{m+1}$, $\beta_j := \frac{1}{\delta t}\alpha_j + \frac{C_D}{\rho_g}\alpha_g |\boldsymbol{u}_g^m - \boldsymbol{u}_l^m|$,

$$\boldsymbol{L}_j := \frac{1}{\delta t}\alpha_j \boldsymbol{u}_l^m \circ X_j^m + \frac{C_D}{\rho_g}\alpha_g |\boldsymbol{u}_g^m - \boldsymbol{u}_l^m| \boldsymbol{u}_{!j}^m, \quad f := {\rho_l}^{-1} K \alpha_l (c_g^{m+1} - c_{sat})^+ \left(\rho_g^{-1} - \rho_l^{-1}\right). \tag{3.43}$$

doi:10.6342/NTU202200609

and where $!g = l,\ !l = g$.

Note that the above is a semi-linearization of (3.32),(3.33). However in algorithm 1 below, the nonlinear problem is solved by an iterative fixed point which uses (3.42)-(3.43).

The LBB theorem says that the solution of (3.42) exists and is unique because, for every $p \in P^{m+1}$ there is a (non-unique) $\boldsymbol{w} \in \boldsymbol{V}_0^{m+1}$ with

$$(\nabla \cdot \boldsymbol{w}, \widehat{q}) = (f, \widehat{q}), \quad \forall \widehat{q} \in P^{m+1},$$

provided that $\int_{\Gamma_{in}} \boldsymbol{u}_{in} \cdot \boldsymbol{n} = \int_{\Omega^{m+1}} f dx$. Let us show stability in the special case $f = 0$ because one can always subtract $\boldsymbol{w}$ from $\frac{\alpha_g}{\rho_g}\boldsymbol{u}_g + \frac{\alpha_l}{\rho_l}\boldsymbol{u}_l$ so as to work with $\boldsymbol{u}_{g,in} = \boldsymbol{u}_{l,in} = 0$ and $f = 0$.

Thus, setting $\widehat{\boldsymbol{v}}_g = \boldsymbol{u}_g$, $\widehat{\boldsymbol{v}}_l = \boldsymbol{u}_l$ and $\widehat{q} = p$ leads to

$$\frac{1}{\delta t}\left\|\sqrt{\alpha_g}\boldsymbol{u}_g\right\|_{L^2}^2 + \frac{1}{2}\left\|\sqrt{\alpha_g}D(\boldsymbol{u}_g)\right\|_{L^2}^2 + \frac{1}{\delta t}\left\|\sqrt{\alpha_l}\boldsymbol{u}_l\right\|_{L^2}^2 + \frac{1}{2}\left\|\sqrt{\alpha_l}D(\boldsymbol{u}_l)\right\|_{L^2}^2 \leq (\boldsymbol{L}_g, \boldsymbol{u}_g) + (\boldsymbol{L}_l, \boldsymbol{u}_l)\,. \tag{3.44}$$

By the same argument used above, it implies that $\boldsymbol{u}_j,\ j = g, l$ is bounded. Indeed, assuming $\alpha^m \geq 0$,

$$\begin{aligned}
&\delta t\,(\boldsymbol{L}_j, \boldsymbol{u}_j) = \int_{\Omega^{m+1}} \alpha_j \boldsymbol{u}_j^m \circ X_j^m \cdot \boldsymbol{u}_j dx \leq \left\|\sqrt{\alpha_j}\boldsymbol{u}_j\right\|_{L^2} \left(\int_{\Omega^{m+1}} \alpha_j \left|\boldsymbol{u}_j^m \circ X_j^m\right|^2 dx\right)^{\frac{1}{2}} \\
&= \left\|\sqrt{\alpha_j}\boldsymbol{u}_j\right\|_{L^2} \left(\int_{\Omega^{m+1}} \left(\alpha_j^m \circ X_j^m - \alpha\delta t(\nabla \cdot \boldsymbol{u}_l^m + \frac{1}{\rho_l}K(c_g^m - c_{sat})^+)\right) \left|\boldsymbol{u}_j^m \circ X_j^m\right|^2 dx\right)^{\frac{1}{2}} \\
&\leq \left\|\sqrt{\alpha_j}\boldsymbol{u}_j\right\|_{L^2} \left(\int_{\Omega^{m+1}} \left(\alpha_j^m \circ X_j^m - \alpha\delta t\nabla \cdot \boldsymbol{u}_l^m\right) \left|\boldsymbol{u}_j^m \circ X_j^m\right|^2 dx\right)^{\frac{1}{2}} \\
&\leq \left\|\sqrt{\alpha_j}\boldsymbol{u}_j\right\|_{L^2} \left(\int_{\Omega^{m+1}} \alpha_j^m \circ X_j^m \left(1 - \delta t\nabla \cdot \boldsymbol{u}_l^m + O(\delta t^2)\right) \left|\boldsymbol{u}_j^m \circ X_j^m\right|^2 dx\right)^{\frac{1}{2}} \\
&= \left\|\sqrt{\alpha_j}\boldsymbol{u}_j\right\|_{L^2} \left(\int_{\Omega^m} \left(\alpha_j^m(1 + O(\delta t^2))\right) \left|\boldsymbol{u}_j^m\right|^2 dx\right)^{\frac{1}{2}}
\end{aligned}$$

doi:10.6342/NTU202200609

$$\leq \left\|\sqrt{\alpha_j}\boldsymbol{u}_j\right\|_{L^2}(1+\delta t^2 C(\|c_g^m\|_{L^\infty},\|\nabla^2\boldsymbol{u}_l^m\|_{L^\infty}))\left\|\sqrt{\alpha_j^m}\boldsymbol{u}_j^m\right\|_{L^2} \tag{3.45}$$

for some generic constant C depending on $\|c_g^m\|_{L^\infty}$ and $\|\nabla^2\boldsymbol{u}_l^m\|_{L^\infty}$.

Finally, we obtain

$$|||\boldsymbol{u}_g^{m+1},\boldsymbol{u}_l^{m+1}|||_{m+1}\leq(1+C\delta t^2)|||\boldsymbol{u}_g^m,\boldsymbol{u}_l^m|||_m+\delta t\frac{C_D}{\rho_g}\|\frac{\alpha_g}{\alpha_j^m}(\boldsymbol{u}_g^m-\boldsymbol{u}_l^m)\|_{L^\infty}|||\boldsymbol{u}_g^m,\boldsymbol{u}_l^m|||_m \tag{3.46}$$

where

$$|||\boldsymbol{u}_g,\boldsymbol{u}_l|||_m^2:=\sum_{j=g,l}\left\|\sqrt{\alpha_{j,h}^m}\boldsymbol{u}_j\right\|_{L^2}^2+\tfrac{1}{2}\delta t\left\|\sqrt{\alpha_{l,h}^m}D(\boldsymbol{u}_j)\right\|_{L^2}^2,\quad m=0,\ldots,N.$$

This estimate is optimal, but for the constant C which is the drawback of the characteristic method and for the L^∞ norm which is consequence of the unsophisticated treatment of the nonlinearity. Nevertheless, would these two be bounded, the scheme would be H^1 stable.

4. Note that we have swept under the rug the fact that at level m the domain of definition of the functions is Ω^m and at level $m+1$ it is Ω^{m+1}. The problem can be solved but at the cost of difficult notations and iterations between y^{m+1} and $\boldsymbol{u}^{m+1}$; for details see [64].

3.4 Finite element implementation

For simplicity, the physical domain $\Omega(t)$ is assumed to be a two-dimensional polygonal domain.

doi:10.6342/NTU202200609

3.4.1 Mesh

Let $\{\mathcal{K}_h(t)\}_{h>0}$ be an affine, shape regular (in the sense of Ciarlet[65]) family of mesh conforming to $\Omega(t)$. The conforming Lagrange finite element space of degree p on $\Omega(t)$ is

$$X^p_{h,t} = \{v \in C^0(\Omega(t)) : \ v|_K \in P^p, \ \forall K \in \mathcal{K}_h(t)\}, \tag{3.47}$$

where P^p is the space of polynomials of degree p of $\mathbb{R}^2$.

Let $\{\phi_1, \dots \phi_{N_q}\}$ be the nodal Lagrange basis of $X^1_{h,t}$. If the vertices are denoted by $\{\boldsymbol{q}^i\}_1^{N_q}$, then $\phi_i(\boldsymbol{q}_j) = \delta_{ij}$. Let S_i be the support of ϕ_i and let $S_{ij} := S_i \cap S_j$. If E is a union of triangles, define $\mathcal{I}(E) := \{i \in \{1, \dots, N_q\} : \ |S_i \cap E| \neq 0\}$. Finally, the local minimum mesh size of $K \in \mathcal{K}_h(t)$ is $h_K(t) := 1/\max_{i\in\mathcal{I}(K)} \|\nabla\phi_i\|_{L^\infty(K)}$, and the global minimum mesh size is $h(t) := \min_{K\in\mathcal{K}_h} h_K(t)$.

We assume that the connectivity of the mesh $\mathcal{K}_h(t)$ never changes with time.

3.4.2 Spatial discretization

We use the Hood-Taylor element: the velocities are in $\boldsymbol{V}_h(t) := (X^2_{h,t})^2$ and the pressure is in $P_h(t) := X^1_{h,t}$. For the volume fractions and the concentrations we use also $P_h(t)$.

Recall that the nodes of $X^2_{h,t}$ are the vertices and the middle of the edges. Denote by $\{\psi_1, \dots, \psi_{N_a}\}$ the nodal Lagrange basis of associated with the

doi:10.6342/NTU202200609

nodes $\{\boldsymbol{a}_1, \ldots, \boldsymbol{a}_{N_a}\}$ for $X^2_{h,t}$. For convenience, we define $\Omega^m := \Omega(t^m)$, $P^m_h = X^1_{h,t^m}$ and $\boldsymbol{V}^m_h = (X^2_{h,t^m})^2$.

On the boundaries where Dirichlet conditions are set, the functions are known. We denote P^m_{0h} and $\boldsymbol{V}^m_{0h}$, the corresponding spaces where basis functions attached to a Dirichlet node are removed.

Volume fractions

Given $\alpha^m_{l,h}, c^m_{g,h} \in P^m_h$ and $\boldsymbol{u}^m_{l,h} \in \boldsymbol{V}^m_h$, find $\alpha^{m+1}_{l,h} \in P^{m+1}_h$ satisfying the Dirichlet boundary conditions and such that

$$\frac{1}{\delta t}\left(\alpha^{m+1}_{l,h} - \alpha^m_{l,h} \circ X^m_{l,h}, \widehat{q}_h\right) + \left(\alpha^{m+1}_{l,h}(\nabla \cdot \boldsymbol{u}^m_{l,h} + \rho_l^{-1} K(c^m_{g,h} - c_{sat})^+), \widehat{q}_h\right) = 0, \ \forall \widehat{q}_h \in P^{m+1}_{0h}, \tag{3.48}$$

where $X^m_{j,h}(x) = x - \delta t \boldsymbol{u}^m_{j,h}(x)$ for $x \in \Omega^m$, $j = g, l$. Then we let $\alpha^{m+1}_{g,h} = \rho_g(1 - \rho_l^{-1}\alpha^{m+1}_{l,h})$.

Remark 3.4.1 A modification similar to (3.40) will insure the positivity of $\alpha^{m+1}_{l,h}$.

Concentration profiles

Given $\alpha^{m+1}_{l,h} \in P^{m+1}_h, \alpha^m_{l,h} \in P^m_h$, $\boldsymbol{u}^m_{l,h} \in \boldsymbol{V}^m_h$, $C^m_h \in (P^{m+1}_h)^{2+k_M}$, find $C^{m+1}_h \in (P^{m+1}_h)^{2+k_M}$ such that

$$\frac{1}{\delta t}\left(\alpha^{m+1}_{l,h}(C^{m+1}_h - C^m_h \circ X^m_l), \widehat{w}_h\right) + \left(\alpha^{m+1}_{l,h}\boldsymbol{D}\nabla C^{m+1}_h, \nabla \widehat{w}_h\right) + \left(M_g K \alpha^m_{l,h}(c^m_{g,h} - c_{sat})^+, \widehat{w}_{g,h}\right) + \left(I(E^{m+1}_{mix,h})(C^{m+1}_h)^\kappa, \widehat{w}_h\right)_{L^2(S(t^{m+1}))} = 0 \ \ \forall \widehat{w}_h \in (P^{m+1}_{0h})^{2+k_M}, \tag{3.49}$$

doi:10.6342/NTU202200609

subject to

$$\sum_{j=s,k} i_j(E^{m+1}_{mix,h})(c^{m+1}_{j,h})^{\kappa_j}(\boldsymbol{q}_i) = 0, \quad \text{for each nodal point } \boldsymbol{q}_i \text{ on } S^m \tag{3.50}$$

where $\widehat{w}_{g,h}$ is the last component of $\widehat{w}_h$ and

$$I(E^{m+1}_{mix,h}) = \operatorname{diag}\left(\frac{|i_s(E^{m+1}_{mix,h})|}{z_s F}, \frac{|i_k(E^{m+1}_{mix,h})|}{z_k F}, -\frac{\beta|i_s(E^{m+1}_{mix,h})|}{z_s F}\right),$$

$$(C^{m+1}_h)^{\kappa} = \left((c^{m+1}_{s,h})^{\kappa_s}, (c^{m+1}_{k,h})^{\kappa_k}, (c^{m+1}_{s,h})^{\kappa_s}\right)^T$$

for i_s, i_k defined by (3.20).

Two phase flow

Given $\alpha^{m+1}_{j,h} \in P^{m+1}_h$, $j = g, l$, $c^{m+1}_{g,h} \in P^{m+1}_h$, and $\boldsymbol{u}^m_{j,h} \in \boldsymbol{V}^m_h$, find $\boldsymbol{u}^{m+1}_{j,h} \in \boldsymbol{V}^{m+1}_h$, $j = g, l$ and $p^{m+1}_h \in P^{m+1}_h/\mathbb{R}$ such that

$$\sum_{j=g,l}\Big\{\frac{1}{\delta t}\left(\alpha^{m+1}_{j,h}(\boldsymbol{u}^{m+1}_{j,h} - \boldsymbol{u}^m_j \circ X^m_{j,h}), \widehat{\boldsymbol{v}}_{j,h}\right) + \frac{1}{2}\nu_j\left(\alpha^{m+1}_j D(\boldsymbol{u}^{m+1}_{j,h}), D(\boldsymbol{v}_{j,h})\right)$$

$$+ \gamma_j \rho_g^{-1} C_D\left(\alpha^{m+1}_{g,h}|\boldsymbol{u}^{m+1}_{g,h} - \boldsymbol{u}^{m+1}_{l,h}|(\boldsymbol{u}^{m+1}_{g,h} - \boldsymbol{u}^{m+1}_{l,h}), \widehat{\boldsymbol{v}}_{j,h}\right) - \left(p^{m+1}_h, \nabla\cdot(\rho_j^{-1}\alpha^{m+1}_{j,h}\widehat{v}_{j,h})\right)\Big\} = 0 \tag{3.51}$$

$$\left(\widehat{q}_h, \nabla\cdot(\rho_g^{-1}\alpha^{m+1}_{g,h}\boldsymbol{u}^{m+1}_{g,h} + \rho_l^{-1}\alpha^{m+1}_{l,h}\boldsymbol{u}^{m+1}_{l,h})\right) = \left(\widehat{q}_h, \frac{K}{\rho_l}\alpha^{m+1}_{l,h}(c^{m+1}_{g,h} - c_{sat})^+\left(\rho_g^{-1} - \rho_l^{-1}\right)\right) \tag{3.52}$$

for all $\widehat{\boldsymbol{v}}_{j,h} \in \boldsymbol{V}^{m+1}_{0h}$, $j = g, l$ and $\widehat{q}_h \in P^{m+1}_h/\mathbb{R}$.

3.4.3 Fixed point iterative solution of (3.51), (3.52)

The system (3.51)-(3.52) is nonlinear. An iterative algorithm is described in Algorithm 1.

doi:10.6342/NTU202200609

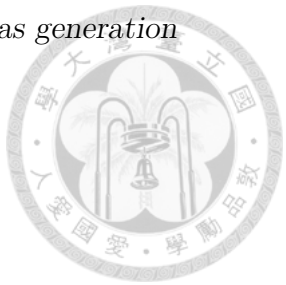

Algorithm 1: A semi-lineariazation for solving (3.51)-(3.52).

1 Let $\boldsymbol{L}_g,\ \boldsymbol{L}_l,\ f$ be defined by (3.43).

Data: Set $\boldsymbol{u}_j = \boldsymbol{u}_{j,h}^m,\ j = g, l.$

2 **for** $n = 1 \dots N$ **do**

3 Set $\beta_j = \left(\frac{1}{\delta t} \alpha_{j,h}^{m+1} + \frac{C_D}{\rho_g} \alpha_{g,h}^{m+1} |\boldsymbol{u}_g - \boldsymbol{u}_l| \right),$

4 Find $\boldsymbol{u}_g, \boldsymbol{u}_l$ and p sastifying the Dirichlet conditions and such that,

$$\forall \widehat{\boldsymbol{v}}_g, \widehat{\boldsymbol{v}}_l \in \boldsymbol{V}_{0h}^{m+1} \text{ and } \forall \widehat{q} \in P_h^{m+1}/\mathbb{R}$$

$$\begin{aligned} &(\beta_g \boldsymbol{u}_g, \widehat{\boldsymbol{v}}_g) + (\beta_l \boldsymbol{u}_l, \widehat{\boldsymbol{v}}_l) + \frac{1}{2} \left(\alpha_{g,h}^{m+1} D(\boldsymbol{u}_g), D(\widehat{\boldsymbol{v}}_g) \right) + \frac{1}{2} \left(\alpha_{l,h}^{m+1} D(\boldsymbol{u}_l), D(\widehat{\boldsymbol{v}}_l) \right) \\ &- \left(p, \nabla \cdot (\frac{\alpha_{g,h}^{m+1}}{\rho_g} \widehat{\boldsymbol{v}}_g + \frac{\alpha_{l,h}^{m+1}}{\rho_l} \widehat{\boldsymbol{v}}_l) \right) + \left(\widehat{q}, \nabla \cdot (\frac{\alpha_{g,h}^{m+1}}{\rho_g} \boldsymbol{u}_g + \frac{\alpha_{l,h}^{m+1}}{\rho_l} \boldsymbol{u}_l) \right) \\ &= (\boldsymbol{L}_g, \widehat{\boldsymbol{v}}_g) + (\boldsymbol{L}_l, \widehat{\boldsymbol{v}}_l) + (\widehat{q}, f)\,. \end{aligned} \tag{3.53}$$

5 **end**

6 Set $\boldsymbol{u}_j^{n+1} = \boldsymbol{u}_j,\ j = g, l.$

doi:10.6342/NTU202200609

3.4.4 Consistence and Stability

Variational formulations discretized by finite element methods inherit the stability and consistency of the continuous equations. The LBB theorem applies also to the Hood-Taylor element for velocity pressure problems. Therefore, as in the continuous case, the H^1 norms of $\alpha_j^{m+1}, \boldsymbol{u}_j^{m+1}, C_j^{m+1}$ are less than $(1 + C(\|\nabla^2 \boldsymbol{u}_l^m\|_{L^\infty})\delta t)$ times the H^1 norms of $\alpha_j^m, \boldsymbol{u}_j^m, C_j^m$. If we could show that $C(\ )$ is bounded, then it would imply that the scheme converges when $\delta t \to 0$.

3.4.5 Solvability of the linear system in matrix form

Let $\boldsymbol{\zeta} = (\boldsymbol{\zeta}_g, \boldsymbol{\zeta}_l) \in (\boldsymbol{V}_h^{m+1})^2$, $\alpha_{j,h}^{m+1} \in P_h^{m+1}$, $\alpha_{j,h} \geq \epsilon$ for some constant $\epsilon > 0$, $j = g, l$.

To study the solvability of (3.51)-(3.52), we consider a simpler case with $\boldsymbol{u}_g = \boldsymbol{u}_l = 0$ on $\partial\Omega^{m+1} \setminus \Gamma_{out}$, and take the linearized approximation on the drag force terms. The problem reads: Find $\boldsymbol{u}_h^{m+1} := (\boldsymbol{u}_{g,h}^{m+1}, \boldsymbol{u}_{l,h}^{m+1}) \in (\boldsymbol{V}_{0h}^{m+1})^2$ and $p_h^{m+1} \in \boldsymbol{P}_h^{m+1}/\mathbb{R}$ satisfying

$$a_{\boldsymbol{\zeta}}(\boldsymbol{u}_h^{m+1}, \widehat{\boldsymbol{v}}_h) + b(p_h^{m+1}, \widehat{\boldsymbol{v}}_h) = F(\widehat{\boldsymbol{v}}_h), \quad b(\widehat{q}_h, \boldsymbol{u}_h^{m+1}) \ = G(\widehat{q}_h), \tag{3.54}$$

doi:10.6342/NTU202200609

where, for $\boldsymbol{u}=(\boldsymbol{u}_g,\boldsymbol{u}_l), \boldsymbol{v}=(\boldsymbol{v}_g,\boldsymbol{v}_l)\in(\boldsymbol{v}_{0h}^{m+1})^2$, $q\in P_h^{m+1}$,

$$
\begin{aligned}
a_{\boldsymbol{\zeta}}(\boldsymbol{u},\boldsymbol{v}) &= \sum_{j=g,l}\left[\frac{1}{\delta t}\left(\alpha_{j,h}^{m+1}\boldsymbol{u}_j,\boldsymbol{v}_j\right)+\frac{1}{2}\nu_j\left(\alpha_{j,h}^{m+1}D(\boldsymbol{u}_j),D(\boldsymbol{v}_j)\right)\right]\\
&\quad+\rho_g^{-1}C_D\left(\alpha_{g,h}^{m+1}|\boldsymbol{\zeta}_g-\boldsymbol{\zeta}_l|(\boldsymbol{u}_g-\boldsymbol{u}_l),\boldsymbol{v}_g-\boldsymbol{v}_l\right)\\
b(q,\boldsymbol{v}) &= -\left(q,\nabla\cdot(\rho_g^{-1}\alpha_{g,h}^{m+1}\boldsymbol{v}_g+\rho_l^{-1}\alpha_{l,h}^{m+1}\boldsymbol{v}_l)\right)\\
F(\boldsymbol{v}) &= \sum_{j=l,g}\frac{1}{\delta t}\left(\alpha_{j,h}^{m+1}\boldsymbol{u}_{j,h}^m(X_{j,h}^m(x)),\boldsymbol{v}_j\right)\quad G(q)=\left(q,\rho_l^{-1}K\alpha_{l,h}^{m+1}(c_{g,h}^{m+1}-c_{sat})^+(\rho_g^{-1}-\rho_l^{-1})\right).
\end{aligned}
\tag{3.55}
$$

On the basis of $\boldsymbol{V}_h^{m+1}$ and P_h^{m+1}, we can write

$$
\boldsymbol{u}_{g,h}^{m+1}=\sum_{i=1}^{2N_a}u_{g,i}^{m+1}\boldsymbol{\psi}_i,\quad \boldsymbol{u}_{l,h}^{m+1}=\sum_{i=1}^{2N_a}u_{l,i}^{m+1}\boldsymbol{\psi}_i,\quad p_h^{m+1}=\sum_{i=1}^{N_q}p_i^{m+1}\phi_i,
\tag{3.56}
$$

More precisely $\{\boldsymbol{\psi}_1,\ldots,\boldsymbol{\psi}_{2N_a}\}$ is $\{\psi_1\boldsymbol{e}_1,\ldots,\psi_{N_a}\boldsymbol{e}_1,\psi_1\boldsymbol{e}_2,\ldots,\psi_{N_a}\boldsymbol{e}_2\}$ for $\boldsymbol{e}_1=(1,0)^T$ and $\boldsymbol{e}_2=(0,1)^T$.

Problem (3.54) can be formally expressed as a system of linear equations:

$$
\boldsymbol{\Phi}\boldsymbol{U}^{m+1}=\boldsymbol{F}^m,
\tag{3.57}
$$

where $\boldsymbol{\Phi}$ is a $(4N_a+N_q)\times(4N_a+N_q)$ matrix, $\boldsymbol{U}^{m+1}$ and $\boldsymbol{F}^m$ are $(4N_a+N_q)$ vectors. Note that $\boldsymbol{\Phi}$ has the form

$$
\boldsymbol{\Phi}=\begin{pmatrix}A & B\\ B^T & O\end{pmatrix},\ \text{with } A=\begin{pmatrix}A_g & A_{mix}\\ A_{mix} & A_l\end{pmatrix}.
\tag{3.58}
$$

In the above,

$$
A_k=\left(\frac{1}{\delta t}\left(\alpha_{k,h}^{m+1}\boldsymbol{\psi}_i,\boldsymbol{\psi}_j\right)+\frac{1}{2}\nu_k\left(\alpha_{k,h}^{m+1}D(\boldsymbol{\psi}_i),D(\boldsymbol{\psi}_j)\right)+\rho_g^{-1}C_D\left(\alpha_{g,h}^{m+1}|\boldsymbol{\zeta}_g-\boldsymbol{\zeta}_l|\boldsymbol{\psi}_i,\boldsymbol{\psi}_j\right)\right)_{i,j=1,\ldots,2N_a},\quad k
$$

$$
A_{mix}=\left(-\rho_g^{-1}C_D\left(\alpha_{g,h}^{m+1}|\boldsymbol{\zeta}_g-\boldsymbol{\zeta}_l|\boldsymbol{\psi}_i,\boldsymbol{\psi}_j\right)\right)_{i,j=1,\ldots,2N_a},
$$

$$
B=\begin{pmatrix}-\left(\phi_j,\nabla\cdot(\rho_g^{-1}\alpha_{g,h}^{m+1}\boldsymbol{\psi}_i)\right)\\ -\left(\phi_j,\nabla\cdot(\rho_l^{-1}\alpha_{l,h}^{m+1}\boldsymbol{\psi}_i)\right)\end{pmatrix}_{i=1,\ldots,4N_a;j=1,\ldots,N_q}.
$$

doi:10.6342/NTU202200609

Proposition 3.4.1 The linear system (3.57) is uniquely solvable.

Proof. According to the Ladyzhenskaya-Babuska-Brezzi theorem [63] the saddle point problem (3.53) is well posed when for $p \in P_h^{m+1}/\mathbb{R}$, there exists $\boldsymbol{v} \in \boldsymbol{V}_{0h}^{m+1}$ such that

$$\frac{(p, \nabla \cdot \boldsymbol{v})}{\|\boldsymbol{v}\|_{H^1}} \geq c\|p\|_{L^2/\mathbb{R}} \text{ for some } c > 0. \tag{3.59}$$

Therefore $\boldsymbol{\Phi}$ has full rank and is non singular.

3.4.6 Iterative process

At each time step, (3.48), is solved first, then (3.49)-(3.50) is solved iteratively by using a semi-linearization of the nonlinear boundary terms. Then (3.51),(3.52) is solved iteratively by a semi-linearization of the nonlinear terms; each block involves the solution of a well posed symmetric linear system. Finally S^m is updated by (3.23). Algorithm 2 summarises the procedure.

Note that the computational domain is $\Omega^m = \{(x, y), 0 < x < L,\ 0 < y < y^m(x)\}$.

doi:10.6342/NTU202200609

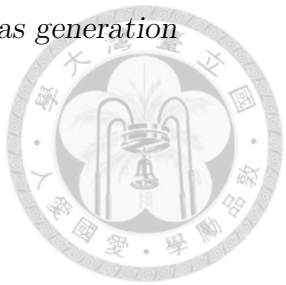

Algorithm 2: Algorithm for solving the full system of equations.

Data: $\alpha_{g,h}^m$, $\alpha_{l,h}^m$, $\boldsymbol{u}_{g,h}^m$, $\boldsymbol{u}_{l,h}^m$, p_h^m, $c_{s,h}^m$, $c_{k,h}^m$, $c_{g,h}^m$, $E_{mix,h}^m$, and y^m

Set initial data $\alpha_{g,h}^0$, $\alpha_{l,h}^0$, $\boldsymbol{u}_{g,h}^0$, $\boldsymbol{u}_{l,h}^0$, $c_{s,h}^0$, $c_{k,h}^0$, $c_{g,h}^0$, $E_{mix,h}^0$;

for m **do**

  Solve (3.48) to get $\alpha_{g,h}^{m+1}$, $\alpha_{l,h}^{m+1}$;

  Initial guess: $E_{mix,h}^{m+1,0} = E_{mix,h}^m$, $C_h^{m+1,0}$ = solution to (3.49) when mixed potential is $E_{mix,h}^{m+1,0}$;

  while $\|C_h^{m+1,k+1} - C_h^{m+1,k}\| \geq tolerance$ **do**

    Initial guess: $E_{mix,h}^{m+1,k+1,0} = E_{mix,h}^{m+1,k}$;

    while $\|E_{mix,h}^{m+1,k+1,l+1} - E_{mix,h}^{m+1,k+1,l}\|_{L^2(S^m)} \geq tolerance$ **do**

      Solve (3.49) to get $c_{s,h}^{m+1,k+1,l+1}$, $c_{k,h}^{m+1,k+1,l+1}$, $c_{g,h}^{m+1,k+1,l+1}$;

      Solve (3.50) to get $E_{mix,h}^{m+1,k+1,l^*}$;

      $E_{mix,h}^{m+1,k+1,l+1} = \xi E_{mix,h}^{m+1,k+1,l^*} + (1-\xi) E_{mix,h}^{m+1,k+1,l}$, $0 < \xi < 1$;

    end

  end

  Solve (3.51)-(3.52) to get, $\boldsymbol{u}_{g,h}^{m+1}$, $\boldsymbol{u}_{l,h}^{m+1}$, p_h^{m+1} (Using Algorithm 1);

  For the free boundary case change the mesh by $y^{m+1} = y^m + \delta t u_{2\,g,h}^{m+1}$;

end

doi:10.6342/NTU202200609

3.5 Numerical simulation

3.5.1 One-dimensional electroless nickel plating problem

Here we reproduce, with a two dimensional computation, the one-dimensional study by Kim and Sohn [1]. In their work, the electroless nickel plating process on a rotating disk with constant angular velocity is considered. In this situation, the velocity field near the surface of the rotating disk can be approximated by a uniformly distributed flow towards the plating surface. In addition, the thickness of diffusion layer is assumed uniform on the surface. Consequently, for the modeling, the domain becomes one-dimensional. Given that the gas generation is not considered and only the steady state is computed in [1], a single phase recovery $r_l = 1$, $c_g = 0$ is applied. Finally, four partial reactions in the electroless nickel plating process are considered:

$$H_2PO_2^- + H_2O = H_2PO_3^- + 2H^+ + 2e^- \qquad \text{(anodic)} \qquad (3.60a)$$

$$H_2PO_2^- + 2H^+ + e^- = P + 2H_2O \qquad \text{(cathodic)} \qquad (3.60b)$$

$$Ni^{2+} + 2e^- = Ni \qquad \text{(cathodic)} \qquad (3.60c)$$

$$2H^+ + 2e^- = H_2 \qquad \text{(cathodic)} \qquad (3.60d)$$

All chemical species are labeled as follows: c_1 is the concentration of the anodic hypophosphite ($H_2PO_2^-$), c_2 the concentration of the cathodic hypophosphite, c_3 the concentration of the nickel ion (Ni^{2+}), and c_4 the con-

doi:10.6342/NTU202200609

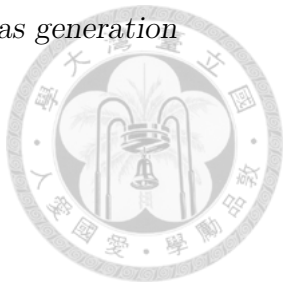

Table 3.1: Physical parameters used in the simulation by Kim and Sohn [1], which are valid for $pH = 4.5$ and the concentration of $H_2PO_2^- = 0.3$ M

	H^+	Ni^{2+}	$H_2PO_2^-$(cathodic)	$H_2PO_2^-$(anodic)
i_0 (A/cm^2)	1.5×10^{-4} [a]	1.5×10^{-7} [b]	6.0×10^{-4}	8.9×10^{-3}
D (cm^2/s)	4.5×10^{-5} [a]	0.5×10^{-6} [c]	1.7×10^{-5}	1.7×10^{-5}
α	0.79 [a]	0.79 [c]	0.2	0.9
β	0.21 [a]	0.21 [c]	0.8	0.1
z	1	2	1	4
γ	1.0 [a]	1.0 [c]	0.3	1.0
E_0 (V) [d]	-0.101	-0.147	-0.806	-0.878
c_0 (M)	3.162×10^{-5} [e]	0.1	0.3	0.3
subscript j	4	3	2	1

[a] Estimated from the literature [66]. [b] Assumed in this study. [c] Taken from the literature [67] . [d] Calculated based on the literature [68]. all values except E_{03} (Ni^{2+}) depend on pH (see (3.66)). [e] If $pH = x$, then $c_{04} = 10^{-x}$ (M). i_0: Exchange current density, D: Diffusion coefficient. α: Anodic transfer coefficient, β Cathodic transfer coefficient. z: Number of electron transport, γ: Reaction order, E_0: Equilibrium potential (90^oC) c_0 inlet and initial concentration

doi:10.6342/NTU202200609

Table 3.2: Conditions assumed in [1] for performing our simulations

Experimental conditions	
Angular velocity ω	400 rpm
Kinematic viscosity ν	1.2×10^{-2} cm^2/s
Temperature θ	90 ^oC

Composition of electrolytes	
$NiSO_4$ (nickel sulfate)	0.1 M
NaH_2PO_2 (sodium hypophosphite)	0.3 M
pH	$4.0 - 5.3$

centration of the hydrogen ion (H^+). Now the two-dimensional analogue can be formulated: Let $\Omega = (0, \delta_3) \times (0, \epsilon)$, where δ_3 is the thickness of the diffusion layer for nickel and $\epsilon << \delta_3$ is a small positive number. The thickness of the diffusion layer for species j is given in [13]:

$$\delta_j = 1.61 D_j^{1/3} \omega^{-1/2} \nu^{1/6}. \tag{3.61}$$

The governing equation for the concentration profile is given by

$$\partial_t c_j + \boldsymbol{u} \cdot \nabla c_j - D_j \Delta c_j = 0 \quad \text{in } \Omega, \tag{3.62}$$

doi:10.6342/NTU202200609

subject to the boundary conditions

$$\begin{aligned} &c_j = c_{0j} \ \text{ at } x = \delta_3, \qquad -D_j \frac{\partial c_j}{\partial n} = 0 \ \text{ at } y = 0, \epsilon, \\ &-D_j \frac{\partial c_j}{\partial n} = \frac{|i_1(E_{mix})|}{z_1 F} \left(\frac{(1-r)c_1}{c_{01}} \right)^{\gamma_1} + \frac{|i_2(E_{mix})|}{z_2 F} \left(\frac{r c_2}{c_{02}} \right)^{\gamma_2} \qquad j = 1, 2, \\ &-D_j \frac{\partial c_j}{\partial n} = \frac{|i_j(E_{mix})|}{z_j F} \left(\frac{c_1}{c_{01}} \right)^{\gamma_j} \qquad j = 3, 4 \ \text{ at } x = 0. \end{aligned} \tag{3.63}$$

with the electron balance constraint

$$\sum_{j=1}^{4} \frac{i_j(E_{mix})}{z_j F} \left(\frac{c_j}{c_{0j}} \right)^{\gamma_j} = 0. \tag{3.64}$$

The velocity field can be expressed as in [13]:

$$\boldsymbol{u} = (-a x^2 \omega^{3/2} \nu^{-1/2}, 0)^T \tag{3.65}$$

where $a = 0.51023$ is an experimental constant, $r = 0.995$ is the ratio between the hypophosphite anodic part and the cathodic part on the reacting surface. The equilibrium potential E_{0j} for species j can be approximated by the Nernst equation, with $pH = \log(c_{04})$:

$$\begin{aligned} &E_{01} = -0.878 + \frac{0.25 R\theta}{F} \log\left(10^{4.5} c_{04}\right), \quad E_{02} = -0.806 + \frac{0.3 R\theta}{F} \log\left(10^{4.5} c_{04}\right), \\ &E_{03} = -0.147, \quad E_{04} = -0.101 + \frac{R\theta}{F} \log\left(10^{4.5} c_{04}\right). \end{aligned} \tag{3.66}$$

By simulating system (3.62), (3.63), and (3.64), with the physical constants given in Table 3.1, until a steady state is reached, the numerical tests show that the present model agrees well with the previous 1D studies of Kim and Sohn [1]: see Figures 3.3 and 3.4.

doi:10.6342/NTU202200609

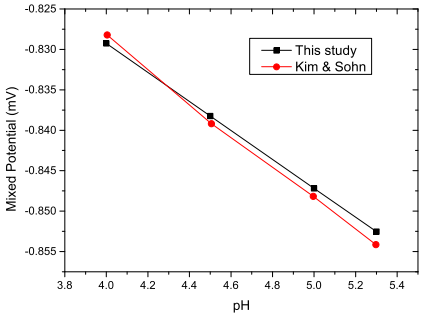

Figure 3.3: In red, the mixed potential E_{mix} computed by the one dimensional system (3.63) versus pH$= \log c_{04}$. In black, the same but computed with the full two dimensional system.

Regarding (3.60), atomic nickel and phosphorus are deposited on the surface during the electroless process. The deposition thickness can be estimated in terms of the current densities:

$$\left(\frac{i_2(E_{mix})\,(c_2|_{x=0}/c_{02})\,V_P}{z_2 F} + \frac{i_3(E_{mix})\,(c_3|_{x=0}/c_{03})\,V_{Ni}}{z_3 F} \right) t, \tag{3.67}$$

where V_P, V_{Ni} are molar volumes of phosphorus and nickel, respectively, and t is the deposition time.

3.5.2 Two species in a gas-liquid two phase flow

Let the initial domain Ω be a rectangular of size 0.01×0.001 (in meters). We consider complexed (by tartrate, denoted by L) copper ions, formaldehyde, and hydrogen dissolved in water, which are denoted by the subscriptions s, k, g, respectively, for the chemical species transport equations.

The chemical reaction can be expressed as the following two partial reac-

doi:10.6342/NTU202200609

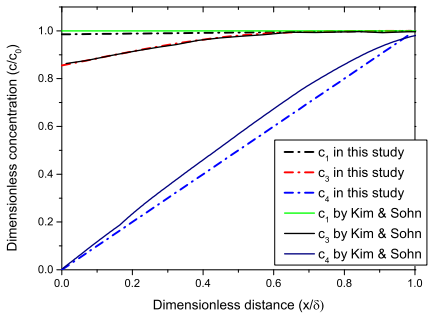

Figure 3.4: Concentration profiles of three chemical species versus x computed by the one dimensional system (3.63) and compared with the results of the full two dimensional system.

tions:

$$Cu(OH)_2L_2^{-4} = Cu + 2OH^- + 2L^{-2} \tag{3.68a}$$

$$2HCHO + 4OH^- = 2HCOO^- + H_2 + 2H_2O + 2e^- \tag{3.68b}$$

Given the above equations, we also use the subscriptions s and k to represent the quantities corresponding to (3.68a) and (3.68b), respectively.

The values of the physical constants are listed in Table 3.3.

doi:10.6342/NTU202200609

physical quantity	value	physical quantiy	value
ρ_l (kg/m^3)	995.65	ρ_g (kg/m^3)	1.161
ρ_0 (kg/m^3)	1.161	μ_g $(kg/m \cdot s)$	1.86×10^{-5}
μ_l $(kg/m \cdot s)$	7.977×10^{-4}	d_0 (m)	0.001
u_0 (m/s)	0.001	c_{sat} (mol/m^3)	0
i_g (A/m^2)	1.0×10^{-2}	i_s (A/m^2)	1.0×10^{-2}
i_k (A/m^2)	10	R $(J/K \cdot mol)$	8.314
K $(kg/mol \cdot s)$	3.87×10^{-4}	M_g (mol/kg)	500
$c_{g,0}$ (mol/m^3)	1	$c_{s,0}$ (mol/m^3)	39.34
$c_{k,0}$ (mol/m^3)	77.58	D_g (m^2/s)	2×10^{-8}
D_s (m^2/s)	7×10^{-10}	D_k (m^2/s)	1.2×10^{-9}
z_s (1)	2	z_k (1)	4
α_s (1)	0.67	α_k (1)	0.37
β_s (1)	0.33	β_k (1)	0.63
θ (K)	363.15	E_s (V)	-0.266
E_k (V)	1.5	C_D (1)	242220
α (1)	0.0005		

Table 3.3: Parameters used in Section 3.5.2.

doi:10.6342/NTU202200609

For convenience, the following scalings are applied:

$$L \to \frac{L}{d_0} \ (L \text{ is any length}), \quad \rho_l \to \frac{\rho_l}{\rho_0}, \quad \rho_g \to \frac{\rho_g}{\rho_0},$$
$$\mu_l \to \frac{\mu_l}{\rho_0 d_0 u_0}, \quad \mu_g \to \frac{\mu_g}{\rho_0 d_0 u_0}, \quad c_g \to \frac{c_g}{c_{g0}}, \quad c_k \to \frac{c_k}{c_{k0}}, \quad c_s \to \frac{c_s}{c_{s0}}, \quad K \to \frac{d_0 c_{g0}}{\rho_0 u_0} K,$$
$$L_g \to \frac{L_g}{u_0 c_{g0} z_s F}, \quad L_s \to \frac{L_s}{u_0 c_{s0} z_s F}, \quad L_k \to \frac{L_k}{u_0 c_{k0} z_k F}, \quad D_g \to \frac{D_g}{u_0 d_0}, \quad D_s \to \frac{D_s}{u_0 d_0}, \quad D_k \to \frac{D_k}{u_0 d_k},$$
$$i_g \to \frac{i_g}{u_0 c_{g0} z_s F}, \quad i_s \to \frac{i_s}{u_0 c_{s0} z_s F}, \quad i_k \to \frac{i_k}{u_0 c_{k0} z_k F}. \tag{3.69}$$

The initial conditions are set to: constant phase ratio and Poiseuille flow:

$$r_g^0 = \epsilon, \quad r_l^0 = 1 - \epsilon, \quad \boldsymbol{u}_g^0 = \boldsymbol{u}_l^0 = (0.69y(1-y), 0)^T, \tag{3.70}$$

with $\epsilon = 0.0001$. Also, let $C^0 = (c_s^0, c_k^0, c_g^0)^T$ satisfies

$$-\nabla \cdot (r_l^0 \boldsymbol{D} \nabla C^0) = 0, \quad C^0|_{\Gamma_{in}} = (1,1,0)^T, \quad \frac{\partial C^0}{\partial n}|_{\Gamma_{out} \cup \Gamma_{wall}} = 0 \tag{3.71}$$

plus the first equation in (3.73) subject to (3.21). The inflow values are

$$\boldsymbol{u}_g^{m+1}|_{\Gamma_{in}} = \boldsymbol{u}_l^{m+1}|_{\Gamma_{in}} = (y(1-y), 0)^T, \ c_g|_{\Gamma_{in}} = 0, \ c_s|_{\Gamma_{in}} = c_k|_{\Gamma_{in}} = 1, \ r_l|_{\Gamma_{in}} = 1-\epsilon. \tag{3.72}$$

The boundary conditions on $S(t^{m+1})$ are

$$-D_p \frac{\partial c_p^{m+1}}{\partial n} = \chi r_l^{m+1} |i_p^{m+1}| c_p^{m+1}, \ p = s, g, k, \ \boldsymbol{u}_g^{m+1} = \boldsymbol{u}_l^{m+1} = \alpha \chi r_l^{m+1} |i_s^{m+1}| c_s^{m+1}, \tag{3.73}$$

doi:10.6342/NTU202200609

where $\alpha = 0.0005$ and

$$\chi(x,y) = \begin{cases} x - \frac{3}{4} + \frac{1}{4}\sin\left(2\pi(x-\frac{1}{4})\right), & 1 \le x < 1.5, \\ 1, & 1.5 \le x < 5.5, \\ \frac{17}{4} - x - \frac{1}{4}\sin\left(2\pi(x-\frac{19}{4})\right), & 5.5 \le x < 6, \\ 0, & 0 \le x < 1 \text{ or } 6 \le x \le 10. \end{cases} \tag{3.74}$$

Boundary conditions on Γ_{out} and Γ_{wall} are as in Section 3.2.4. See also Figure 3.1.

Remark 3.5.1 We note that $\alpha = 0.0005$ is much larger than the experimental values; the numerical simulations produce u_{g_2} (and u_{l2}) of magnitude in the order $O(10^{-4})$. On the other hand, the deposition rate in a typical experiment is of order 1 μm per hours [69], which is not larger than $O(10^{-6})$. Yet the numerical test is conducted to validate the numerical method when the evolution of the domain is larger than real life values.

Convergence

First, we conduct the convergence test for different time step with a fixed mesh. To obtain a "reference solution", the system (3.48)-(3.52) is solved with a 50×10 uniform mesh and a small time step $\delta t = 0.01$ and $T = 10$. The convergence with respect to δt is studied without changing the mesh; results are given in Table 3.4 and the rate of convergence for each variable is presented in Figure 3.5. Numerical tests for solving two phase flow problem

doi:10.6342/NTU202200609

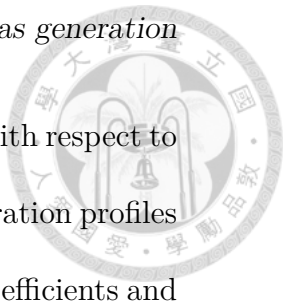

and volume fraction problem present a linear decay of L^2 error with respect to the time step. However, the convergence for solving the concentration profiles does not reach the expectation due to extremely low diffusion coefficients and large current densities.

Second, we conduct the convergence tests for different time step and mesh pairs. The reference solution is obtained with 200×20 uniform mesh and $\delta t = 0.05$ at $T = 10$. We always keep the time step being proportional to the mesh size. Figure 3.6 and Table 3.5 present a linear decay of L^2 error with respect to the time step for each variable.

Third, the convergence tests for different time step and mesh pairs are performed until a larger final time. The reference solution is obtained with 200×20 uniform mesh and $\delta t = 0.3$ at $T = 120$. Same as the second test, we always keep the time step being proportional to the mesh size. Figure 3.7 and Table 3.6 present a nearly linear decay of L^2 error with respect to the time step for each variable. In this test, r_g and c_k are of the worst convergence. Their intensity maps are given in Figures 3.8 and 3.9. Except for tests with time step $\delta t = 1.2$, the intensity maps for the tests with $\delta t \leq 0.6$ present no significant difference with the reference solutions.

Robustness for large time steps

With a large time step $\delta t = 1$ and 100×10 uniform mesh, the product of the maximal liquid fluid speed with the time step is around 1.5 times of the mesh

doi:10.6342/NTU202200609

Table 3.4: L^2 error with respect to the reference solution provided with time step $\delta t = 0.01$, 50×10 uniform mesh, and $\alpha = 0.0005$ for numerical simulation in Section 3.5.2 at $T = 10$.

δt	$\boldsymbol{u}_g$	$\boldsymbol{u}_l$	p	α_g	c_s	c_k	c_g
1	5.56×10^{-4}	5.49×10^{-4}	1.45×10^{-3}	9.11×10^{-2}	9.12×10^{-3}	3.77×10^{-4}	1.74×10^{-2}
0.5	2.77×10^{-4}	2.73×10^{-4}	7.17×10^{-4}	4.50×10^{-2}	6.80×10^{-3}	2.64×10^{-4}	8.74×10^{-3}
0.1	4.85×10^{-5}	4.84×10^{-5}	1.28×10^{-4}	8.07×10^{-3}	3.87×10^{-3}	2.01×10^{-4}	1.72×10^{-3}
0.05	2.25×10^{-5}	2.24×10^{-5}	5.75×10^{-5}	3.58×10^{-3}	3.00×10^{-3}	1.55×10^{-4}	8.77×10^{-4}

Table 3.5: L^2 error with respect to the reference solution provided with time step $\delta t = 0.05$, 200×20 uniform mesh, and $\alpha = 0.0005$ for numerical simulation in Section 3.5.2 at $T = 10$.

$(\delta t, \text{mesh})$	$\boldsymbol{u}_g$	$\boldsymbol{u}_l$	p	α_g	c_s	c_k	c_g
$(1, 25 \times 3)$	2.03×10^{-2}	2.04×10^{-2}	1.72×10^{-2}	6.24×10^{-1}	1.55×10^{-1}	8.73×10^{-2}	8.57×10^{-1}
$(0.5, 50 \times 5)$	6.50×10^{-3}	6.45×10^{-3}	5.24×10^{-3}	2.18×10^{-1}	4.54×10^{-2}	3.08×10^{-2}	2.78×10^{-1}
$(0.1, 100 \times 10)$	1.47×10^{-3}	1.35×10^{-3}	9.48×10^{-4}	6.09×10^{-2}	1.57×10^{-2}	7.65×10^{-3}	6.58×10^{-2}

Table 3.6: L^2 error with respect to the reference solution provided with time step $\delta t = 0.3$, 200×20 uniform mesh, and $\alpha = 0.0005$ for numerical simulation in Section 3.5.2 at $T = 120$.

$(\delta t, \text{mesh})$	$\boldsymbol{u}_g$	$\boldsymbol{u}_l$	p	α_g	c_s	c_k	c_g
$(1.2, 50 \times 5)$	1.73×10^{-2}	1.73×10^{-2}	6.48×10^{-3}	3.71×10^{-1}	3.97×10^{-2}	1.56×10^{-2}	2.73×10^{-1}
$(0.6, 100 \times 10)$	1.22×10^{-2}	1.23×10^{-2}	4.07×10^{-3}	2.20×10^{-1}	1.35×10^{-2}	1.18×10^{-2}	2.11×10^{-1}
$(0.4, 150 \times 15)$	6.40×10^{-3}	6.41×10^{-3}	2.23×10^{-3}	1.19×10^{-1}	6.60×10^{-3}	6.23×10^{-3}	1.11×10^{-1}

doi:10.6342/NTU202200609

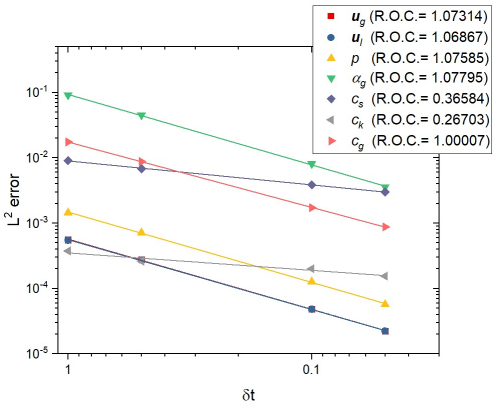

Figure 3.5: Convergence with respect to δt for the case described in Section 3.5.2 with fixed mesh: log-log plot of the error for each unknown; (note that the curves for $\boldsymbol{u}_g$ and $\boldsymbol{u}_l$ overlap) . R.O.C. means "Rate Of Convergence". The reference solution is a computation with a very small time step.

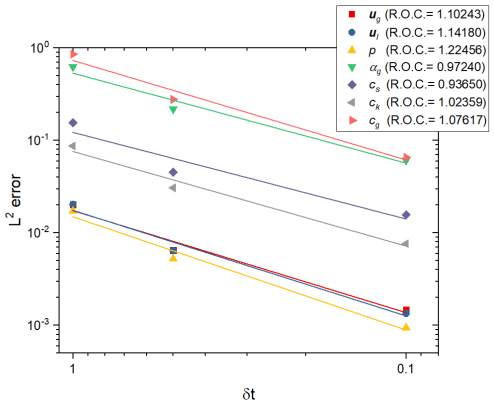

Figure 3.6: Convergence with respect to δt and mesh size for the case described in Section 3.5.2 (see Table 3.5 for the time step and mesh size pair): log-log plot of the error for each unknown; (note that the curves for $\boldsymbol{u}_l$ and $\boldsymbol{u}_l$ overlap) .

doi:10.6342/NTU202200609

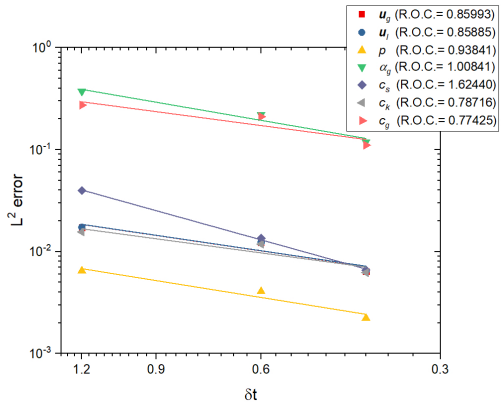

Figure 3.7: Convergence with respect to δt and mesh size for the case described in Section 3.5.2 (see Table 3.5 for the time step and mesh size pair): log-log plot of the error for each unknown; (note that the curves for $\boldsymbol{u}_g$ and c_k overlap and the curve of $\boldsymbol{u}_l$ is closed to them).

size, which is optimal for the Galerkin-Characteristic method. solutions are displayed in Figure 3.10-3.15.

CPU time

With $\delta t = 1$ and 100×10 uniform mesh, it took 5832 seconds to reach the final time $T = 180$ with an Intel Core i7-8750H @ 2.20GHz. During the computation, it took 0.086% of the total CPU for solving the volume fraction problem, 7.66% for solving the chemical species transport problem and 91.93% for solving the two velocities/pressure flow problem.

The computer program is written using the `FreeFEM++` toolkit [70].

doi:10.6342/NTU202200609

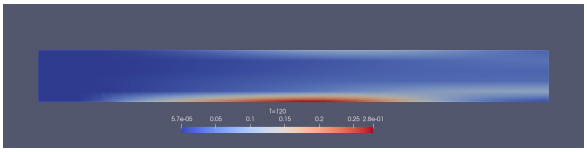

(a) Intensity map of r_g at $t = 120$ with $\delta t = 1.2$ and 50×5 uniform mesh.

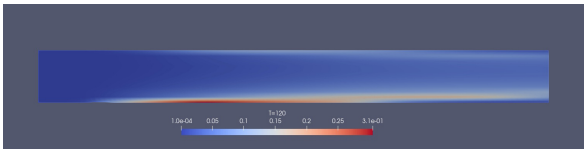

(b) Intensity map of r_g at $t = 120$ with $\delta t = 0.6$ and 100×10 uniform mesh.

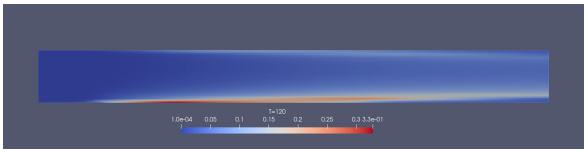

(c) Intensity map of r_g at $t = 120$ with $\delta t = 0.4$ and 150×15 uniform mesh.

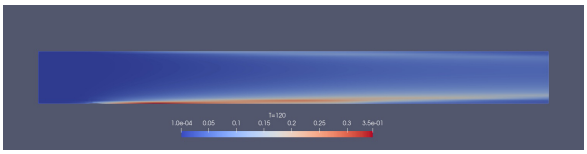

(d) Intensity map of r_g at $t = 120$ with $\delta t = 0.3$ and 200×20 uniform mesh.

Figure 3.8: For Section 3.5.2: The intensity maps of r_g for different time step and mesh size pairs.

doi:10.6342/NTU202200609

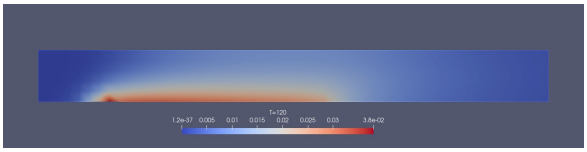

(a) Intensity map of c_g at $t = 120$ with $\delta t = 1.2$ and 50×5 uniform mesh.

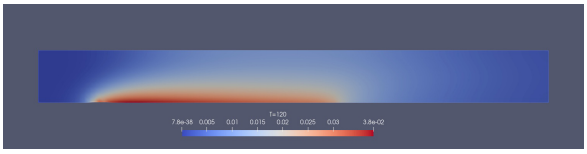

(b) Intensity map of c_g at $t = 120$ with $\delta t = 0.6$ and 100×10 uniform mesh.

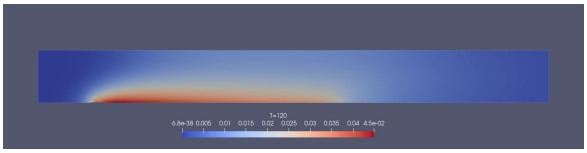

(c) Intensity map of c_g at $t = 120$ with $\delta t = 0.4$ and 150×15 uniform mesh.

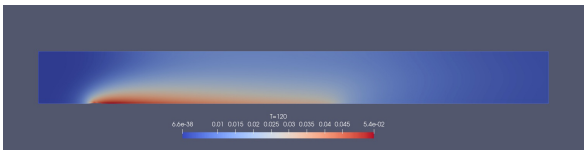

(d) Intensity map of c_g at $t = 120$ with $\delta t = 0.3$ and 200×20 uniform mesh.

Figure 3.9: For Section 3.5.2: The intensity maps of c_g for different time step and mesh size pairs.

doi:10.6342/NTU202200609

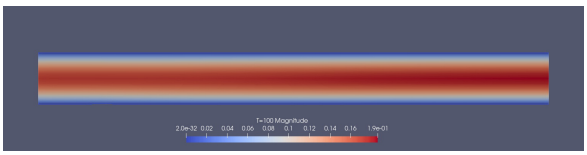

(a) Intensity map of $\boldsymbol{u}_g$ at $t = 100$.

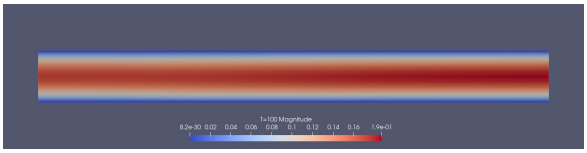

(b) Intensity map of $\boldsymbol{u}_l$ at $t = 100$.

Figure 3.10: For Section 3.5.2: The velocity magnitudes of $\boldsymbol{u}_g$ and $\boldsymbol{u}_l$.

Results

On Figure 3.10a and 3.10b the velocity vector fields $\boldsymbol{u}_g$ and $\boldsymbol{u}_l$ are seen to be almost parabolic in y (Poiseuille flow). but the phase change and moving boundary induce a non-zero asymmetric vertical component u_{2g} (see Figure 3.14); both play important roles for the bubble distribution. Bubble density can be inferred by analyzing c_g and r_g (see Figure 3.17). The color maps of Figure 3.11 displays a high gas volume fraction area near the top and bottom plates . Figure 3.12 shows how the steady state is established and how the electrolyte disappears in the plating region due to the plating. Figure 3.13 explains why it is always of the highest volume fraction of gaseous phase near the reacting surface. The deposition-induced movement of S is presented in Figure 3.16. Figure 3.17b shows that the region of the highest bubble density is moving away from the inlet as the electroless plating proceeds.

doi:10.6342/NTU202200609

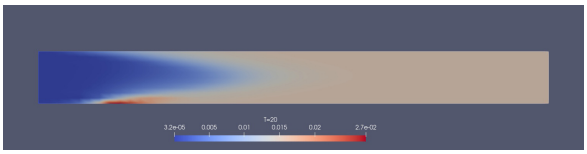

(a) Intensity map of r_g at $t = 20$.

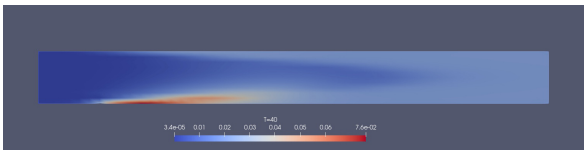

(b) Intensity map of r_g at $t = 40$.

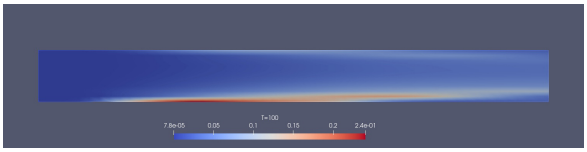

(c) Intensity map of r_g at $t = 100$.

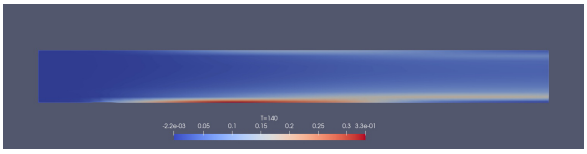

(d) Intensity map of r_g at $t = 140$.

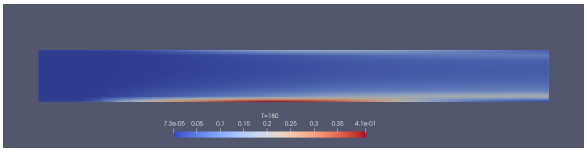

(e) Intensity map of r_g at $t = 180$.

Figure 3.11: For Section 3.5.2: intensity maps of the volume fraction of the gas phase r_g computed with $\delta t = 1$ and a 100×10 uniform mesh.

doi:10.6342/NTU202200609

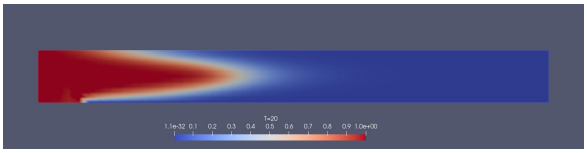

(a) Intensity map of c_s at $t = 20$.

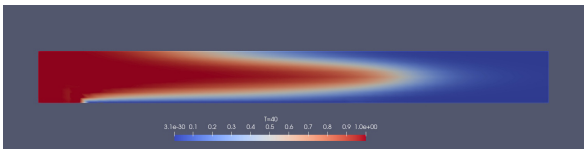

(b) Intensity map of c_s at $t = 40$.

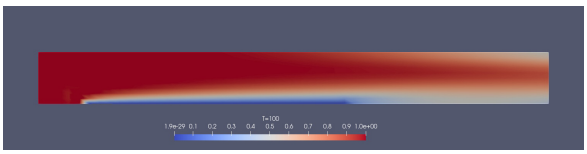

(c) Intensity map of c_s at $t = 100$.

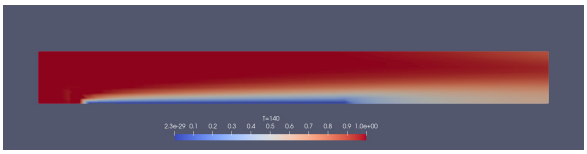

(d) Intensity map of c_s at $t = 140$.

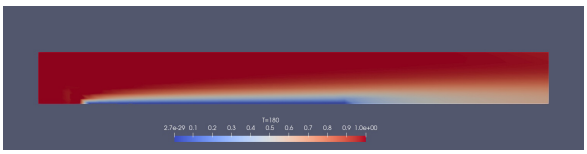

(e) Intensity map of c_s at $t = 180$.

Figure 3.12: For Section 3.5.2: intensity maps of the concentration electrolyte ions c_s computed with $\delta t = 1$ and a 100×10 uniform mesh. The blue zone in the plating region, on the lower plate shows that the electrolyte is absorbed by the plating process.

doi:10.6342/NTU202200609

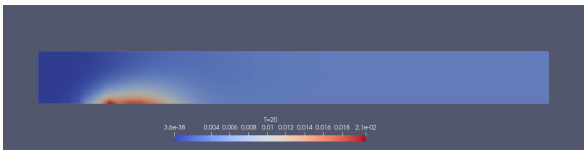

(a) Intensity map of c_g at $t = 20$.

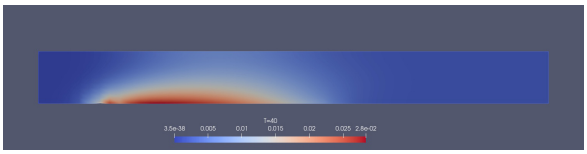

(b) Intensity map of c_g at $t = 40$.

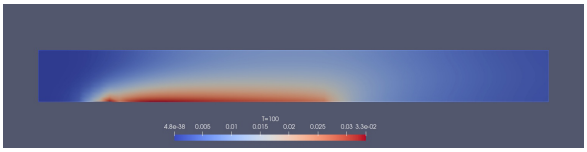

(c) Intensity map of c_g at $t = 100$.

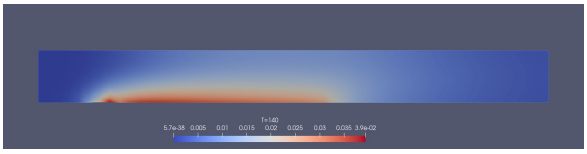

(d) Intensity map of c_g at $t = 140$.

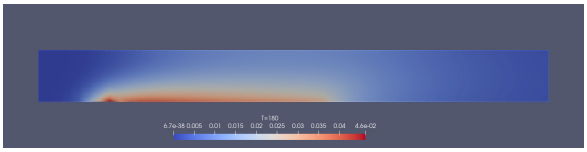

(e) Intensity map of c_g at $t = 180$.

Figure 3.13: For Section 3.5.2: intensity maps of the concentration of dissolved gas.

doi:10.6342/NTU202200609

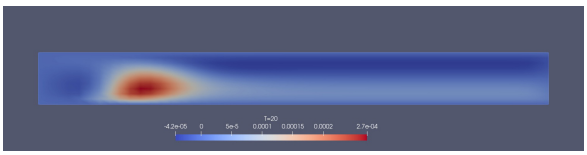

(a) Intensity map of u_{2g} at $t = 20$.

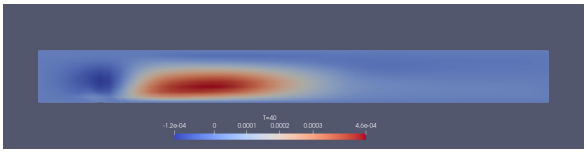

(b) Intensity map of u_{2g} at $t = 40$.

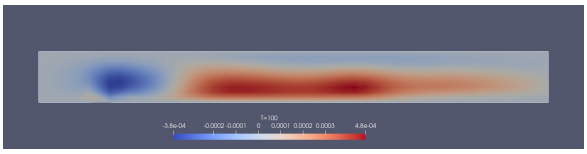

(c) Intensity map of u_{2g} at $t = 100$.

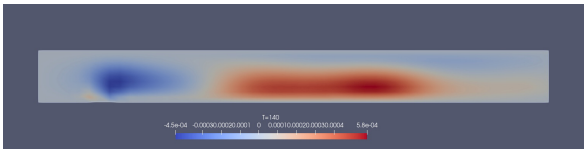

(d) Intensity map of u_{2g} at $t = 140$.

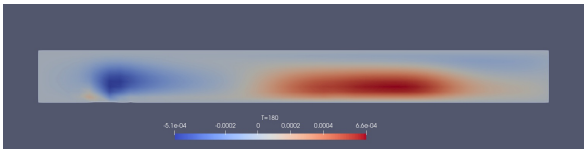

(e) Intensity map of u_{2g} at $t = 180$.

Figure 3.14: For Section 3.5.2: The vector fields $\boldsymbol{u}_g$ and $\boldsymbol{u}_l$ are very closed to Poisseuille flow. In this case, phase change and moving boundary contribute to the second component of $\boldsymbol{u}_g$ (and $\boldsymbol{u}_l$) together. The numerical test is conducted with $\delta t = 1$ and 100×10 uniform mesh. The intensity maps indicate the bubble rising in the red region. Indeed, their exists high gas volume fraction region near the top side (see Figure 3.11).

doi:10.6342/NTU202200609

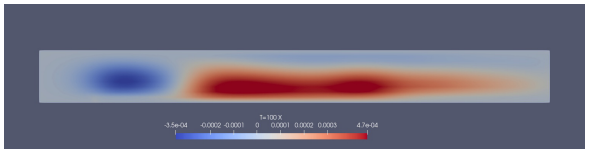

(a) Intensity map of u_{l2} at $t = 100$.

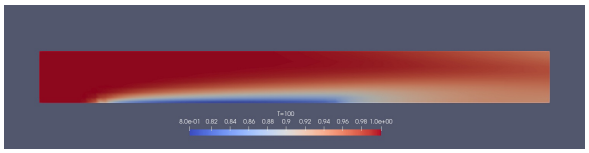

(b) Intensity map of c_k at $t = 100$.

Figure 3.15: For Section 3.5.2: Intensity maps of u_{l2} and c_k at $t = 100$.

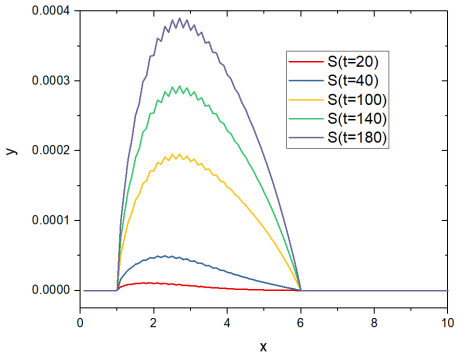

Figure 3.16: The thickness of the deposition is given by the motion of $S(t)$, plotted here at 5 instants of time, with respect to x-axis (in mm). Notice that the motion $t \to S(t)$ is very small; the oscillations are blown-out of proportions by the scaling used in the graphic.

doi:10.6342/NTU202200609

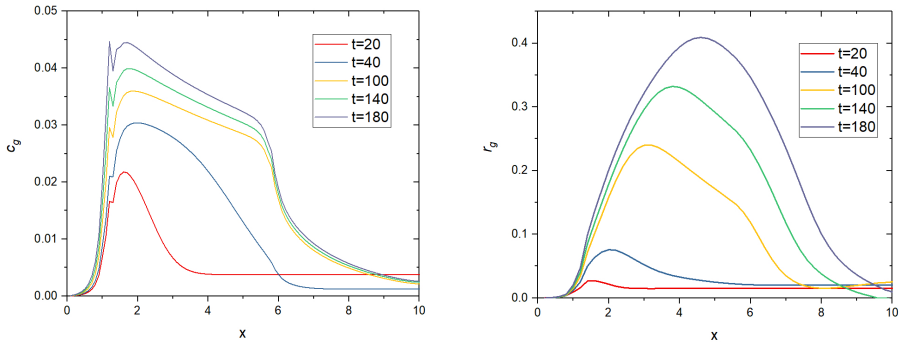

(a) For Section 3.5.2: Intensity map of c_g on S versus x.

(b) For Section 3.5.2: Intensity map of r_g on S versus x.

Figure 3.17: Plots of r_g and c_g versus x on the reaction surface S.The gas bubble density in the plating reaction zone can be observed.

3.6 Comparison with experimental results

To validate the numerical method on a real-life problem, an experiment for reproducing the numerical study in Section 3.5.2 is conducted. Here, we shall show that the experimental result can be qualitatively fitted by the numerical simulation.

The experimental setting is described as the following: A micro-channel is enclosed by two sheet glasses of size 8 $mm \times 8$ mm and another two of size 8 $mm \times 1$ mm, which form a rectangular channel. The electrolyte goes in the channel from the left and exit on the right. One piece of the square sheet glasses is partially glued on a copper plate of size 8 $mm \times 4$ mm, where the longer side of the copper plate coincides with an edge of the inlet (see Figure 3.18 for geometry setting). The inflow is set to be of average velocity

doi:10.6342/NTU202200609

0.115 mm/s. At inlet, the copper ion concentration is $c_{s0} = 39.34\ mol/m^3$ and the formaldehyde concentration is $c_{k0} = 77.5883\ mol/m^3$. Here, the inlet concentrations c_{g0} and c_{k0} are the reference concentrations for copper ion and formaldehyde, respectively. We further define the reference concentration of the hydrogen gas to be $c_{g0} = 1\ mol/m^3$. Other physical parameters are given by Table 3.3. Some parameters, for example, reference current densities i_s, i_k, and i_g, may not be exactly same as what are given in Table 3.3. Nevertheless, they are acceptably closed to the reality, or at least in a same order.

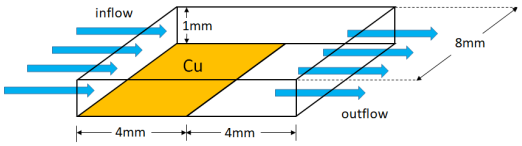

Figure 3.18: The geometry setting for both experiment and numerical simulation. Here, the yellow region indicates the copper plate glued on the sheet glass.

3.6.1 Experimental

To fabricate the test vehicle, a 4 $inch$ glass wafer was first sputtered with 30 nm chromium and 200 nm copper which served as adhesion layer and seed layer, respectively. The wafer was then diced into each 8 $mm \times 8\ mm$ glass dies. To ensure a significant comparison between the regions being plated or not, each test die was half immersed in SPS ($Na_2S_2O_8$) solution and hydrochloric acid to remove copper and chromium layer. The glass die

doi:10.6342/NTU202200609

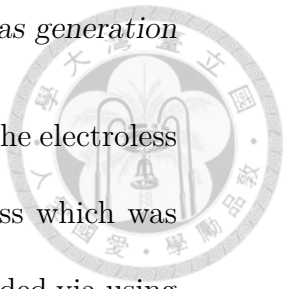

turned out half transparent and half coated with copper where the electroless copper plating took place. Thereafter, a fully transparent glass which was identical to the size of test die, was face-to-face aligned and bonded via using flip-chip die-bonder in order to obtain a clear observation view. Two tungsten wire which were 8 mm in length and 2 mm in diameter were glued by UV gel and placed on the periphery of the test die for the purpose of restricting the flow direction and defining the height between the dies (see Figure 3.19).

The test vehicle was then subjected to micro-fluidic system composed of a PDMS mode containing micro-fluidic channel and a bottom glass. Clips were used to sealed the micro-fluidic system and prevented the leakage of electrolyte. A peristatic pump was used to control the flow and connect the micro-fluidic system with silicone tube. Prior to the electroless plating, the test vehicle was immersed in 10% sulfuric acid to remove copper oxide. Finally, the electroless copper plating was conducted in a water tank controlled at 50 $^{\circ}C$ with in-situ recording via stereomicroscope (charged coupled device digital camera CCD). The electrolyte PHE-1 Uyemura possessing the given reference concentrations c_{s0} of (complexed) copper ion and c_{k0} of formaldehyde was used for the experiment. A complete equipment setup is described in Figure 3.20.

doi:10.6342/NTU202200609

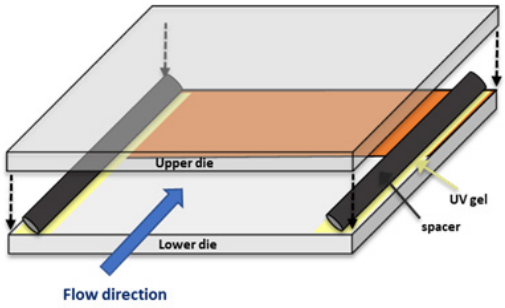

Figure 3.19: Test vehicle formation.

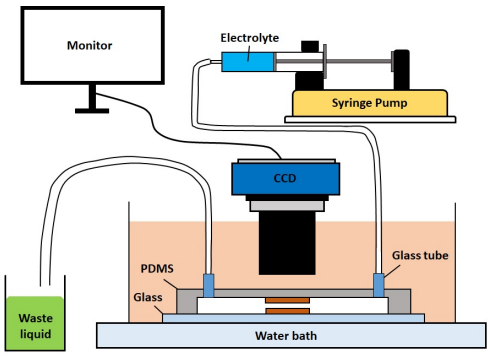

Figure 3.20: Electroless copper plating via using microfluidic system.

3.6.2 Results

Experimental results (see Figure 3.21) show that the bubbles are not only appearing on the copper plate, but also appearing on the top. In video, one can see that there were several bubbles going to the top from the center or the bottom side of the channel. The region above the glass becomes darker with time. The simulation results (see Figure 3.11) qualitatively arrive at the same conclusion. The experiment indicates that the clustering of bubbles happens on both top side and the bottom side of the channel. Second, the numerical simulation predicts that most bubbles are generated at an early

doi:10.6342/NTU202200609

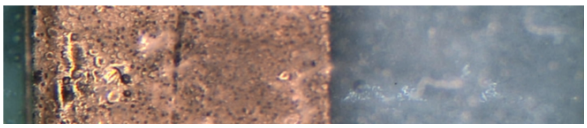

(a) The initial profile of the micro-channel.

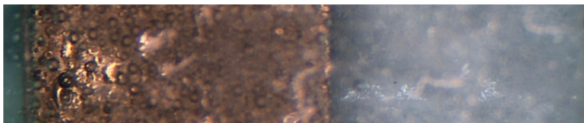

(b) micro-channel at $t = 20\ s$.

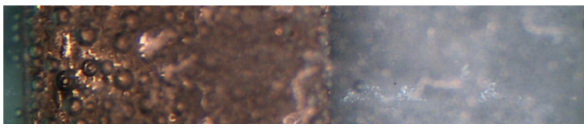

(c) micro-channel at $t = 40\ s$.

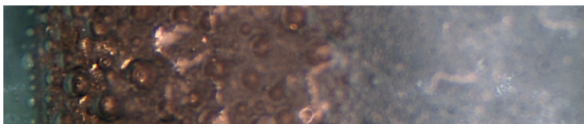

(d) micro-channel at $t = 100\ s$.

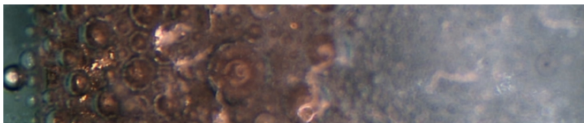

(e) micro-channel at $t = 140\ s$.

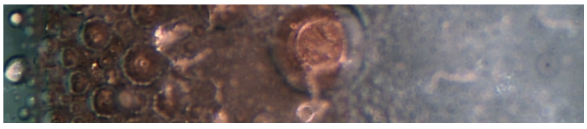

(f) micro-channel at $t = 180\ s$.

Figure 3.21: The pictures are taken from the top side and the region near the center between two 8 $mm \times 1\ mm$ sheet glasses. The brown region is covered by the copper plate, where the surface reaction occurs.

doi:10.6342/NTU202200609

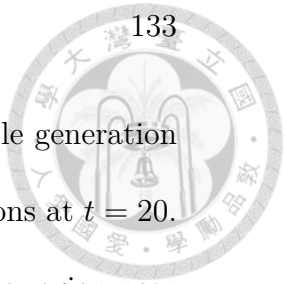

stage and near the inlet. The experiment shows that the bubble generation is more exuberant near the inlet in comparison with other regions at $t = 20$. This observation coincides with that of Figs 3.13 and 3.17a. The region near the inlet at $t = 20$ is of the highest concentration of dissolving hydrogen gas. In addition, large bubbles were observed at the back end of the copper plates (i.e. region near (x,y) = (6,0) corresponding Figure 3.1), which is also the case in Figure 3.17b.

3.6.3 Discussion

For an electroless plating process accompanying gas generation, the bubble distribution with respect to time, in the micro-channel, is the most important index for evaluating the quality of deposition. To measure it quantitatively, a high-quality optical system installed in the micro-channel is indispensable. For example, several types of fiber optical probe have been used to measure the particle (or bubble) size and distribution in a channel flow (or micro-channel flow) [71, 72, 73, 74]. However, such optical system is difficult to be installed in our case because there is no appropriate place to setup the light source and the detector in the micro-channel. The signal interference caused by the copper plate or glued gel on two sides is almost inevitable.

doi:10.6342/NTU202200609

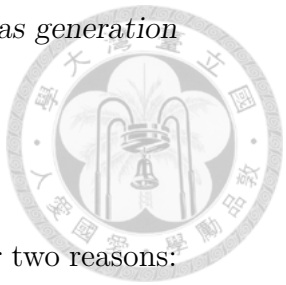

3.7 Conclusion

The numerical simulation of an electroless plating is difficult for two reasons: the multi-phase modeling and the nonlinearities. We have proposed a phase averaged liquid-gas two fluid velocities/one pressure system combined with phase densities and chemical concentration equations. The nonlinearities being similar to those of the Navier-Stokes equations, we have used a semi-Eulerian time discretization leading to a generalized Stokes operator for the two velocities/one pressure system; the inf-sup saddle point theorem has lead to a proof of stability and well posedness of the discretized system by the Hood-Taylor finite element method. The two phase flow model is compatible with single phase models when the volume fraction of gas and the concentration of the gas in the liquid phase are set to zero. The model is also compatible with the one dimensional model proposed in [1]. The numerical results confirm the robustness of the method. To validate the model a real life experiment has been performed. The numerical results agree qualitatively with the experiment for the repartition of bubbles near the plating boundary. We believe that in the future the computer code will be used to design industrial and experimental systems. However, as to the measurement of the deposition rate, It takes at least one hour to obtain an observable thickness of plating. In this case, bubbles have accumulated everywhere in the micro-channel and there is ground for an extension of the present code with a level set or phase field model which tracks the liquid to

doi:10.6342/NTU202200609

gas interface. To establish a mathematical model suitable for a larger time simulation is left as a future work.

3.A Estimation of the interfacial terms

Let V_0 be a local volume to be observed which is occupied by gas and liquid. In a liquid-gas two phase system, we have $A_l = A_g$ and further $\rho_l(\boldsymbol{w}_l - \boldsymbol{u}_l) \cdot \boldsymbol{n}_l = -\rho_g(\boldsymbol{w}_g - \boldsymbol{u}_g) \cdot \boldsymbol{n}_g$ on the interface. If the size of each single bubble in the electrolyte is small enough, then we can assume that the bubbles are spherical. Assuming that there is a typical radius for all bubbles $R_B > 0$ such that $1/R_B^2$ is the average of $1/R^2$ among all bubbles in the system, the growth rate of bubbles governed by the local mass loss prescribed by Eq. (3.3) can be computed by the relation

$$4\pi R_B^2 N_q \frac{dR}{dt} = \int_{V_0} \frac{\dot{S}_g}{\rho_g} dV, \tag{3.75}$$

where N_q is the amount of bubbles in a local volume V_0. Therefore, we have the following formulae on A_g and A_l, respectively

$$(\boldsymbol{u}_g - \boldsymbol{w}_g) \cdot \boldsymbol{n}_g = -\frac{1}{4\pi N_q R^2} \int_{V_0} \frac{\dot{S}_g}{\rho_g} dV \tag{3.76}$$

$$(\boldsymbol{u}_l - \boldsymbol{w}_l) \cdot \boldsymbol{n}_l = \frac{1}{4\pi N_q R^2} \int_{V_0} \frac{\dot{S}_g}{\rho_l} dV. \tag{3.77}$$

The quantity R_B is useful when the fluid velocity is large enough so that each bubble won't stay at the observed physical domain, because every bubble hasn't been far from the state that is just after nucleation.

doi:10.6342/NTU202200609

Given a small cube V_0 of size $|V_0| = d \times d \times d$ and a typical radius R_B, the ratio of its surface area and volume is $\frac{4\pi N_q R_B^2}{d^3}$, where N_q can be estimated by

$$N_q = \frac{r_g d^3}{\frac{4}{3}\pi R_B^3} \tag{3.78}$$

Therefore, if d is small enough so that the physical quantities in $\boldsymbol{F}_\alpha$ defined in Section 3.2.3 can be assumed uniform, then we have the approximation

(3.79)

$$\boldsymbol{F}_l \approx \left(\frac{4\pi N_q R_B^2}{d^3}\right) \cdot \rho_l \cdot \left(-\frac{d^3 \dot{S}_g}{4\pi N_q R_B^2 \rho_l}\right) \boldsymbol{u}_l = -\dot{S}_g \boldsymbol{u}_l = \dot{S}_l \boldsymbol{u}_l. \tag{3.80}$$

Similarly,

$$\boldsymbol{F}_g \approx \dot{S}_g \boldsymbol{u}_g \tag{3.81}$$

The same approximation can be applied to G_j occurring at (3.5) and (3.6):

$$G_j \approx \dot{S}_l c_j, \quad j = s, k, \quad G_g \approx \dot{S}_l c_g - M_g K \rho_l r_l (c_g - c_{sat})^+ \tag{3.82}$$

doi:10.6342/NTU202200609

Appendix A

Preliminaries and notations

A.1 Lebesgue spaces $L^p(\Omega)$ and Sobolev spaces $W^{k,p}(\Omega)$

A.1.1 L^p space

Let $1 \leq p \leq \infty$ and $\Omega \subset \mathbb{R}^d$ a bounded domain. We denote by $L^p(\Omega)$ the set of all measurable functions from Ω to $\mathbb{C}$ or $\mathbb{R}$ which satisfy

$$\|f\|_p := \begin{cases} \left(\int_\Omega |f|^p dx\right)^{1/p} < \infty & 1 \leq p < \infty; \\ \operatorname{ess\,sup}_{x\in\Omega} |f| & p = \infty. \end{cases} \tag{A.1}$$

In particular, $L^2(\Omega)$ is a Hilbert space with the inner product $(\cdot,\cdot)$ defined by

$$(f,g) := \int_\Omega f(x)\overline{g(x)}dx, \quad f,g \in L^2(\Omega), \tag{A.2}$$

which induces the norm $\| \ \|_0$.

doi:10.6342/NTU202200609

A.1.2 Sobolev space

Let k be a natrual number, $\alpha = (\alpha_1, \ldots, \alpha_d)$ a multi-index with norm $|\alpha| = \alpha_1 + \cdots + \alpha_d$. We define

$$D^\alpha f = \frac{\partial^{|\alpha|} f}{\partial x_1^{\alpha_1} \cdots \partial x_d^{\alpha_d}}$$

The Sobolev space $W^{k,p}(\Omega)$ is defined as

$$W^{k,p}(\Omega) := \{f \in L^p(\Omega) : \ D^\alpha f \in L^p(\Omega) \ \forall |\alpha| \leq k\} \tag{A.3}$$

A common way to define the norm of $W^{k,p}(\Omega)$ is

$$\|f\|_{W^{k,p}(\Omega)} := \begin{cases} \left(\sum_{\alpha \leq k} \|D^\alpha f\|^p_{L^p(\Omega)}\right)^{\frac{1}{p}} & 1 \leq p < \infty; \\ \max_{\alpha \leq k} \|D^\alpha f\|_{L^\infty(\Omega)} & p = \infty. \end{cases} \tag{A.4}$$

For the particular case $p = 2$, the space $H^k(\Omega) := W^{k,2}(\Omega)$ is a Hilbert space. Moreover, we denote by $H^1_{\Gamma_D}(\Omega)$ the closed subspace of $H^1(\Omega)$ defined by

$$H^1_{\Gamma_D}(\Omega) := \{f \in H^1(\Omega) : \ f|_{\Gamma_D} = 0\}. \tag{A.5}$$

If the number k is non-integer, we define the fractional Sobolev space in two cases: If $0 < k < 1$, we define $W^{k,p}$ for $1 \leq p < \infty$ by

$$W^{k,p}(\Omega) := \left\{ f \in L^p(\Omega) : \frac{|f(x) - f(y)|}{|x - y|^{\frac{d}{p}+k}} \in L^p(\Omega \times \Omega) \right\} \tag{A.6}$$

which endowed with the norm

$$\|f\|_{W^{k,p}(\Omega)} := \left(\int_\Omega |f|^p dx + \int_\Omega \int_\Omega \frac{|f(x) - f(y)|}{|x - y|^{\frac{d}{p}+k}} dx dy \right)^{\frac{1}{p}}. \tag{A.7}$$

doi:10.6342/NTU202200609

When $k > 1$ and it is not an integer, we write $k = m + s$, where m is an integer and $0 < s < 1$. The space $W^{k,p}(\Omega)$ is defined by

$$W^{k,p}(\Omega) := \{f \in W^{m,p} : \ D^\alpha f \in W^{s,p} \ \forall \alpha \text{ s.t. } |\alpha| = m\}. \tag{A.8}$$

The above space is equipped with the norm

$$\|f\|_{W^{k,p}(\Omega)} := \left(\|f\|^p_{W^{m,p}(\Omega)} + \sum_{|\alpha|=m} \|D^\alpha f\|^p_{W^{s,p}(\Omega)} \right)^{\frac{1}{p}}. \tag{A.9}$$

In particular, $H^k(\Omega) := W^{k,p}(\Omega)$ is again a Hilbert space when k is non-integer.

For convenience, we denote the norm of $H^k(\Omega)$ by $\|\cdot\|_k$ for real $k \geq 0$.

A.1.3 Traces

Theorem A.1.1 Let $\Omega \subset \mathbb{R}^d$ be bounded with Lipschitz boundary. Then there exists a bounded linear operator $T : W^{1,p}(\Omega) \to L^p(\partial\Omega)$ such that

$$\begin{aligned} Tu &= u|_{\partial\Omega}, \quad u \in W^{1,p}(\Omega) \cap C(\overline{\Omega}) \\ \|Tu\|_{L^p(\partial\Omega)} &\leq c(p,\Omega)\|u\|_{W^{1,p}(\Omega)}, \quad u \in W^{1,p}(\Omega) \end{aligned} \tag{A.10}$$

Remark A.1.1 For $1 < p < \infty$, the trace operator T maps maps $W^{1,p}(\Omega)$ continuously onto the space $W^{1-\frac{1}{p},p}(\partial\Omega)$.

A.1.4 Bochner space

Given $I := [0, T]$ a time interval and a Sobolev space $W^{k,p}(\Omega)$, the Bochner space $L^r(I; W^{k,p}(\Omega))$ is the space of all measurable function $u : I \to W^{k,p}(\Omega)$

doi:10.6342/NTU202200609

such that the associated norm is finite:

$$\|u\|_{L^r(I;W^{1,p}(\Omega))} := \left(\int_0^T \|u(t)\|^r_{W^{k,p}(\Omega)} dt\right)^{\frac{1}{p}} < +\infty, \quad 1 \le r < \infty$$
$$\|u\|_{L^\infty(I;W^{k,p}(\Omega))} := \operatorname*{ess\,sup}_{t\in I} \|u(t)\|_{W^{k,p}(\Omega)} < +\infty, \quad r = \infty. \tag{A.11}$$

A.2 Weighted Sobolev space

Definition A.2.1 (Weighted space $L^p_\rho(\Omega, d, m)$ and $W^{1,p}_\rho(\Omega, d, m)$) Let (Ω, d, m) be a metric measure space, where m is a locally finite Borel regular measure on Ω. Let $p > 1$ and $\rho : \Omega \to [0, \infty]$ a Borel function satisfying $\rho^{-1} \in L^{\frac{1}{p-1}}m$; we define the weighted space $L^p(\Omega, d, m)$ and sobolev space $W^{1,p}_\rho(\Omega, d, m)$ by

$$L^p_\rho(m) := \left\{ f \in L^1(\Omega, d, m) \mid \int_\Omega |f|^p \rho dm < +\infty \right\},$$
$$W^{1,p}_\rho(m) := \left\{ f \in W^{1,1}(\Omega, d, m) \mid \int_\Omega |f|^p \rho dm + \int_\Omega |\nabla f|^p \rho dm < +\infty \right\},$$

respectively. The above spaces are endowed with the norms

$$\|f\|^p_{L^p_\rho} := \int_\Omega |f|^p \rho dm + \int_\Omega |\nabla f|^p \rho dm.$$
$$\|f\|^p_{W^{1,p}_\rho} := \int_\Omega |f|^p \rho dm + \int_\Omega |\nabla f|^p \rho dm.$$

If $\Omega \subset \mathbb{R}^n$ endowed with standard Euclidean metric, we shorten the notations by $L^p_\rho(\Omega) := L^p_\rho(\Omega, d, m)$, $W^{1,p}_\rho(\Omega) := W^{1,p}_\rho(\Omega, d, m)$, respectively

Proposition A.2.1 $\forall p > 1$, the weighted Sobolev space $(W^{1,p}_\rho(\Omega, d, m), \| \cdot \|_\rho)$ is a Banach space whenever $\rho^{-1} \in L^{\frac{1}{p-1}}(\Omega)$

Definition A.2.2 (Doubling) A locally finite Borel measure m on (Ω, d) is doubling if it gives finite positive measure to balls and there is a constant

doi:10.6342/NTU202200609

$C > 0$ such that

$$m(B(x,2r)) \leq Cm(B(x,r)), \quad \forall x \in \Omega,\ r > 0$$

Definition A.2.3 (p-Poincaré) For $p \in [1,\infty)$, we say that a p-Poincaré inequality holds for Lipschitz functions if there are constants $\tau, \Lambda > 0$ such that $\forall f \in \mathrm{Lip}(\Omega)$, $\forall x \in \mathrm{supp}(m),\ r > 0$, the following inequality holds:

$$\frac{1}{m(B(x,r))}\int_{B(x,r)} |f - f_{B(x,r)}|dm \leq \tau\left(\frac{1}{m(B(x,\Lambda r))}\int_{B(x,\Lambda r)} |\nabla f|^p dm\right)^{\frac{1}{p}},$$

where

$$f_A := \frac{1}{m(A)}\int_A f dm.$$

Definition A.2.4 A doubling metric measure space satisfying p-Poincaré inequality is called PI_p space.

Remark A.2.1 Euclidean space endowed with normal euclidean distancing is PI_p for all $p \geq 1$.

Theorem A.2.1 [75] Suppose that (Ω, d, m) is a PI_1 metric measure space, $\rho \in L^1_{loc}(m)$ and $\rho^{-1} \in L^{\frac{1}{p-1}}(m)$. Then $W^{1,p}_\rho(\Omega, d, m)$ is reflexive for all $p > 1$.

Corollary A.2.1 Let $\Omega \subset \mathbb{R}^d$ be a open bounded domain, $W^{1,p}_\rho$ is a reflexive Banach space if $p > 1$, $\rho \in L^1_{loc}(\Omega)$, and $\rho^{-1} \in L^{\frac{1}{p-1}}(\Omega)$.

Remark A.2.2 Let $\Omega \subset \mathbb{R}^d$ and $p = 2$, we denote $W^{1,p}_\rho(\Omega)$ by $H^1_\rho(\Omega)$, which is a Hilbert space endowed with the inner product

$$(u,v)_{\rho,1} = \int_\Omega u(x)v(x)\rho(x)dx + \int_\Omega (\nabla u(x)\cdot\nabla v(x))\rho(x)dx.$$

doi:10.6342/NTU202200609

We also denote the inner product for $L^2_\rho(\Omega)$ by

$$(u,v)_{\rho,0} = \int_\Omega u(x)v(x)\rho(x)dx.$$

The norm of $H^k_\rho(\Omega)$, $k \in \mathbb{N} \cup \{0\}$ is denoted by $\|\cdot\|_{\rho,k}$.

Theorem A.2.2 (compact embedding) [76] Let $\Omega \subset \mathbb{R}^d$, $1 \le s \le r < \frac{dq}{d-q}$, $q \le p$, $1 < p < +\infty$, and

$$K(w) := \max\left\{\|w^{-\frac{1}{p}}\|_{L^{\frac{pq}{p-q}}(\Omega)}, \|w^{\frac{1}{s}}\|_{L^{\frac{rs}{r-s}}(\Omega)}\right\} < +\infty. \tag{A.12}$$

Note that we take $+\infty$ if $p-q=0$ or $r-s=0$ in (A.12). Then the embedding operator

$$i : W^{1,p}_w(\Omega) \hookrightarrow L^s_w(\Omega)$$

is a compact operator. For $r = dq/(d-q)$, the embedding operator i is bounded only.

A.3 Weak convergence in Banach spaces

Lemma A.3.1 Let E be a Banach space, $\|\cdot\|$ its norm, and $f_n : E \to \mathbb{R}$ a sequence of functions for $n = 1, 2, \ldots$. If f_n is equicontinuous and pointwisely convergent on a dense subset $D \subset E$, then f_n is pointwisely convergent everywhere.

Proof. Let $a \in E$. Since D is dense in E, there is a $b \in D$ such that for every ϵ there is a δ such that $\|a-b\| < \delta$ and $|f_n(b) - f_n(a)| < \frac{\epsilon}{3}$. For any $m > n$,

doi:10.6342/NTU202200609

we have

$$|f_m(a) - f_n(a)| \leq |f_m(a) - f_m(b)| + |f_m(b) - f_n(b)| + |f_n(b) - f_n(a)|$$
$$< \frac{2\epsilon}{3} + |f_m(b) - f_n(b)|$$

But $f_n(b)$ is convergent, it is shown that $f_n(a)$ is a Cauchy sequence. Q.E.D.

Lemma A.3.2 Let E be a normed space, $\|\cdot\|$ its norm and $\|\cdot\|_{E'}$ the norm of its dual space. Let x_n be a sequence in E for $n = 1, 2, \ldots$, $x \in E$. The followings are equivalent:

(i) $x_n \to x$ in E weakly

(ii) x_n is bounded and for all $S \subset E'$ such that $\overline{span\ S} = E'$ satisfies $\lim_{n\to\infty} f(x_n) = f(x)$ for all $f \in S$.

Proof. (i)⇒(ii). Assuming that $x_n \to x$ in E weakly, then x_n is bounded. Moreover, for all $f \in E'$, we have $\lim_{n\to\infty} f(x_n) = f(x)$. Hence for all $S \subset E'$ such that $\overline{span\ S} = E'$ we have $\lim_{n\to\infty} f(x_n) = f(x)$ for all $f \in S$.

(ii)⇒ (i). Assume that $\|x_n\|$ is bounded by some constant $M > 0$ and for all $S \subset E'$ such taht $\overline{span\ S} = E'$ satisfies $\lim_{n\to\infty} f(x_n) = f(x)$ for all $f \in S$. Take arbitrary $g \in span\ S$, then $g = \sum_{k=1}^{m} \alpha_k f_k$ for $\alpha_k \in \mathbb{R}$ and $f_k \in S$. This gives us $\lim_{n\to\infty} g(x_n) = g(x)$. Now, take arbitrary $g \in E' = \overline{span\ S}$, then $g = \lim_{k\to\infty} g_k$ for some sequence g_k in $span\ S$. Fix $\epsilon > 0$. Since $g = \lim_{k\to\infty} g_k$,

doi:10.6342/NTU202200609

there is $K \in \mathbb{N}$ such that $\|g - g_k\|_{E'} \leq \epsilon$ for all $k > K$. Then

$$\begin{aligned} |g(x_n) - g(x)| &\leq |g(x_n) - g_k(x_n)| + |g_k(x_n) - g_k(x)| + |g_k(x) - g(x)| \\ &\leq \|g - g_k\|_{E'}\|x_n\| + |g_k(x_n) - g_k(x)| + \|g_k - g\|_{E'}\|x\| \\ &\leq \epsilon M + |g_k(x_n) - g_k(x)| + \epsilon\|x\| \end{aligned} \tag{A.13}$$

We take a limit $n \to \infty$ in the above inequality, then

$$\limsup_{n\to\infty} |g(x_n) - g(x)| \leq \epsilon M + \lim_{n\to\infty} |g_k(x_n) - g_k(x)| + \epsilon\|x\|$$

Since $g_k \in \mathit{span}\ S$, we have $\lim_{n\to\infty} |g_k(x_n) - g_k(x)| = 0$ and we get

$$\limsup_{n\to\infty} |g(x_n) - g(x)| \leq \epsilon M + \epsilon\|x\|.$$

Since $\epsilon > 0$ is arbitrary, we obtain $\limsup_{n\to\infty} |g(x_n) - g(x)| = 0$. This implies that $\lim_{n\to\infty} g(x_n) = g(x)$. Since $g \in E^{'}$ is arbitrary, the proof is completed. Q.E.D.

Lemma A.3.3 Let X be a Banach space, D a dense subset of $X^{'}$, x_n, $n = 1, 2, \ldots$ the bounded sequence in X. If $g(x_n) \to g(x)$ for all $g \in D$, then $x_n \to x$ weakly in X.

Proof. If x_n is a bounded sequence in X, it is an equicontinuous sequence as a sequence of functions $X^{'} \to \mathbb{R}$. And x_n is pointwisely convergent on D by the hypothesis. Using Lemma A.3.1, x_n is pointwisely convergent. By Lemma A.3.2, since x_n is bounded in norm by the hypothesis, we conclude that x_n is weakly convergent to x in X. Q.E.D.

doi:10.6342/NTU202200609

Lemma A.3.4 Let X, Y be two normed space and $T : X \to Y$ the bounded linear operator. If $x_n \to x$ weakly in X, then $Tx_n \to Tx$.

Proof. Let $y^* \in Y'$. We can define $x^* = y^*T \in X'$. So

$$y^*(Tx_n) = (y^*T)(x_n) = x^*(x_n) \to x^*(x) = (y^*T)(x) = y^*(Tx).$$

Q.E.D.

Corollary A.3.1 Let $\Gamma \subset \partial\Omega$. There is a trace operator $Tr : L^2(0,T;H^1(\Omega)) \to L^2(0,T;H^{\frac{1}{2}}(S))$ such that: If $x_n \to x$ weakly in $L^2(0,T;H^1(\Omega))$, then $Trx_n \to Trx$ weakly in $L^2(0,T;H^{\frac{1}{2}}(\Gamma))$.

Proof. By Section 5.7 in [77], there exists a trace operator $Tr : L^2(0,T;H^1(\Omega)) \to L^2(0,T;H^{\frac{1}{2}}(\Gamma))$ which is linear and bounded. By Lemma A.3.4, the proof is completed. Q.E.D.

doi:10.6342/NTU202200609

doi:10.6342/NTU202200609

Appendix B

A simplified model with surface reaction

We assume that $\Omega \subset \mathbb{R}^d$ be a bounded open domain. For Sobolov space, the norm of $W^{k,p}(\Omega)$ space is denoted by $\|\cdot\|_{k,p}$ for $p > 0,\ k \geq 0$. If $p = 2$, the norm is denoted by $\|\cdot\|_k$. For weighted Sobolev space, we denote the norm of $H^k_\rho(\Omega)$ by $\|\cdot\|_{\rho,k}$ for $k \in \mathbb{N}$, ρ any function satisfying $\rho, \dfrac{1}{\rho} \in L^1(\Omega)$. If $k = 0$, we denote the norm of $L^2_\rho(\Omega)$ by $\|\cdot\|_\rho$ for simplicity. We denote the inner product for $L^2_\rho(\Omega)$ by $(\cdot,\cdot)_\rho$. For convenience, we denote the generic constant by C or C_j, $j = 1, 2, \ldots$.

B.1 Modeling equations

We assume that there are two chemical species s and k involving in the surface reaction in terms of the mixed potential (see (3.20)). Let E_j be the

doi:10.6342/NTU202200609

constant with subscripts $j = s, k$ representing the ion to be plated and the anodic ion involving in the surface reaction, respectively. Without loss of generality, we assume that $0 > E_s > E_k$. For the physical system, we assume that the chemical reaction satisfying electron balance on the reaction surface $S \subset \partial\Omega$, the convective effect in system (3.26)-(3.26) is negligible, and the densities satisfy $\rho_l >> \rho_g > 0$. For simplicity, we further assume that the saturation concentration can be neglected. That is, we require that

$$\boldsymbol{u}_g = \boldsymbol{u}_l = 0, \quad c_{sat} = 0. \tag{B.1}$$

Employing (B.1) into (3.3), we get

$$\partial_t r_l = -\frac{K}{\widetilde{\rho_g}} r_l c_g, \tag{B.2}$$

where $\dfrac{1}{\widetilde{\rho_g}} := \dfrac{1}{\rho_g} - \dfrac{1}{\rho_l}$. The assumption (B.1) tells us that the momentum balance equations (3.27) are dropped. The remaining equations (3.5) with the assumption (B.1) can be rewritten as

$$\begin{aligned} &r_l \partial_t c_j - D_j \nabla \cdot (r_l \nabla c_j) = 0, \quad j \neq g \\ &r_l \partial_t c_g - D_g \nabla \cdot (r_l \nabla c_g) + \frac{K_g M_g}{\rho_l} r_l c_g = 0 \end{aligned} \tag{B.3}$$

Since there are only two chemical species s and k involving in the surface reaction, (B.2), (B.3) and the boundary conditions (3.19)-(3.20) with electrical neutrality assumption lead to the system:

doi:10.6342/NTU202200609

$$\begin{aligned}
\partial_t r_l &= -\frac{K}{\rho_g} r_l c_g, \quad \text{in } \Omega \times (0,T], \\
r_l \partial_t c_g - D_g \nabla \cdot (r_l \nabla c_g) + \frac{K_g M_g}{\rho_l} r_l c_g &= 0, \quad \text{in } \Omega \times (0,T], \\
r_l \partial_t c_s - D_s \nabla \cdot (r_l \nabla c_s) &= 0, \quad \text{in } \Omega \times (0,T], \\
r_l \partial_t c_k - D_k \nabla \cdot (r_l \nabla c_k) &= 0, \quad \text{in } \Omega \times (0,T],
\end{aligned} \tag{B.4}$$

subject to the boundary conditions

$$\begin{aligned}
-D_s \frac{\partial c_s}{\partial \mathbf{n}} = \frac{|I_s|}{z_s F}, \quad -D_k \frac{\partial c_k}{\partial \mathbf{n}} = \frac{|I_k|}{z_k F}, \quad -D_g \frac{\partial c_g}{\partial \boldsymbol{n}} = -\frac{\beta |I_s|}{z_s F} \quad \text{on } S, \\
\frac{\partial c_s}{\partial \mathbf{n}} = \frac{\partial c_k}{\partial \mathbf{n}} = \frac{\partial c_g}{\partial \mathbf{n}} 0, \quad \text{on } \partial\Omega \setminus S \times (0,T]
\end{aligned} \tag{B.5}$$

for some constant $\beta > 0$. The initial conditions $r_l(0) = r_l^0$, $c_s(0) = c_s^0$, $c_k(0) = c_k^0$, $c_g(0) = c_g^0$ are all in $H^1(\Omega)$ satisfying

$$0 < c_s^0, c_k^0, c_g^0 \leq 1, \quad 0 < \epsilon < r_l^0 \leq 1 \ \text{ in } \Omega \tag{B.6}$$

for some constant $\epsilon > 0$. In the above, I_s and I_k satisfy (3.20) with $j = s, k$ respectively and we further assume that $\gamma_s = \gamma_k = 1$. For electron balance, we have the constrain:

$$I_s + I_k = 0, \quad \text{on } S. \tag{B.7}$$

We shall note that we replace $\widetilde{\rho_g}$ with ρ_g in (B.4) by an abuse of notation.

Remark B.1.1 In (B.4), we employ c_g instead of c_g^+ in the second term of the first equation and the third term of the second equation. We will show that c_g is nonnegative with a proper initial condition.

doi:10.6342/NTU202200609

B.2 Time-discrete problem

Let $N > 0$ be an integer and $\delta t = T/N$ be the time step. To study the existence and the stability of (B.4)-(B.7), we consider the time-discrete problem:

$$\begin{aligned}
&\frac{r_l^{m+1} - r_l^m}{\delta t} = -\frac{K_g}{\rho_g} r_l^{m+1} c_g^m \\
&\frac{r_l^{m+1} c_g^{m+1} - r_l^{m+1} c_g^m}{\delta t} - \nabla \cdot (D_g r_l^{m+1} \nabla c_g^{m+1}) + \frac{M_g K_g}{\rho_l} r_l^{m+1} c_g^{m+1} = 0 \\
&\frac{r_l^{m+1} c_s^{m+1} - r_l^{m+1} c_s^m}{\delta t} - \nabla \cdot (D_s r_l^{m+1} \nabla c_s^{m+1}) = 0 \\
&\frac{r_l^{m+1} c_k^{m+1} - r_l^{m+1} c_k^m}{\delta t} - \nabla \cdot (D_k r_l^{m+1} \nabla c_k^{m+1}) = 0
\end{aligned} \tag{B.8}$$

with boundary conditions on S:

$$-D_s \frac{\partial c_s^{m+1}}{\partial \mathbf{n}} = \frac{1}{z_s F} |i_s(E_{mix}^{m+1})| c_s^{m+1}, \ -D_k \frac{\partial c_k^{m+1}}{\partial \mathbf{n}} = \frac{1}{z_k F} |i_k(E_{mix}^{m+1})| c_k^{m+1}, \ -D_g \frac{\partial c_g^{m+1}}{\partial \boldsymbol{n}} = \beta D_s \frac{\partial c_s^{m+1}}{\partial \mathbf{n}} \tag{B.9}$$

where

$$i_s(E_{mix}^{m+1}) = L_s \left(\exp\left(\frac{\alpha_s z_s F (E_{mix}^{m+1} - E_s)}{R\theta} \right) - \exp\left(\frac{-\beta_s z_s F (E_{mix}^{m+1} - E_s)}{R\theta} \right) \right),$$

$$i_k(E_{mix}^{m+1}) = L_k \left(\exp\left(\frac{\alpha_k z_k F (E_{mix}^{m+1} - E_k)}{R\theta} \right) - \exp\left(\frac{-\beta_k z_k F (E_{mix}^{m+1} - E_k)}{R\theta} \right) \right),$$

$$i_s(E_{mix}^{m+1}) c_s^{m+1} + i_k(E_{mix}^{m+1}) c_k^{m+1} = 0.$$

In the following context, we define $i_s^{m+1} := |i_s(E_{mix}^{m+1})|$, $i_k^{m+1} := |i_k(E_{mix}^{m+1})|$.

Let us begin with the upper bound and the lower bound of r_l.

Lemma B.2.1 Assume that $0 < \epsilon < r_l^j < 1$, $c_g^j \geq 0$, $c_g^j \in H^1(\Omega) \cap L^\infty(\Omega)$ and $r_l^j \in H^1(\Omega)$ for all integer $0 \leq j \leq m$, then

(i) $0 < \dfrac{\epsilon}{1 + K\delta t/\rho_g} < r_l^{m+1} < 1.$

doi:10.6342/NTU202200609

(ii) $\dfrac{1}{r_l^{m+1}} \in L^\infty(\Omega)$

(iii) $r_l^{m+1} \in H^1(\Omega)$

Proof. By the first equation of (B.8), we have

$$\left(1 + \frac{K\delta t}{\rho_g} c_g^m\right) r_l^{m+1} = r_l^m. \tag{B.10}$$

By the assumption $c_g^m \geq 0$, we have

$$r_l^{m+1} \leq 1, \quad \frac{\epsilon}{1 + K\delta t/\rho_l} < r_l^{m+1}.$$

This proves (i). Since $1 < \dfrac{1}{r_l^{m+1}} < \dfrac{1 + K\delta t/\rho_l}{\epsilon}$, we have proved (ii).

Taking the derivative with respect to x_i in (B.10), we have

$$\left(1 + \frac{K\delta t}{\rho_g} c_g^m\right) \partial_{x_i} r_l^{m+1} = -\frac{K\delta t}{\rho_g} r_l^{m+1} \partial_{x_i} c_g^m + \partial_{x_i} r_l^m. \tag{B.11}$$

Since $\partial_{x_i} r_l^m$, $r_l^{m+1} \partial_{x_i} c_g^m$ are bounded in $L^2(\Omega)$, we can conclude that $\partial_{x_i} r_l^{m+1}$ is bounded in $L^2(\Omega)$. This proves (iii). Q.E.D.

The weak formulation regarding the system (B.8) except its first equation can be expressed as:

Problem $(\widetilde{P_c})$:

Let $0 < r_l^m, r_l^{m+1} \leq 1$, $r_l^m, r_l^{m+1} \in H^1(\Omega)$, $0 < c_s^m, c_k^m \leq 1$, $c_g^m \geq 0$, $c_s^m, c_k^m, c_g^m \in H^1_{r_l^m}(\Omega)$. Find $c_s^{m+1}, c_k^{m+1}, c_g^{m+1} \in H^1_{r_l^{m+1}}(\Omega)$ and $E_{mix}^{m+1} \in L^2(S)$ such that

$$\frac{1}{\delta t}(c_s^{m+1}, w_s)_{r_l^{m+1}} + D_s(\nabla c_s^{m+1}, \nabla w_s)_{r_l^{m+1}} + \frac{1}{z_s F}(r_l^{m+1} i_s^{m+1} c_s^{m+1}, w_s)_{L^2(S)} = \frac{1}{\delta t}(c_s^m, w_s)_{r_l^{m+1}} \tag{B.12}$$

doi:10.6342/NTU202200609

$$\frac{1}{\delta t}(c_k^{m+1}, w_k)_{r_l^{m+1}} + D_k(\nabla c_k^{m+1}, \nabla w_k)_{r_l^{m+1}} + \frac{1}{z_k F}(r_l^{m+1} i_k^{m+1} c_k^{m+1}, w_k)_{L^2(S)} = \frac{1}{\delta t}(c_k^m, w_k)_{r_l^{m+1}} \tag{B.13}$$

$$\frac{1}{\delta t}(c_g^{m+1}, w_g)_{r_l^{m+1}} + D_g(\nabla c_g^{m+1}, \nabla w_g)_{r_l^{m+1}} - \frac{\beta}{z_s F}(r_l^{m+1} i_s^{m+1} c_s^{m+1}, w_g)_{L^2(S)} + (\frac{M_g K_g}{\rho_l} c_g^{m+1}, w_g)_{r_l^{m+1}} = \frac{1}{\delta t}(c_g^m, w_g)_{r_l^{m+1}} \tag{B.14}$$

$$(i_s(E_{mix}^{m+1}) + i_k(E_{mix}^{m+1}), w)_{L^2(S)} = 0 \tag{B.15}$$

for all $w_s, w_k, w_g \in H^1(\Omega)$ and $w \in L^2(S)$.

B.3 Existence of the time-discrete problem

Proposition B.3.1 If $E_{mix}^{m+1} \in B := \{w \in L^2(S) |\ E_k \leq w \leq E_s \text{ a.e.}\}$ is given, There exist unique solutions $(c_s^{m+1}, c_k^{m+1}, c_g^{m+1})$ for Problem $(\widetilde{P_c})$.

Proof. The existence and uniqueness for c_s^{m+1}, c_k^{m+1} and c_g^{m+1} can be guaranteed by a classic theory since (B.12)-(B.14) are linear.

If E_{mix}^{m+1} is given, we can further obtain the positivity for c_s^{m+1}, c_k^{m+1} and c_g^{m+1}.

Proposition B.3.2 Let $E_{mix}^{m+1} \in B$, if $c_s^m, c_k^m, c_g^m \geq 0$ a.e., then $c_s^{m+1}, c_k^{m+1}, c_g^{m+1} \geq 0$ a.e..

Proof. Similar to the proof of Proposition 2.4.2, the nonnegativity of $c_s^{m+1}, c_k^{m+1}, c_g^{m+1}$ can be guaranteed by letting $w_s = (c_s^{m+1})^-$, $w_k = (c_k^{m+1})^-$, $w_g = (c_g^{m+1})^-$.

Q.E.D.

doi:10.6342/NTU202200609

Proposition B.3.3 Let $E_{mix}^{m+1} \in B$, $0 < c_s^j, c_k^j \leq 1$, $E_{mix}^j \in B$, for all $0 \leq j \leq m$. Furthermore, we assume that $0 \leq c_g^0 < M$ for some positive constant M, we have

$$c_s^{m+1}, c_k^{m+1} \leq 1 \tag{B.16}$$

and there exists a positive constant C depending only on Ω, D_g, T, such that

$$c_g^{m+1} \leq C, \tag{B.17}$$

Proof. To obtain (B.16), we can take $w_s = (w_s - 1)^+$ and $w_k = (w_k - 1)^+$ in (B.12) and (B.13), respectively. The proof of (B.17) is extremely technical which can be referred to Lemma II 5.7 and Theorem II 6.2 in [78]. Q.E.D.

If the value of mixed potential E_{mix}^{m+1} is restricted in $[E_k, E_s]$, the L^∞ norms of i_s^{m+1}, i_k^{m+1} are uniformly bounded in terms of E_{mix}^{m+1}, respectively. By Thoerem 4 in [79], we have the following:

Lemma B.3.1 (Strong positivity for c_s^{m+1} amd c_k^{m+1}) Let $c_s^m, c_k^m \geq 0$, $E_{mix}^{m+1} \in B$. Assuming further that there are constant $\eta_s^m, \eta_k^m > 0$ such that $c_s^m \geq \eta_s^m$ and $c_k^m \geq \eta_k^m$ a.e., there are constants $\eta_s^{m+1}, \eta_s^{m+1} > 0$ such that $c_s^{m+1} \geq \eta_s^{m+1}$, and $c_k^{m+1} \geq \eta_k^{m+1}$ a.e.. Moreover, c_s^{m+1} and c_k^{m+1} are Hölder continuous in $\overline{\Omega}$ for some exponent $0 < \alpha < 1$.

Corollary B.3.1 Assuming that $\|c_s^j\|_{L^\infty(\Omega)}$ is uniformly bounded for all $0 \leq j \leq N$, there is a generic constant $C > 0$ such that

$$\|\frac{r_l^{j+1} - r_l^j}{\delta t}\|_{L^\infty(\Omega)} \leq C \tag{B.18}$$

doi:10.6342/NTU202200609

for all $0 \le j \le N$.

To show the existence for the full problem $(\widetilde{P_c})$, the Browder fixed point theorem can be applied:

Theorem B.3.1 (Schauder fixed point theorem) Let K be a nonempty closed convex set in a Banach space. If a function $f : K \to K$ is compact, then f has a fixed point.

Lemma B.3.2 $B := \{w \in L^2(S) |\ E_k \le w \le E_s \text{ a.e.}\}$ is a closed bounded convex subset in $L^2(S)$.

Proof. Since S is of finite measure, it is obvious that B is bounded. Let $\theta \in (0,1)$, for $w_1, w_2 \in B$ we have $\theta E_k \le \theta w_1 \le \theta E_s$ and $(1-\theta)E_k \le (1-\theta)w_2 \le (1-\theta)E_s$. Therefore $E_k \le \theta w_1 + (1-\theta)w_2 \le E_s$. This implies that B is convex. Finally, let x be a limit point of B, there exists a sequence $\{x_n\}_{n=1}^{\infty} \subset B$ such that

$$\|x_n - x\|_{L^2(S)} \to 0 \quad \text{as } n \to \infty$$

This shows that $E_k \le x \le E_s$ almost everywhere on S. This completes the proof. Q.E.D.

We define the space $W_\eta := \{w \in H^1_{r_l^{m+1}}(\Omega) \mid \eta \le w \le 1 \text{ a.e.}\}$. Given Lemma B.3.1, we define $\eta_s^{m+1}, \eta_k^{m+1}$ to be the essential infimum of c_s^{m+1}, c_k^{m+1}, respectively. Let us define the mapping $\Gamma_1 : B \to \mathbf{H} := W_{\eta_s^{m+1}} \times W_{\eta_k^{m+1}}$ such that $\Gamma_1(E)$ is the set of solutions to $(\widetilde{P_{c_s}})$, and $(\widetilde{P_{c_k}})$, respectively, when letting $E_{mix}^{m+1} = E$.

doi:10.6342/NTU202200609

Lemma B.3.3 Γ_1 is a bounded operator.

Proof. Let $w_s = c_s^{m+1}$ in (B.12), we have

$$\begin{aligned}
&\frac{1}{\delta t}\|c_s^{m+1}\|^2_{r_l^{m+1}} + D_s\|\nabla c_s^{m+1}\|^2_{r_l^{m+1}} + (r_l^{m+1} i_s^{m+1} c_s^{m+1}, c_s^{m+1})_{L^2(S)} \\
&= \frac{1}{\delta t}(c_s^m, c_s^{m+1})_{r_l^{m+1}} \\
&\leq \frac{1}{\delta t}\|c_s^m\|_{r_l^m}\|c_s^{m+1}\|_{r_l^{m+1}} \\
&\leq \|c_s^m\|_{r_l^m}\left(\|c_s^{m+1}\|^2_{r_l^{m+1}} + D_s\delta t\|\nabla c_s^{m+1}\|^2_{r_l^{m+1}}\right)^{\frac{1}{2}}
\end{aligned} \tag{B.19}$$

This shows that the bound for c_s^{m+1} is independent of i_s. By the same argument, we can show that c_k^{m+1} is uniformly bounded as well. We recall that the element in B has a minimal norm $\|E_s\|_{L^2(S)}$. There must exists a sufficiently large constant $M > 0$ such that

$$\begin{aligned}
&\delta t\left(\frac{K}{\rho_l}\|c_g^{m+1}\|_{L^\infty(\Omega)} + \frac{1}{\delta t}\left(\left\|\frac{1}{r_l^{m+1}}\right\|_{L^\infty(\Omega)}\|r_l^m\|_{L^\infty(\Omega)}\right)^{\frac{1}{2}}\|c_s^m\|_{r_l^m}\right) \\
&\leq M\|E_s\|_{L^2(S)} \leq M\|E\|_{L^2(S)}
\end{aligned} \tag{B.20}$$

for all $E \in B$. Q.E.D.

By Corollary 7.3 in [80], we have:

Lemma B.3.4 The trace operator $T : \mathbf{H} \to L^2(S) \times L^2(S)$ is compact.

Now we define the operator $\Gamma_2 : T(\mathbf{H}) \to L^2(S)$ by

$$\Gamma_2(c_s, c_k) = \frac{c_s}{c_k}, \quad (c_s, c_k) \in \mathbf{H}.$$

doi:10.6342/NTU202200609

Lemma B.3.5 Γ_2 is a bounded operator.

Proof. Let $(c_s, c_k) \in T(\mathbf{H})$, we have, pointwisely

$$\left|\frac{c_s}{c_k}\right| \leq \frac{1}{\eta_k^{m+1}}|c_s|. \tag{B.21}$$

Therefore,

$$\begin{aligned}\left\|\frac{c_s}{c_k}\right\|^2_{L^2(S)} &\leq \frac{1}{(\eta_k^{m+1})^2}\int_S |c_s|^2 d\sigma \leq \frac{1}{(\eta_k^{m+1})^2}\int_S |c_s|^2 + |c_k|^2 d\sigma \\ &= \frac{1}{(\eta_k^{m+1})^2}(\|c_s\|^2_{L^2(S)} + \|c_k\|^2_{L^2(S)})\end{aligned} \tag{B.22}$$

This completes the proof. Q.E.D.

Finally, we define $\Gamma_3 : \Gamma_2(T(\mathbf{H})) \to B$ by

$$\Gamma_3 : \zeta \mapsto E,$$

where E satisfying $i_s(E)\zeta + i_k(E) = 0$ pointwisely.

Lemma B.3.6 Γ_3 is a bounded operator.

Proof. We write $\zeta = \zeta(E)$, we have $\zeta(E) = -\dfrac{i_k(E)}{i_s(E)}$. Observing that $i_k(E) > 0$ and $i_s(E) < 0$ for $E \in (E_k, E_s)$, since $i_k(E)$ is strictly increasing and $-i_s(E)$ is strictly decreasing, we have $\zeta(E)$ is strictly increasing. Therefore, Γ_3 is the inverse of ζ. Since $i_k(E)$ and $i_s(E)$ are linear combinations of exponential function of E, respectively, and $i_s(E) < 0$ for $E \in (E_k, E_s)$, $\zeta(E)$ is differentiable in (E_k, E_s). Therefore, we have

$$\zeta^{'}(E) = \frac{1}{\Gamma_3^{'}(\zeta)}.$$

For any element $c = (c_s, c_k)$ in $T(\mathbf{H})$, we always have

$$\min(\eta_k^{m+1}, \eta_s^{m+1}) \leq \frac{c_k}{c_s} \leq \frac{1}{\min(\eta_k^{m+1}, \eta_s^{m+1})}.$$

doi:10.6342/NTU202200609

Now we are going to seek the upper bound of $\Gamma_3^{'}(\zeta)$ for $\zeta \in [\min(\eta_k^{m+1}, \eta_s^{m+1}), \frac{1}{\min(\eta_k^{m+1}, \eta_s^{m+1})}]$. By the strict monotonity of ζ, there are constants m and M such that $E_k < m < M < E_s$ so that

$$\Gamma_3([\min(\eta_k^{m+1}, \eta_s^{m+1}), \frac{1}{\min(\eta_k^{m+1}, \eta_s^{m+1})}]) \subset [m, M].$$

Let $\alpha_1 = \dfrac{\alpha_s z_s F}{R\theta}$, $\alpha_2 = \dfrac{\alpha_k z_k F}{R\theta}$, $\beta_1 = \dfrac{\beta_s z_s F}{R\theta}$, $\beta_2 = \dfrac{\beta_k z_k F}{R\theta}$, we have

$$\begin{aligned}
&\zeta^{'}(E) \\
&= -\frac{L_k}{L_s}\frac{1}{(e^{\alpha_1(E-E_s)} - e^{-\beta_1(E-E_s)})^2}\Big[(e^{\alpha_1(E-E_s)} - e^{-\beta_1(E-E_s)})(\alpha_2 e^{\alpha_2(E-E_k)} + \beta_2 e^{\beta_2(E-E_k)}) \\
&- (e^{\alpha_2(E-E_k)} - e^{\beta_2(E-E_k)})(\alpha_2 e^{\alpha_2(E-E_k)} + \beta_2 e^{\beta_2(E-E_k)})\Big]
\end{aligned} \tag{B.23}$$

For $m \le E \le M$, we have

$$\zeta^{'}(E) \ge \frac{L_k}{L_s}\frac{(e^{-\beta_1(M-E_s)} - e^{\alpha_1(M-E_s)})(\alpha_2 e^{\alpha_2(m-E_k)} + \beta_2 e^{-\beta_2(m-E_k)})}{(e^{\alpha_1(m-E_s)} - e^{-\beta_1(m-E_s)})^2} \tag{B.24}$$

Therefore, there is a constant $\widetilde{M}$ such that $|\Gamma_3^{'}(\zeta)| \le \widetilde{M}$ for all $\zeta \in [\min(\eta_k^{m+1}, \eta_s^{m+1}), \frac{1}{\min(\eta_k^{m+1}, \eta_s^{m+1})}]$. Finally we have

$$|\Gamma_3(\zeta)| \le \min(\eta_k^{m+1}, \eta_s^{m+1}) + \widetilde{M}|\zeta| \le (\widetilde{M} + 1)|\zeta|.$$

The proof can be completed by integrating the square of the above inequality.

Q.E.D.

Proposition B.3.4 The operator $\Gamma = \Gamma_3 \circ \Gamma_2 \circ T \circ \Gamma_1 : B \to B$ has a fixed point.

Proof. Since B is convex and closed by Lemma B.3.2 and the composition of

doi:10.6342/NTU202200609

bounded operator with compact operator (also their commutation) is compact, the existence of the fixed point can be proved by the Schauder fixed point theorem with Lemmas B.3.3,B.3.4,B.3.5,B.3.6. Q.E.D.

Now, we have the theorem

Theorem B.3.2 If $\delta t > 0$ is sufficiently small, the system Problems $(\widetilde{P_c})$ is well-posed.

Proof. It remains to prove the uniqueness of the system. Assuming that $(c_{s1}, c_{k1}, E_1), (c_{s2}, c_{k2}, E_2) \in W_{\eta_s}^{m+1} \times W_{\eta_k}^{m+1} \times B$ are two different solutions. If $E_1 = E_2$, then we must have $c_{s1} = c_{s2}$ and $c_{k1} = c_{k2}$ by the uniqueness of Problems $(\widetilde{P_c})$. Therefore, we may assume that $E_1 \neq E_2$ for all $\delta t > 0$. By (B.12) and (B.13), we have

$$\begin{aligned}
&(c_{s1} - c_{s2}, w_s)_{r_l^{m+1}} + \delta t D_s(\nabla(c_{s1} - c_{s2}), w_s)_{r_l^{m+1}} \\
&+ \frac{1}{z_s F}(r_l^{m+1}(|i_s(E_1)|c_{s1} - |i_s(E_2)|c_{s2}), w_s)_{L^2(S)} \\
&+ (c_{k1} - c_{k2}, w_k)_{r_l^{m+1}} + \delta t D_k(\nabla(c_{k1} - c_{k2}), w_k)_{r_l^{m+1}} \\
&+ \frac{1}{z_k F}(r_l^{m+1}(|i_k(E_1)|c_{k1} - |i_k(E_2)|c_{k2}), w_k)_{L^2(S)} \\
&= 0.
\end{aligned} \tag{B.25}$$

To estimate the boundary term, we observe pointwisely:

$$|i_s(E_1)|c_{s1} - |i_s(E_2)|c_{s2} = |i_s(E_1)|(c_{s1} - c_{s2}) - c_{s2}(|i_s(E_1)| - |i_s(E_2)|). \tag{B.26}$$

doi:10.6342/NTU202200609

Using notations in Lemma B.3.6, we have, pointwisely

$$
\begin{aligned}
&||i_s(E_1)| - |i_s(E_2)|| = L_s \left|(e^{\alpha_1(E_1-E_s)} - e^{-\beta_1(E_1-E_s)}) - (e^{\alpha_1(E_2-E_s)} - e^{-\beta_1(E_2-E_s)}\right| \\
&\leq L_s \left(\alpha_1 + \beta_1 e^{\beta_1(E_s-E_k)}\right) |E_1 - E_2| \\
&\leq L_s \left(\alpha_1 + \beta_1 e^{\beta_1(E_s-E_k)}\right) \widetilde{M} \left|\frac{c_{s1}}{c_{k1}} - \frac{c_{s2}}{c_{k2}}\right| \\
&\leq L_s \left(\alpha_1 + \beta_1 e^{\beta_1(E_s-E_k)}\right) \frac{\widetilde{M}}{(\eta_k^{m+1})^2} (|c_{s1} - c_{s2}| + |c_{k1} - c_{k2}|)
\end{aligned} \tag{B.27}
$$

Similarly, we have

$$
|i_s(E_1)| - |i_s(E_2)| \leq L_k(\alpha_2 e^{\alpha_2(E_s-E_k)} + \beta_2) \frac{\widetilde{M}}{(\eta_k^{m+1})^2} (|c_{s1} - c_{s2}| + |c_{k1} - c_{k2}|). \tag{B.28}
$$

Now letting $w_s = c_{s1} - c_{s2}$ and $w_k = c_{k1} - c_{k2}$ in (B.25) and by (B.26)-(B.28) with Hölder inequality, there is a generic constant C such that

$$
\begin{aligned}
&\|c_{s1} - c_{s2}\|^2_{r_l^{m+1}} + \|c_{k1} - c_{k2}\|^2_{r_l^{m+1}} + \delta t D_s \|\nabla(c_{s1} - c_{s2})\|^2_{r_l^{m+1}} + \delta t D_k \|\nabla(c_{k1} - c_{k2})\|^2_{r_l^{m+1}} \\
&\leq C\delta t(\|c_{s1} - c_{s2}\|^2_{L^2(S)} + \|c_{k1} - c_{k2}\|^2_{L^2(S)})
\end{aligned} \tag{B.29}
$$

Since $\|\frac{1}{r_l}\|_{L^\infty(0,T;L^\infty(\Omega))}$ is bounded, we also have

$$
\begin{aligned}
&\|c_{s1} - c_{s2}\|_0^2 + \|c_{k1} - c_{k2}\|_0^2 + \delta t D_s \|\nabla(c_{s1} - c_{s2})\|_0^2 + \delta t D_k \|\nabla(c_{k1} - c_{k2})\|_0^2 \\
&\leq C\delta t(\|c_{s1} - c_{s2}\|^2_{L^2(S)} + \|c_{k1} - c_{k2}\|^2_{L^2(S)})
\end{aligned} \tag{B.30}
$$

for some constant $C > 0$. Applying the trace inequality, there is a constant

doi:10.6342/NTU202200609

$C_1 > 0$ such that

$$\|c_{s1} - c_{s2}\|^2_{L^2(S)} \leq C_1 \|c_{s1} - c_{s2}\|_0 \|c_{s1} - c_{s2}\|_1$$
$$\leq \frac{C_1}{2\epsilon_1}\|c_{s1} - c_{s2}\|_0^2 + \frac{C_1\epsilon_1}{2}\|c_{s1} - c_{s2}\|_1^2 = (\frac{C_1}{2\epsilon_1} + \frac{C_1\epsilon_1}{2})\|c_{s1} - c_{s2}\|_0^2 + \frac{C_1\epsilon_1}{2}\|\nabla(c_{s1} - c_{s2})\|_0^2 \tag{B.31}$$

for all $\epsilon_1 > 0$. Similarly, there is a constant $C_2 > 0$ such that

$$\|c_{k1} - c_{k2}\|^2_{L^2(S)} \leq (\frac{C_2}{2\epsilon_2} + \frac{C_2\epsilon_2}{2})\|c_{k1} - c_{k2}\|_0^2 + \frac{C_2\epsilon_2}{2}\|\nabla(c_{k1} - c_{k2}\|_0^2 \tag{B.32}$$

for all $\epsilon_2 > 0$. Choosing $\epsilon_1 = \dfrac{2D_s}{C_1}$, $\epsilon_2 = \dfrac{2D_k}{C_2}$ and

$$\delta t \leq \min\left(\frac{1}{2\left(\frac{C_1^2}{4D_s} + D_s\right)}, \frac{1}{2\left(\frac{C_2^2}{4D_k} + D_k\right)}\right),$$

we have

$$\frac{1}{2}\|c_{s1} - c_{s2}\|_0^2 + \frac{1}{2}\|c_{k1} - c_{k2}\|_0^2 \leq 0. \tag{B.33}$$

This implies that $c_{s1} = c_{s2}$ and $c_{k1} = c_{k2}$. Since $c_{s1}, c_{s2}, c_{k1}, c_{k2} \in C(\overline{\Omega})$, the unique solvability for (B.15) implies that $E_1 = E_2$ on S. This leads to the contradiction. Q.E.D.

Remark B.3.1 In the above theorem, the choice of δt is independent of the data of the previous step $(c_s^m, c_k^m, E_{mix}^m)$. Therefore, the unique solution for time-discrete problem at time $t = T$ can be reached in finite steps.

B.4 Stability analysis

Since the uniform bounds independent of E_{mix}^{m+1} have been found for L^∞ boundedness of c_s^m and c_k^m, $m = 0, \ldots, N$. Now we provide some results of stability:

doi:10.6342/NTU202200609

Lemma B.4.1 Let $0 \le c_j^0 \le 1$, $c_j^0 \in H^1(\Omega)$ for $j = s, k, g$, and $E_{mix}^0 \in B$.

There are generic constants $C > 0$ such that

$$\delta t \sum_{j=s,k,g} \sum_{m=0}^{N-1} \|\nabla c_j^{m+1}\|_{r_l^{m+1}}^2 \le C \tag{B.34}$$

Proof. Letting $w_s = c_s^{m+1}$ in (B.12), we have

$$\begin{aligned} &\|c_s^{m+1}\|_{r_l^{m+1}}^2 + \delta t D_s \|\nabla c_s^{m+1}\|_{r_l^{m+1}}^2 + \delta t (r_l^{m+1} i_s^{m+1} c_s^{m+1}, c_s^{m+1})_{L^2(S)} \\ &= (c_s^m, c_s^{m+1})_{r_l^{m+1}} \le \|c_s^m\|_{r_l^m} \|c_s^{m+1}\|_{r_l^{m+1}} \\ &\le \frac{1}{2}\|c_s^m\|_{r_l^m}^2 + \frac{1}{2}\|c_s^{m+1}\|_{r_l^{m+1}}^2. \end{aligned} \tag{B.35}$$

Similarly, letting $w_k = c_k^{m+1}$ in (B.13), we have

$$\begin{aligned} &\|c_k^{m+1}\|_{r_l^{m+1}}^2 + \delta t D_k \|\nabla c_k^{m+1}\|_{r_l^{m+1}}^2 + \delta t (r_l^{m+1} i_k^{m+1} c_k^{m+1}, c_k^{m+1})_{L^2(S)} \\ &\le \frac{1}{2}\|c_k^m\|_{r_l^m}^2 + \frac{1}{2}\|c_k^{m+1}\|_{r_l^{m+1}}^2. \end{aligned} \tag{B.36}$$

Once more, letting $w_g = c_g^{m+1}$ in (B.14), we have

$$\begin{aligned} &\|c_g^{m+1}\|_{r_l^{m+1}}^2 + \delta t D_g \|\nabla c_g^{m+1}\|_{r_l^{m+1}}^2 + \delta t \frac{M_g K_g}{\rho_l} \|c_g^{m+1}\|_0^2 \\ &= (c_g^m, c_g^{m+1})_{r_l^{m+1}} + \beta \delta t (r_l^{m+1} i_s^{m+1} c_s^{m+1}, c_s^{m+1})_{L^2(S)} \\ &\le \frac{1}{2}\|c_g^m\|_{r_l^m}^2 + \frac{1}{2}\|c_g^{m+1}\|_{r_l^{m+1}}^2 + \beta \delta t (r_l^{m+1} i_s^{m+1} c_s^{m+1}, c_g^{m+1}) \\ &\le \frac{1}{2}\|c_g^m\|_{r_l^m}^2 + \frac{1}{2}\|c_g^{m+1}\|_{r_l^{m+1}}^2 + \beta \delta t \|i_s\|_{L^2(S)} \|c_g\|_{L^2(S)} \\ &\le \frac{1}{2}\|c_g^m\|_{r_l^m}^2 + \frac{1}{2}\|c_g^{m+1}\|_{r_l^{m+1}}^2 + \beta \delta t (\frac{1}{2\epsilon}\|i_s\|_{L^2(S)}^2 + \frac{\epsilon}{2}\|c_g\|_{L^2(S)}) \\ &\le \frac{1}{2}\|c_g^m\|_{r_l^m}^2 + \frac{1}{2}\|c_g^{m+1}\|_{r_l^{m+1}}^2 + C \delta t (\frac{1}{2\epsilon}\|i_s\|_{L^2(S)}^2 + \frac{\epsilon}{2}\|c_g\|_1^2) \end{aligned} \tag{B.37}$$

Therefore, we have

$$(1+\delta t \frac{M_g K_g}{\rho_l} - C\epsilon\delta t)\|c_g^{m+1}\|_{r_l^{m+1}}^2 + \delta t(2D_g - C\epsilon)\|\nabla c_g\|_{r_l^{m+1}}^2 \le \frac{C\delta t}{\epsilon}\|i_s\|_{L^2(S)} + \|c_g^m\|_{r_l^m}^2 \tag{B.38}$$

doi:10.6342/NTU202200609

Taking $\epsilon = \dfrac{D_g}{C}$ sufficiently small so that and using the fact that c_g^{m+1} has a uniform L^∞ bound. We can conclude that there exists a generic constant $C > 0$ such that

$$\|\nabla c_g^{m+1}\|_0^2 \leq C \tag{B.39}$$

Collecting (B.35), (B.36), and (B.39) and taking the summation from 0 to $\dfrac{T}{\delta t} - 1$, the proof is completed. Q.E.D.

Since $\|\frac{1}{r_l^{m+1}}\|_{L^\infty(\Omega)}$ is bounded for all $m = 0, \ldots, N$, we have

Corollary B.4.1 There are generic constants $C > 0$ such that

$$\delta t \sum_{j=s,k,g} \sum_{m=0}^{N-1} \|\nabla c_j^{m+1}\|_0^2 \leq C \tag{B.40}$$

Lemma B.4.2 There are generic constants $C > 0$ such that

$$\sum_{j=s,k,g} \sum_{m=0}^{N-1} \|r_l^{m+1}(c_j^{m+1} - c_j^m)\|_0^2 \leq C. \tag{B.41}$$

Proof. The proof is almost identical to Lemma B.4.1 with the fact that

$$\begin{aligned} &(r_l^{m+1}c_j^{m+1} - c_j^m, c_j^{m+1}) \\ &= \frac{1}{2}\|c_j^{m+1}\|_{r_l^{m+1}}^2 + \frac{1}{2}\|c_j^m - c_j^m\|_{r_l^{m+1}}^2 - \frac{1}{2}\|c_j^m\|_{r_l^{m+1}}^2 \\ &\leq \frac{1}{2}\|c_j^{m+1}\|_{r_l^{m+1}}^2 + \frac{1}{2}\|c_j^m - c_j^m\|_{r_l^{m+1}}^2 - \frac{1}{2}\|c_j^m\|_{r_l^m}^2 \end{aligned} \tag{B.42}$$

Q.E.D.

Lemma B.4.3 There are generic constants $C > 0$ such that

$$\delta t \sum_{j=s,k,g} \sum_{m=0}^{N-1} \left\| \frac{r_l^{m+1}(c_j^{m+1} - c_j^m)}{\delta t} \right\|_{(H^1(\Omega))'}^2 \leq C \tag{B.43}$$

doi:10.6342/NTU202200609

Proof. We only look for the boundedness of c_s and the case is similar for k and dis. By definition

$$\left\| \frac{r_l^{m+1}(c_s^{m+1}-c_s^m)}{\delta t} \right\|_{(H^1(\Omega))'} = \sup_{w_s \in H^1(\Omega)} \left\langle \frac{r_l^{m+1}(c_s^{m+1}-c_s^m)}{\delta t}, w_s \right\rangle \tag{B.44}$$

By (B.12), with $w = \dfrac{w_s}{\|w_s\|_1} \in H^1(\Omega)$,

$$\begin{aligned} &\left\| \frac{r_l^{m+1}(c_s^{m+1}-c_s^m)}{\delta t} \right\|_{(H^1(\Omega))'} \\ &= \sup_{w \in H^1(\Omega), \|w\|_1 = 1} \left\{ -D_s(\nabla c_s^{m+1}, \nabla w)_{r_l^{m+1}} - \frac{1}{z_s F}(r_l^{m+1} | i_s^{m+1} | c_s^{m+1}, w)_{L^2(S)} \right\} \end{aligned} \tag{B.45}$$

We estimate all terms on the right hand side of (B.45):

$$\begin{aligned} &- D_s(\nabla c_s^{m+1}, \nabla w)_{r_l^{m+1}} \le D_s \|\nabla c_s^{m+1}\|_{r_l^{m+1}} \|\nabla w\|_{r_l^{m+1}} \\ &\le D_s \|\nabla c_s^{m+1}\|_{r_l^{m+1}} \|\nabla w\| \le D_s \|\nabla c_s^{m+1}\|_{r_l^{m+1}} \|w\|_1 \le D_s \|\nabla c_s^{m+1}\|_{r_l^{m+1}}, \end{aligned} \tag{B.46}$$

$$\begin{aligned} &- \frac{1}{z_s F}(r_l^{m+1} | i_s^{m+1} | c_s^{m+1}, w)_{L^2(S)} \le \frac{1}{z_s F} |i_s(E_k)| \|c_s^{m+1}\|_{L^2(S)} \|w\|_{L^2(S)} \\ &\le C \|c_s^{m+1}\|_1 \|w\|_1 = C \|c_s^{m+1}\|_1, \end{aligned} \tag{B.47}$$

Collecting (B.46)-(B.47) and multiplying by δt gives

$$\delta t \left\| \frac{r_l^{m+1}(c_s^{m+1}-c_s^m)}{\delta t} \right\|^2_{(H^1(\Omega))'} \le C \delta t (\|c_s^m\|_1^2 + \|c_s^{m+1}\|_1^2). \tag{B.48}$$

Taking the summation from 0 to $N-1$ and the boundedness given by Corollaray B.4.1 and Lemma B.3.3, we have the desired estimate. Q.E.D.

Corollary B.4.2 There are generic constants $C > 0$ such that

$$\delta t \sum_{j=s,k,g} \sum_{m=0}^{N-1} \left\| \frac{c_j^{m+1} - c_j^m}{\delta t} \right\|^2_{(H^1(\Omega))'} \le C \tag{B.49}$$

doi:10.6342/NTU202200609

Proof. This is the direct result from Lemma B.4.3 and the fact that r_l^{m+1} is bounded in $L^\infty(\Omega)$. Q.E.D.

Corollary B.4.3 There are generic constants $C > 0$ such that

$$\delta t \sum_{j=s,k,g} \sum_{m=0}^{N-1} \left\| \frac{r_j^{m+1} c_j^{m+1} - r_j^m c_j^m}{\delta t} \right\|^2_{(H^1(\Omega))'} \leq C \tag{B.50}$$

Proof. By the relation

$$r_l^{m+1} c_j^{m+1} - r_l^m c_j^m = r_l^{m+1}(c_j^{m+1} - c_j^{m+1}) + c_s^m (r_l^{m+1} - r_l^m), \quad 0 \leq m \leq M-1,$$

the desired result can be obtained by collecting Lemma B.4.3, Corollary B. 4.2 and the L^∞ boundedness of r_l^m for all $0 \leq m \leq N$. Q.E.D.

Lemma B.4.4 Assuming that $r_l^j \in H^1(\Omega)$, $0 < r_l^j \leq 1$, $c_g^j \in H^1(\Omega) \cap L^\infty(\Omega)$, $c_g^j \geq 0$ for all $0 \leq j \leq m \leq N$, then we have the estimate

$$\|\nabla r_l^k\|_0^2 \leq \exp\left(\frac{K_g T}{\rho_g}\right) (\|\nabla r_l^0\|_0^2 + \frac{K_g \delta t}{\rho_g} \sum_{m=0}^{N-1} \|\nabla c_g^m\|_0^2). \tag{B.51}$$

Proof. Multiplying (C.11) with $\partial_{x_i} r_l^{m+1}$ and integrating the both sides with respect to Ω, we have

$$\begin{aligned}
&\int_\Omega (1 + \frac{K\delta t}{\rho_g} c_g^m) |\nabla r_l^{m+1}|^2 dx = -\frac{K\delta t}{\rho_g} \int_\Omega \nabla c_g^m \cdot \nabla r_l^{m+1} dx + \int_\Omega \nabla r_l^m \cdot \nabla r_l^{m+1} dx \\
&\leq \frac{K\delta t}{\rho_g} \|\nabla c_g^m\|_0 \|\nabla r_l^{m+1}\|_0 + \|\nabla r_l^m\|_0 \|\nabla r_l^{m+1}\|_0 \\
&\leq \frac{1}{2} \|\nabla r_l^m\|_0^2 + \frac{1}{2}(1 + \frac{K\delta t}{\rho_g}) \|\nabla r_l^{m+1}\|_0^2 + \frac{1}{2} \frac{K\delta t}{\rho_g} \|\nabla c_g^m\|_0^2.
\end{aligned} \tag{B.52}$$

The above inequality leads to

$$(1 - \frac{K\delta t}{\rho_g}) \|\nabla r_l^{m+1}\|_0^2 \leq \|\nabla r_l^m\|_0^2 + \frac{K\delta t}{\rho_g} \|\nabla c_g^m\|_0^2. \tag{B.53}$$

doi:10.6342/NTU202200609

Taking the summation from 0 to $N-1$, we have

$$\|\nabla r_l^j\|_0^2 \le \left(1 - \frac{K\delta t}{\rho_g}\right)^{-N} (\|\nabla r_l^0\|_0^2 + \frac{K\delta t}{\rho_g} \sum_{m=0}^{N-1} \|\nabla c_g^m\|_0^2) \tag{B.54}$$

for all $0 \le j \le N$. Since $\delta t = T/N$, we have

$$(1 - \frac{K_g \delta t}{\rho_g})^{-N} = (1 - \frac{K_g T}{N\rho_g})^{-N} \le \exp(\frac{K_g T}{\rho_g})$$

Employing the above inequality to (B.54), the proof is completed. Q.E.D.

B.5 Passage to limit $\delta t \to 0$

Let us define

$$r_{l,\delta} : [0,T] \to H^1(\Omega), \quad r_{l,\delta}(t) = r_l^j \quad \text{if } t \in ((j-1)\delta t, j\delta t], \tag{B.55}$$

$$r_{l,h} : [0,T] \to H^1(\Omega), \ r_{l,h}(t) = \frac{t-(j-1)\delta t}{\delta t} r_l^j + \frac{j\delta t - t}{\delta t} r_l^{j-1} \quad \text{if } t \in ((j-1)\delta t, j\delta t], \tag{B.56}$$

$$c_{dis,\delta} : [0,T] \to H^1(\Omega), \quad c_{g,\delta}(t) = c_g^j \quad \text{if } t \in ((j-1)\delta t, j\delta t], \tag{B.57}$$

$$c_{s,\delta} : [0,T] \to H^1(\Omega), \quad c_{s,\delta}(t) = c_s^j \ \text{ if } t \in ((j-1)\delta t, j\delta t] \tag{B.58}$$

$$c_{k,\delta} : [0,T] \to H^1(\Omega), \quad c_{k,\delta}(t) = c_k^j \ \text{ if } t \in ((j-1)\delta t, j\delta t] \tag{B.59}$$

$$\begin{aligned} &c_{dis,h} : [0,T] \to H^1(\Omega), \\ &c_{dis,h}(t) = \frac{t-(j-1)\delta t}{\delta t} c_g^j + \frac{j\delta t - t}{\delta t} c_g^{j-1} \quad \text{if } t \in ((j-1)\delta t, j\delta t], \end{aligned} \tag{B.60}$$

$$\begin{aligned} &c_{s,h} : [0,T] \to H^1(\Omega), \\ &c_{s,h}(t) = \frac{t-(j-1)\delta t}{\delta t} c_s^j + \frac{j\delta t - t}{\delta t} c_s^{j-1} \quad \text{if } t \in ((j-1)\delta t, j\delta t], \end{aligned} \tag{B.61}$$

doi:10.6342/NTU202200609

$$c_{k,h} : [0,T] \to H^1(\Omega),$$
$$c_{k,h}(t) = \frac{t-(j-1)\delta t}{\delta t} c_k^j + \frac{j\delta t - t}{\delta t} c_k^{j-1} \quad \text{if } t \in ((j-1)\delta t, j\delta t], \tag{B.62}$$

$$c_{dis,\delta-} : [0,T] \to H^1(\Omega), \quad c_{dis,\delta}(t) = c_g^{j-1} \ \text{ if } t \in ((j-1)\delta t, j\delta t] \tag{B.63}$$

$$c_{s,\delta-} : [0,T] \to H^1(\Omega), \quad c_{is,\delta}(t) = c_s^{j-1} \ \text{ if } t \in ((j-1)\delta t, j\delta t] \tag{B.64}$$

$$c_{k,\delta-} : [0,T] \to H^1(\Omega), \quad c_{k,\delta}(t) = c_k^{j-1} \ \text{ if } t \in ((j-1)\delta t, j\delta t] \tag{B.65}$$

$$E_{mix,\delta} : [0,T] \to L^2(S), \quad E_{mix,\delta}(t) = E_{mix}^{j} \ \text{ if } t \in ((j-1)\delta t, j\delta t] \tag{B.66}$$

$$(r_l c_g)_h : [0,T] \to H^1(\Omega), \ (r_l c_g)_h(t) = \frac{t-(j-1)\delta t}{\delta t} r_l^j c_g^j + \frac{j\delta t - t}{\delta t} r_l^{j-1} c_g^{j-1} \quad \text{if } t \in ((j-1)\delta t, j\delta t], \tag{B.67}$$

$$(r_l c_s)_h : [0,T] \to H^1(\Omega), \ (r_l c_s)_h(t) = \frac{t-(j-1)\delta t}{\delta t} r_l^j c_s^j + \frac{j\delta t - t}{\delta t} r_l^{j-1} c_s^{j-1} \quad \text{if } t \in ((j-1)\delta t, j\delta t], \tag{B.68}$$

$$(r_l c_k)_h : [0,T] \to H^1(\Omega), \ (r_l c_k)_h(t) = \frac{t-(j-1)\delta t}{\delta t} r_l^j c_k^j + \frac{j\delta t - t}{\delta t} r_l^{j-1} c_k^{j-1} \quad \text{if } t \in ((j-1)\delta t, j\delta t], \tag{B.69}$$

With the above notations, the system of discrete equations can be expressed as:

$$\langle \partial_t r_{l,h}, w \rangle + \left(\frac{K_g}{\rho_g} r_{l,\delta} c_{dis,\delta-}\right) = 0 \tag{B.70}$$

$$\begin{aligned} &\langle r_{l,\delta} \partial_t c_{dis,h}, w_g \rangle + D_g (r_{l,\delta} \nabla c_{dis,\delta}, \nabla w_g) + \frac{M_g K_g}{\rho_l} (r_{l,\delta} c_{dis,\delta}, w_g) \\ &= \frac{\beta}{z_s F} (r_{l,\delta} | i_g(E_{mix,\delta}) | c_{dis,\delta}, w_g)_{L^2(S)}, \end{aligned} \tag{B.71}$$

$$\langle r_{l,\delta} \partial_t c_{s,h}, w_s \rangle + D_s (r_{l,\delta} \nabla c_{s,\delta}, \nabla w_s) + \frac{1}{z_s F} (r_{l,\delta} | i_s(E_{mix,\delta}) | c_{s,\delta}, w_s)_{L^2(S)} = 0, \tag{B.72}$$

$$\langle r_{l,\delta} \partial_t c_{k,h}, w_k \rangle + D_k (r_{l,\delta} \nabla c_{k,\delta}, \nabla w_k) + \frac{1}{z_k F} (r_{l,\delta} | i_k(E_{mix,\delta}) | c_{k,\delta}, w_k)_{L^2(S)} = 0 \tag{B.73}$$

doi:10.6342/NTU202200609

Here we collect the boundedness of functions given by (B.58)-(B.66): By Lemmas B.3.2, B.3.3 and B.4.1, $c_{dis,\delta}, c_{s,\delta}, c_{k\delta}, c_{dis,\delta-}, c_{s,\delta-}, c_{k,\delta-}$ are uniformly bounded in $L^2(0,T;H^1(\Omega))$. Since $E_{mix,\delta}$ is always bounded in B for all time, $E_{mix,\delta}$ is uniformly bounded in $L^2(0,T;L^2(S))$. Therefore, there are $r_l, r_l^*, c_g, c_s, c_k, c_g^*, c_s^*, c_k^*, E_{mix}$ such that there exist subsequences of $r_{l,\delta}, r_{l,h}, c_{dis,\delta}, c_{s,\delta}$, $c_{k,\delta}, c_{dis,\delta-}, c_{s,\delta-}, c_{k,\delta-}$ (still denote by same notations) satisfying

$$r_{l,\delta} \to r_l \quad \text{in } L^2(0,T;H^1(\Omega)) \text{ weakly}, \tag{B.74}$$

$$r_{l,h} \to r_l^* \quad \text{in } L^2(0,T;H^1(\Omega)) \text{ weakly}, \tag{B.75}$$

$$c_{dis,\delta} \to c_g \quad \text{in } L^2(0,T;H^1(\Omega)) \text{ weakly}, \tag{B.76}$$

$$c_{s,\delta} \to c_s \quad \text{in } L^2(0,T;H^1(\Omega)) \text{ weakly}, \tag{B.77}$$

$$c_{k,\delta} \to c_k \quad \text{in } L^2(0,T;H^1(\Omega)) \text{ weakly}, \tag{B.78}$$

$$c_{dis,\delta-} \to c_g^* \quad \text{in } L^2(0,T;H^1(\Omega)) \text{ weakly}, \tag{B.79}$$

$$c_{s,\delta-} \to c_s^* \quad \text{in } L^2(0,T;H^1(\Omega)) \text{ weakly}, \tag{B.80}$$

$$c_{k,\delta-} \to c_k^* \quad \text{in } L^2(0,T;H^1(\Omega)) \text{ weakly}, \tag{B.81}$$

$$E_{mix,\delta} \to E_{mix} \quad \text{in } L^2((0,T)\times S) \text{ weakly}. \tag{B.82}$$

doi:10.6342/NTU202200609

For the time derivatives, by Lemma B.4.3, Corollaries B.4.2 and B.4.2, there are $g_1, g_2, g_3, g_4, g_5, g_6, g_7$ such that

$$\partial_t r_{l,h} \to g_1 \qquad \text{in } L^2(0,T;L^2(\Omega)) \text{ weakly}, \tag{B.83}$$

$$\partial_t c_{dis,h} \to g_2 \qquad \text{in } L^2(0,T;(H^1(\Omega))') \text{ weakly}, \tag{B.84}$$

$$\partial_t c_{s,h} \to g_3 \qquad \text{in } L^2(0,T;(H^1(\Omega))') \text{ weakly}, \tag{B.85}$$

$$\partial_t c_{k,h} \to g_4 \qquad \text{in } L^2(0,T;(H^1(\Omega))') \text{ weakly}, \tag{B.86}$$

$$\partial_t (r_l c_g)_h \to g_5 \qquad \text{in } L^2(0,T;(H^1(\Omega))') \text{ weakly}, \tag{B.87}$$

$$\partial_t (r_l c_s)_h \to g_6 \qquad \text{in } L^2(0,T;(H^1(\Omega))') \text{ weakly}, \tag{B.88}$$

$$\partial_t (r_l c_k)_h \to g_7 \qquad \text{in } L^2(0,T;(H^1(\Omega))') \text{ weakly}, \tag{B.89}$$

Remark B.5.1 By the $L^2(0,T;H^1(\Omega))$ boundedness of $r_{l,\delta}c_{j,\delta}$ for $j = s, k, dis$, it is easy to conclude that

$$r_{l,\delta}c_{j,\delta} \to r_l c_j \quad \text{in } L^2(0,T;H^1(\Omega)) \text{ weakly}. \tag{B.90}$$

Lemma B.5.1 There are generic constants $C > 0$ such that

$$\sum_{j=s,k,g} \int_0^T \|r_{l,\delta}(c_{j,\delta} - c_{j,h})\|_0^2 dt \le C\delta t \tag{B.91}$$

Proof. By the definition of (B.55), (B.58), and (B.61), we have

$$\int_{(j-1)\delta t}^{j\delta t} \|r_{l,\delta}(c_{s,\delta} - c_{s,h})\|_0^2 dt = \frac{\delta t}{3} \|r_l^j (c_s^j - c_s^{j-1})\|_0^2 \tag{B.92}$$

doi:10.6342/NTU202200609

Taking the summation from $j = 1$ to $j = T/\delta t$, we get

$$\int_0^T \|r_{l,\delta}(c_{s,\delta} - c_{s,h})\|_0^2 dt = \sum_{j=1}^{N} \int_{(j-1)\delta t}^{j\delta t} \|r_{l,\delta} c_{s,\delta} - (r_l c_s)_h\|_0^2 dt$$
$$= \frac{\delta t}{3} \sum_{j=0}^{m} \|r_l^j (c_s^j - c_s^{j-1})\|_0^2 \leq C\delta t \tag{B.93}$$

for some constant $C > 0$ by Lemma B.4.2. The same proof can be used to show the boundedness for $r_{l,\delta}(c_{k,\delta} - c_{k,h})$ and $r_{l,\delta}(c_{dis,\delta} - c_{dis,h})$. Q.E.D.

Lemma B.5.2

$$c_g = c_g^*, \quad c_s = c_s^*, \quad c_k = c_k^*, \quad \text{a.e. in } [0,T] \times \Omega \tag{B.94}$$

Proof. Since there is a uniform L^∞ bound of $\dfrac{1}{r_l^m}$ for all $0 \leq m \leq N$, there is a constant $C > 0$ such that

$$C\|c_j^{m+1} - c_j^m\|_0 \leq \|r_l^{m+1}(c_j^{m+1} - c_j^m)\|_0, \quad j = s, k, dis. \tag{B.95}$$

Lemma B.4.2 directly leads to the desired result.Q.E.D.

Remark B.5.2 By a classical argument, see for instance [41], we have

$$g_1 = \partial_t r_l, \;\; g_2 = \partial_t c_g, \;\; g_3 = \partial_t c_s, \;\; g_4 = \partial_t c_k, \;\; g_5 = \partial_t(r_l c_g), \;\; g_6 = \partial_t(r_l c_s), \;\; g_7 = \partial_t(r_l c_k) \tag{B.96}$$

In order to pass the limit in (B.70)-(B.73), we look into (B.72) firstly and take any $w = v(x)\lambda(t)$, where $v \in W^{1,\infty}(\Omega)$ and $\lambda \in W_0^{1,\infty}(0,T)$. Then

$$-\int_0^T ((r_l c_s)_h, v)\lambda'(t)dt - \int_0^T (c_{s,\delta-}\partial_t r_{l,h}, v)\lambda(t)dt + \int_0^T D_s(r_{l,\delta}\nabla c_{s,\delta}, \nabla v)\lambda dt$$
$$+ \frac{1}{z_s F}\int_0^T (r_{l,\delta}|i_s(E_{mix,\delta})|c_{s,\delta}, v)_{L^2(S)}\lambda dt = 0 \tag{B.97}$$

doi:10.6342/NTU202200609

For the first term in (B.72), we have

$$-\int_0^T ((r_l c_s)_h, v)\lambda'(t)dt \to -\int_0^T (r_l c_s, v)\lambda'(t)dt = \int_0^T \langle \partial_t (r_l c_s), v\rangle_{(H^1(\Omega))', H^1(\Omega)} \lambda(t)dt. \tag{B.98}$$

Since $\partial_t r_{l,\delta}$ converges to $\partial_t r_l$ weakly in $L^2((0,T)\times\Omega)$ and $c_{s,\delta-}$ converges to c_s in $L^2(0,T)\times\Omega)$ by Aubin-Lions lemma, we have

$$\int_0^T (c_{s,\delta-}\partial_t r_{l,h}, v)\lambda(t)dt \to \int_0^T (c_s \partial_t r_l, v)\lambda(t)dt. \tag{B.99}$$

Since $r_{l,\delta}$ is strongly convergent in $L^2((0,T)\times\Omega)$ (by Aubin-Lions lemma) and $\partial_{x_i} c_{s,\delta}$ is weakly convergent in $L^2((0,T)\times\Omega)$ for any direction x_i, we have

$$\int_0^T D_s(r_{l,\delta}\nabla c_{s,\delta}, \nabla v)\lambda dt \to \int_0^T D_s(r_l \nabla c_s, \nabla v)\lambda dt. \tag{B.100}$$

To deal with the fourth term, Theorem 1 in [81] can be applied. By the Rellich-Kondrachov theorem, we have the compact embedding $H^1(\Omega) \hookrightarrow H^s(\Omega)$ for all $0 \le s < 1$. On the other hand, H^s is continuously embedded in $(H^1(\Omega))'$. Let u be an arbitrary function defined on $[0,T]\times\Omega$. We define $\sigma_\tau u(t,x) = u(t-\tau, x)$ in $[\tau, T]\times\Omega$ for $0 < \tau < T$. We claim that $\delta t^{-1}\|r_{l,\delta}c_{s,\delta} - \sigma_{\delta t}(r_{l,\delta}c_{s,\delta})\|_{L^1(\delta t, T; (H^1(\Omega))')}$ is uniformly bounded.

Lemma B.5.3 There are generic constants $C_1, C_2 > 0$ such that

$$\|r_{l,\delta}c_{s,\delta} - \sigma_{\delta t}(r_{l,\delta}c_{s,\delta})\|_{L^1(\tau,T;(H^1(\Omega))')} \le C_1\delta t, \;\; \|r_{l,\delta}c_{k,\delta} - \sigma_{\delta t}(r_{l,\delta}c_{k,\delta})\|_{L^1(\tau,T;(H^1(\Omega))')} \le C_2\delta t \tag{B.101}$$

doi:10.6342/NTU202200609

Proof. We prove the bound for $c_{s,\delta}$ only. By definition of $c_{s,\delta}$, we have

$$\|r_{l,\delta}c_{s,\delta} - \sigma_{\delta t}(r_{l,\delta}c_{s,\delta})\|_{L^1(\tau,T;(H^1(\Omega))')} = \int_\tau^T \|r_{l,\delta}c_{s,\delta} - \sigma_{\delta t}(r_{l,\delta}c_{s,\delta})\|_{(H^1(\Omega))'}dt$$
$$= \sum_{m=1}^{N-1}\int_{m\delta t}^{(m+1)\delta t} \|r_{l,\delta}c_{s,\delta} - \sigma_{\delta t}(r_{l,\delta}c_{s,\delta})\|_{(H^1(\Omega))'}dt \le \delta t \sum_{m=0}^{N-1} \|r_s^{m+1}c_s^{m+1} - r_s^m c_s^m\|_{(H^1(\Omega))'}$$
$$= \delta t^2 \sum_{m=0}^{N-1} \left\| \frac{r_s^{m+1}c_s^{m+1} - r_s^m c_s^m}{\delta t} \right\|_{(H^1(\Omega))'}$$
$$\le \delta t^2 \sum_{m=0}^{N-1} \left(\left\| \frac{r_s^{m+1}c_s^{m+1} - r_s^m c_s^m}{\delta t} \right\|^2_{(H^1(\Omega))'} + \frac{1}{2} \right) \le (C + \frac{1}{2}T)\delta t$$

for some generic constant $C > 0$ (by Lemma B.4.3). Q.E.D.

Now using Theorem 1 in [81], we have in particular

$$r_{l,\delta}c_{s,\delta} \to r_l c_s \quad \text{in } L^2(0,T;H^{\frac{3}{4}}(\Omega)) \text{ strongly} \tag{B.102}$$

$$r_{l,\delta}c_{k,\delta} \to r_l c_k \quad \text{in } L^2(0,T;H^{\frac{3}{4}}(\Omega)) \text{ strongly} \tag{B.103}$$

Regarding the trace operator $T_S : L^2(0,T;H^{\frac{3}{4}}(\Omega)) \to L^2(0,T;H^{\frac{1}{2}}(S))$ is continuous, we have

$$r_{l,\delta}c_{s,\delta} \to r_l c_s \quad \text{in } L^2(0,T;H^{\frac{1}{4}}(S)) \text{ strongly} \tag{B.104}$$

$$r_{l,\delta}c_{k,\delta} \to r_l c_k \quad \text{in } L^2(0,T;H^{\frac{1}{4}}(S)) \text{ strongly} \tag{B.105}$$

Since i_s is strongly negative on B, $|i_s| : B \to L^2(S)$ preserves the continuity and boundedness. Therefore, $|i_s(E_{mix,\delta})| \to |i_s(E_{mix})|$ weakly in $L^2((0,T) \times S)$. Likewise, $i_k : B \to L^2(S)$ is continuous. Therefore, $i_k(E_{mix,\delta}) \to i_k(E_{mix})$ weakly in $L^2((0,T) \times S)$. The strong convergence of $r_{l,\delta}c_{s,\delta}$ in $L^2((0,T) \times S)$ implies that

$$\frac{1}{z_s F}\int_0^T (r_{l,\delta}|i_s(E_{mix,\delta})|c_{s,\delta}, v)_{L^2(S)}\lambda dt \to \frac{1}{z_s F}\int_0^T (r_l|i_s(E_{mix})|c_s, v)_{L^2(S)}\lambda dt \tag{B.106}$$

doi:10.6342/NTU202200609

Therefore

$$\int_0^T \langle r_l \partial_t c_s, v\rangle_{(H^1(\Omega))',H^1(\Omega)} + \int_0^T D_s(r_l \nabla c_s, \nabla v)\lambda dt + \frac{1}{z_s F}\int_0^T (r_l |i_s(E_{mix})| c_s, v)_{L^2(S)}\lambda dt = 0 \tag{B.107}$$

for all $\lambda \in W_0^{1,\infty}(0,T)$ and for all $v \in W^{1,\infty}(\Omega)$. By a totally same argument, we have

$$\int_0^T \langle r_l \partial_t c_k, v\rangle_{(H^1(\Omega))',H^1(\Omega)}\lambda dt + \int_0^T D_k(r_l \nabla c_k, \nabla v)\lambda dt + \frac{1}{z_k F}\int_0^T (r_l |i_k(E_{mix})| c_k, v)_{L^2(S)}\lambda dt = 0 \tag{B.108}$$

for all $\lambda \in W_0^{1,\infty}(0,T)$ and for all $v \in W^{1,\infty}(\Omega)$. Moreover, since $i_s(E_{mix,\delta})c_{s,\delta} + i_k(E_{mix,\delta})c_{k,\delta} = 0$ in $(0,T)\times S$ for all δt and

$$\int_0^T (i_s(E_{mix,\delta})c_{s,\delta} + i_k(E_{mix,\delta})c_{k,\delta}, v)\lambda dt \to \int_0^T (i_s(E_{mix})c_s + i_k(E_{mix})c_k, v)\lambda dt \tag{B.109}$$

for all $\lambda \in W_0^{1,\infty}(0,T)$ and for all $v \in W^{1,\infty}(\Omega)$. Therefore the resctriction $i_s(E_{mix})c_s + i_k(E_{mix})c_k = 0$ holds.

Since $r_{l,\delta}$, $c_{dis,\delta}$ are strongly convergent in $L^2((0,T)\times\Omega)$, we have

$$\int_0^T (r_{l,\delta}c_{dis,\delta}, v)\lambda(t)dt \to \int_0^T (r_l c_g, v)\lambda(t)dt \tag{B.110}$$

Employing the same argument as for s and k, we have

$$\int_0^T \langle r_l \partial_t c_g, v\rangle_{(H^1(\Omega))',H^1(\Omega)} + \int_0^T D_g(r_l \nabla c_g, \nabla v)\lambda dt + \frac{K_g M_g}{\rho_l}\int_0^T (r_{l,\delta}c_{dis,\delta}, v)\lambda(t)dt \to \int_0^T (r_l c_g, v)\lambda(t)dt - \frac{\beta}{z_s F}\int_0^T (r_l |i_s(E_{mix})| c_s, v)_{L^2(S)}\lambda dt = 0 \tag{B.111}$$

for all $\lambda \in W_0^{1,\infty}(0,T)$ and for all $v \in W^{1,\infty}(\Omega)$.

doi:10.6342/NTU202200609

To recover the initial conditions, we take $\lambda \in W^{1,\infty}(0,T)$, $\lambda(T) = 0$, $\lambda(0) \neq 0$, and $v \in W^{1,\infty}(\Omega)$. We consider (B.97) such that all terms are identical except the first one:

$$\int_0^T (\partial_t (r_l c_s)_h, v)\lambda dt = \int_0^T \partial_t ((r_l c_s)_h, v)\lambda dt = -\int_0^T ((r_l c_s)_h, v)\lambda'(t)dt - (r_l^0 c_s^0, v)\lambda(0). \tag{B.112}$$

When passing to the limit, we get

$$\begin{aligned}
&\int_0^T \langle \partial_t (r_l c_s)_h, v\rangle_{(H^1(\Omega))',H^1(\Omega)}\lambda dt = -\int_0^T (r_l c_s, v)\lambda'(t)dt - (r_l^0 c_s^0, v)\lambda(0) \\
&= \int_0^T \frac{d}{dt}(r_l c_s, v)\lambda dt + (r_l(0)c_s(0), v)\lambda(0) - (r_l^0 c_s^0, v)\lambda(0) \\
&= \int_0^T \langle \partial_t (r_l c_s), v\rangle_{(H^1(\Omega))',H^1(\Omega)}\lambda dt + (r_l(0)c_s(0), v)\lambda(0) - (r_l^0 c_s^0, v)\lambda(0).
\end{aligned} \tag{B.113}$$

Therefore

$$(r_l(0)c_s(0), v) = (r_l^0 c_s^0, v), \qquad \forall v \in H^1(\Omega) \cap W^{1,\infty}(\Omega)$$

This implies that $r_l(0)c_s(0) = r_l^0 c_s(0) = r_l^0 c_s^0$. Since $r_l^0 > 0$, by copying the same argument for r_l, c_k and c_g, we may conclude the above result by the theorem:

Theorem B.5.1 There exists $r_l, c_g, c_s, c_k \in L^2(0,T;H^1(\Omega))$, E_{mix} in $L^2(0,T;B)$ with $\partial_t r_l, \partial_t c_g, \partial_t c_s, \partial_t c_k \in L^2(0,T;(H^1(\Omega))')$ such that

$$\int_0^T (\partial_t r_l, w)dt + \frac{K_g}{\rho_g}\int_0^T (r_l c_g, w)dt = 0 \tag{B.114}$$

$$\begin{aligned}
&\int_0^T \langle r_l \partial_t c_g, w_g\rangle_{(H^1(\Omega))',H^1(\Omega)}dt + \int_0^T D_g(r_l \nabla c_g, \nabla w_g)dt \\
&- \frac{\beta}{z_s F}\int_0^T (r_l |i_s(E_{mix})|c_s, w_s)_{L^2(S)}dt + \frac{K_g M_g}{\rho_l}\int_0^T (r_l c_g, w_g)dt = 0,
\end{aligned} \tag{B.115}$$

doi:10.6342/NTU202200609

$$\int_0^T \langle r_l \partial_t c_s, w_s \rangle_{(H^1(\Omega))',H^1(\Omega)} dt + \int_0^T D_s(r_l \nabla c_s, \nabla w_s) dt + \frac{1}{z_s F} \int_0^T (r_l | i_s(E_{mix}) | c_s, w_s)_{L^2(S)} dt = 0, \tag{B.116}$$

$$\int_0^T \langle r_l \partial_t c_k, w_k \rangle_{(H^1(\Omega))',H^1(\Omega)} dt + \int_0^T D_k(r_l \nabla c_k, \nabla w_s) dt + \frac{1}{z_k F} \int_0^T (r_l | i_k(E_{mix}) | c_k, w_k)_{L^2(S)} dt = 0, \tag{B.117}$$

satisfying the constraint

$$\int_0^T (i_s(E_{mix}) c_s + i_k(E_{mix}) c_k, w_e)_{L^2(S)} dt \tag{B.118}$$

for all $w, w_g, w_s, w_k \in L^2(0,T;H^1(\Omega))$ and for all $w_e \in L^2((0,T) \times S)$. Moreover, r_l, c_g, c_s, c_k satisfy the initial conditions $r_l(0) = r_l^0$, $c_g(0) = c_g^0$, $c_s(0) = c_s^0$, $c_k(0) = c_k^0$ with $0 < r_l^0 \leq 1$, $0 \leq c_g^0 \leq 1$, $0 < c_s^0, c_k^0 \leq 1$, $r_l^0, c_g^0, c_s^0, c_k^0 \in H^1(\Omega)$.

Remark B.5.3 The solution $(r_l, c_g, c_s, c_k, E_{mix})$ is unique by Theorem B. 3.2.

B.6 Several species case

The results for two species case can be generalized to $N+1$ species case, $N > 2$. Let E_j be the constants defined in Section 2 with subscripts $j = s, k_1, \ldots, k_N$, where s means the ion to be plated and $k_1, \ldots k_N$ mean other ions involving in the surface reaction. We assume that $0 > E_{k_1} > \cdots > E_s > \cdots > E_{k_N}$. Again, we assume that the chemical reaction satisfying electron balance on the reaction surface $S \subset \partial\Omega$ and the convective effect in system

doi:10.6342/NTU202200609

(3.26)-(3.28) can be neglected. We assume the same regularity for r_l and c_g as in two species case. Te system of equations can be expressed as

$$\begin{aligned} \partial_t r_l + \frac{K_g}{\rho_g} c_g &= 0 \quad \text{in } \Omega \times (0,T] \\ r_l \partial_t c_g - \nabla \cdot (r_l D \nabla c_g) + \frac{K_g M_g}{\rho_l} r_l c_g &= 0 \quad \text{in } \Omega \times (0,T] \\ \partial_t (r_l \Theta) - \nabla \cdot (r_l D \nabla \Theta) &= 0 \quad \text{in } \Omega \times (0,T] \end{aligned} \tag{B.119}$$

subject to the boundary conditions

$$-D_j \frac{\partial c_j}{\partial \mathbf{n}} = \frac{|I_j|}{z_j F}, \quad \text{on } S \times (0,T], \quad \frac{\partial c_j}{\partial \mathbf{n}} = 0, \quad \text{on } (\partial\Omega \setminus S) \times (0,T] \tag{B.120}$$

for $j = s, k_1, \ldots, k_N$, and

$$-D_g \frac{\partial c_g}{\partial \mathbf{n}} = \frac{\beta |I_s|}{z_s F}, \quad \text{on } S \times (0,T], \quad \frac{\partial c_g}{\partial \mathbf{n}} = 0, \quad \text{on } (\partial\Omega \setminus S) \times (0,T] \tag{B.121}$$

The initial conditions are given by $r_l(0) = r_l^0 \in H^1(\Omega)$, $c_j(0) = c_j^0 \in H^1(\Omega)$ satisfying

$$0 < c_j^0 \leq 1, \quad 0 < r_l^0 \leq 1, \quad \text{in } \Omega \tag{B.122}$$

for $j = dis, s, k_1, \ldots, k_N$. In the above $\Theta = (c_s, c_{k_1}, \ldots, c_{k_N})^T$. The constraint for electrons balance reads

$$I_s + \sum_{l=1}^{N} I_{k_l} = 0. \tag{B.123}$$

Here, we omit the semi-discrete scheme for solving r_l and c_g since there is nothing different from the two-species case. The time-discrete problem for species $j = s, k_1, \ldots, k_N$ can be expressed as:

$$\frac{r_l^{m+1}(c_j^{m+1} - c_j^m)}{\delta t} - \nabla \cdot (D_j r_l^{m+1} \nabla c_j^{m+1}) = 0 \tag{B.124}$$

doi:10.6342/NTU202200609

with boundary conditions on S

$$-D_j\frac{\partial c_j^{m+1}}{\partial \mathbf{n}} = \frac{1}{z_j F}|i_j(E_{mix}^{m+1})|c_j^{m+1}, \tag{B.125}$$

where

$$i_j(E_{mix}^{m+1}) = L_j\left(\exp\left(\frac{\alpha_j z_j F(E_{mix}^{m+1}-E_j)}{R\theta}\right) - \exp\left(\frac{-\beta_j z_j F(E_{mix}^{m+1}-E_j)}{R\theta}\right)\right),$$

$$\sum_j i_j(E_{mix}^{m+1})c_j^{m+1} = 0 \tag{B.126}$$

for $j = s, k_1, k_2, \ldots, k_N$. In the following, we define $i_j^{m+1} := |i_j(E_{mix}^{m+1})|$.

Now we define the weak problem for the time-discrete problem:

Problem $(\widetilde{P_{c_j}})$

Find c_j^{m+1}, $j = s, k_1, k_2, \ldots, k_N \in H^2_{r_l^{m+1}}(\Omega)$ such that

$$\begin{aligned}&\frac{1}{\delta t}(c_j^{m+1}, w_j)_{r_l^{m+1}} + D_j(\nabla c_j^{m+1}, \nabla w_j)_{r_l^{m+1}} + \frac{1}{z_j F}(r_l^{m+1} i_j^{m+1} c_j^{m+1}, w_j)_{L^2(S)} \\ &= \frac{K}{\rho_l}(c_g^{m+1}c_j^m, w_j)_{r_l^{m+1}} + \frac{1}{\delta t}(c_j^m, w_j)_{r_l^m}\end{aligned} \tag{B.127}$$

subject to the constraint

$$\sum_j \int_S i_j(E_{mix}^{m+1})c_j^{m+1}w_j d\sigma = 0 \tag{B.128}$$

for all $w_j \in H^1(\Omega)$.

Regarding the argument given in the two species case, we need only to show the existence and uniqueness of the fixed point for solving E_{mix}^{m+1} by iteration algorithm. Firstly, we shall justify the solvability for E_{mix}^{m+1} for pointwisely given c_j^{m+1} on S, $j = s, k_1, \ldots, k_N$. Since Thoerem 4 in [79] guar-

doi:10.6342/NTU202200609

antees that there are $\eta_j^{m+1} > 0$ such that $c_j^{m+1} \geq \eta_j^{m+1}$ for $j = s, k_1, \ldots, k_N$, we have

Lemma B.6.1 There is one and only one root $E \in [E_{k_N}, E_{k_1}]$ satisfying

$$\sum_j i_j(E)(c_j) = 0 \tag{B.129}$$

for given $c_j \geq \eta_j^{m+1}$, $j = s, k_1, \ldots, k_N$.

Proof. Let $f(E) = \sum_j i_j(E)(c_j)$. Obviously, we have

$$f(E_{k_1}) > 0, \quad f(E_{k_N}) < 0 \tag{B.130}$$

The continuity of f implies that there is a root in $[E_{k_N}, E_{k_1}]$. Differentiating f with respect to E, we have

$$f'(E) = \sum_{j=1}^{N} \left(\alpha_{k_j} L_{k_j} e^{\alpha_{k_j}(E-E_{k_j})} + \beta_{k_j} L_{k_j} e^{-\beta_{k_j}(E-E_{k_j})}\right) + \alpha_s L_s e^{\alpha_s(E-E_s)} + \beta_s L_s e^{-\beta_s(E-E_s)} > 0 \tag{B.131}$$

for all $E \in (E_{k_N}, E_{k_1})$. This implies that $f(E)$ is strcitly monotone. Therefore, the root is unique. Q.E.D.

Let us define $\Lambda_1 : B \to \mathbf{H}_N := W_{\eta_s^{m+1}} \times W_{\eta_{k_1}^{m+1}} \times \cdots \times W_{\eta_{k_N}^{m+1}}$ such that $\Lambda_1(E)$ is the set of solutions to $(\widetilde{P_{c_j}})$ when letting $E_{mix}^{m+1} = E$.

Lemma B.6.2 Λ_1 is a bounded operator.

Proof. The boundedness of Λ_1 can be shown by the same argument as in Lemma B.3.3. Q.E.D.

By Corollary 7.3 in [80]:

doi:10.6342/NTU202200609

Lemma B.6.3 The trace operator $T_N : \mathbf{H}_N \to (L^2(S))^{N+1}$ is compact.

Finally, we define $\Lambda_2 : T_N(\mathbf{H}_N) \to B$ by

$$\Lambda_2 : (c_s, c_{k1}, \ldots, c_{k_N}) \mapsto E,$$

where E satisfying $\sum_j i_j(E)c_j = 0$ for $j = s, k_1 \ldots, k_N$.

Lemma B.6.4 Λ_2 is a bounded operator.

Proof. Let $\chi = (c_s, c_{k1}, \ldots, c_{k_N}) \in T_N(\mathbf{H}_N)$, we have $E_{k_N} \leq \Lambda_2(\chi) \leq E_{k_1}$. This implies that

$$\|\Lambda_2(\chi)\|^2_{L^2(S)} \leq \|E_{k_N}\|^2_{L^2(S)} \leq M \sum_j \|\eta_j^{m+1}\|_0^2 \leq M \sum_j \|c_j\|_0^2 \leq M \sum_j \|c_j\|_1^2 \tag{B.132}$$

for some constant $M > 0$. This completes the proof. Q.E.D.

Defining $\Lambda = \Lambda_2 \circ T_N \circ \Lambda_1$, we have

Proposition B.6.1 The operator $\Lambda : B \to B$ has a fixed point.

Now the existence result for two species case can be generalized to several species case:

Theorem B.6.1 There exist unique $r_l, c_g, c_j \in L^2(0,T; H^1(\Omega))$, $E_{mix} \in L^2(0,T;B)$ with $\partial_t r_l, \partial_t c_g, \partial_t c_j \in L^2(0,T; (H^1(\Omega))')$ such that

$$\int_0^T (\partial_t r_l, w)dt + \frac{K_g}{\rho_g} \int_0^T (r_l c_g, w)dt = 0 \tag{B.133}$$

$$\begin{aligned} &\int_0^T \langle r_l \partial_t c_g, w_g \rangle_{(H^1(\Omega))', H^1(\Omega)} dt + \int_0^T D_g (r_l \nabla c_g, \nabla w_g)dt \\ &- \frac{\beta}{z_s F} \int_0^T (r_l |i_s(E_{mix})| c_s, w_s)_{L^2(S)} dt + \frac{K_g M_g}{\rho_l} \int_0^T (r_l c_g, w_g)dt = 0, \end{aligned} \tag{B.134}$$

doi:10.6342/NTU202200609

$$\int_0^T \langle \partial_t(r_l c_j), w_j \rangle_{(H^1(\Omega))',H^1(\Omega)} + \int_0^T D_j(r_l \nabla c_j, \nabla w_j)dt + \frac{1}{z_j F}\int_0^T (r_l |i_j(E_{mix})| c_j, w_j)_{L^2(S)}dt = \frac{K}{\rho_l}\int_0^T (r_l c_g c_j, w_j)dt, \tag{B.135}$$

satisfying the constraint

$$\sum_j \int_0^T (i_j(E_{mix})c_s, w_e)_{L^2(S)}dt \tag{B.136}$$

for all $w, w_g, w_j \in L^2(0,T;H^1(\Omega))$ and for all $w_e \in L^2((0,T)\times S)$. Moreover, r_l, c_g, c_j satisfy the initial conditions $r_l(0) = r_l^0$, $c_g(0) = c_g^0$, $c_j(0) = c_j^0$ with $0 < r_l^0 \leq 1$, $0 \leq c_g^0 \leq 1$, $0 < c_j^0 \leq 1$, $r_l^0, c_g^0, c_j^0 \in H^1(\Omega)$.

doi:10.6342/NTU202200609

doi:10.6342/NTU202200609

Reference

[1] Y. S. Kim and H. J. Sohn, "Mathematical modeling of electroless nickel deposition at steady state using rotating disk electrode," *Journal of the Electrochemical Society*, vol. 143, pp. 505–509, 1996. xxix, 9, 12, 28, 31, 61, 83, 107, 108, 109, 110, 134

[2] A. Brenner and G. E. Riddell, "Nickel plating on steel by chemical reduction," *Journal of Research of the National Bureau of Standards*, vol. 37, pp. 31–34, 1946. 1

[3] N. Paunovic, "Electrochemical aspects of electroless deposition of metal," *Plating*, vol. 51, pp. 11–61, 1968. 1

[4] G. O. Mallory and J. B. Hajdu, *Electroless plating: fundamentals and applications*, C. U. Press, Ed., 1990. 1, 2

[5] Y. Shacham-Diamand, T. Osaka, Y. Okinaka, A. Sugiyama, and V. Dubin, "30 years of electroless plating for semiconductor and polymer micro-systems," *Microelectronic Engineering*, vol. 132, pp. 35 – 45, 2015,

doi:10.6342/NTU202200609

micro and Nanofabrication Breakthroughs for Electronics, MEMS and Life Sciences. 2

[6] R. Parkinson, *Properties and Applications of Electroless Nickel*, N. D. I. T. S. no.10081, Ed., 1995. 2

[7] G. O. Mallory and J. B. Hajdu, *Electroless Plating: Fundamentals and Applications*, W. Andrew, Ed., 1990. 2

[8] H. C. Koo, R. Saha, and P. A. Kohl, "Copper electroless bonding of dome-shaped pillars for chip-to-package interconnect," *Journal of the Electrochemical Society*, vol. 158, pp. D698–D703, 2011. 2, 7

[9] J. A. Bard and R. A. Faulkner, *Electrochemical MethodsFundamentals and Applications*, J. W. . Sons, Ed., 2001. 4

[10] S. Yang, H. T. Hung, P. Y. Wu, Y. W. Wang, Y. W. Nishikawa, and C. R. Kao, "Materials merging mechanism of microfluidic electroless interconnection process," *Journal of the Electrochemical Society*, vol. 165, pp. D273–D281, 2018. 7

[11] Y. B. Chen, "Development of interconnects by electroless nickel plating," Master's thesis, Graduate Institute of Materials Science and Engineering, National Taiwan University, 2015. 8

doi:10.6342/NTU202200609

[12] C. Y. Yang, "Application of electroless Ni plating for chip-to-chip direct bonding," Master's thesis, Graduate Institute of Materials Science and Engineering, National Taiwan University, 2019. 8, 9

[13] V. G. Levich and S. Technica, *Physicochemical Hydrodynamics*, P. hall Englewood Cliffs, Ed., 1962. 10, 27, 83, 109, 110

[14] M. Ramasubramanian, B. N. Popov, R. E. White, and K. A. Chen, "Mathematical model for electroless copper deposition on planar substrates," *Journal of the Electrochemical Society*, vol. 146, pp. 111–116, 1999. 11, 28, 31

[15] Lord Rayleigh, Sec R. S., "Xx. on the theory of surface forces.—ii. compressible fluids," *The London, Edinburgh, and Dublin Philosophical Magazine and Journal of Science*, vol. 33, pp. 209–220, 1892. 19

[16] J. D. van der Waals, "Thermodynamische theorie der capillariteit in de onderstelling van continue dichtheidsverandering, verhand," *Verhandelingen der Koninklijke Akademie van Wetenschappen*, vol. 1, p. 56, 1893. 19

[17] H. Abels, H. Garcke, and G. Grün, "Thermodynamically consistent, frame indifferent diffuse interface models for incompressible two-phase flows with different densities," *Mathematical Models and Methods in Applied Sciences*, vol. 22, p. 1150013, 2012. 19, 20, 82

doi:10.6342/NTU202200609

[18] P. C. Hohenberg and B. I. Halperin, "Theory of dynamic critical phenomena," *Reviews of Modern Physics*, vol. 49, pp. 435–479, 1977. 19, 20

[19] J. Lowengrub and L. Truskinovsky, "Quasi-incompressible Cahn-Hilliard fluids and topological transitions," *Proceedings of the Royal Society of London. Series A: Mathematical Physical and Engineering Sciences*, vol. 454, pp. 2617–2654, 1998. 19

[20] J. Shen and X. Yang, "Decoupled, energy stable schemes for phase-field models of two-phase incompressible flows," *SIAM Journal on Numerical Analysis*, vol. 53, pp. 279–296, 2015. 21, 82

[21] M. Hintermuller and V. A. Kovtunenko, "From shape variation to topological changes in constrained minimization: a velocity method-based concept," *Optimization Methods and Software*, vol. 26, pp. 513–532, 2011. 21

[22] G. Tierra and F. Guillén-González, "Numerical methods for solving the Cahn–Hilliard equation and its applicability to related energy-based models," *Archives of Computational Methods in Engineering*, vol. 22, pp. 269–289, 2015. 21

[23] M. Sussman, P. Smereka, S. Osher *et al.*, "A level set approach for computing solutions to incompressible two-phase flow," Ph.D. disserta-

doi:10.6342/NTU202200609

tion, Department of Mathematics, University of California, Los Angeles, 1994. 21, 82

[24] J. Ni and C. Beckermann, "A volume-averaged two-phase model for transport phenomena during solidification," *Metallurgical Transactions B*, vol. 22, pp. 349–361, 1991. 23, 84, 88, 89

[25] D. A. Drew, "Mathematical modeling of two-phase flow," *Annual Review of Fluid Mechanics*, vol. 15, pp. 261–291, 1983. 23, 82, 89

[26] S. Whitaker, "Diffusion and dispersion in porous media," *AIChE Journal*, vol. 13, pp. 420–427, 1967. 24, 86

[27] J. C. Slattery, "Flow of viscoelastic fluids through porous media," *AIChE Journal*, vol. 13, pp. 1066–1071, 1967. 24, 86

[28] N. Perez, *Electrochemistry and Corrosion Science*, Springer, Ed., 2004. 27

[29] O. Pironneau, "On optimum profiles in Stokes flow," *Journal of Fluid Mechanics*, vol. 59, pp. 117–128, 1973. 28, 32, 33

[30] T. C. Rebollo, V. Girault, F. Murat, and O. Pironneau, "Analysis of a coupled fluid-structure model with applications to hemodynamics," *SIAM Journal on Numerical Analysis*, vol. 54(2), pp. 994–1019, 2016. 28, 32

doi:10.6342/NTU202200609

[31] M. Beneš and P. Kučera, "Solutions to the Navier – Stokes equations with mixed boundary conditions in two-dimensional bounded domains," *Mathematische Nachrichten*, vol. 289, no. 2-3, pp. 194–212, 2016. 38

[32] S. Kračmar and J. Neustupa, "Modeling of the unsteady flow through a channel with an artificial outflow condition by the navier–stokes variational inequality," *Mathematische Nachrichten*, vol. 291, no. 11-12, pp. 1801–1814, 2018. 38

[33] M. Braack and P. B. Mucha, "Directional do-nothing condition for the Navier-Stokes equations," *Journal of Computational Mathematics*, vol. 32, pp. 507–521, 2014. 38

[34] M. A. Freedman, "Riemann step function approximation of bochner integrable functions," *Proceedings of the American Mathematical Society*, vol. 96, no. 4, pp. 605–613, 1986. 40

[35] T. Kato, "Linear evolution equations of "hyperbolic" type, II," *Journal of the Mathematical Society of Japan*, vol. 25, no. 4, pp. 648 – 666, 1973. 40

[36] P. G. Ciarlet, *Linear and Nonlinear Functional Analysis with Applications*. SIAM, 2013, vol. 130. 43

[37] G. J. Minty *et al.*, "Monotone (nonlinear) operators in Hilbert space," *Duke Math. J.*, vol. 29, no. 3, pp. 341–346, 1962. 43

doi:10.6342/NTU202200609

[38] G. J. Minty, "On a monotonicity method for the solution of nonlinear equations in Banach spaces," *P. Natl. Acad. Sci. USA*, vol. 50, no. 6, p. 1038, 1963. 43

[39] F. E. Browder, "Nonlinear elliptic boundary value problems," *B. Am. Math. Soc.*, vol. 69, no. 6, pp. 862–874, 1963. 43

[40] A. Pryde, "Second order elliptic equations with mixed boundary conditions," *Journal of Mathematical Analysis and Applications*, vol. 80, no. 1, pp. 203–244, 1981. 44

[41] R. Temam, *Navier-Stokes Equations: Theory and Numerical Analysis*, A. North-Holland, Ed., 1977. 53, 169

[42] P. D. Lax, *Functional Analysis*, Wiley-Interscience, Ed., 2002. 54

[43] T. A. Davis, "Algorithm 832: UMFPACK V4.3—an unsymmetric-pattern multifrontal method," *ACM Trans. Math. Softw.*, vol. 30, no. 2, p. 196–199, 2004. 63, 64

[44] M. Bercovier and O. Pironneau, "Error estimates for finite element method solution of the Stokes problem in the primitive variables," *Numerische Mathematik*, vol. 33, pp. 211–224, 1979. 63

[45] H. Hung, S. Yang, Y. Chen, and C. Kao, "Chip-to-chip direct interconnections by using controlled flow electroless Ni plating," *Journal of Electronic Materials*, vol. 46, pp. 4321–4325, 2017. 66, 70

doi:10.6342/NTU202200609

[46] C. Lochovsky, S. Yasotharan, and A. Günther, "Bubbles no more: in-plane trapping and removal of bubbles in microfluidic devices," *Lab on a Chip*, vol. 12, pp. 595–601, 2012. 81

[47] A. Hibara, S. Iwayama, S. Matsuoka, M. Ueno, Y. Kikutani, M. Tokeshi, and T. Kitamori, "Surface modification method of microchannels for gas-liquid two-phase flow in microchips," *Analytical Chemistry.*, vol. 77, pp. 943–947, 2005. 81

[48] Z. Yang, S. Matsumoto, and R. Maeda, "A prototype of ultrasonic micro-degassing device for portable dialysis system," *Sensors and Actuators A: Physical*, vol. 95, pp. 274–280, 2002. 81

[49] K. A. Triplett, S. M. Ghiaasiaan, S. I. Abdel-Khalik, and D. L. Sadowski, "Gas–liquid two-phase flow in microchannels part I: two-phase flow patterns," *International Journal of Multiphase Flow*, vol. 25, pp. 377–394, 1999. 82

[50] K. A. Triplett, S. M. Ghiaasiaan, S. I. Abdel-Khalik, A. LeMouel, and B. N. McCord, "Gas–liquid two-phase flow in microchannels part II: void fraction and pressure drop," *International Journal of Multiphase Flow*, vol. 25, pp. 395–410, 1999. 82

[51] M. K. Akbar, D. A. Plummer, and S. M. Ghiaasiaan, "On gas-liquid two-phase flow regimes in microchannels," *International Journal of Multiphase Flow*, vol. 29, pp. 855–866, 2003. 82

doi:10.6342/NTU202200609

[52] E. Delnoij, F. A. Lammers, J. A. M. Kuipers, and W. P. M. van Swaaij, "Dynamic simulation of dispersed gas-liquid two-phase flow using a discrete bubble model," *Chemical Engineering Science*, vol. 52, pp. 1429–1458, 1997. 82

[53] T. Fukano and A. Kariyasaki, "Characteristics of gas-liquid two-phase flow in a capillary tube," *Nuclear Engineering and Design*, vol. 141, pp. 59–68, 1993. 82

[54] E. Olsson and G. Kreiss, "A conservative level set method for two phase flow," *Journal of Computational Physics*, vol. 210, pp. 225–246, 2005. 82

[55] M. Ishii and T. Hibiki, *Thermo-fluid dynamics of two-phase flow*, S. S. . B. Media, Ed., 2010. 82

[56] N. Zuber and J. Findlay, "Average volumetric concentration in two-phase flow systems," *Journal of Heat Transfer*, vol. 87. Serie C, pp. 453–462, 1965. 82

[57] V. Girault, O. Pironneau, and P. Y. Wu, "Analysis of an Electroless Plating Problem," *IMA Journal of Numerical Analysis*, 2021. 83

[58] O. Pironneau, "On the transport-diffusion algorithm and its applications to the Navier-Stokes equations," *Numerische Mathematik*, vol. 38, pp. 309–332, 1982. 83

doi:10.6342/NTU202200609

[59] A. E. Nielsen, *Kinetics of precipitation.* Pergamon, 1964, vol. 18. 87

[60] S. Wachi and A. G. Jones, "Mass transfer with chemical reaction and precipitation," *Chemical Engineering Science*, vol. 46, no. 4, pp. 1027–1033, 1991. 87

[61] D. Bresch, B. Desjardins, J.-M. Ghidaglia, E. Grenier, and M. Hilliairet, "Multifluid models including compressible fluids," *Handbook of Mathematical Analysis in Mechanics of Viscous Fluids*, pp. 2927–2978, 2018. 89

[62] D. Bresch and M. Renardy, "Well-posedness of two-layer shallow-water flow between two horizontal rigid plates," *Nonlinearity*, vol. 24, no. 4, pp. 1081–1088, 2011. 89

[63] V. Girault and P.-A. Raviart, "Finite element methods for navier-stokes equations," vol. 5, 1986. 96, 105

[64] F. Hecht and O. Pironneau, "An energy stable monolithic eulerian fluid-structure finite element method," *International Journal for Numerical Methods in Fluids*, vol. 85, no. 7, pp. 430–446, 2017. 98

[65] P. G. Ciarlet, *The Finite Element Method for Elliptic Problems.* SIAM, 2002. 99

doi:10.6342/NTU202200609

[66] C. Arana, J. Tabib, J. Dukovic, and L. T. Romankiw, "Electrodeposition of nickel-iron alloys," *Journal of the Electrochemical Society*, vol. 136, pp. 1336–1340, 1989. 108

[67] S. Hessami and C. W. Tobias, "A mathematical model for anomalous codeposition of nickel-iron on a rotating disk electrode," *Journal of the Electrochemical Society*, vol. 136, pp. 3611–3616, 1989. 108

[68] C. M. Criss and J. W. Cobbie, "The thermodynamic properties of high temperature aqueous solutions," *Journal of the American Chemical Society*, vol. 86, pp. 5385–5390, 1964. 108

[69] S. Yang, H. T. Hung, P. Y. Wu, Y. W. Wang, H. Nishikawa, and C. R. Kao, "Materials merging mechanism of microfluidic electroless interconnection process," *J. Electrochem. Soc.*, vol. 165, no. 7, pp. D273–D281, 2018. 115

[70] F. Hecht, "New developments in Freefem++ (www.freefem.org)," *J. Numer. Math.*, vol. 20, pp. 251–265, 2012. 119

[71] A. Cartellier, "Simultaneous void fraction measurement bubble velocity and size estimate using a single optical probe in gas−liquid two-phase flows," *Review of Scientific Instruments*, vol. 63, pp. 5442–5453, 1992. 133

doi:10.6342/NTU202200609

[72] R. Blue and D. Uttamchandani, "Recent advances in optical fiber devices for microfluidics integration," *Journal of Biophotonics*, vol. 9, pp. 13–25, 2016. 133

[73] H. Ide, R. Kimura, and M. Kawaji, "Optical measurement of void fraction and bubble size distributions in a microchannel," *Heat Transfer Engineering*, vol. 28, pp. 713–719, 2007. 133

[74] "Measurement accuracy of a mono-fiber optical probe in a bubbly flow," *International Journal of Multiphase Flow*, vol. 36, pp. 533 – 548, 2010. 133

[75] L. Ambrosio, A. Pinamonti, and G. Speight, "Weighted Sobolev spaces on metric measure spaces," *Journal für die reine und angewandte Mathematik*, vol. 2019, pp. 39–65, 2019. 141

[76] V. Gol'dshtein and A. Ukhlov, "Weighted Sobolev spaces and embedding theorems," *Transactions of the American Mathematical Society*, vol. 361, pp. 3829–3850, 2009. 142

[77] J. L. Vazquez, *The Porous Medium Equation: Mathematical Theory*, C. Press, Ed., 2006. 145

[78] O. A. Ladyzhenskaia, V. A. Solonnikov, and N. N. Ural'tseva, *Linear and quasi-linear equations of parabolic type*. American Mathematical Soc., 1988, vol. 23. 153

doi:10.6342/NTU202200609

[79] D. Le and H. Smith, "Strong positivity of solutions to parabolic and elliptic equations on nonsmooth domains," *Journal of Mathematical Analysis and Applications*, vol. 275, pp. 208–221, 2002. 153, 176

[80] M. Biegert, "On traces of Sobolev functions on the boundary of extension domains," *Proceedings of the American Mathematical Society*, vol. 137, pp. 4169–4176, 2009. 155, 177

[81] M. Dreher and A. Jüngel, "Compact families of piecewise constant functions in $L^p(0,T;B)$," *Nonlinear Analysis: Theory, Methods and Applications*, vol. 75, pp. 3072 – 3077, 2012. 170, 171

doi:10.6342/NTU202200609